50,000 years of paleoenvironmental change recorded in meteoric waters and coeval paleoecological and cryostratigraphic indicators from the Klondike goldfields, Yukon, Canada

by

Matthew E. Mahony

A thesis submitted in partial fulfillment of the requirements for the degree of

Master of Science

Department of Earth and Atmospheric Sciences
University of Alberta

Abstract

A 50,000 year record of meteoric water isotopes ($\delta^2H/\delta^{18}O$) and paleoenvironmental conditions is presented from syngenetic ice-rich permafrost and macrofossils from eight sites in the Klondike area of central Yukon. Four sedimentary units are recognized based on cryostratigraphy, paleoecological indicators, and $\delta^2H/\delta^{18}O$ of associated ground ice. Unit 1 (50,000-36,000 cal yrs BP) contains boreal indicators (large woody macrofossils indicating trees and shrubs) near the base of the unit and is bounded near the top by the appearance of arctic ground squirrel nests. The presence of arctic ground squirrel nests, a reliable indicator of steppe-tundra, coupled with the largely massive organic-rich silts and large syngenetic ice wedges, defines Unit 2 (36,000-27,000 cal yrs BP). Unit 3 (27,000-13,150 cal yrs BP) includes abundant arctic ground squirrel nests, while the silts are generally grey and less organic-rich, and ice wedges through the unit are rare. Unit 4 (13,150 cal yrs BP to present) lacks arctic ground squirrel nests and contains shrubs near the base of the unit and full-boreal indicators in the upper sections. $\delta^2H/\delta^{18}O$ tracks large-scale climate trends with a shift from near-modern values near the base of Unit 1 to more depleted values, reaching a minima at the Last Glacial Maximum (LGM). Isotopic values increase abruptly at 15,000 cal yrs BP, marking a climate amelioration reaching maximum values during the early Holocene, followed by subsequent cooling after 9,000 cal yrs BP. Deuterium (d) excess shows no clear trends except a +9‰ anomaly from 29,000-22,000 cal yrs BP coinciding with the LGM. This period likely represents an enhanced seasonality of precipitation, either from increased winter or reduced summer precipitation. This multi-proxy permafrost record provides new insights on late Pleistocene-Holocene climate and environmental change in eastern Beringia, and highlights the potential to develop similar records in other unglaciated regions.

Acknowledgments

Financial support for this thesis was provided by the Geological Society of America and the Canadian Circumpolar Institute at the University of Alberta. I would also like to thank the EnviroNorth training program for their support of student research in northern environments.

Dr. Duane Froese is responsible for providing me with this wonderful opportunity to advance my academic career. He introduced me to the Klondike and eastern Beringia and helped me create this fun and rewarding research project. I also deeply appreciate all the time and effort he gave to help me successfully navigate through the completion of the requirements for a masters degree. I would also like to thank Dr. Trevor Porter, who provided many great ideas and interpretations of the stable isotope record and northern environments. Additional thanks to my thesis committee members, Dr. Jeff Kavanaugh and Dr. Alberto Reyes, for their time and contributions in the development of this thesis.

This work would not have been possible if it also weren't for Dr. Fabrice Calmels, Joel Pumple, Lauren Davies, Ann Hammad, and Sasiri Bandara for their assistance in the field and lab over the last few years.

I would also like to thank my family: Ed, Sarah, and Kasey, for their perpetual support throughout my academic career – even when it requires me moving to the great white north, eh?

Table of Contents

List of Tables

(Ch 2)

List of Figures

(Ch 1)

List of Appendices

Chapter 1: Introduction

Spanning from Siberia through Yukon, Beringia is the subcontinental region that existed during Pleistocene cold stages as the shallow marine shelves connecting the two continents became exposed during times of lowered sea level, enabling biogeographic exchanges between the Old and New worlds. The North American portion of Beringia, eastern Beringia, was dissimilar to much of the arctic during the Last Glacial Maximum (LGM) in that it was largely unglaciated (Figure 1-1), preserving a rich depositional record dating back through the late Neogene (Westgate et al., 1990; Ehlers and Gibbard, 2004; Froese et al., 2009).

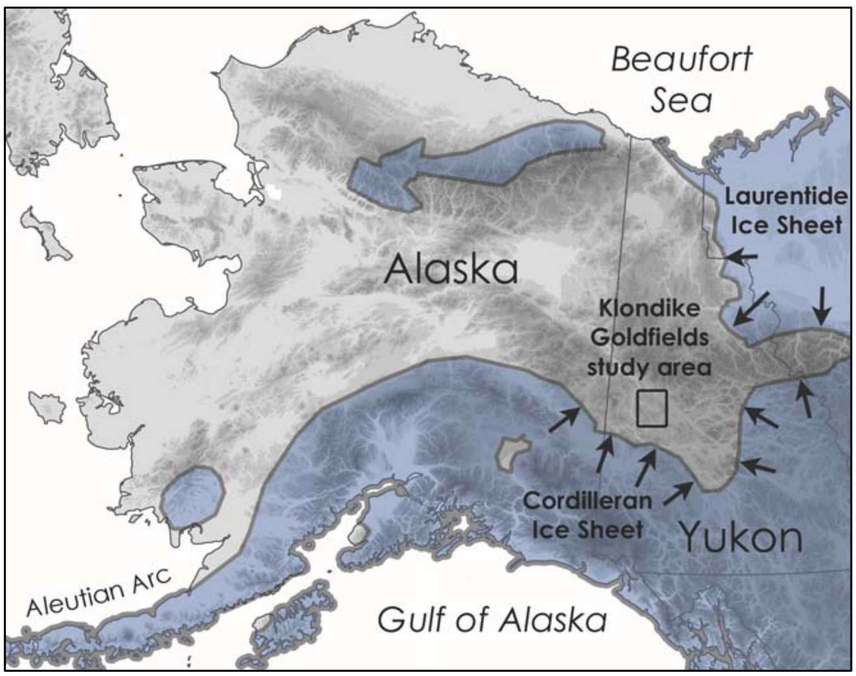

Figure 1-1: Study area and surrounding glacial ice during the LGM (from Ehlers and Gibbard, 2004).

The lack of glaciation in Beringia was a result of the pronounced aridity of the region. This aridity was due in large part to the presence of mountain ranges (Wrangell-St. Elias, Alaska Range, and Coast mountains) that border the region to the southwest. Moisture in the interior of Yukon and Alaska is largely derived from the North Pacific and has to travel over the mountains, which results in large amounts of precipitation locally and much drier air masses that continue into the interior (Figure 1-2) (PRISM Climate Group, 2000). This was likely most pronounced during cold stages and would have intensified the already arid conditions that would have been present largely due to increased winds, clear sunny days, and dry weather (Guthrie, 1990, 2001).

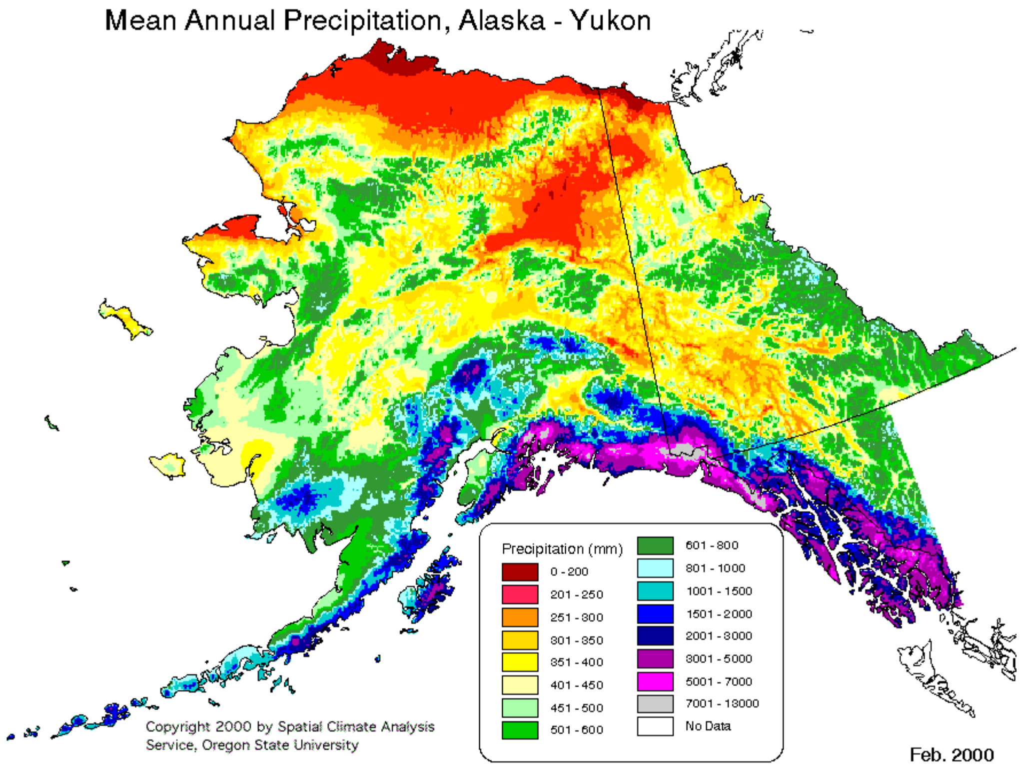

Figure 1-2: Mean annual precipitation in Alaska and Yukon (from PRISM Climate Group, 2000).

Widespread fine-grained sedimentary deposits blanket much of Beringia. This fine-grained sediment was readily reworked subaerially in periglacial environments by increased winds during cold stages. In eastern Beringia, this windblown sediment, or loess, is the most abundant surficial deposit and was largely deposited across much of this region during cold stages of the Pleistocene (Péwé, 1975). In areas of permafrost, deposition of sediments results in the upward migration of the permafrost table, resulting in aggradational, or syngenetic permafrost. Across much of Beringia, active loess deposition during the cold stages led to widespread syngenetic permafrost (Schirrmeister et al., 2013). In contrast, many areas of Beringia during interglacials, such as the Holocene, are characterized by a permafrost table that is relatively stable, or epigenetic permafrost. The numerous exposures of permafrost through the Klondike region, because of their long temporal history, provide the opportunity to study the dynamics of permafrost under changing climate conditions of the past.

Klondike permafrost

The Klondike region is within the area of extensive discontinuous permafrost, a region where permafrost is strongly controlled by elevation, slope, aspect, and vegetation cover. Permafrost is generally present on north-facing slopes, and within narrow valleys, but may be sporadic to absent on south-facing slopes. The bedrock in this region is blanketed by thick regolith and Pliocene gold-bearing gravels overlain by Quaternary material within valleys. This is an area of widespread placer gold-mining operations located in close proximity to Dawson City, Yukon (64° 3' 35.8" N, 139° 24' 39.02" W). Throughout much of the Klondike, permafrost is seen as an impediment to gold mining, as it slows the excavation of auriferous gravels. The frozen silts that overlie these gravels are locally known as "muck", a vernacular term for ice-rich silts and fine sand exposed in Klondike valley-bottoms (*e.g.* McConnell, 1905; Fraser and Burn, 1997; Froese et al., 2009).

Klondike muck deposits are generally divided into two units by a distinct unconformity between relatively organic-poor Pleistocene silt and organic-rich Holocene deposits (Fraser and Burn, 1997). Late Pleistocene silts in Siberia are similar to the Klondike muck, but are termed "Ice Complex" or more commonly "yedoma". The stratotype for yedoma includes sandy silt with a layered cryostructure, large syngenetic wedges, and plant and animal material. Schirrmeister et al. (2013) apply the yedoma definition to all syngenetic ice-rich silts in Beringia that formed during late Pleistocene cold-climate conditions. Their definition incorporates late Pleistocene "muck" of the Klondike into the western "yedoma" definition, however in my experience there are a significant number of exposures dating to the last cold stage that are relatively ice-rich but lack the large ice wedges characteristic of yedoma. Because of this, central Yukon permafrost tends not to agree with the strict definition of late Pleistocene Beringian permafrost always containing large ice wedges. In addition, yedoma deposits are considered to be late Pleistocene by definition while "muck" includes the organic-rich material of the Holocene, which is a significant part of this study. For the sake of simplicity, and also due to incongruities with the current yedoma definition, I continue referring to Klondike syngenetic permafrost as muck.

Thick ice-rich muck deposits in Klondike valley-bottoms are an excellent archive of late Pleistocene environments (Fraser and Burn, 1997; Kotler and Burn, 2000; Froese et al., 2009). In addition to various paleoecological indicators, such as plant and animal fossils, abundant syngenetic ground ice preserves the geochemical signatures of past precipitation. These ancient waters can be utilized as a powerful proxy for past climate (*e.g.* Meyer et al., 2000; Schirrmeister et al., 2002; Popp et al., 2006) and are a major focus of this thesis.

Ground ice as a paleoenvironmental proxy

Ground ice in syngenetic permafrost deposits can form either as interstitial (pore or textural) ice, segregated lenses of ice varying from a few mm to m in thickness, or as distinct ice bodies such as ice wedges, buried snowbanks, or icings (Mackay, 1972; French, 2011). These ice bodies provide information on the past environmental conditions by virtue of the geocryological properties which indicate past landscape processes at the time of formation or the conditions that led to their preservation. The variability in the type and amount of ground ice therefore can also assist in correlation of contemporary deposits.

In addition to the geocryological properties that inform the origin of ground ice, the isotopic composition of the ice can be used as an archive of past meteoric water (Meyer et al., 2000; Kotler and Burn, 2000; Lacelle, 2011). One of the central questions of this thesis is the extent to which pore ice in permafrost can be viewed as record of meteoric precipitation. The water in precipitation (*i.e.* meteoric water) can be used to construct paleoclimate records by virtue of two interrelated effects: the temperature dependence of fractionation factors between liquid and vapor phases, and Rayleigh Distillation (Dansgaard, 1964; Jouzel et al., 1997; Bowen, 2008; Birks and Edwards, 2009). Since the isotopic composition of precipitation is correlated with temperature, it may provide a robust paleoclimate proxy. The development of long-term records, such as the one in this study, is instrumental to furthering our understanding of regional and global climate dynamics. This study attempts to add another long-term record to the existing North American records, which up to this point has only been possible from ice cores, such as those recovered from Greenland and Mt. Logan, Yukon.

Developing proxy records from permafrost is a complex task. There are only a few reliable techniques for dating the material, including radiocarbon dating of plant macrofossils and animal remains, optically stimulated luminescence dating, and correlation of interbedded volcanic ash (tephra) layers. In this study the main techniques used are radiocarbon dating and the identification of interbedded tephra beds. The only distinct tephra bed in this study is the Dawson tephra, which erupted from the Emmons Lake volcanic center in the Aleutian arc approximately 30,000 cal yrs BP (Froese et al., 2002; Demuro et al., 2008). This bed is a particularly useful marker in the field as it erupted right around the onset of cold and dry conditions of the LGM (Zazula et al., 2006).

Beringian paleoecology

The bones and teeth of Ice Age mammals are common across Beringia and may be exceptionally preserved in relict permafrost (*e.g.* Guthrie, 1990). Numerous teeth and bones of large herbivores have been dated through the LGM, indicating Beringia hosted sufficient vegetation to support herds of grazing megafauna and associated carnivores (Guthrie, 1990; Zazula et al., 2007). The connection of North America to Eurasia resulted in unique combinations of North American and Asian flora and fauna that migrated across the land bridge (Schweger, 1997; Shapiro et al., 2004). R. Dale Guthrie has worked extensively with late Pleistocene mammal fossils and proposed the 'mammoth-steppe' as a full glacial steppe-tundra environment (Guthrie, 1990). More recently, paleoecological investigations have reinforced the interpretation that the mammoth-steppe was productive enough to support the "Pleistocene megafauna" (Froese et al., 2009), which included horse, bison, mammoth, short-faced bear, and Beringian lions, to name a few.

One of the most remarkable datasets to address this question of the nature of the full-glacial ecosystem of Beringia has come from the nests and seed caches of arctic ground squirrels from Yukon (Zazula et al., 2003, 2005, 2007), Alaska (Guthrie, 1990; Gaglioti et al., 2011), and Siberia (Zanina et al., 2011). Analyses of more than 100 arctic ground squirrel nests from central Yukon permafrost have characterized plant macrofossils and revealed prairie sage, bunch-grasses, and forbs from an open, steppe-tundra environment. Gaglioti et al. (2011) confirmed similar findings in fossil plant taxa from arctic ground squirrel nests in interior Alaska, as did Zanina et al. (2011) in Siberia. These data support the existence of a widespread mammoth-steppe in Beringia during the late Pleistocene. Paleoecological studies such as these have helped develop our modern understanding of LGM environments in eastern Beringia as being open, steppe-tundra with well-drained loessal soils and deep active layers (Zazula et al., 2003; Froese et al., 2009; Blinnikov et al., 2011).

Marine Isotope Stage 2 ended with abrupt warming associated with a precession-driven increase in insolation during the last glacial-interglacial transition that drastically altered the vegetation of the mammoth-steppe. The timing of this transition is only approximately known from lake sediment archives (Edwards and Barker, 1994; Bigelow and Edwards, 2001) and a handful of plant macrofossil studies that date to this transition. During this time the Bering land bridge was resubmerged by rising sea levels, severing the connection between Eurasia and North America and effectively putting an end to Beringia and the mammoth-steppe. Proxy records from vegetation indicate shrub expansion, peat formation, and eventual expansion of boreal vegetation northward as warmer and wetter conditions of the early Holocene developed (Ritchie, 1984). The shrub-dominated environment of the early Holocene thermal maximum was eventually replaced by boreal forest that has persisted to the modern day (Figure 1-3) (Guthrie, 2006). Of the widespread "Pleistocene megafauna", only a few of the large mammals survived the environmental changes and associated environmental shifts that occurred during the last glacial-interglacial transition.

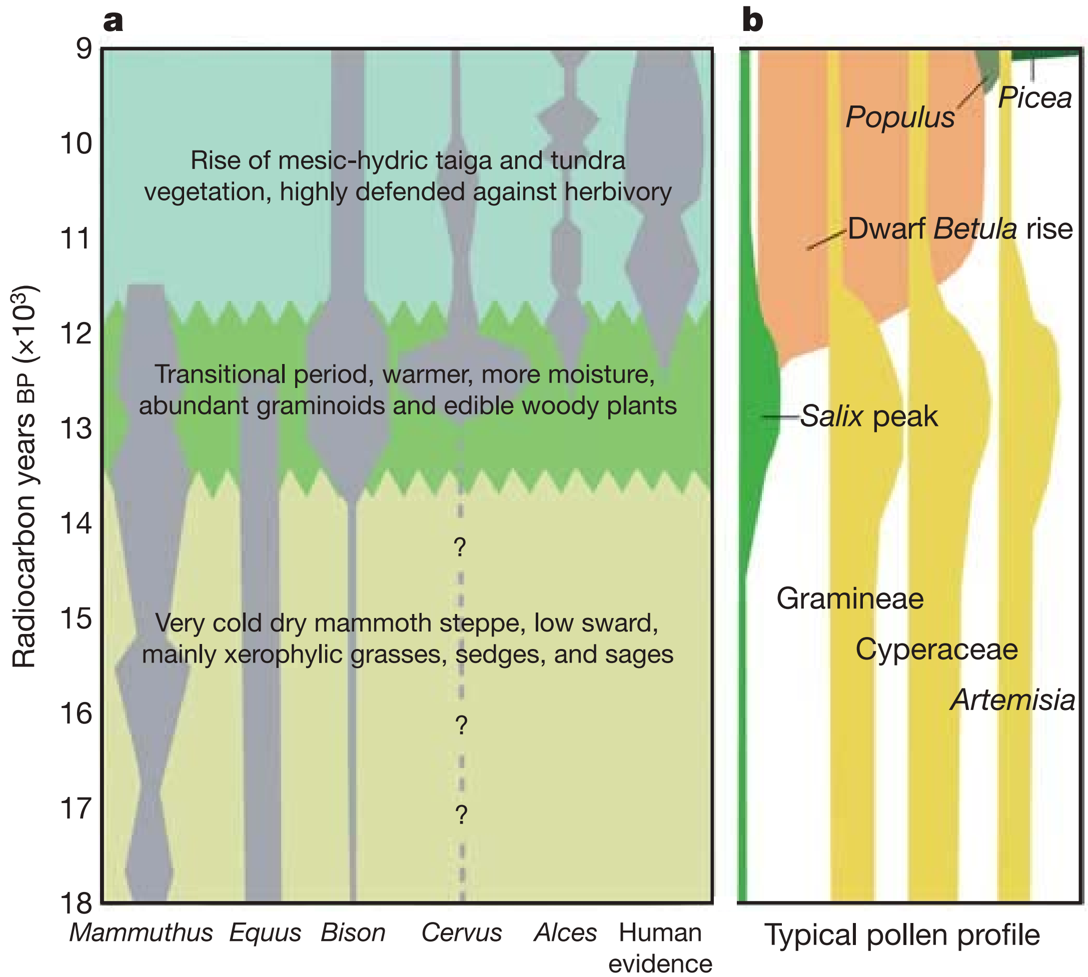

Figure 1-3 : (a) Climate-vegetation dynamics overlain by radiocarbon dates of large mammal fossils from 18,000 to 9,000 radiocarbon years, (b) generalized pollen patterns from several pollen studies across Alaska and Yukon (from Guthrie, 2006).

Thesis objectives and organization

This thesis presents a new record of meteoric waters and paleoenvironmental proxies up to the limits of radiocarbon dating methods *ca.* 50,000 calendar years before present (cal yrs BP). This timeframe includes the three most recent marine isotope stages (MIS): MIS 1 Holocene interglacial, MIS 2 late Wisconsinan cold stage (glacial), and late MIS 3 interstadial, to the limits of radiocarbon dating (Figure 1-4). These proxies include hydrogen and oxygen ($\delta^2H/\delta^{18}O$) isotopic ratios from pore and wedge ice, paleoecological indicators, and cryostratigraphic observations.

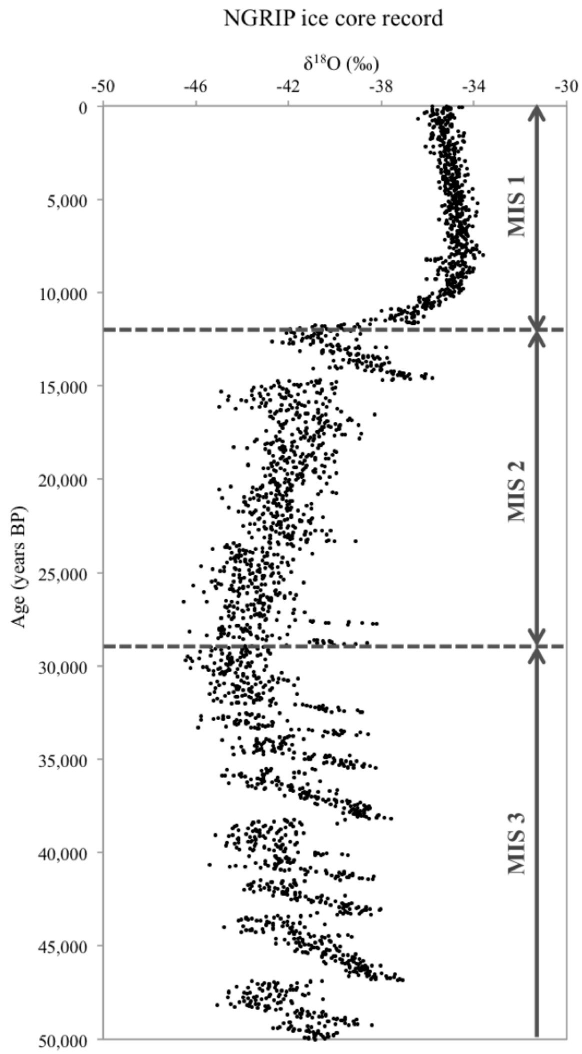

Figure 1-4 : Timing of paleoclimatic events through the last 50,000 cal yrs BP (Lowe et al., 2008).

Utilizing these proxies we define four distinct units spanning the last 50,000 cal yrs BP. The physical characteristics of these units can hopefully help with age estimations of unknown exposures during future fieldwork in the Klondike. This study can also help shed light on environmental and permafrost dynamics under changing climate regimes, which may be beneficial to understanding the potential impacts of future warming in the subarctic. Klondike permafrost could theoretically be developed into the longest paleoclimate record in the Northern Hemisphere, as locally there is permafrost over 700,000 years old in central Yukon (Froese et al., 2008).

The objectives of this study are:

1) Define the main depositional units of the Klondike muck deposits based on cryostratigraphic, isotopic, and paleoecological indicators;

2) Determine whether the meteoric water isotopes from these perennially-frozen deposits provide a regionally coherent climate proxy between sites and over time from associated water isotopes in pore and wedge ice; and

3) Describe the timing and nature of the last glacial-interglacial transition from Klondike permafrost.

Organization of thesis

Chapter 2 describes the field and laboratory techniques used to construct this record. Also included is a detailed study into the effectiveness of the isotope analyzers when measuring isotopic ratios of permafrost waters. Chapter 3 describes the general lithostratigraphic, cryostratigraphic, chronostratigraphic, isotopic, and paleoecological indicators of the eight permafrost exposures included in this study. At the end of the chapter is a brief summary of paleoenvironmental interpretations based on the characteristics of each site. Chapter 4 presents the complete meteoric water record and main permafrost units based on the multiple proxy records. A discussion of the findings is included at the end of the chapter. Chapter 5 presents the general conclusions and recommendations for future research.

References

Bigelow, N.H., Edwards, M.E., 2001. A 14,000 yr paleoenvironmental record from Windmill Lake, Central Alaska: Late glacial and Holocene vegetation in the Alaska range. Quaternary Science Reviews, 20, 203–215.

Birks, S.J., Edwards, T.W.D., 2009. Atmospheric circulation controls on precipitation isotope–climate relations in western Canada. Tellus B, 61 (3), 566-576.

Blinnikov, M.S., Gaglioti, B.V., Walker, D.A., Wooller, M.J., Zazula, G.D., 2011. Pleistocene graminoid-dominated ecosystems in the Arctic. Quaternary Science Reviews, 30 (21–22), 2906-2929.

Bowen, G.J., 2008. Spatial analysis of the intra-annual variation of precipitation isotope ratios and its climatological corollaries. Journal of Geophysical Research: Atmospheres (1984–2012), 113, D05113.

Dansgaard, W., 1964. Stable isotopes in precipitation. Tellus, 16 (4), 436-468.

Demuro, M., Roberts, R.G., Froese, D.G., Arnold, L.J., Brock, F., Ramsey, C.B., 2008. Optically stimulated luminescence dating of single and multiple grains of quartz from perennially frozen loess in western Yukon Territory, Canada: comparison with radiocarbon chronologies for the late Pleistocene Dawson tephra. Quaternary Geochronology, 3 (4), 346-364.

Edwards, M.E., Barker Jr, E.D., 1994. Climate and vegetation in northeastern Alaska 18,000 yr BP–present. Palaeogeography, Palaeoclimatology, Palaeoecology, 109 (2), 127-135.

Ehlers, J., Gibbard, P.L., 2004. Developments in Quaternary Science: Quaternary Glaciations—Extent and Chronology, Part II: North America. Elsevier, Amsterdam.

Fraser, T.A., Burn, C.R., 1997. On the nature and origin of "muck" deposits in the Klondike area, Yukon Territory. Canadian Journal of Earth Sciences, 34 (10), 1333-1344.

French, H., 2011. Frozen sediments and previously-frozen sediments. Geological Society, London, Special Publications, 354 (1), 153-166.

Froese, D.G., Westgate, J.A., Preece, S.J., Storer, J., 2002. Age and significance of the late Pleistocene Dawson tephra in eastern Beringia. Quaternary Science Reviews, 21 (20), 2137-2142.

Froese, D.G., Westgate, J.A., Reyes, A.V., Enkin, R.J., Preece, S.J., 2008. Ancient permafrost and a future, warmer arctic. Science, 321 (5896), 1648.

Froese, D.G., Zazula, G.D., Westgate, J.A., Preece, S.J., Sanborn, P.T., Reyes, A.V., Pearce, N.J.G., 2009. The Klondike goldfields and Pleistocene environments of Beringia. GSA Today, 19 (8), 4-10.

Gaglioti, B.V., Barnes, B.M., Zazula, G.D., Beaudoin, A.B., Wooller, M.J., 2011. Late

Pleistocene paleoecology of arctic ground squirrel (*Urocitellus parryii*) caches and nests from Interior Alaska's mammoth steppe ecosystem, USA. Quaternary Research, 76 (3), 373-382.

Guthrie, R.D., 1990. Frozen fauna of the mammoth-steppe: The story of Blue Babe. The University of Chicago, Chicago, Illinois.

Guthrie, R.D., 2001. Origin and causes of the mammoth steppe: a story of cloud cover, woolly mammal tooth pits, buckles, and inside-out Beringia. Quaternary Science Reviews, 20 (1), 549-574.

Guthrie, R.D., 2006. New carbon dates link climatic change with human colonization and Pleistocene extinctions. Nature, 441 (7090), 207-209.

Jouzel, J., Alley, R.B., Cuffey, K.M., Dansgaard, W., Grootes, P., Hoffmann, G., Johnsen, S.J., Koster, R.D., Peel, D., Shuman, C.A., Stievenard, M., Stuiver, M., White, J., 1997. Validity of the temperature reconstruction from water isotopes in ice cores. Journal of Geophysical Research: Oceans (1978–2012), 102 (C12), 26471-26487.

Kotler, E., Burn, C.R., 2000. Cryostratigraphy of the Klondike “muck” deposits, west-central Yukon Territory. Canadian Journal of Earth Sciences, 37, 849–861.

Lowe, J.J., Rasmussen, S.O., Björck, S., Hoek, W.Z., Steffensen, J.P., Walker, M.J., Yu, Z.C., the INTIMATE group, 2008. Synchronisation of palaeoenvironmental events in the North Atlantic region during the Last Termination: a revised protocol recommended by the INTIMATE group. Quaternary Science Reviews, 27 (1), 6-17.

Lacelle, D., 2011. On the $\delta^{18}O$, δD and D-excess relations in meteoric precipitation and during equilibrium freezing: theoretical approach and field examples. Permafrost and Periglacial Processes, 22 (1), 13-25.

Mackay, J. R., 1972. The world of underground ice. Annals of the Association of American Geographers, 62 (1), 1-22.

McConnell, R.G., 1905. Report on the Klondike gold fields, in: Annual Report for 1901, vol. XIV, part B. Geological Survey of Canada Publication, 884, 1-71.

Meyer, H., Schönicke, L., Wand, U., Hubberten, H.W., Friedrichsen, H., 2000. Isotope studies of hydrogen and oxygen in ground ice – experiences with the equilibration technique. Isotopes in Environmental and Health Studies, 36 (2), 133-149.

Péwé, T. L., 1975. Quaternary geology of Alaska. US Government Printing Office.

Popp, S., Diekmann, B., Meyer, H., Siegert, C., Syromyatnikov, I., Hubberten, H.W., 2006. Palaeoclimate signals as inferred from stable-isotope composition of ground ice in the Verkhoyansk foreland, Central Yakutia. Permafrost and Periglacial Processes, 17 (2), 119-132.

PRISM Climate Group, Oregon State University, http://prism.oregonstate.edu, created February 2000.

Ritchie, J.C., 1984. Past and Present Vegetation of the Far Northwest of Canada. University of Toronto Press, Toronto, Ontario.

Schirrmeister, L., Siegert, C., Kuznetsova, T., Kuzmina, S., Andreev, A., Kienast, F., Meyer, H., Bobrov, A., 2002. Paleoenvironmental and paleoclimatic records from permafrost deposits in the Arctic region of Northern Siberia. Quaternary International, 89 (1), 97-118.

Schirrmeister, L., Froese, D.G., Tumskoy, V., Grosse, G., Wetterich, S., 2013. Yedoma: Late Pleistocene ice-rich syngenetic permafrost of Beringia, in: Elias, S.A. (Ed.), Encyclopedia of Quaternary Sciences, second ed. Elsevier, B.V., Amsterdam, pp. 542-552.

Schweger, C.E., 1997. Late Quaternary paleoecology of the Yukon: A review, in: Danks, H.V., Downes, J.A. (Eds.), Insects of the Yukon. Biological Survey of Canada, Ottawa, pp. 59-72.

Shapiro, B., Drummond, A.J., Rambaut, A., Wilson, M.C., Matheus, P.E., Sher, A.V., Pybus, O.G., Gilbert, M.T.P., Barnes, I., Binladen, J., Willerslev, E., Hansen, A.J., Baryshnikov, G.F., Burns, J.A., Davydov, S., Driver, J.C., Froese, D.G., Harington, C.R., Keddie, G., Kosintsev, P., Kunz, M.L., Martin, L.D., Stephenson, R.O., Storer, J., Tedford, R., Zimov, S., Cooper, A., 2004. Rise and fall of the Beringian steppe bison. Science, 306 (5701), 1561-1565.

Westgate, J.A., Stemper, B.A., Péwé, T.L., 1990. A 3 my record of Pliocene-Pleistocene loess in interior Alaska. Geology, 18 (9), 858-861.

Zanina, O.G., Gubin, S.V., Kuzmina, S.A., Maximovich, S.V., Lopatina, D.A., 2011. Late-Pleistocene (MIS 3-2) palaeoenvironments as recorded by sediments, palaeosols, and ground-squirrel nests at Duvanny Yar, Kolyma lowland, northeast Siberia. Quaternary Science Reviews, 30 (17), 2107-2123.

Zazula, G.D., Froese, D.G., Schweger, C.E., Mathewes, R.W., Beaudoin, A.B., Telka, A.M., Harington, C.R., Westgate, J.A., 2003. Palaeobotany: Ice-age steppe vegetation in east Beringia. Nature, 423 (6940), 603.

Zazula, G.D., Froese, D.G., Westgate, J.A., La Farge, C., Mathewes, R.W., 2005. Paleoecology of Beringian "packrat" middens from central Yukon Territory, Canada. Quaternary Research, 63, 189–198.

Zazula, G.D., Froese, D.G., Elias, S.A., Kuzmina, S., La Farge, C., Reyes, A.V., Sanborn, P.T., Schweger, C.E., Scott Smith, C.A., Mathewes, R.W., 2006. Vegetation buried under Dawson tephra (25,300 ^{14}C years BP) and locally diverse late Pleistocene paleoenvironments of Goldbottom Creek, Yukon, Canada. Palaeogeography, Palaeoclimatology, Palaeoecology, 242 (3-4), 253-286.

Zazula, G.D., Froese, D.G., Elias, S.A., Kuzmina, S., Mathewes, R.W., 2007. Arctic ground squirrels of the mammoth-steppe: paleoecology of Late Pleistocene middens (~ 24,000–29,450 ^{14}C yr BP), Yukon Territory, Canada. Quaternary Science Reviews, 26 (7), 979-1003.

Chapter 2: Methods

The geochemical, geochronological, and cryostratigraphical characterization of perennially frozen sediments (permafrost) is important to understanding their origins and paleoclimatic significance. The focus of this thesis is to develop a long-term multi-proxy record that includes lithostratigraphy, cryostratigraphy, water isotopes, vegetation, and various paleoecological indicators (*e.g.* presence of arctic ground squirrel nests, carbon and nitrogen abundance, and large mammal fossils).

This chapter is organized into sections that detail the methods for each component of this study. These descriptions outline the stratigraphy, radiocarbon dating, carbon and nitrogen totals, dissolved organic carbon content, and water isotopes. The water isotope section includes a study into the effectiveness of absorption spectrometry for permafrost waters.

Stratigraphy

Multiple permafrost samples were recovered from each of the eight sites with photos, sketches, and observations. The location of sites were recorded with a handheld GPS, while elevations for samples were measured via a laser range finder (Lasertech 200XL) with 0.1 m vertical precision; given challenges with operator position and target accuracy, I estimate vertical accuracy to 0.5 m. The record of each exposure consists of overall site characteristics, unit descriptions, and the type and abundance of ground ice.

The categorization of ground ice in permafrost is an important tool for understanding the source waters and processes during freezing (Mackay, 1972). The common forms of ground ice are pore, segregated, aggradational, thermokarst-cave, pool, vein, and wedge ice. Pore ice is found in permafrost that has an absence of excess ice and consists of waters that have filled the voids between grains at the time of freezing. Segregated ice is the result of water migration due to negative pressure at the freezing front, resulting in an ice lens that exceeds the pore space (French, 2007). Aggradational ice is formed in layers at the base of the active layer in syngenetic permafrost (Mackay, 1972). Thermokarst-cave ice and pool ice forms as massive ice bodies from the freezing of pools of water and in underground cavities in permafrost made by running water (Mackay, 1997; Kanevskiy et al., 2011). Vein ice forms from the infilling of thermal contraction cracks by windblown snow and/or snowmelt (French and Shur, 2010). Repeated cracking and infilling results in ice wedges, which can range from several cm to several m wide and have syngenetic, epigenetic, or anti-syngenetic histories (Mackay, 1995).

An understanding of ice structure and abundance can provide information on the conditions during formation and the history of the permafrost (French and Shur, 2010; French, 2011). Cryostratigraphy is used to define these relations and is similar to sedimentology, but includes the structure and distribution of ice within frozen sediments. Cryostratigraphy is a broad term that encompasses several aspects of geocryology. This includes identification of ice bodies, contacts between units, and details regarding the nature of the ice and sediment. The relations between ice and sediment are defined by the cryotextures, cryostructures, and cryofacies. More information about these three elements are presented below.

Cryotextures describe microscopic features, such as grain and ice crystal size and shape, and the contacts between them (Murton and French, 1994). Cryotextures were not included as a part of this study.

Cryostructures describe the macroscopic features of the ice and sediment. The shape and distribution of ice depends on the amount of water in the sediment prior to freezing, sediment grain size distribution, and the rate of freezing, which largely controls the extent of moisture migration during freezing (French, 2011). Certain cryostructures are considered to indicate freezing histories that were either syngenetic (forming at or near the same time as sediment deposition) or epigenetic (forming some time after sediments were deposited) (Mackay, 1974; Murton and French, 1994; Shur et al., 2004; Bray et al., 2006; French and Shur, 2010; French, 2011). Cryostructures in permafrost are most simply and concisely defined by Murton and French (1994) and are divided into six categories: lenticular, layered, reticulate, structureless, crustal, and suspended (Figure 2-1). If the ice is generally less than 0.5 mm thick, the prefix micro- may be added (*e.g.* microlenticular, microlayered, *etc.*) (French and Shur, 2010). Layered and lenticular cryostructures are generally thought to be associated with syngenetic permafrost, while reticulate may typically reflect an epigenetic history (Shur et al., 2004; Bray et al., 2006).

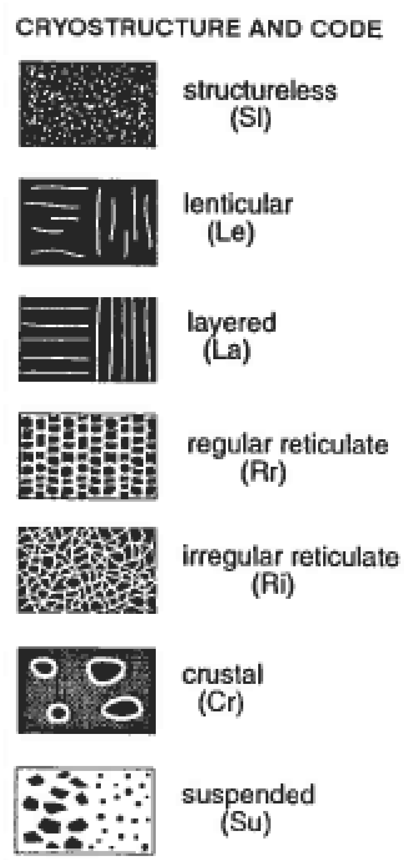

Figure 2-1 : Diagram illustrating the basic cryostructures in permafrost (adapted from Murton and French, 1994). The ice is white and sediment is black in this figure.

Structureless, also known as massive or pore ice, is the term used when no excess ice is visible. Several studies have suggested that structureless permafrost indicates an epigenetic history (*e.g.* Bray et al., 2006), however Ping et al. (2008) found it in the upper permafrost of well-drained sites in the North American arctic. Structureless, or pore, ice is present in many syngenetic samples in this study.

A lenticular structure refers to discontinuous lenses of ice of any orientation. Lenticular, as well as layered, ice can be characterized as parallel or non-parallel structures that are planar, wavy, or curved (Figure 2-2) (French and Shur, 2010). Lenticular ice is thought to form in syngenetic deposits when water migrates to freezing fronts through cryosuction and results in excess ice (French, 2007). Microlenticular is one of the most common forms found in this study and likely reflects rapid sedimentation (Figure 2-3).

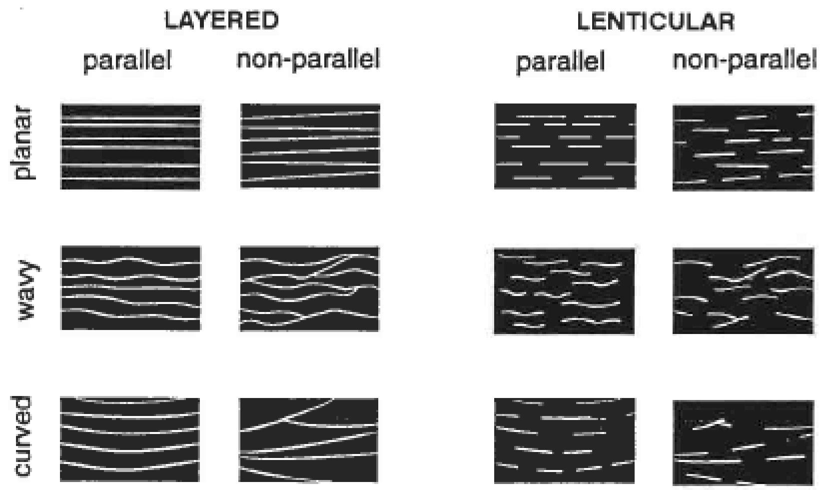

Figure 2-2 : Classification scheme denoting the relations between layered and lenticular ice to create comprehensive descriptions of cryostructures (adapted from Murton and French, 1994).

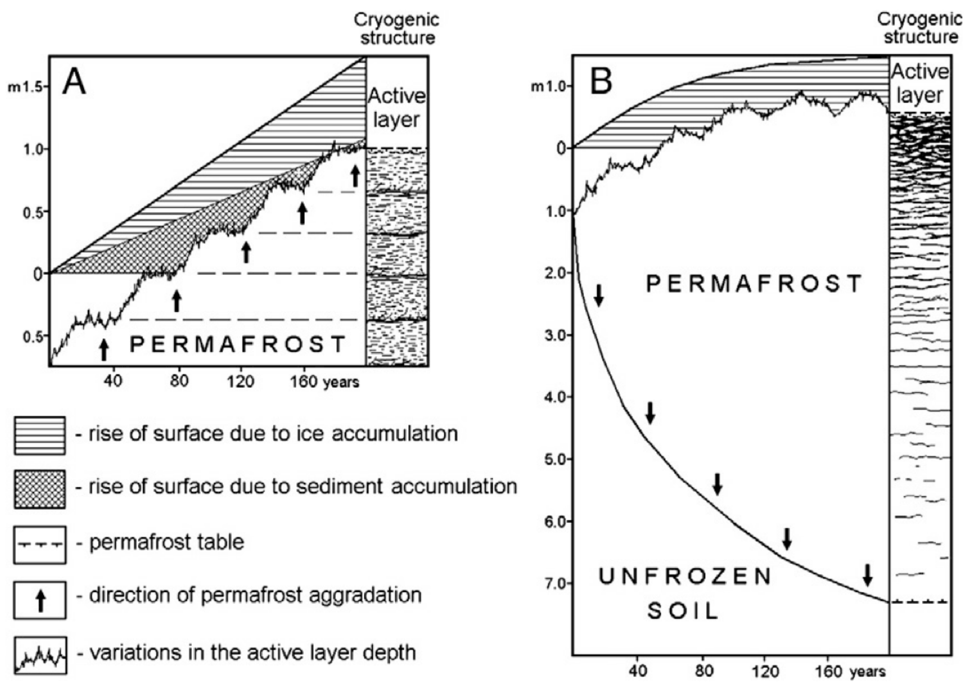

Figure 2-3: Relation of (a) syngenetic and (b) epigenetic permafrost and their respective cryogenic structures over time (from French and Shur, 2010).

Layered ice consists of bands of continuous ice that can have any orientation. Layered ice is thought to form in syngenetic deposits when water migrates to freezing front and results in excess ice (Murton and French, 1994).

Reticulate ice is a three-dimensional net-like structure that can be regular (uniform) or irregular (non-uniform) (Murton and French, 1994). It is thought be the result of the desiccation and shrinkage of sediments, and therefore suggests an epigenetic origin. Reticular-chaotic is an additional descriptor, which consists of randomly oriented ice lenses (Bray et al., 2006).

Crustal ice forms around frost-susceptible material in the permafrost, such as wood fragments or rock clasts (Murton and French, 1994). This is an uncommon structure that was only found in one sample in this study.

Suspended, or ataxitic, cryostructure denotes that grains or blocks of sediment are suspended in a matrix of ice. This is most common in ice bodies or just below the top of permafrost (Murton and French, 1994).

Cryofacies are defined by the nature and abundance of ice found within sediment (French and Shur, 2010). The following cryofacies have been defined based on volumetric ice by Murton and French (1994): pure ice, sediment-poor ice (> 75% ice), sediment-rich ice (75 – 50% ice), ice-rich sediment (50 – 25% ice), and ice-poor sediment (< 25% ice). Cryofacies may be subdivided based on cryostructure (Murton and French, 1994). A distinct cryostratigraphic unit comprised of associated cryofacies can be grouped to form a cryofacies assemblage (Murton and French, 1994; French and Shur, 2010).

Volumetric ice contents of 18 pore ice samples were determined at the University of Alberta. To do this, water displacement was measured when the frozen samples were immersed briefly in cold water. The mass of the samples were noted before immersion into the water and then after the sample was subsequently dried in an oven. Volumetric ice content (VIC) is reported as a percent of the total volume, where:

$$VIC\ (\%) = \frac{(M_t - M_d)\times 0.9167}{V_t}\times 100$$

In which M_t is the total frozen mass of the sample, M_d is the total dry mass, V_t is the total frozen volume, and 0.9167 g/cm^3 is the density of ice. The number of samples analyzed using this technique was a small percentage of the total samples. For the remaining samples, we estimated which cryofacies the samples fit into based on the amount of visible ground ice.

Radiocarbon dating

In order to understand the chronology of Klondike permafrost exposures, this study utilizes 85 radiocarbon dates (^{14}C yrs BP) of organic material. ^{14}C is produced in the upper atmosphere and incorporated into the biological structures of organisms through uptake of CO_2 while the organism is alive (*e.g.* bones, leaves, *etc.*). Once an organism dies, it ceases to exchange carbon with the environment, preserving the atmospheric ^{14}C/^{12}C ratio and allowing organics up to *ca.* 50,000 cal yrs BP to be precisely dated.

^{14}C atoms decay at a steady rate, with a half-life of 5,730 years. By measuring the relative abundance of radioactive ^{14}C atoms to the stable ^{12}C atoms, the age of organic samples can be determined up to approximately 10 half-lifes, or *ca.* 53,000 ^{14}C yrs BP. Radiocarbon dates up to 43,200 ^{14}C years BP (*ca.* 46,800 cal yrs BP) are included in this study from woody macrofossils, grass rootlets, ground squirrel nesting material, and fecal pellets. This age range was selected since samples to *ca.* 43,000 ^{14}C years have good reproducibility in our experience even at relatively low sample masses.

Organic samples require pre-treatment for ^{14}C dating to remove contamination. For pre-treatment, samples were placed in sterilized glass culture tubes and underwent an acid-base-acid (ABA) wash. This consisted of heating samples to 70°C and soaking them for 30 minutes in 1M HCl, followed by 60 minute washes of 1M NaOH until the solution was clear, and finally a 30 minute 1M HCl wash. Samples were then rinsed with ultrapure water until neutral and freeze-dried. Prepared samples were shipped to the W.M. Keck Carbon Cycle Accelerator Mass Spectrometer facility at the University of California, Irvine for combustion, graphitization, and measurement of ^{14}C activity by AMS.

Organic samples were grouped into batches of 12 samples during the preparatory steps, which included 1 – 2 standards and at least one non-finite 'blank' (Table 2-1). Standards were matched as closely as possible in terms of their estimated age and type of material to the samples to be dated.

Table 2-1: Laboratory standards for radiocarbon analyses.

Standards	Age (^{14}C BP)	Material	Reference
FIRI-D	4,510	Wood shavings	Boaretto et al., 2002
FIRI-F	4,510	Wood shavings	Boaretto et al., 2002
IAEA C5	11,800	Wood powder	Rozanski et al., 1992
QUEETS-A	Non-finite	Wood shavings	J. Southon 2014, *pers. comm.*
AVR07-PAL	Non-finite, last interglacial (MIS 5e)	Wood shavings	Reyes et al., 2010

Radiocarbon dates need to be calibrated to calendar years, as the amount of ^{14}C produced in the atmosphere is known to have fluctuated over the last 60,000 years, requiring "^{14}C years" to be adjusted via the 'IntCal13' calibration curve (Reimer et al., 2013). Ages were calibrated using OxCal Online and reported as calendar years before present (cal yrs BP), with "Before Present" being defined as before 1950 AD (Bronk Ramsey, 2009).

Total carbon, total nitrogen, and dissolved organic carbon content

Total carbon and nitrogen analyses of Klondike soils were preformed at the University of Alberta. Samples were extracted with water, filtered, and analyzed using a Shimadzu TOC-V/TN instrument. Dissolved organic carbon (DOC) contents of permafrost pore waters were determined by the Biogeochemical Laboratory at the University of Alberta.

Water isotopes and laser absorption spectrometry (LAS)

Frozen samples were collected after cleaning the surface of the exposure by removing a small hand sample with an ice axe, or by drilling either horizontal or vertical cores. Horizontal samples were taken using a small hand drill with a core barrel 8 cm in diameter and 40 cm long. Vertical drill cores up to ~6 m were recovered at sites using a light, portable drill similar to that in Calmels et al. (2005) (Figure 2-4). Vertical core samples were drilled with a 10 cm wide and 40 cm long core barrel. All samples were placed in plastic bags after sampling and kept frozen until subsampling.

Figure 2-4 : The permafrost drilling process, beginning with coring (left), core catching (top right), and the retrieval of the permafrost core (bottom right).

In order to prepare the samples for water isotope ($\delta^2H/\delta^{18}O$) analysis, the pore, ice wedge and segregated ground ice subsamples were placed in re-sealable zipper storage bags that were vacuum packed and placed in a refrigerator to thaw. Pore waters were extracted with a syringe and injected into 2 ml glass vials through a 0.2 micron filter. Extraction was either done directly from the plastic bag or, more frequently, after centrifuging the samples for several minutes to separate the water from the sediment.

Traditionally, isotope-ratio mass spectroscopy (IRMS) has been the only reliable method to measure the isotopic ratios ($^{18}O/^{16}O$ and $^2H/^1H$) of water samples. This method utilizes physical separation of molecules based on mass and quantifies the relative abundance of the isotopes. Modern techniques have been developed over the last few decades however that use laser absorption spectrometry (LAS), which measures the interaction of matter and radiated energy to quantify the isotopic ratios of atoms.

Paldus and Kachanov (2005) describe LAS as the measurement of transmitted light (*i.e.* light that passes through a substance) as a function of wavelength to quantify changes in transmitted light intensity caused by absorbing molecules. To measure the isotopic ratios, a detector measures the voltage of the laser, which fluctuates due to interferences from water molecules in the optical cavity. Measurements of interference at specific wavelengths are related to the molar ratios of $^{18}O/^{16}O$ and $^{2}H/^{1}H$, which are measured simultaneously (Figure 2-5).

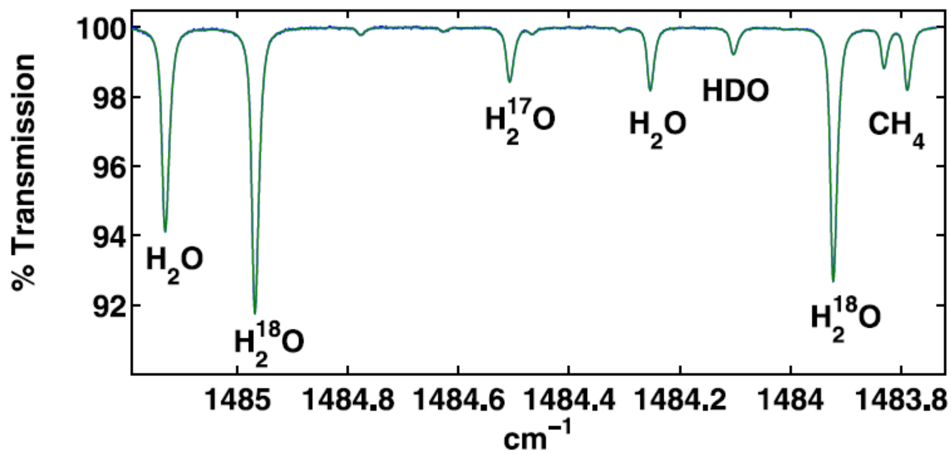

Figure 2-5: Example of simultaneous δ^2H and $\delta^{18}O$ measurement by relating transmissivity of molecules at specific wavelengths (adapted from Moyer et al., 2008).

Isotopic ratios are reported in δ-notation in parts per thousand (‰), where:

$$\delta = \left(\frac{R_{sample}}{R_{standard}} - 1\right) \times 1000\ ‰$$

In which R_{sample} is the molar ratio (*e.g.* H^2/H^1) of a specific sample, and $R_{standard}$ is the molar ratio of Vienna Standard Mean Ocean Water (VSMOW). Two LAS instruments were used in this study. The majority of samples were measured via off-axis integrated-cavity output spectroscopy (OA-ICOS) using a Los Gatos Research (LGR) model DLT-100 (Figure 2-6). The second technique, used for the majority of samples at the Lucky Lady II site, uses continuous-wave cavity ring-down spectroscopy (CW-CRDS) in a Picarro model L2130-i (Figure 2-7). These methods are very accurate in part due to a long path length that is achieved by reflecting the light between high-reflectivity mirrors many times in the optical cavity, effectively creating transmitted light that has interacted with water molecules over a path thousands of meters long. Both of these LAS methods have been shown to be as or more reliable than IRMS (Kerstel and Gianfrani, 2008; Lis et al., 2008; Wassenaar et al., 2008; Gupta et al., 2009; Wassenaar et al., 2012).

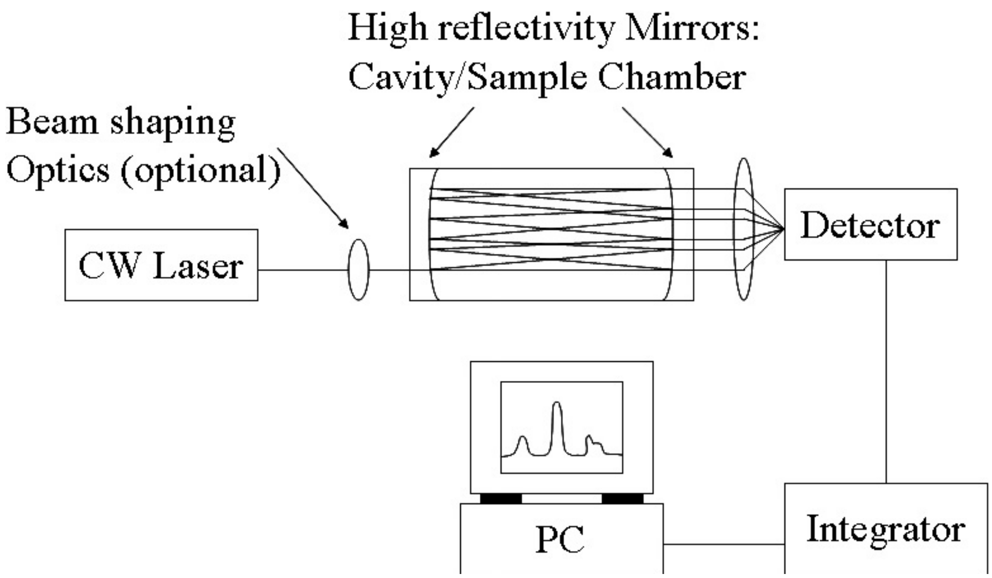

Figure 2-6: Typical OA-ICOS setup (from Paldus and Kachanov, 2005).

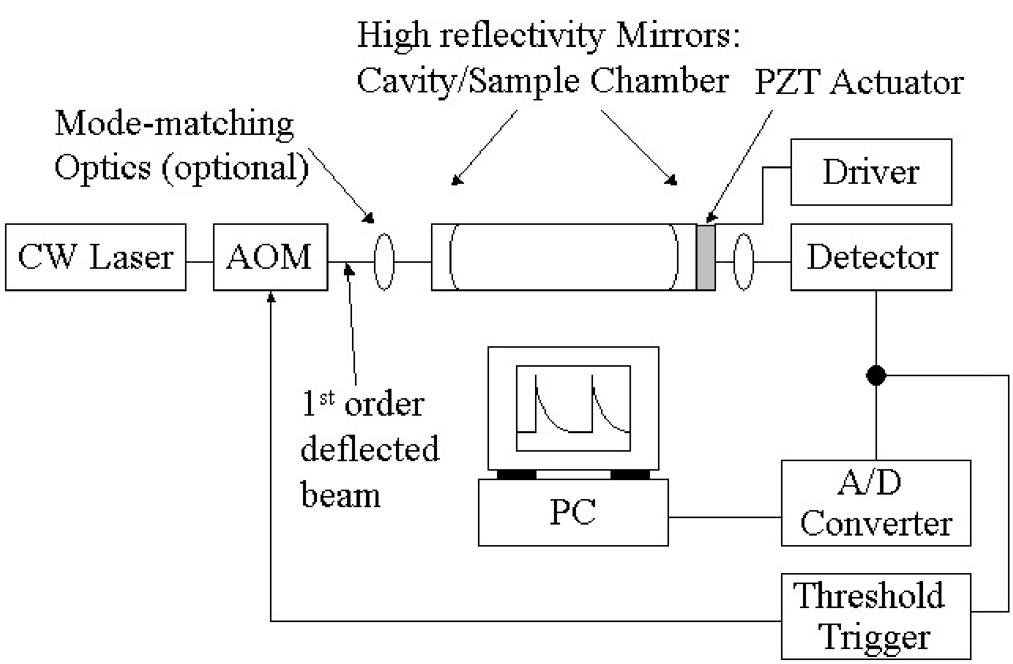

Figure 2-7: Typical CW-CRDS setup (from Paldus and Kachanov, 2005).

The LGR is set up to analyze 10 – 30 unknown samples per ‘run’. Throughout each run, 2 – 5 unknown samples are grouped together between an enriched and a depleted standard. The difference in the measured isotopic ratio relative to the known isotopic ratio of the depleted and enriched standards on either side of each group allows for normalization of the unknown samples in between. At least three Quality Control (QC) standards with known isotopic ratios are included in each run, placed within groups of unknowns, to verify the accuracy of the measurement and data normalization. Calibration standards included in this study are outlined in Table 2-2.

Table 2-2 : Water isotope standards used in this study.

Standard	δ^2H (‰)	δ^{18}O (‰)	Reference
USGS45	-10.3	-2.24	U.S. Geological Survey, 2012a
Vancouver Ocean Water	-24.4	-3.43	A. Kwan 2011, *pers. comm.*
Evian	-73.7	-10.29	Chesson et al., 2010
USGS46	-235.8	-29.80	U.S. Geological Survey, 2012b
LW2	-271.8	-33.94	A. Kwan 2011, *pers. comm.*

The Picarro analyzes three standards at the beginning of the run with varying isotopic ratios spanning the range of the unknowns. This determines a linear relationship in which to correct unknown values based on their isotopic values. One to three Evian water QC standards are placed throughout the run to assure the accuracy of the measurements and corrections.

The Biogeochemical Analytical Service Laboratory at the University of Alberta uses the same LGR, which accepts all QC values at or below ±1.6‰ δ^2H and ±0.3‰ δ^{18}O deviation from the known value. Values outside this range are individually inspected and either accepted or re-run. The primary QC for this study is Evian bottled water, which was analyzed by Chesson et al. (2010) many times (n=4400) and shown to have a 1σ error of 1.7‰ δ^2H and 0.21‰ δ^{18}O. The standard deviation for all QC samples in this study was ±0.6‰ δ^2H and ±0.17‰ δ^{18}O, with maximum accepted values of ±2.6‰ δ^2H and ±0.74‰ δ^{18}O (see Chapter 4). The isotopic ratios for water molecules are based on the average of multiple injections for each sample, the details of which are explained in the following section.

LAS measurements and results

LAS measurements are sensitive to minute changes between injections, such as the number of water molecules in the optical cavity. This requires scrutiny and an understanding of the measurements from each injection to get the most accurate results.

Injection volume

One of the most significant factors influencing LAS analysis is the volume of each injection. Injection volumes may change significantly due to degradation of the syringe or septa. Fluctuating injection volumes can be minimized from routine procedures, including regular cleaning of syringes and replacement of septa after ~500 injections. It is critical that injection volumes are consistent between the standards and unknowns because the unknown samples are calibrated to the measured standard. Injection volumes are deemed acceptable if they are within 1.5 standard deviations (1.5σ) of the average for the entire run, with injections outside this range being inspected and typically discarded.

Memory effect

Isotopic ratios are measured by taking the average value of a series of injections for each sample (6 – 9 injections/sample). The first few injections for each sample can be problematic however because remnants of the previous sample are typically present in small quantities (Figure 2-8). This occurs when water molecules from previous injections are not completely evacuated from the system and become incorporated into the subsequent measurement. This is known as the memory effect and it can have a significant influence on the isotopic ratios of the first few injections of a sample, especially if there is a large isotopic difference between the previous sample, which regularly occurs in permafrost studies (Lis et al., 2008). After 2 – 3 injections this effect is negligible, therefore we use the average of injections 4 – 6 to determine the isotopic ratio of the sample.

The previously mentioned factors are a reflection of the variability of the instrument when analyzing pure water samples, but additional considerations may need to be taken when analyzing waters containing impurities, as they may cause additional laser interference. Permafrost pore waters can range from clear to a dark yellow, suggesting these may include impurities. This has prompted a study into the effectiveness of LAS for measuring permafrost pore water isotopes, which was performed by comparing results from LAS (LGR and Picarro) and IRMS, the details of which are presented in the following section.

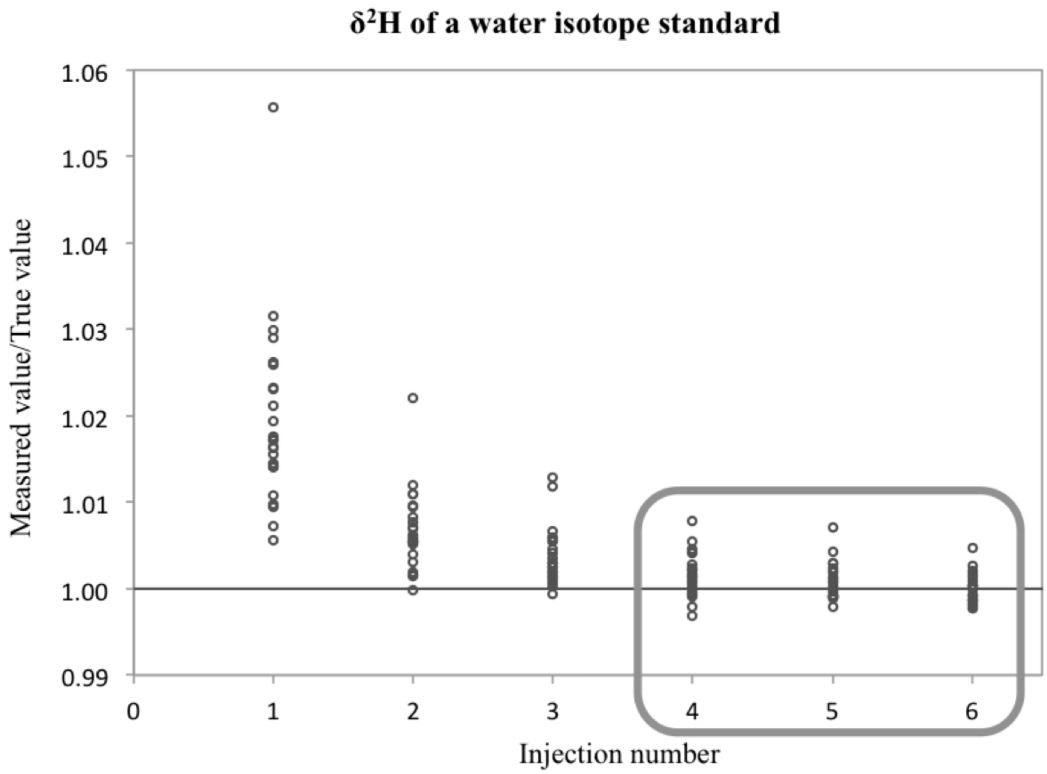

Figure 2-8: Example of memory effect on δ^2H measurements from series of injections on the LGR of a laboratory standard. In this study we excluded the first three injections to avoid the memory effect.

Effectiveness of LAS for measuring Klondike permafrost isotopes (δ^2H/δ^{18}O)

Absorption spectroscopy is a quick and effective method for measuring water isotopes, however some compounds can be vaporized along with water that will negatively affect measurements. If there are a significant number of molecules that absorb photons at similar wavelengths as water they may skew the isotopic results. This is due to the fact that the area under the curve would have a double peak, one for the water, and another for the interfering molecules (Hendry et al., 2011). For example, Schultz et al. (2011) recorded LAS interferences from leaf waters that affected isotopic ratios up to 9.3‰ for δ^{18}O and 15.7‰ for

δ^2H. This offset occurred because waters extracted directly from plants contain large numbers of dissolved organic carbon (DOC) molecules, typically in the form of short-chain alcohols, which effect the transmissivity of the laser beam at important frequencies. Associated soil water in the Schultz et al. (2011) study did not have measureable interference.

While interfering DOC molecules, such as methane, methanol and ethanol have been shown to have strong optical absorption that interfere with $\delta^2H/\delta^{18}O$ analyses, the DOCs in runoff, such as humic acid, do not cause measurable interference (Brand et al., 2009; Hendry et al., 2011). Technical support at Picarro informed me that this is because larger molecules which contain –OH groups will have much weaker absorption than small alcohols, and these absorptions are so broad they are detected as a very weak offset (~0.1% increase in the background absorption) (D. Vu 2011, *pers. comm.*). Permafrost pore and wedge ice is essentially a paleoarchive of soil and run off waters, and therefore should not contain significant amounts of problematic compounds.

While previous studies have focused on soil and runoff waters to study spectral interferences with laser absorption spectrometry (*e.g.* West et al., 2010; Schultz et al., 2011), no studies have focused specifically on investigating permafrost waters. The following sections present a study into the effectiveness of LAS for permafrost waters in order to assess the accuracy of these analyses.

Methods

Water samples for this study were selected to have a wide range of colour (clear to dark yellow) (Figure 2-9). We obtained DOC values for all samples in order to test the relationship between colour, DOC, and any significant deviation between IRMS and LAS results. Waters from 10 samples were sent to the Center for Stable Isotope Biogeochemistry at the University of California (Berkley) for IRMS. Hydrogen isotopes were measured using a ThermoFinnigan H/Device connected to a Delta Plus mass spectrometer. Oxygen isotopes were measured using a ThermoFinnigan GasBench II connected to a Delta Plus XL mass spectrometer. In addition to 10 unknown samples, 4 standards were assigned random sample numbers and included in the batch as a secondary QC check. All samples were calibrated with USGS45 and USGS46.

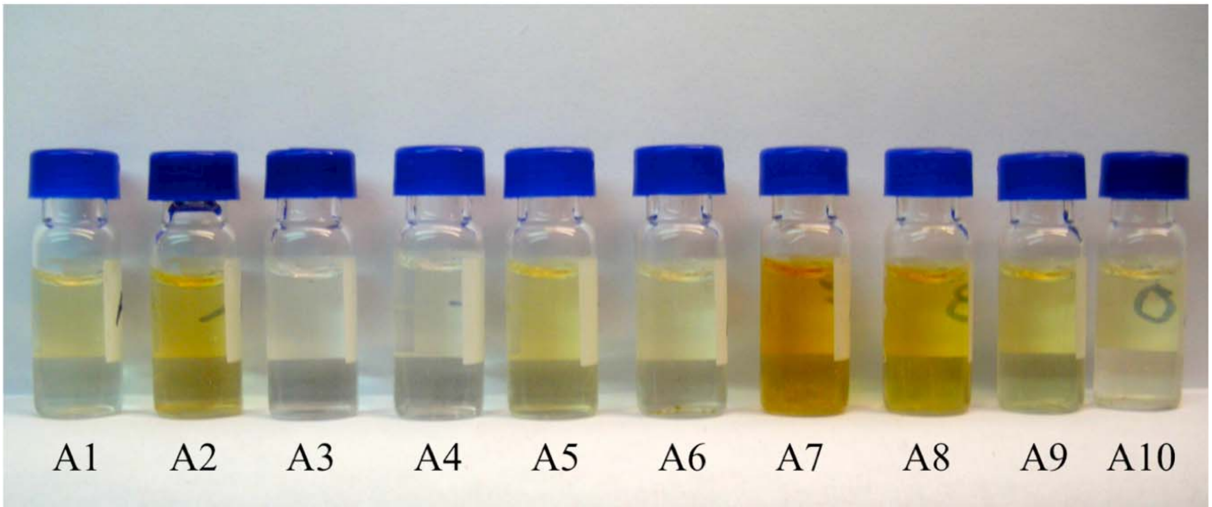

Figure 2-9 : Varying colours of the unknown permafrost water samples.

Results

The four standards that were sent for IRMS analysis were in excellent agreement with the known values (1σ = ±0.3‰ δ^2H; ±0.14‰ δ^{18}O) (Table 2-3). This gives us a high degree of confidence in the 10 unknown permafrost waters, which were in excellent agreement between the two methods (1σ = ±0.6‰ δ^2H; ±0.11‰ δ^{18}O) (Figure 2-10, 2-11). The DOC contents of the unknown samples ranged from 12.1 to 1,648.0 C mg/L, with no apparent correlation between DOC content and relative deviation between the LGR and IRMS results (Table 2-4, Figure 2-12).

Table 2-3 : Deviation from reported values for three water isotope standards submitted as unknowns for IRMS analysis. LW2 standard submitted twice as separate unknown samples.

Standards	δ^{18}O (‰)	δ^2H (‰)	d-excess
USGS 46	0.12	0.0	0.9
Evian	0.05	0.6	0.2
LW2 (1)	0.35	0.5	-2.3
LW2 (2)	0.26	0.5	-1.6

Table 2-4 : Deviation of 10 unknown Klondike permafrost samples (A1 – A10) analyzed via LAS (LGR and Picarro) and IRMS, reported as absolute values. DOC contents are included.

		LGR vs. IRMS			Picarro vs. IRMS		
	D.O.C. C mg/L	δ^2H difference	$\delta^{18}O$ difference	d-excess difference	δ^2H difference	$\delta^{18}O$ difference	d-excess difference
A1	202.6	1.7	0.19	3.2	3.6	0.07	3.1
A2	424.1	0.0	0.15	1.2	2.0	0.01	2.0
A3	12.1	1.0	0.14	2.1	1.7	0.04	1.4
A4	19.9	0.2	0.24	1.7	1.2	0.05	0.9
A5	144.6	0.7	0.03	0.9	1.4	0.02	1.5
A6	55.8	0.3	0.15	0.9	1.1	0.02	1.3
A7	1,648.0	0.9	0.05	0.5	3.0	0.06	2.5
A8	1,323.0	0.3	0.09	0.4	2.5	0.03	2.2
A9	995.7	0.3	0.01	0.4	1.3	0.05	1.7
A10	183.0	0.4	0.04	0.1	1.8	0.03	1.5

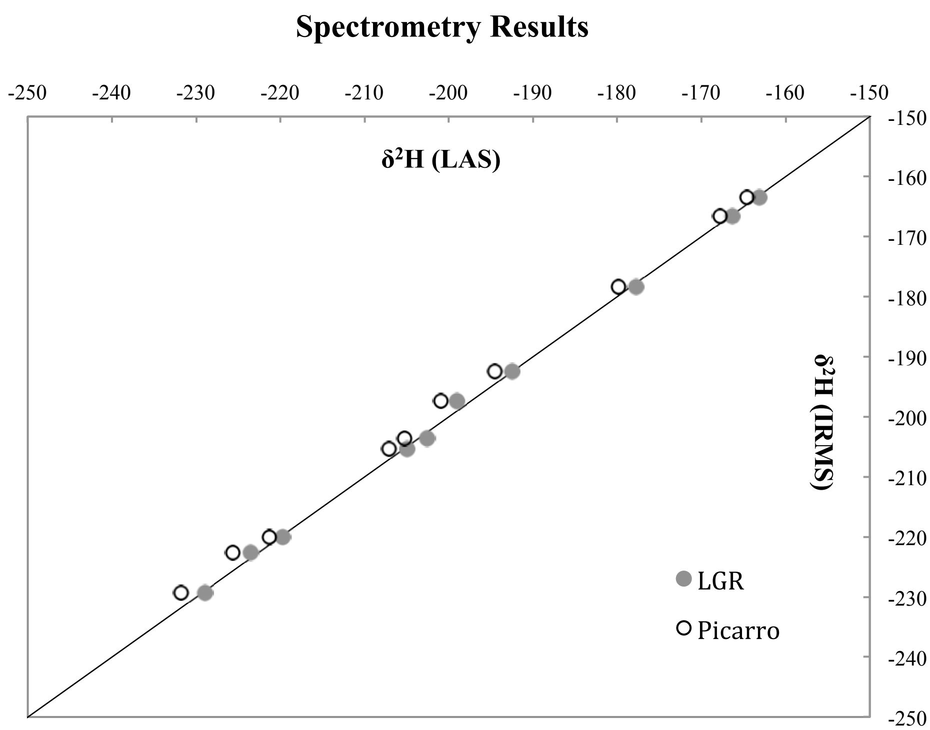

Figure 2-10 : δ^2H results for 10 unknown permafrost waters analyzed via LAS and IRMS.

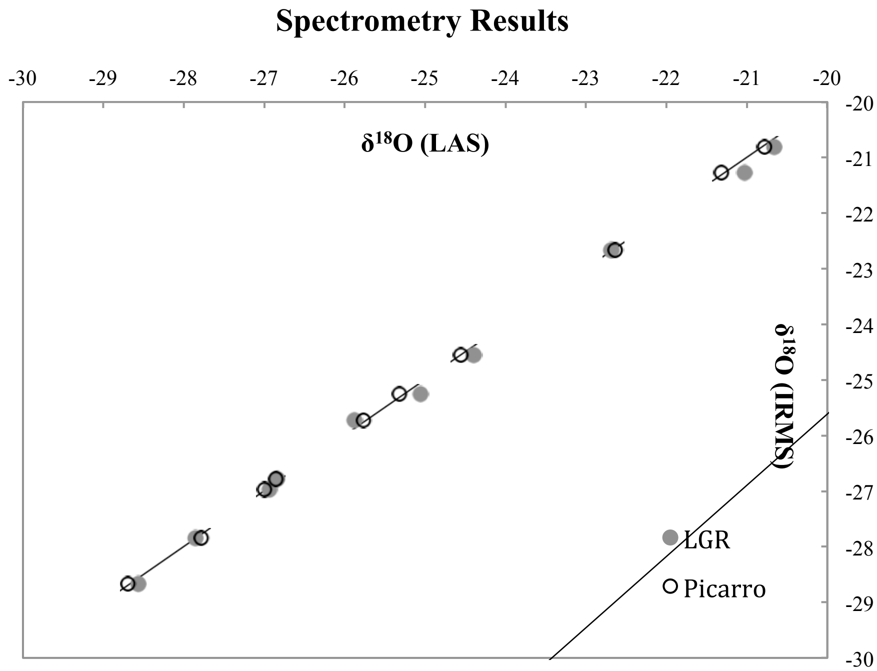

Figure 2-11 : $\delta^{18}O$ results for 10 unknown permafrost waters analyzed via LAS and IRMS.

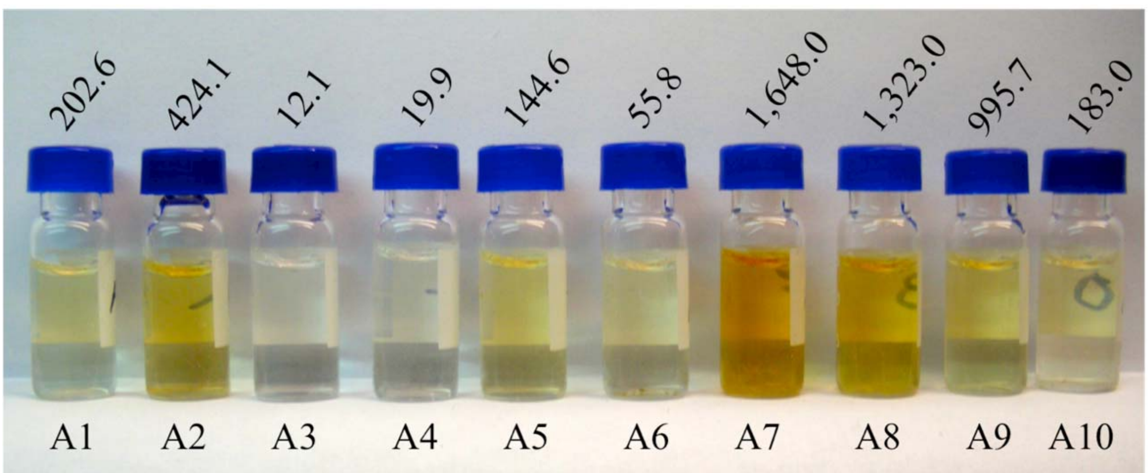

Figure 2-12 : Permafrost waters from 10 samples and DOC concentrations (C mg/L).

Discussion and conclusions

The isotopic results of the two spectroscopic methods are in excellent agreement across a large range of isotopic values, regardless of permafrost water colour or DOC content. There is a systematic offset between the two LAS techniques and IRMS, with the LGR being in better agreement with δ^2H and the Picarro in better agreement with δ^{18}O. This may be due to a number of factors during the measurement and normalization of the isotopic values, however these factors do not significantly affect the results for this study. The close correlation between these methods gives a high degree confidence that LAS is an effective alternative to IRMS for permafrost water analyses and yields a firm estimate of the errors involved in the remaining parts of this thesis. Based on these results, there do not appear to be significant amounts of problematic DOCs in Klondike pore and wedge ice. Future identification of DOC species in permafrost waters could determine if spectral interferences are just insignificant or nonexistent.

References

Boaretto, E., Bryant, C., Carmi, I., Cook, G., Gulliksen, S., Harkness, D., Heinemeier, J., McClure, J., McGee, E., Naysmith, P., Possnert, G., Scott, M., van der Plicht, H., van Strydonck, M., 2002. Summary findings of the fourth international radiocarbon intercomparison (FIRI) (1998-2001). Journal of Quaternary Science, 17, 633-637.

Brand, W.A., Geilmann, H., Crosson, E.R., Rella, C.W., 2009. Cavity ring-down spectroscopy versus high-temperature conversion isotope ratio mass spectrometry; a case study on δ^2H and δ^{18}O of pure water samples and alcohol/water mixtures. Rapid Communications in Mass Spectrometry, 23 (12), 1879-1884.

Bray, M.T., French, H.M., Shur, Y., 2006. Further cryogenic investigations in the CRREL permafrost tunnel, Fox, Alaska. Permafrost and Periglacial Processes, 17, 233-243.

Bronk Ramsey, C., 2009. Bayesian analysis of radiocarbon dates. Radiocarbon, 51 (1), 337-360. Oxcal Version 4.2, http://c14.arch.ox.ac.uk/oxcal.html.

Calmels, F., Gagnon, O., Allard, M., 2005. A portable Earth-drill system for permafrost studies. Permafrost and Periglacial Processes, 16 (3), 311-315.

Chesson, L.A., Bowen, G.J., Ehleringer, J.R., 2010. Analysis of the hydrogen and oxygen stable isotope ratios of beverage waters without prior water extraction using isotope ratio infrared spectroscopy. Rapid Communications in Mass Spectrometry, 24, 3205-3213.

French, H.M., 2007. The Periglacial Environment, 3rd edition. John Wiley and Sons Ltd., Chichester, UK, 458 p.

French, H.M., 2011. Frozen sediments and previously-frozen sediments. Geological Society, London, Special Publications, 354, 153-166.

French, H.M., Shur, Y., 2010. The principles of cryostratigraphy. Earth Science Reviews, 101, 190-206.

Gupta, P., Noone, D., Galewsky, J., Sweeny, C., Vaughn, B.H., 2009. Demonstration of high-precision continuous measurements of water vapor isotopologues in laboratory and remote field deployments using wavelength-scanned cavity ring-down spectroscopy (WS-CRDS) technology. Rapid Communications in Mass Spectrometry, 23 (16), 2534-42.

Hendry, M.J., Richman, B., Wassenaar, L.I., 2011. Correcting for methane interferences on δ^2H and $\delta^{18}O$ measurements in pore water using $H_2O_{(liquid)}$-$H_2O_{(vapor)}$ equilibration laser spectroscopy. Analytical Chemistry, 83 (14), 5789-5796.

Kanevskiy, M., Shur, Y., Fortier, D., Jorgenson, M.T., Stephani, E., 2011. Cryostratigraphy of late Pleistocene syngenetic permafrost (yedoma) in northern Alaska, Itkillik River exposure. Quaternary Research, 75 (3), 584-596.

Kerstel, E., Gianfrani, L., 2008. Advances in laser-based isotope ratio measurements: selected applications. Applied Physics B, 92, 439-449.

Lis, G., Wassenaar, L.I., Hendry, M.J., 2008. High-precision laser spectroscopy D/H and $^{18}O/^{16}O$ measurements of microliter natural water samples. Analytical Chemistry, 80 (1), 287-293.

Mackay, J.R., 1972. The world of underground ice. Annals of the Association of American Geographers, 62 (1), 1-22.

Mackay, J.R., 1974. Reticulate ice veins in permafrost, Northern Canada. Canadian Geotechnical Journal, 11 (2), 230-237.

Mackay, J.R., 1995. Ice wedges on hillslopes and landform evolution in the late Quaternary, western Arctic coast, Canada. Canadian Journal of Earth Sciences, 32 (8), 1093-1105.

Mackay, J.R., 1997. A full-scale field experiment (1978-1995) on the growth of permafrost by means of lake drainage, western Arctic coast: A discussion of the method and some results. Canadian Journal of Earth Sciences, 34 (1), 17-33.

Moyer, E.J., Sayres, D.S., Engel, G.S., Clair, J.S., Keutsch, F.N., Allen, N.T., Kroll, J.H., Anderson, J.G., 2008. Design considerations in high-sensitivity off-axis integrated cavity output spectroscopy. Applied Physics B, 92 (3), 467-474.

Murton, J.B., French, H.M., 1994. Cryostructures in permafrost, Tuktoyaktuk coastlands, western Arctic Canada. Canadian Journal of Earth Sciences, 31, 737-747.

Paldus, B.A., Kachanov, A.A., 2005. An historical overview of cavity-enhanced methods. Canadian Journal of Physics, 83 (10), 975-999.

Ping, C.L., Michaelson, G.J., Kimble, J.M., Romanovsky, V.E., Shur, Y.L., Swanson, D.K., Walker, D.A., 2008. Cryogenesis and soil formation along a bioclimate gradient in Arctic North America. Journal of Geophysical Research, 113, G03S12.

Reimer, P.J., Baillie, M.G.L., Bard, E., Bayliss, A., Beck, J.W., Blackwell, P.G., Bronk Ramsey, C., Buck, C.E., Burr, G.S., Edwards, R.L., Friedrich, M., Grootes, P.M., Guilderson, T.P., Hajdas, I., Heaton, T., Hogg, A.G., Hughen, K.A., Kaiser, K.F., Kromer, B., McCormac, F.G., Manning, S.W., Reimer, R.W., Richards, D.A., Southon, J.R., Talamo, S., Turney, C.S.M., van der Plicht, J., Weyhenmeyer, C.E., 2013. IntCal13 and Marine13 radiocarbon age calibration curves 0–50,000 years cal BP. Radiocarbon, 55 (4), 1869-1887.

Reyes, A.V., Froese, D.G., Jensen, B.J.L., 2010. Permafrost response to last interglacial warming field evidence from non-glaciated Yukon and Alaska. Quaternary Science Reviews, 29 (23-24), 3256-3274.

Rozanski, K., Stichler, W., Gonfiantini, R., Scott, E.M., Beukens, R.P., Kromer, B., Van der Plicht, J., 1992. The IAEA ^{14}C intercomparison exercise 1990. Radiocarbon, 34, 506-519.

Schultz, N.M., Griffis, T.J., Lee, X., Baker, J.M., 2011. Identification and correction of spectral contaminations in $^2H/^1H$ and $^{18}O/^{16}O$ measured in leaf, stem, and soil water. Rapid Communications in Mass Spectrometry, 25, 3360-3368.

Shur, Y., French, H.M., Bray, M.T., Anderson, D.A., 2004. Syngenetic permafrost growth: cryostratigraphic observations from the CRREL Tunnel near Fairbanks, Alaska. Permafrost and Periglacial Processes, 15 (4), 339-347.

U.S. Geological Survey, 2012a. Report of Stable Isotopic Composition, Reference Material USGS45, Reston, VA. http://isotopes.usgs.gov/lab/referencematerials/USGS45.pdf.

U.S. Geological Survey, 2012b. Report of Stable Isotopic Composition, Reference Material USGS46, Reston, VA. http://isotopes.usgs.gov/lab/referencematerials/USGS46.pdf.

Wassenaar, L.I., Hendry, M.J., Chostner, V.L., Lis, G.P., 2008. High resolution pore water δ^2H and $\delta^{18}O$ measurements by $H_2O_{(liquid)}$-$H_2O_{(vapor)}$ equilibration laser spectroscopy. Environmental Science and Technology, 42 (24), 9262-9267.

Wassenaar, L.I., Ahmad, M., Aggarwal, P., Duren, M., Pöltenstein, L., Araguas, L., Kurttas, T., 2012. Worldwide proficiency test for routine analysis of δ^2H and $\delta^{18}O$ in water by isotope-ratio mass spectrometry and laser absorption spectroscopy. Rapid Communications in Mass Spectrometry, 26 (15), 1641-1648.

West, A.G., Goldsmith, G.R., Brooks, P.D., Dawson, T.E., 2010. Discrepancies between isotope ratio infrared spectroscopy and isotope ratio mass spectrometry for the stable isotope analysis of plant and soil waters. Rapid Communications in Mass Spectrometry, 24 (14), 1948-1954.

Chapter 3: Lithostratigraphy, cryostratigraphy, and paleoecological indicators from late Quaternary Klondike permafrost

This chapter details the characteristics of the sediment, ice, and other paleoenvironmental indicators from permafrost units at the eight sites included in this study. The chapter is organized into descriptions and paleoenvironmental interpretations for each site based on the lithostratigraphy, cryostratigraphy, chronostratigraphy, and paleoecological indicators. Because this thesis is organized as a hybrid between a traditional thesis and a paper-format thesis, there is some duplication between these detailed field observations, presented here to provide a full record, and the paper that follows in Chapter 4.

Site Descriptions and Interpretations

Individual site descriptions begin with a general overview of the sediments, organic material, and general characteristics followed by a description of each unit and then associated paleoenvironmental interpretations for all units. Site locations in Table 3-1 are shown in Figure 3-1. Radiocarbon dates are presented in Appendix A. Aggradation rates are estimated for units via OxCal depositional models, which are based on the vertical distance between calibrated radiocarbon dates (Bronk Ramsey, 2008, 2009; Bronk Ramsey and Lee, 2013). The models are presented in each unit description, and the rates are compiled in Appendix B.

Table 3-1: Site details for Klondike permafrost exposures (all locations with respect to NAD83 datum).

Locality	Elevation (m)	Latitude	Longitude	Aspect
Black Hills	634	63° 30.769'	138° 55.794'	W
Upper Quartz	620	63° 49.806'	139° 00.895'	WNW
Lower Quartz	578	63° 49.455'	139° 01.597'	NW
Upper Goldbottom	618	63° 53.879'	138° 59.506'	W
Lucky Lady II	615	63° 44.225'	138° 51.368'	NE
Brimstone	617	63° 44.400'	138° 50.867'	SW
Upper Hunker	491	63° 57.536'	138° 56.957'	NNW
Lower Hunker	390	64° 01.014'	139° 09.220'	NNE

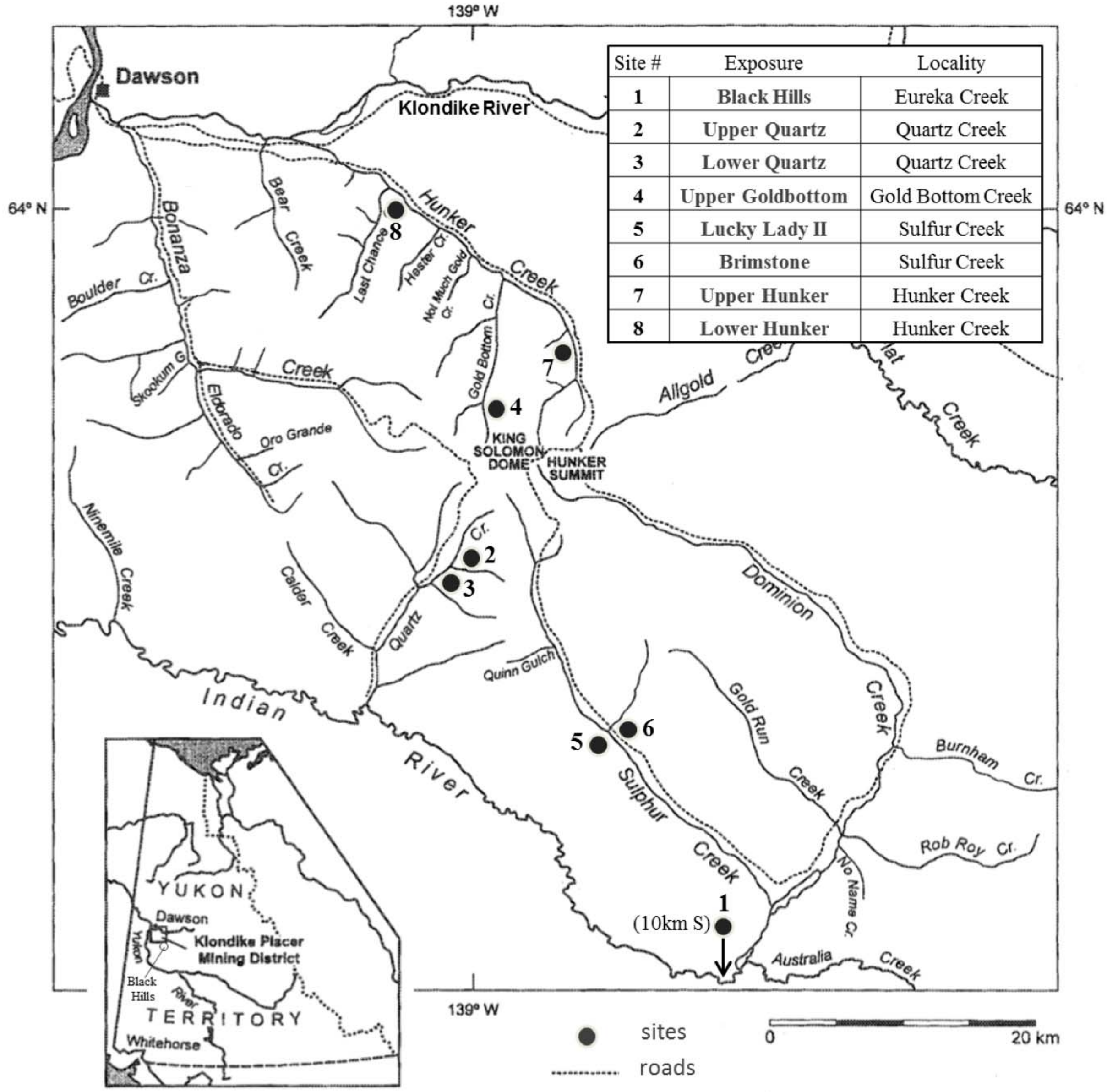

Site #	Exposure	Locality
1	Black Hills	Eureka Creek
2	Upper Quartz	Quartz Creek
3	Lower Quartz	Quartz Creek
4	Upper Goldbottom	Gold Bottom Creek
5	Lucky Lady II	Sulfur Creek
6	Brimstone	Sulfur Creek
7	Upper Hunker	Hunker Creek
8	Lower Hunker	Hunker Creek

Figure 3-1 : Map of Klondike sites in this study (base map adapted from Fraser and Burn, 1997).

Black Hills

The Black Hills site is located in the middle of a broad valley 66 km southeast of Dawson on a tributary to the Stewart River. The Black Hills site has a 7 m section that can be subdivided into three units, from bottom to top: (1) 4 m of grey and brown silts with graminoid vegetation, (2) 1.1 m of organic-rich grey and black silts with wood and fibrous vegetation, and (3) 1.9 m of organic-rich grey and black silts with large roots in growth position at the base (Figure 3-2, 3-3). Contacts between units are sharp. No large mammal fossils are present.

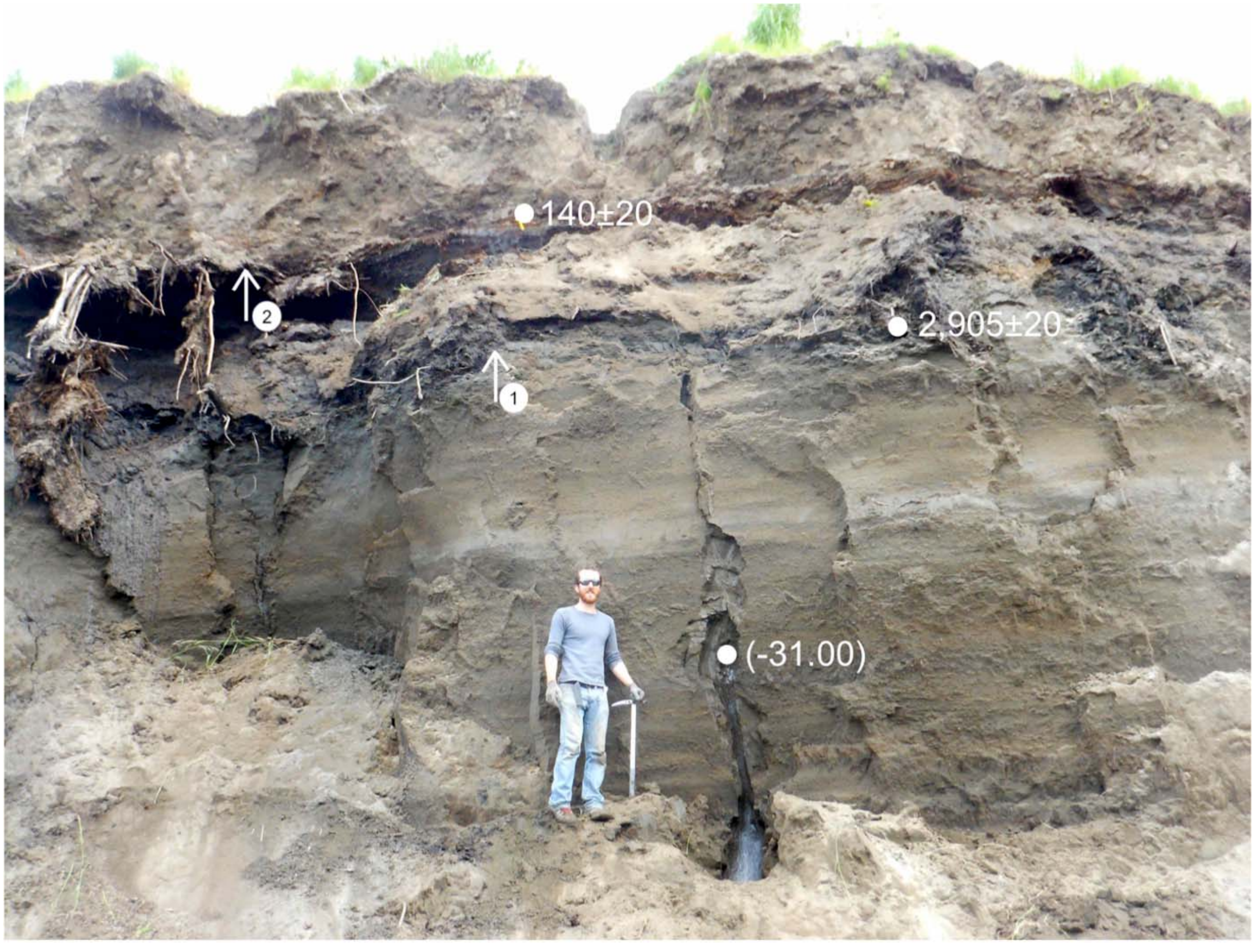

Figure 3-2 : The Black Hills site, which is divided into three units. Samples are indicated by markers which include $\delta^{18}O$ (‰) values and/or radiocarbon dates where applicable. The lowermost unit, exposed from 0 to 4.0 m, consists of grey-brown silt including an arctic ground squirrel nest (just out of frame to right) dating to 27,575 cal yrs BP (23,360±100, UCIAMS-114718). A single syngenetic ice wedge is present in the upper 2.5 m of silts (at lowermost sample marker). This wedge extends above a series of truncated wedges near the base of the exposure that are ~1 m wide. This unit is overlain by a sharp unconformity at 4.0 m (at the arrow marked "1") which consists of 1.1 m of organic-rich silt deposited 3,040 cal yrs BP (2,905±20, UCIAMS-114902). The uppermost unit, exposed from 5.1 to 7.0 m, consists of organic-rich silt with a sharp basal contact (above the arrow marked "2"), which dates to 145 cal yrs BP (140±20, UCIAMS-114904). Ice axe in photo is 80 cm high.

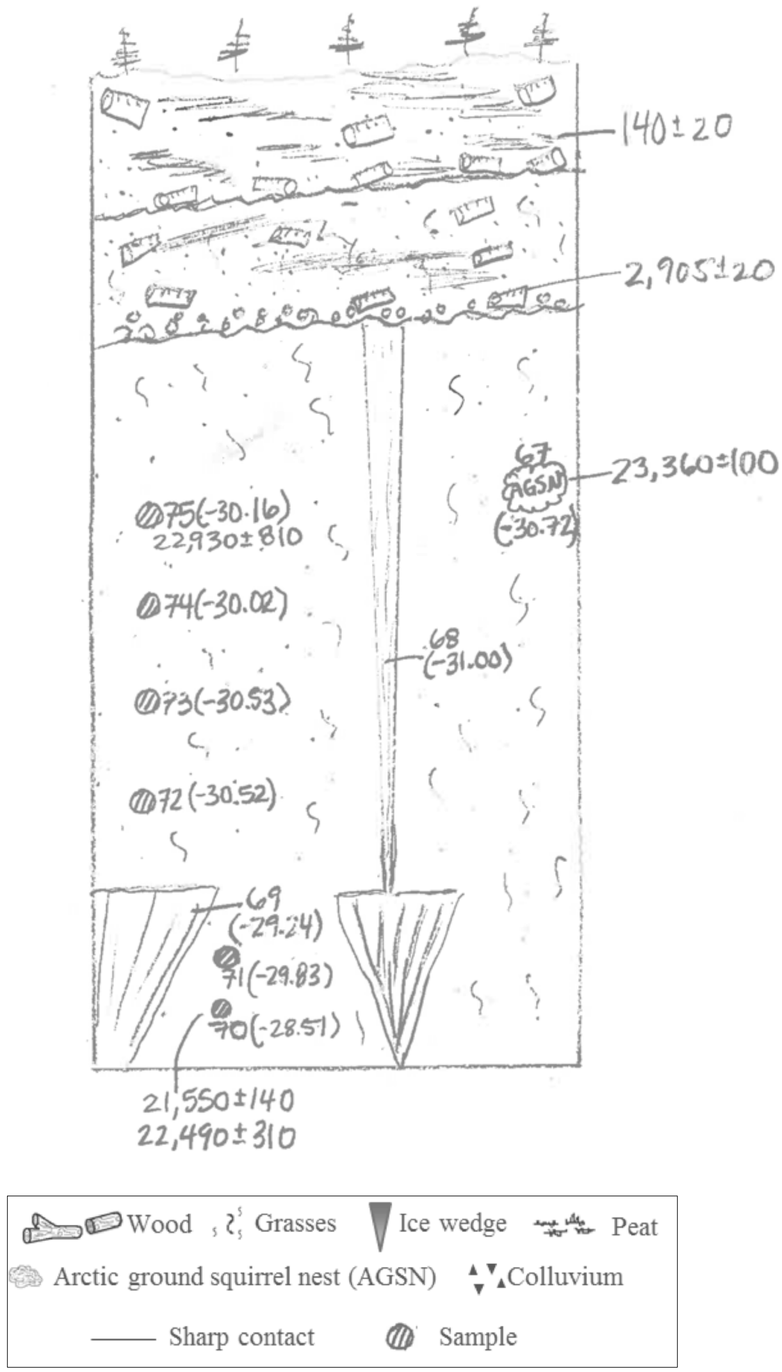

Figure 3-3 : Stratigraphic sketch of the Black Hills section. Numbers next to features correspond to MM12 sample numbers (*e.g*. 67 is sample MM12-67). This is a reference figure for the site sketches in this chapter. $\delta^{18}O$ values (‰, VSMOW) are in parentheses and radiocarbon dates are included where applicable. The vertical distances between samples can be found in Appendix D.

Description

The lowermost unit, exposed from 0 to 4.0 m, consists of grey and brown silts containing graminoid vegetation. Total carbon ranges from 1.6 to 3.0% and total nitrogen ranges from 0.1 to 0.3%. Values for all carbon and nitrogen contents in this study are in Appendix C. Both carbon and nitrogen contents are highest at the base of this unit and decrease with height. Four syngenetic ice wedges (~1 m wide) are truncated at 1.5 m. One thin (15 cm wide) syngenetic ice wedge extends 2.5 m up to the overlying contact (Figure 3-4). Parallel, wavy microlenticular and layered (2 mm thick) ice is present in otherwise ice-poor (structureless) silts. Water isotopes from pore and ice wedge ice samples show little difference within the lower section, averaging -30.1 ± 0.9‰ $\delta^{18}O$ and -224.5 ± 5.5‰ $\delta^{2}H$. Values for all water isotopes in this study are in Appendix D. This unit has five radiocarbon dates between 27,575 and 25,840 cal yrs BP[1] (23,360±100, UCIAMS-114718; 21,550±140, UCIAMS-114923). Grasses adjacent to one of the truncated ice wedges are dated to 26,775 and 25,840 cal yrs BP (22,490±310, UCIAMS-122279; 21,550±140, UCIAMS-114923) (Figure 3-5). Grasses from 1.8 m above the truncated ice wedge date to 27,220 cal yrs BP (22,930±810, UCIAMS-131097), a reversal in age from grasses adjacent to the ice wedge. One arctic ground squirrel nest found at 2.9 m dates to 27,575 cal yrs BP (23,360±100, UCIAMS-114718). Ages of all arctic ground squirrel nests in the Klondike area are in Appendix E.

[1] Throughout the text calibrated radiocarbon dates are presented as mean age estimates. Full radiocarbon calibration ranges are in Appendix A.

Figure 3-4 : The lowermost unit at the Black Hills site is exposed from 0 to 4.0 m and consists of grey and brown ice-poor silts with *in situ* graminoid vegetation. A single thin (~15 cm wide) secondary syngenetic ice wedge extends above the lower ice wedge (~1 m wide) below (not pictured). An arctic ground squirrel nest in this unit (not pictured) dates to 27,575 cal yrs BP (23,360±100, UCIAMS-114718) and has an $\delta^{18}O$ pore ice value of -30.72‰. Ice axe is 80 cm high.

Figure 3-5 : One of four truncated ice wedges at the Black Hills site. Grasses from one sample adjacent to the ice wedge are dated to 26,775 and 25,840 cal yrs BP (22,490±310, UCIAMS-122279; 21,550±140, UCIAMS-114923). Truncation of the ice wedge is indicated by the arrow. Shovel is ~1.2 m high.

The second unit, exposed from 4.0 to 5.1 m, consists of interbedded layers (3 – 25 cm thick) of dark grey and black organic silts, fibrous organics, abundant woody macrofossils, and lenses of rust-brown quartz-rich gravel (Figure 3-6). The underlying contact is sharp and undulating. No ice wedges are present. No water isotope samples or cryostructural observations were made in this unit. One wood sample is dated to 3,040 cal yrs BP (2,905±20, UCIAMS-114902).

Figure 3-6 : Grey silts of the underlying unit are sharply overlain (at arrow) by the second unit, exposed from 4.0 to 5.1 m, which consists of organic-rich black and grey silt with woody roots, fibrous organics, and interbedded sands and gravels dating to the late Holocene. A woody macrofossil from the upper unit is dated to 3,040 cal yrs BP (2,905±20, UCIAMS-114902). Ice axe head is 21 cm wide.

The uppermost unit, exposed from 5.1 to 7.0 m, consists of dark grey and black organic silts, fibrous organics, abundant woody macrofossils, with a single radiocarbon date of 145 cal yrs BP (140±20, UCIAMS-114904) (Figure 3-7). No other observations were made.

Figure 3-7 : Large 3 – 6 cm thick roots (at arrow) at the sharp contact with the second unit in the Black Hills section. Organic material from this unit dates to 145 cal yrs BP (140±20, UCIAMS-114904). This unit is likely the result of anthropogenic disturbance at the site.

Interpretations

Radiocarbon dates from lowermost exposure suggest that the sediment from 0 to 4.0 m was deposited near the beginning of the last cold stage. The basal contact of this unit is obscured by slumped material. The presence of graminoid-dominated vegetation and an arctic ground squirrel nest suggest steppe-tundra vegetation (Zazula et al., 2005, 2007). The sediment in this unit is organic-poor and most likely had well-drained, deep active layers (Froese et al., 2009). Decreasing carbon and nitrogen contents suggest reduced vegetation cover going into the last cold stage. Syngenetic ice wedges, present at the base of this unit, are notably absent from 1.5 to 4.0 m, albeit with one thin syngenetic ice wedge that formed *ca.* 26,000 cal yrs BP, possibly suggesting increased aridity and/or other environmental factors. Additional hypotheses explaining reduced ice wedge formation during the last cold stage are discussed in detail in Chapter 4. Microlenticular and layered cryostructures in otherwise structureless (ice-poor) sediments suggest syngenetic aggradation of this unit in arid conditions. Ice-poor sediments are common in the permafrost units in this study, suggesting arid conditions, which may be amplified during cold stage conditions. Water isotopes are consistent throughout this unit and are among the most depleted in this study, suggesting cold temperatures associated with cold stage conditions *ca.* 27,000 cal yrs BP. Aggradation rates are not estimated, due to unclear relations between radiocarbon ages. This could be from local reworking of older grass fragments, which may suggest local denudation during the last cold stage, or may be from sampling across dipping bedding planes in the *ca.* 30 m long exposure (see Figure 3-2). Cryostratigraphy and paleoenvironmental indicators in this unit are in good agreement with units that are similar in age from the Upper Goldbottom and Upper Hunker sites in this study. This unit may be comparable to the Quartz Creek Member from Kotler and Burn (2000).

Radiocarbon dates from the second unit suggest that the sediment from 4.0 to 5.1 m was deposited during the late Holocene. The contact with the underlying unit is undulating and unconformable, and is characterized by a thin layer of basal sands and gravels, suggesting it is an erosional surface from local fluvial conditions. Wood and graminoid vegetation appears to be largely *in situ*. Cryostructures, total carbon and nitrogen, and other paleoecological indicators in this unit are not defined. This unit may be comparable to the "Organic unit" from Kotler and Burn (2000).

Radiocarbon dates from uppermost sediments suggest the sediment from 5.1 to 7.0 m is most likely reworked material from modern gold mining operations. The basal contact of this unit is sharp and erosional. This interpretation is consistent with a distinct buried layer of large *in situ* roots at the base of this unit. Cryostructures, total carbon and nitrogen, and other paleoecological indicators in this unit are not defined.

Upper Quartz

The Upper Quartz site is located in a narrow valley 33 km south of Dawson on a tributary to the Indian River. The Upper Quartz site has a 7 m section that can be subdivided into three units, from bottom to top: (1) 2.8 m of massive to crudely-stratified grey silts with *in situ* graminoid vegetation; (2) 1 m of grey silts with shrub and graminoid vegetation; and (3) over

3.2 m of black and grey organic-rich silts with abundant fibrous and woody macrofossils (Figure 3-8, 3-9, 3-10). The amount of ice in the section generally increases from the bottom to the top of the exposure, and the contacts between units are sharp. No large mammal fossils are present *in situ*.

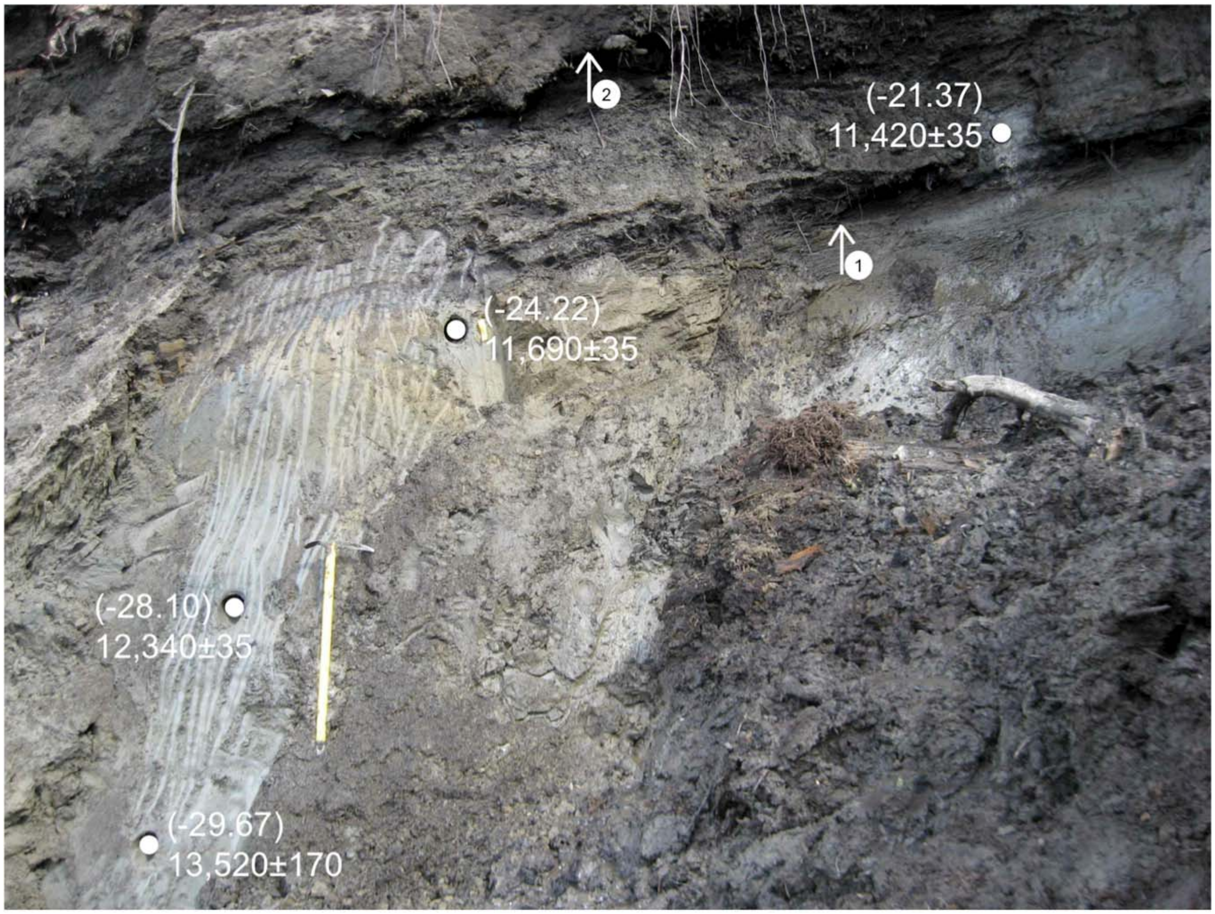

Figure 3-8 : General view of the Upper Quartz section from 2013. The lowermost unit is exposed from 0 to 2.8 m and consists of grey and brown silts with *in situ* graminoid vegetation. A sharp contact at 2.8 m separates this unit from a distinct black organic layer 10 cm thick (arrow "1") in organic-rich black and grey silts with *in situ* graminoid and shrub vegetation. This is overlain by a sharp contact (arrow "2") defining the base of the uppermost unit from 3.8 to 7.0 m, which consists of organic-rich black and grey silts including abundant randomly-oriented reworked shrub and large wood macrofossils. Ice axe is 74 cm high.

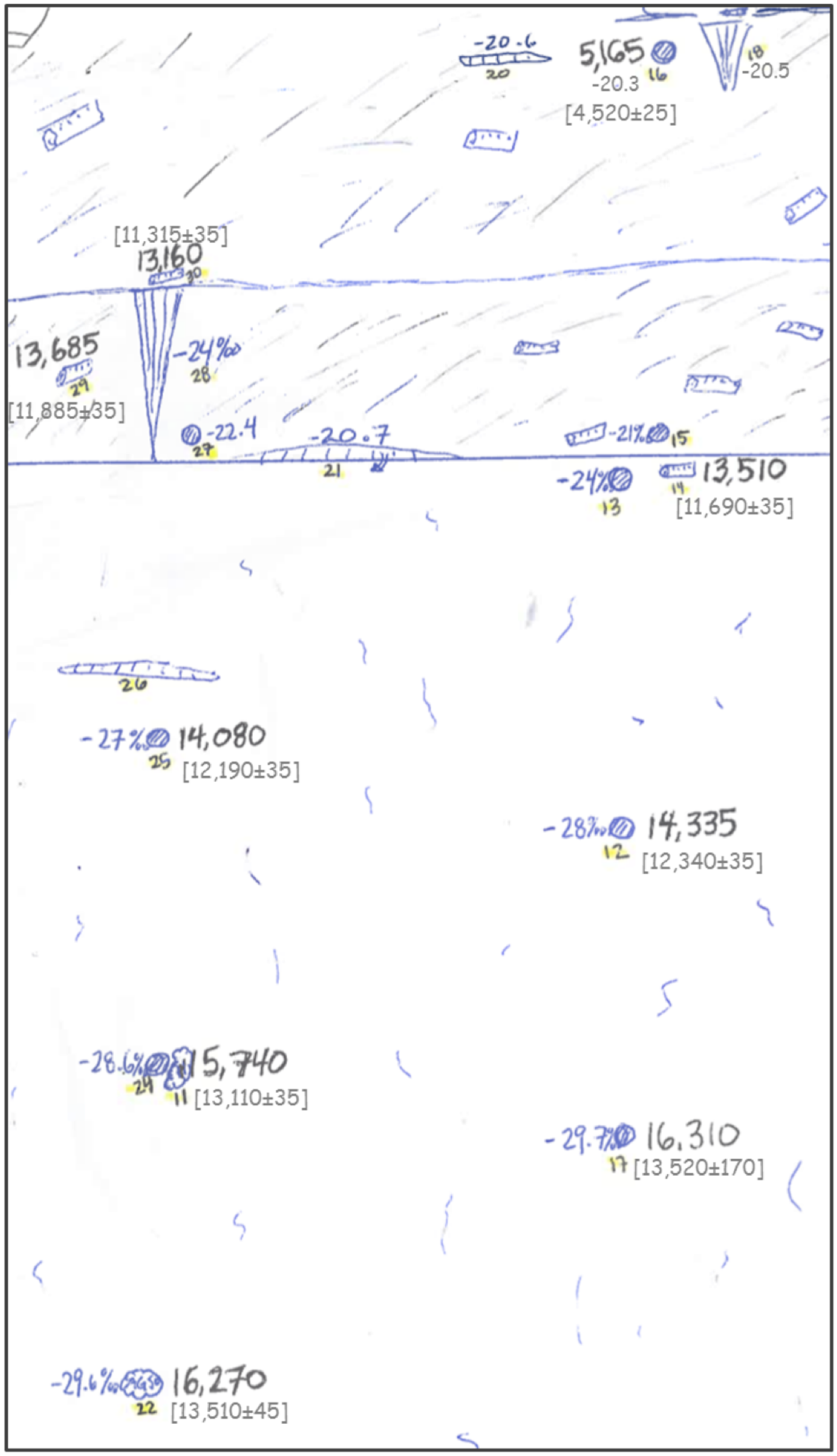

Figure 3-9 : Stratigraphic sketch of the Upper Quartz sections from 2013. Ages are in calibrated years BP with radiocarbon ages in brackets. Sample numbers correspond to MM13 samples.

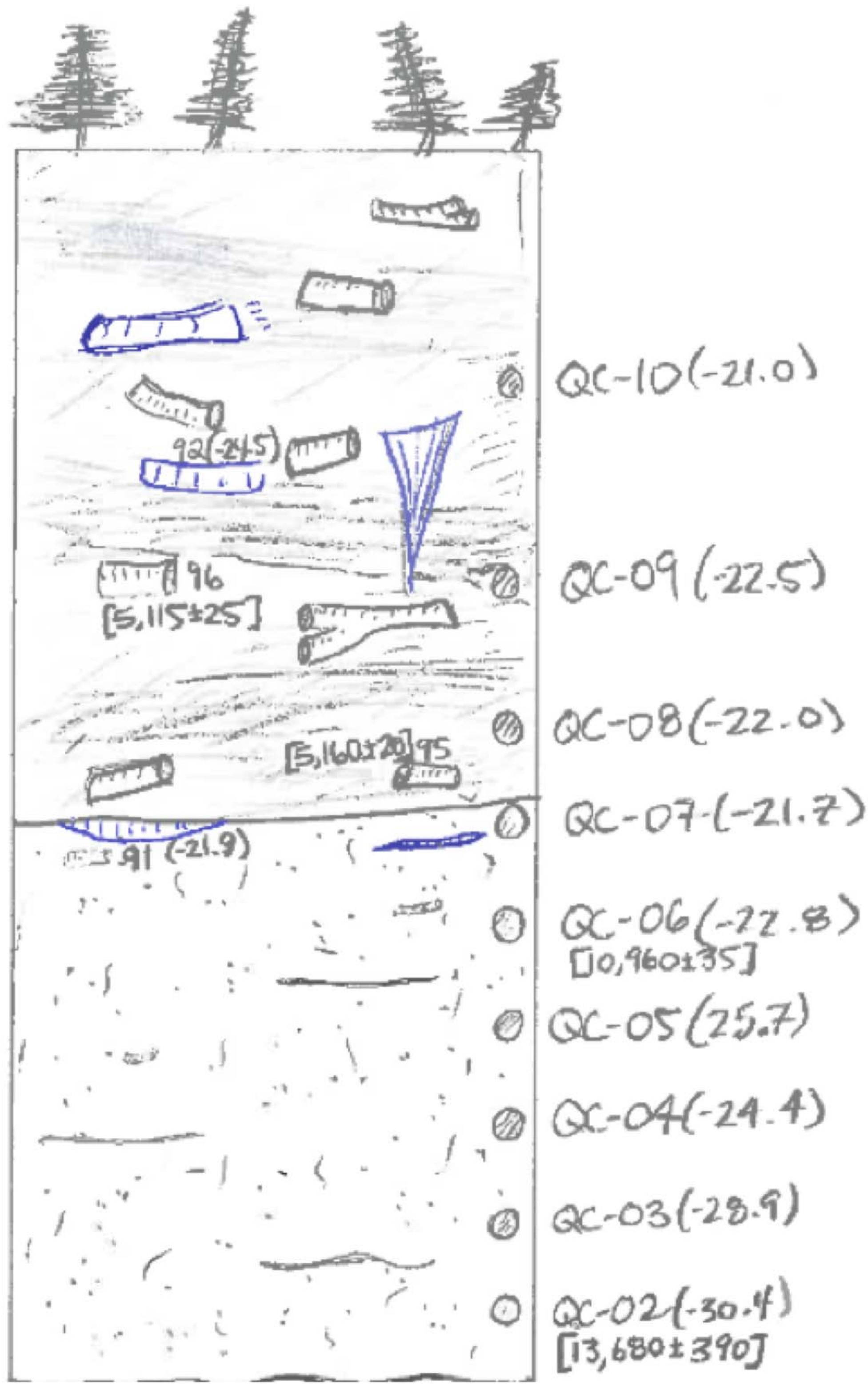

Figure 3-10 : Stratigraphic sketch of the Upper Quartz site in 2012. Sample numbers correspond to MM12 samples (*e.g.* QC-06 is MM12-QC-06).

Description

The lowermost unit, exposed from 0 to 2.8 m, consists of grey and brown silts with abundant macrofossils of *in situ* graminoid vegetation (Figure 3-11). In the upper ~1 m, several thin (1 – 3 cm) discontinuous black organic lenses and rare detrital woody macrofossils are present. Total carbon ranges from 0.9 to 1.1% and total nitrogen ranges from 0.05 to 0.06%. Pore ice samples in the lower 1.5 m are largely structureless, albeit interspersed with parallel, wavy layered to microlayered lenses of ice (up to 2 mm thick) with one occurrence of a reticulate-chaotic cryostructure at 1.5 m. The upper 1 m is characterized by non-parallel wavy lenticular (2 – 20 mm) and microlenticular ice, with one 10 cm thick lens of thermokarst-cave ice at 1.8 m. The most depleted water isotope sample (-30.43‰ $\delta^{18}O$; -234.5‰ $\delta^{2}H$) is from the base of the exposure, and the uppermost sample is the most enriched (-21.72‰ $\delta^{18}O$; -166.8‰ $\delta^{2}H$). Seven radiocarbon dates from the section range from 16,560 to 13,510 cal yrs BP (13,680±390, UCIAMS-114710; 11,680±35, UCIAMS-131100). Two arctic ground squirrel nests, at 0 and 0.75 m, date to 16,270 and 15,740 cal yrs BP, respectively (13,510±45, UCIAMS-131096; 13,110±35, UCIAMS-142195). Arctic ground squirrel nests are excellent paleoecological indicators because they contain vegetation and waters from the surface, which is stratigraphically higher in the section (Zazula et al., 2005, 2007). Excavations of modern arctic ground squirrel burrows have indicated that the nests are typically found immediately above the top of the permafrost in active layers ~1 m deep (Buck and Barnes, 1999). In this study, we assume that arctic ground squirrel nests are located at least 80 cm below the original surface, near the base of the active layer. Independent estimates of paleoactive layer depth can also be made from the depth of translocated organics in cold stage paleosols and truncated ice wedges (*e.g.* Zazula et al., 2005; Sanborn et al., 2006). This offset is taken into account when estimating aggradation rates inferred from one or more dated arctic ground squirrel nests. Aggradation rates for this unit are estimated to range from 0.06 to 0.14 cm/year over this interval (Figure 3-12, 3-13).

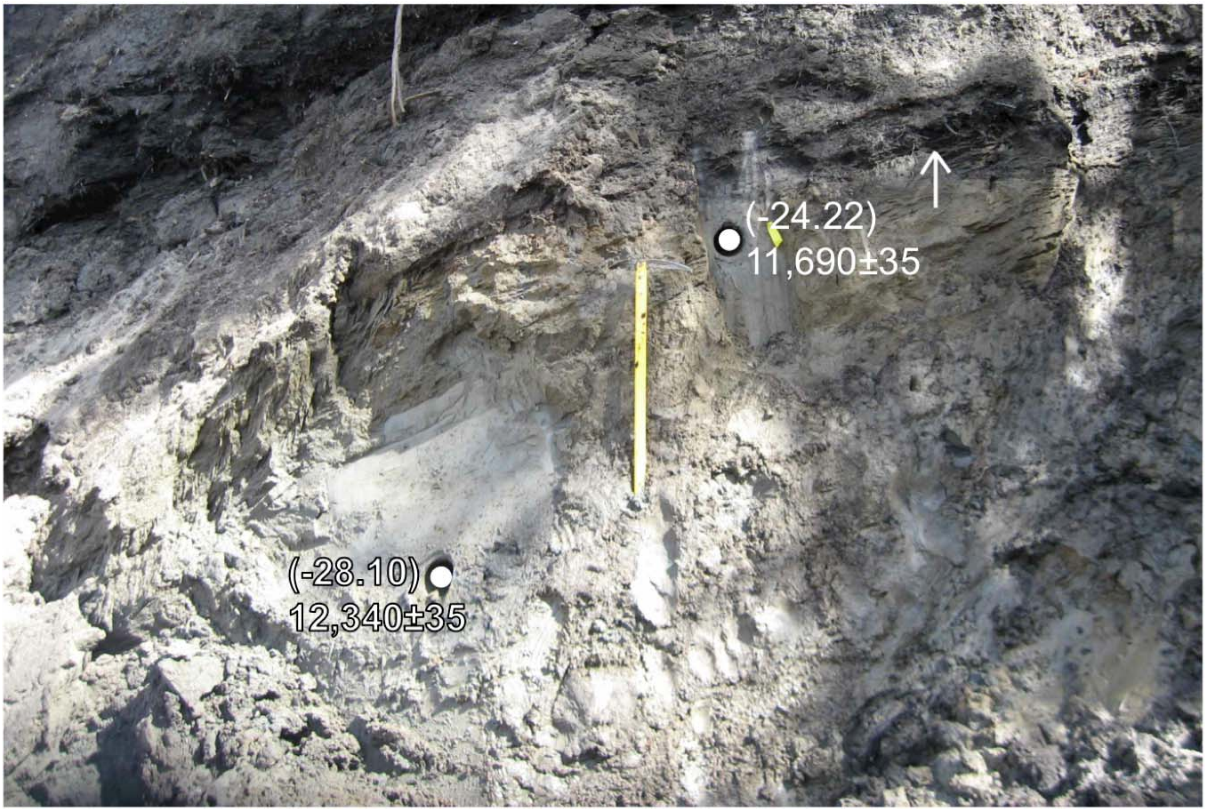

Figure 3-11 : Upper Quartz grey and brown silts with *in situ* graminoid vegetation. The lowermost unit, exposed from 0 to 2.8 m, is largely free of excess ice except in the upper 1 m which includes layers of ice up to 2 cm thick. This upper meter also contains organic silt lenses (1 – 3 cm thick) containing *in situ* graminoid vegetation and reworked twigs. Two arctic ground squirrel nests (not pictured) are in the lower 75 cm and date to 16,270 and 15,740 cal yrs BP (13,510±45, UCIAMS-131096; 13,110±35, UCIAMS-142195). The overlying contact is sharp and distinguished by a 10 cm thick laterally-continuous black organic layer (indicated by arrow). Ice axe is 74 cm high.

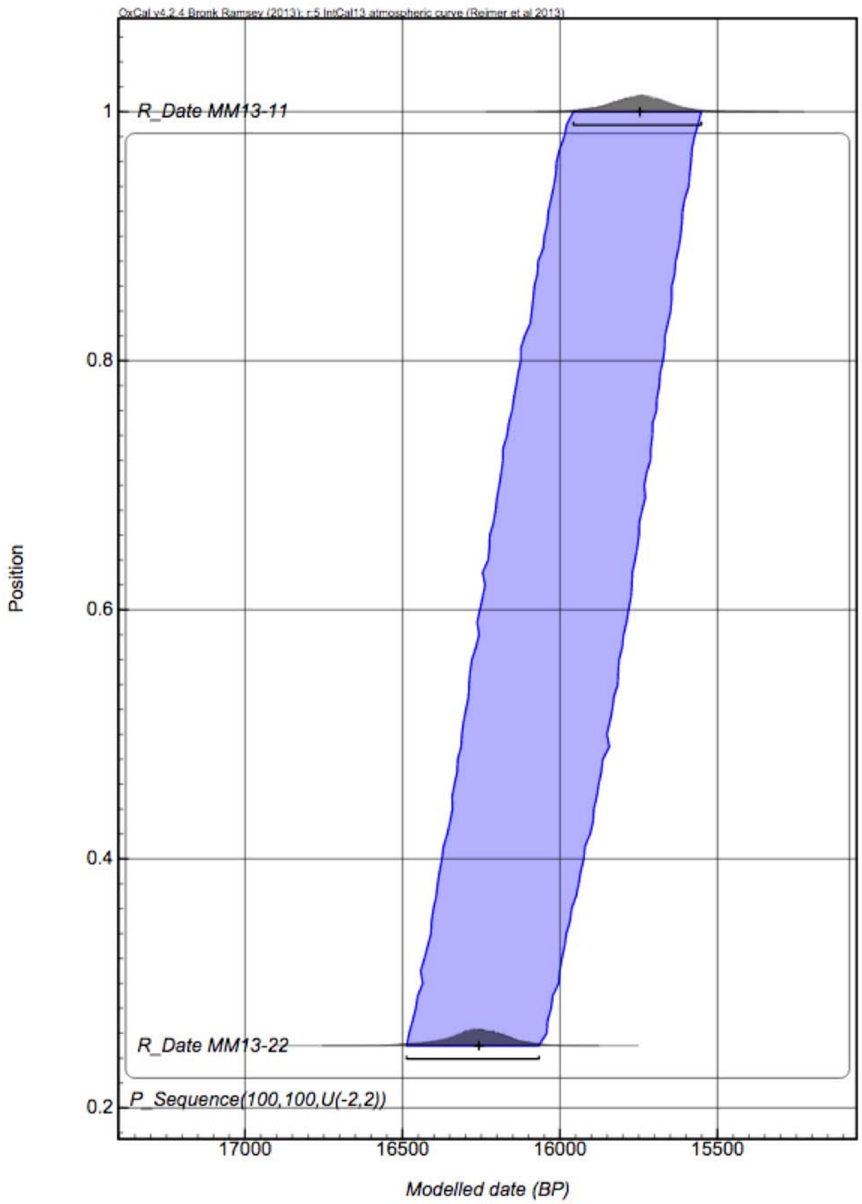

Figure 3-12 : Deposition model for the lowermost unit based on two radiocarbon dates at 0.25 and 1.0 m collected at the Upper Quartz site in 2013. 1σ calibrated age ranges are indicated by brackets below samples. Shadowed areas represent the estimated age of sediment from the depositional model at various heights in the section. The estimated aggradation rate for this interval is 0.14 cm/year, based on linear interpolation between calibrated ages for samples MM13-22 and MM13-11. An additional deposition model is presented in the following figure from samples collected at the same site in 2012. The relative position between samples is measured in meters. All of the estimated rates of deposition are compiled in Appendix B.

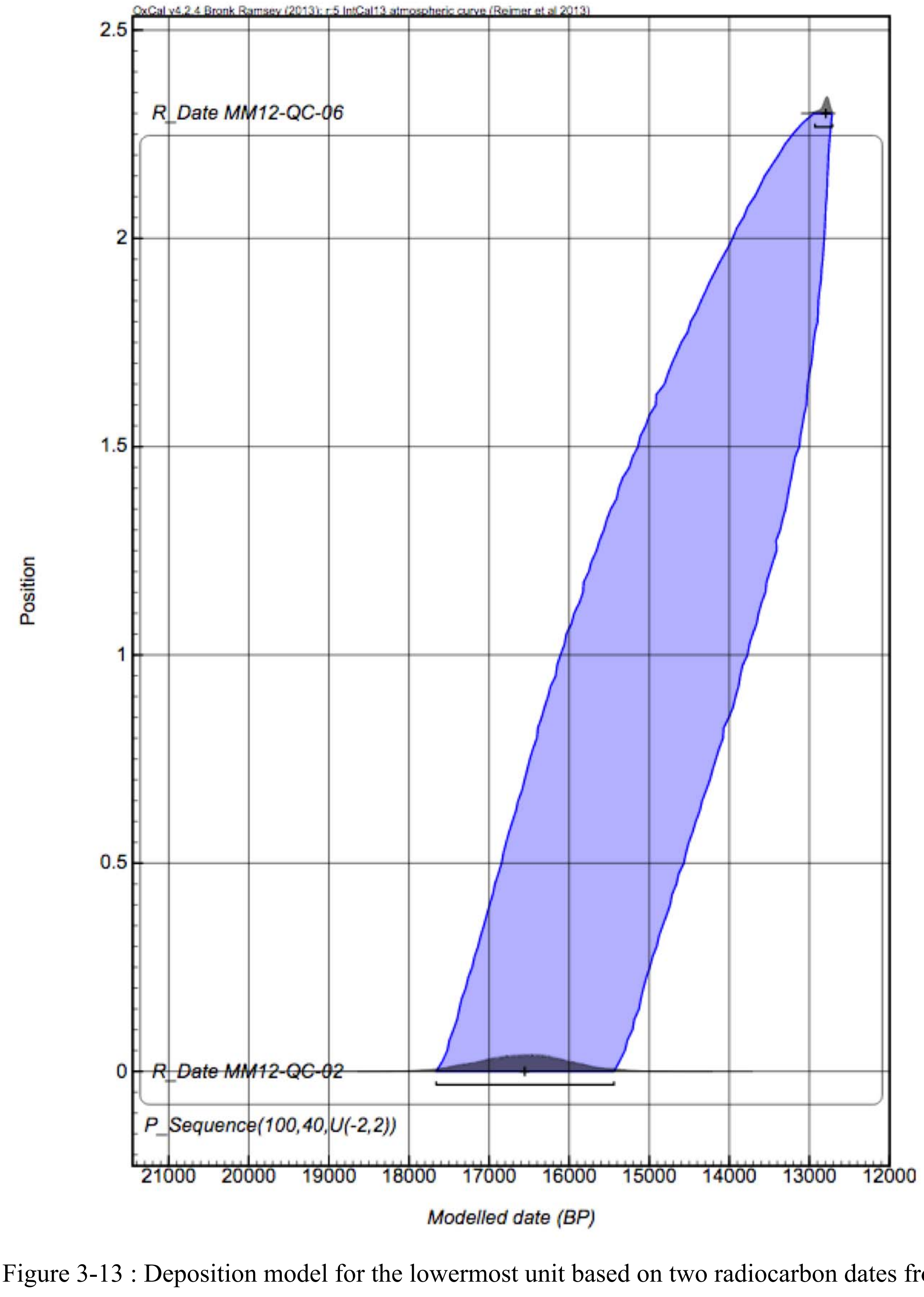

Figure 3-13 : Deposition model for the lowermost unit based on two radiocarbon dates from 0 and 2.3 m collected at the Upper Quartz site in 2012. The estimated aggradation rate for this interval is 0.06 cm/year. The relative position between samples is measured in meters.

The second unit, exposed from 2.8 to 3.8 m, consists of grey and black silts including *in situ* shrubby roots and graminoid vegetation (Figure 3-14). The base of this unit is characterized by a 10 cm thick laterally-continuous black organic-rich layer. Total carbon and nitrogen are not determined. This unit has abundant non-parallel wavy microlenticular cryostructures with several aggradational ice lenses (2 cm thick) interspersed throughout, with one thin (20 cm wide, 1 m tall) syngenetic ice wedge (Figure 3-15). Water isotopes range from -24.61‰ to -20.74‰ $\delta^{18}O$ and -195.5‰ to -162.8‰ $\delta^{2}H$. Shrub macrofossils date between 13,685 and 13,160 cal yrs BP (11,885±35, UCIAMS-142206; 11,315±35, UCIAMS-142205). Estimation of aggradation rates is not possible due to a lack of dated samples from multiple horizons in the unit.

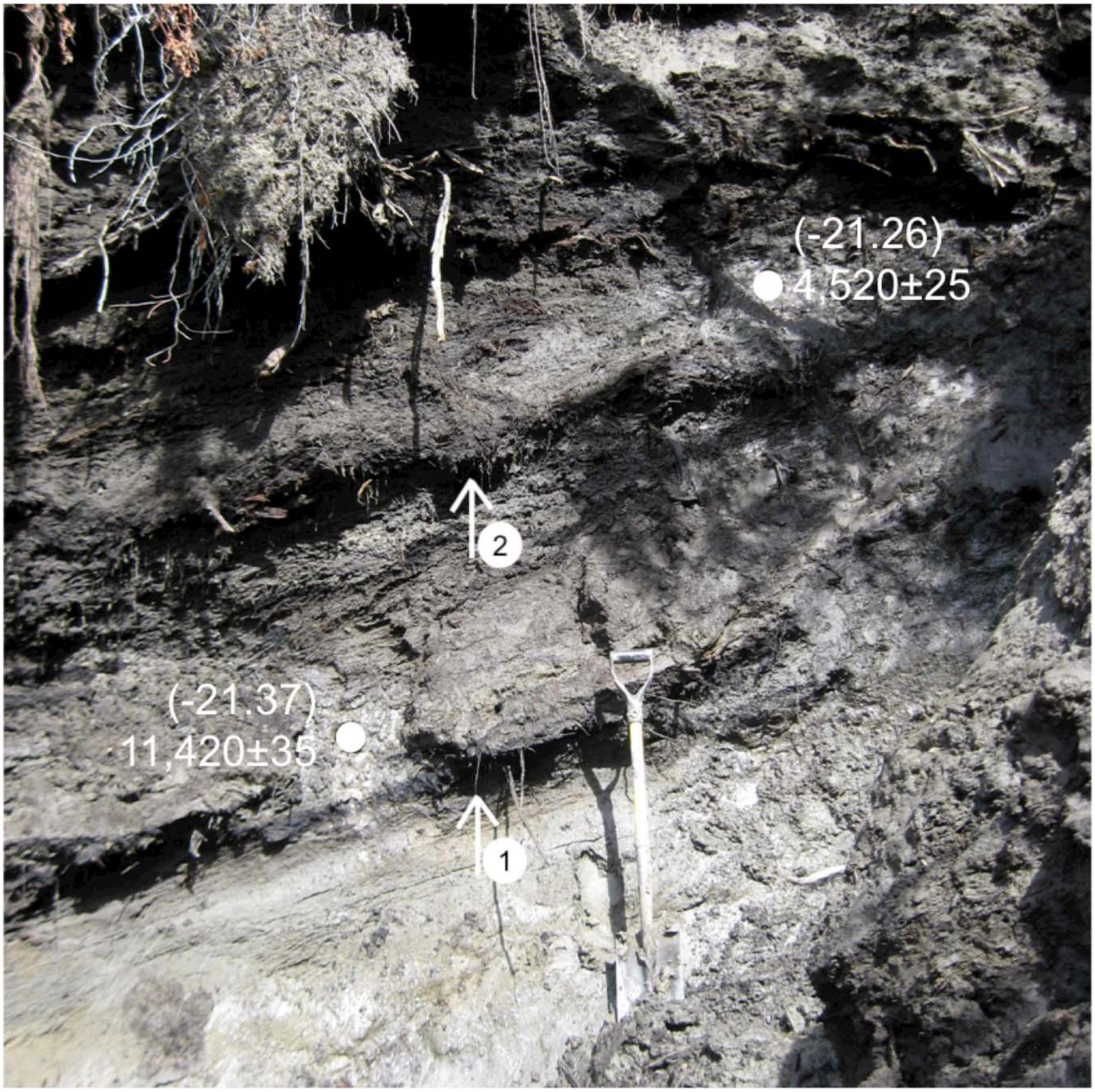

Figure 3-14 : The second unit at the Upper Quartz site is exposed from 2.8 to 3.8 m and consists of organic-rich black and grey silts with *in situ* shrub and graminoid vegetation. A 10 cm thick laterally-continuous black shrubby layer is the base of this unit (arrow “1”) and an overlying sharp contact (arrow “2”) with the uppermost unit. Shovel is ~1.2 m high.

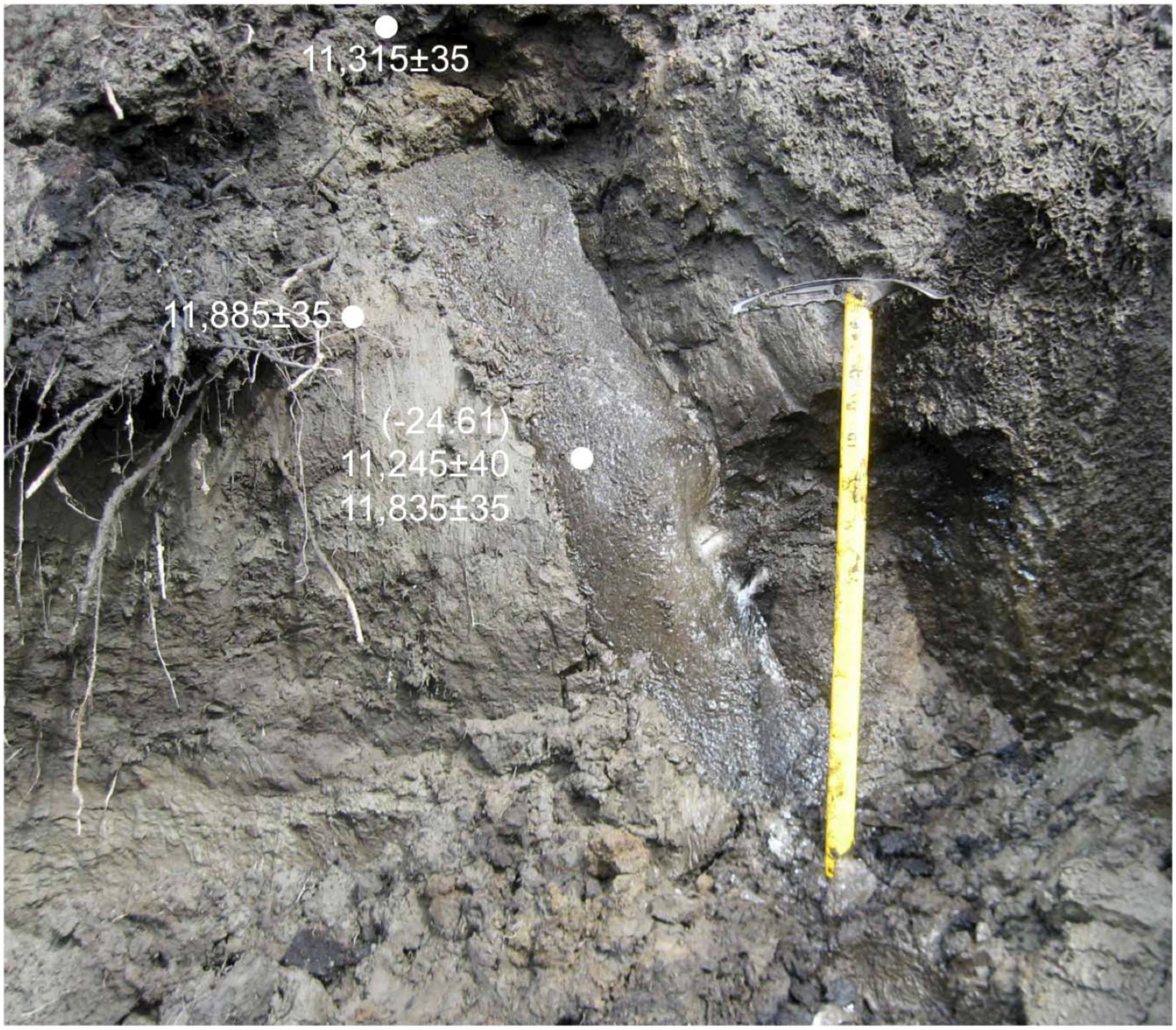

Figure 3-15 : A thin syngenetic ice wedge (~20 cm wide) in the second unit at the Upper Quartz site in organic-rich grey and black silts with *in situ* shrub and graminoid vegetation. Grass and twigs from within the wedge ice are dated to 13,655 and 13,110 cal yrs BP (11,835±35, UCIAMS-150832; 11,245±40, UCIAMS-150828). An ice sample completely transecting the wedge was not taken, however, based on the number of foliations in an 8.3 cm wide sample, there were ~20 – 25 thermal contraction cracking events that created the ice wedge. Ice axe is 74 cm high.

The uppermost unit, exposed from 3.8 to 7.0 m, consists of organic-rich black and grey silts including *in situ* fibrous organics, reworked wood, and interbedded discontinuous diamict and sand lenses 10 – 15 cm thick (Figure 3-16). Sub-horizontal bedding planes of organic material range from ~0.5 to 1 m thick and are characterized by randomly-oriented wood fragments. There is a sharp contact with the underlying unit. Total carbon and nitrogen are not determined. Cryostructures are typically non-parallel wavy lenticular (2 – 6 mm) and microlenticular ice, with one instance of crustal ice around a wood fragment. One truncated syngenetic ice wedge (~50 cm wide) is sampled at 3.95 m. Aggradational ice (up to ~10 cm thick) is present throughout this unit. Water isotopes range from -24.48‰ to -20.59‰ $\delta^{18}O$ and -157.1‰ to -188.8‰ $\delta^{2}H$. Three radiocarbon samples have dates ranging from 5,925 to 5,165 cal yrs BP (5,160±20, UCIAMS-114899; 4,520±25, UCIAMS-142207). Aggradation of this unit appears to have been rapid at times, as two pieces of wood that are dated to 5,925 and 5,840 cal yrs BP (5,160±20, UCIAMS-114899; 5,115±25, UCIAMS-114911) are 1.7 m apart, indicating an aggradation rate of 2.0 cm/year (Figure 3-17).

Figure 3-16 : The uppermost unit at the Upper Quartz site in 2013, which is exposed from 3.8 to 7.0 m and consists of black and grey silts with abundant reworked wood, *in situ* fibrous organics, and diamict and sand lenses 10 – 15 cm thick. This unit was deposited between 5,925 and 5,165 cal yrs BP (5,160±20, UCIAMS-114899; 4,520±25, UCIAMS-142207). A sharp contact with the underlying unit is present (at arrow).

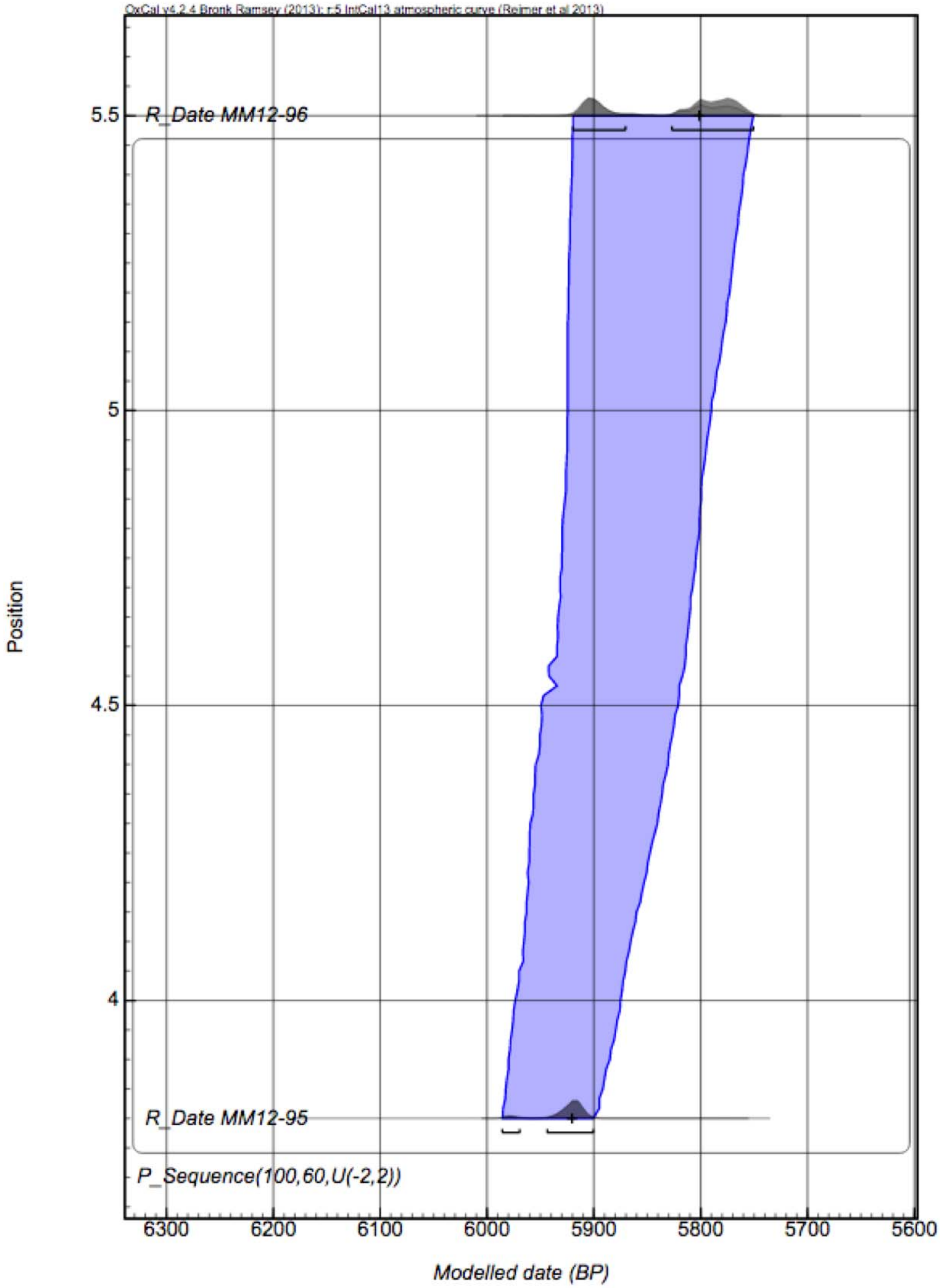

Figure 3-17 : Deposition model for the uppermost unit in the Upper Quartz site sampled in 2012, which is based on two radiocarbon dates at 3.8 and 5.5 m. The estimated aggradation rate for this interval is 2.0 cm/year. The relative position between samples is measured in meters.

Interpretations

Radiocarbon dates from the lowermost unit suggest the sediment from 0 to 2.8 m was deposited just prior to the Bølling-Allerød interstadial during the latest Pleistocene. Basal contact is obscured by slumped material. Mineral soils with graminoid vegetation and arctic ground squirrel nests suggest a steppe-tundra environment with deep, well-drained active layers during this interval. Low carbon and nitrogen contents suggest sparse vegetation cover. Layered to microlayered cryostructures suggest syngenetic aggradation of permafrost. Excess ice has a general increase with height in the section, suggesting a shift to relatively warmer and wetter conditions during this interval. Depleted water isotopes at the base of this unit suggest cold temperatures associated with cold stage conditions. Enrichment of water isotopes with height in the section suggests increasing air temperatures towards the end of the Pleistocene. Aggradation rates are estimated between 0.06 to 0.14 cm/year, which are low compared to the rapid aggradation during the mid-Holocene. Cryostratigraphy and paleoenvironmental indicators in this unit are in good agreement with a unit that is similar in age from the Lucky Lady II site in this study. This unit is comparable to the Quartz Creek Member from Kotler and Burn (2000).

Radiocarbon dates from the second unit suggest that the sediment from 2.8 to 3.8 m was deposited during the Bølling-Allerød interstadial during the latest Pleistocene. The base of this unit has a sharp, conformable contact, which is defined by a 10 cm thick paleosol with *in situ* shrub and graminoid vegetation. The paleosol formed during the Bølling-Allerød as shrub vegetation became established. The earliest shrub macrofossil is dated to 13,685 cal yrs BP (11,885±35, UCIAMS-142206). A lack of arctic ground squirrel nests and the presence of shrub vegetation suggest a shift away from steppe-tundra to shrub-dominated vegetation. The appearance of shrub vegetation suggests the Klondike had relatively warmer and wetter conditions at this time than during formation of the lowermost unit during the late Pleistocene. Total carbon and nitrogen contents are not determined. One thin syngenetic ice wedge and microlenticular cryostructures suggest syngenetic aggradation of permafrost. Abundant excess ice in this unit also suggests that moisture was more readily available during this time, relative to the underlying unit. Water isotopes are similar to slightly depleted compared to late Holocene values, suggesting cooler temperatures associated with interstadial conditions.

Cryostratigraphy and paleoenvironmental indicators in this unit are in good agreement with a unit that is similar in age from the Lucky Lady II site in this study. Aggradation rates are not defined. This unit may be comparable to the Dago Hill Member from Kotler and Burn (2000).

Radiocarbon dates from the uppermost unit suggest that the sediment from 3.8 to 7.0 m was deposited during the mid-Holocene. The basal contact of this unit is sharp and undulating, indicating an erosional unconformity with the underlying latest Pleistocene sediment. Large wood macrofossils suggest boreal forest in relatively warmer and wetter conditions. Total carbon and nitrogen contents are not defined. Syngenetic and epigenetic wedges are present, possibly suggesting fluctuating deposition rates and/or frequency of thermal contraction cracking. Lenticular and microlenticular cryostructures suggest syngenetic aggradation of permafrost. Excess ice also suggests that the environment had more available moisture in the landscape than the cold stage silts of the lowermost unit. Water isotopes are close to modern values, suggesting warm temperatures associated with interglacial conditions. Rapid deposition may have occurred during the mid-Holocene from repeated slumping of thawed material, which is suggested by rapid rates of aggradation, randomly-oriented broken wood macrofossils, and a prominent erosional unconformity with underlying sediment. Cryostratigraphy and paleoenvironmental indicators in this unit are in good agreement with a mid-Holocene deposit from the Upper Goldbottom site in this study. This unit is comparable to the “Organic unit” from Kotler and Burn (2000).

Lower Quartz

The Lower Quartz site is located in a valley 33 km south of Dawson on a tributary to the Indian River. The exposure consists of 5 m of basal gravel and 15 m of overlying ice-rich brown silts with *in situ* graminoid vegetation (Figure 3-18, 3-19).

Description

This exposure consists of brown silts including *in situ* graminoid vegetation from 5.0 to 20.0 m. Dawson tephra is present at 19.2 m. The contact between the gravel and silts is sharp. Total carbon ranges from 2.4 to 4.6% and total nitrogen from 0.2 to 0.4%. Large multi-generational syngenetic ice wedges (up to ~2.5 m wide) are regular throughout the lower 11 m and absent in the upper 9 m. Cryostratigraphy is characterized by non-parallel planar layered (~1 mm thick) to wavy lenticular (1 – 2 mm thick). Water isotopes range from -31.16‰ to -28.14‰ $\delta^{18}O$ and -237.6‰ to -223.6‰ $\delta^{2}H$, with a general trend of more depleted isotopic ratios with height above the gravels. Based on five radiocarbon dates this unit was deposited *ca.* 31,200 to 28,210 cal yrs BP (26,070±180, UCIAMS-101901; 23,990±560, UCIAMS-101864). Aggradation may have been rapid, with an estimated rate of 0.34 cm/year (Figure 3-20). Two arctic ground squirrel nests are present at 10.8 and 15.0 m, which date to 30,160 and 28,210 cal yrs BP, respectively (25,920±180, UCIAMS-101914; 23,990±560, UCIAMS-101864). No *in situ* bones are present, however, detrital mammoth, horse, and bison fossils are common.

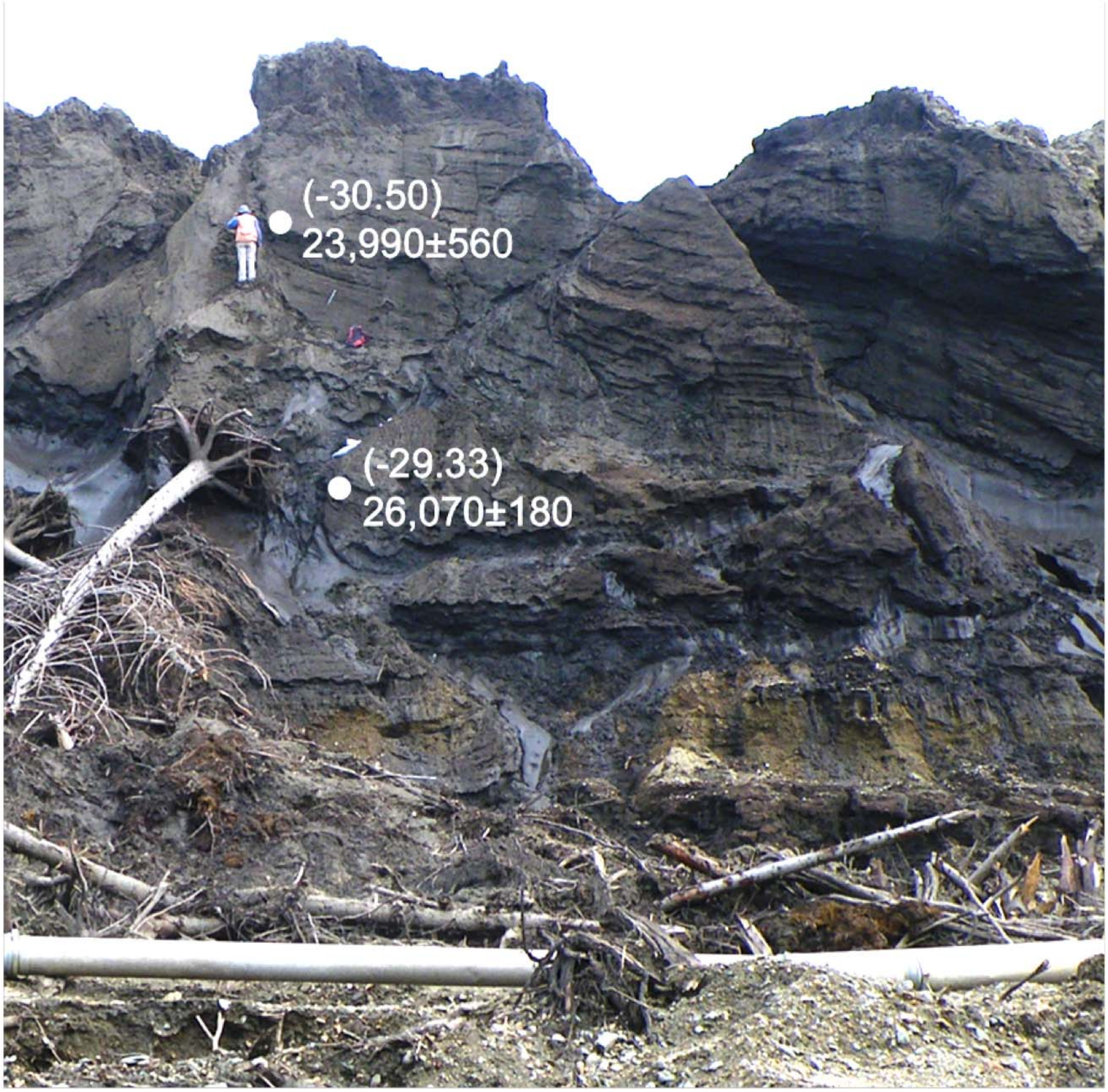

Figure 3-18 : Lower Quartz section containing 5 m of gravel and 15 m of overlying brown silt with large syngenetic ice wedges. This unit, exposed from 5.0 to 20.0 m, consists of brown silts including *in situ* graminoid vegetation and arctic ground squirrel nests.

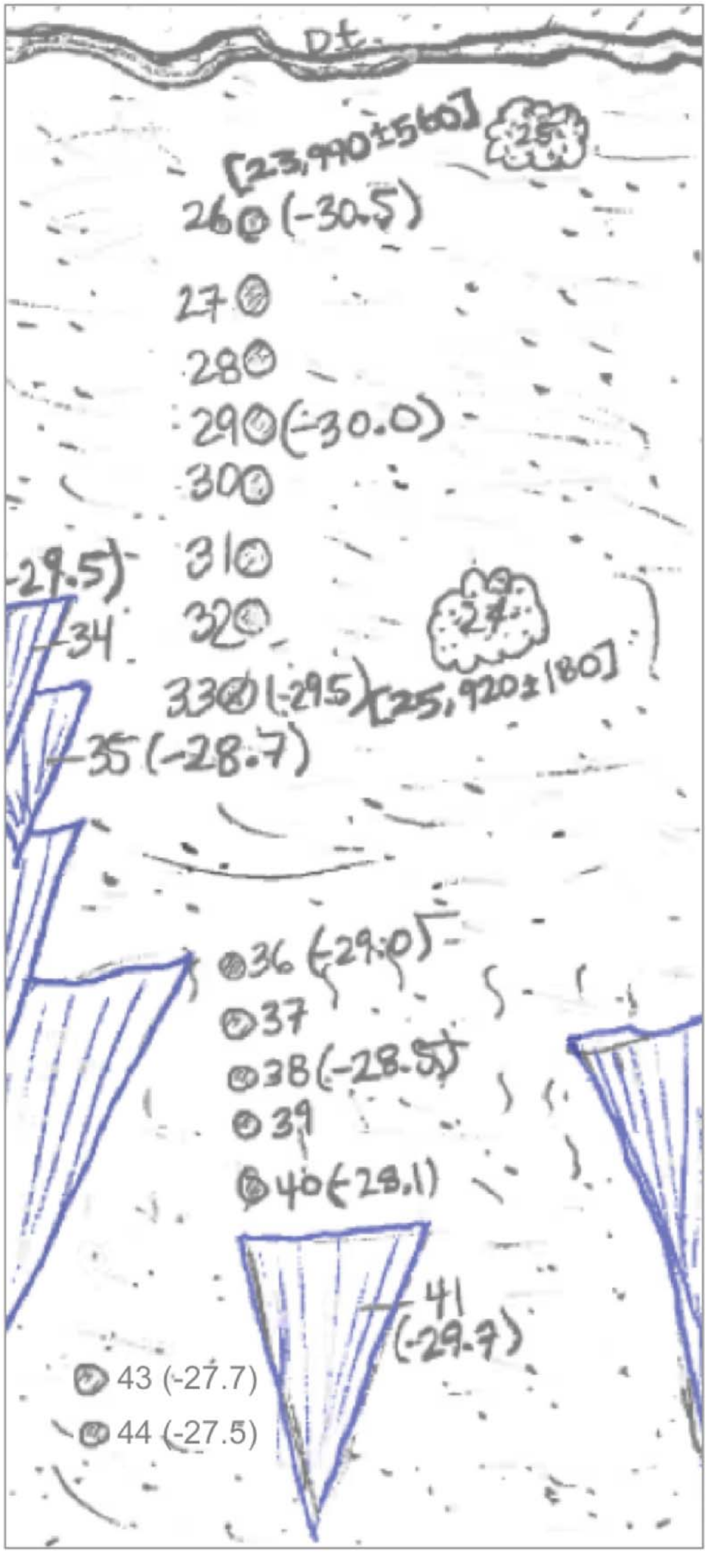

Figure 3-19 : Stratigraphic sketch of the Lower Quartz section. Dawson tephra (D.t.) is present near the top of the exposure. Numbers correspond to DF10 sample numbers (*e.g.* 26 is DF10-26).

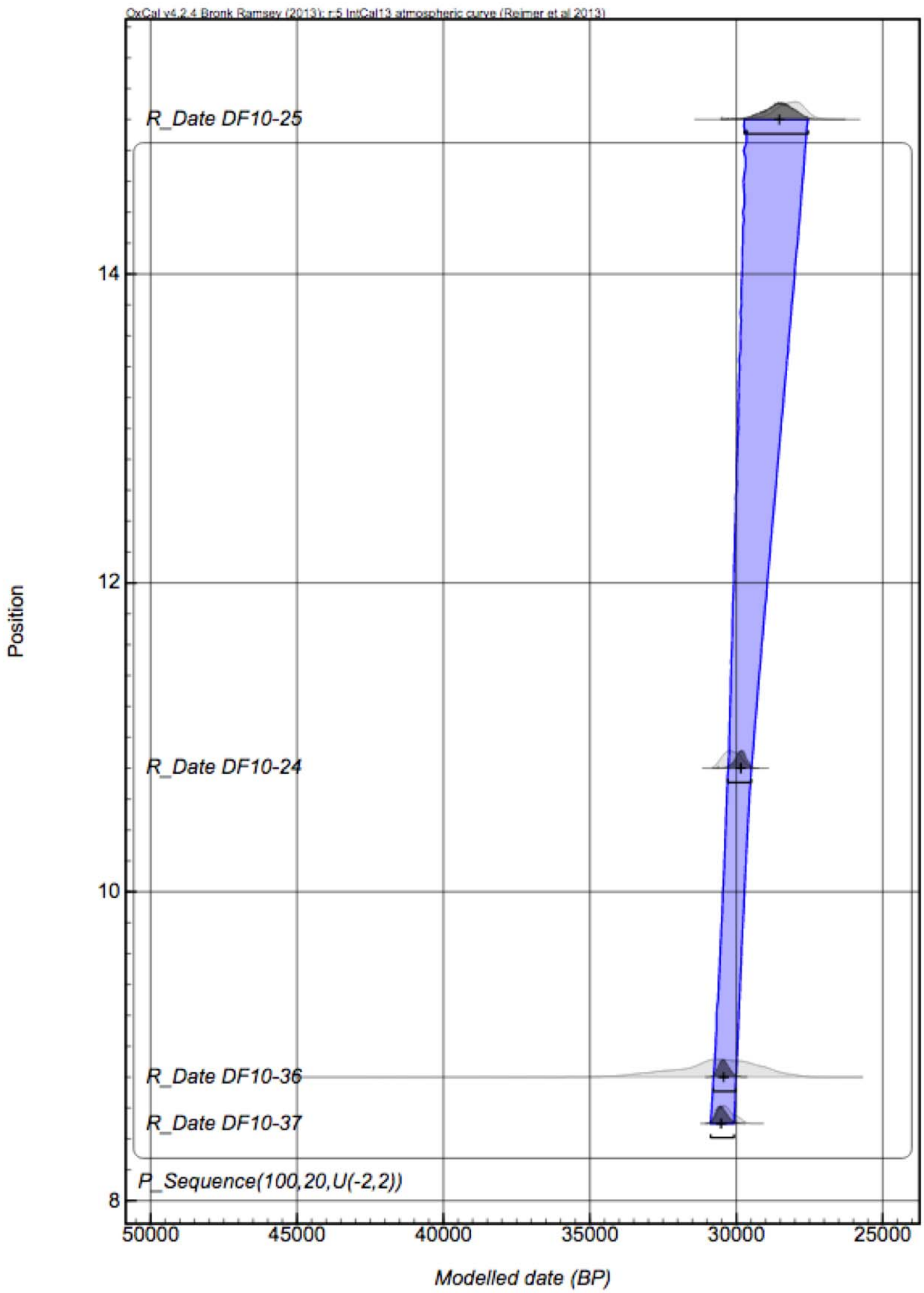

Figure 3-20 : Deposition model based on four radiocarbon dates from 8.5 to 15.0 m in the Lower Quartz exposure. The estimated aggradation rate for this interval is 0.34 cm/year. The relative position between samples is measured in meters.

Interpretations

Radiocarbon dates and the presence of Dawson tephra in this unit suggest the sediment from 5.0 to 20.0 m was deposited during the MIS 3 – MIS 2 transition. The presence of graminoid vegetation and arctic ground squirrel nests indicate cold, arid conditions with steppe-tundra vegetation during this interval. Total carbon and nitrogen have a general decline with height in the section suggesting a reduction in productivity in the landscape or perhaps less incorporation of carbon and nitrogen in sediments due to high aggradation rates. The average total carbon from this unit (3.2%; 1σ = 0.7%) is slightly higher, but comparable to total carbon contents at Quartz Creek reported by Sanborn et al. (2006) (2.5%; 1σ = 1.5%) around Dawson tephra time, *ca.* 29,375 cal yrs BP (25,300 ^{14}C yrs BP) (Zazula et al., 2006). Syngenetic wedges, common in the lower 11 m, are absent in the upper 9 m. Layered and lenticular cryostructures suggest syngenetic aggradation of permafrost. Water isotopes become more depleted with height in the section, suggesting cooling temperatures during the MIS 2 – MIS 3 transition associated with the onset of cold stage conditions. High rates of aggradation may be the result of increase loess production from the expanding ice sheets or it could be from sampling along dipping bedding planes at the site, as suggested by D. Froese (2014, *pers. comm.*). A comparable MIS 3 – MIS 2 transition unit from Upper Goldbottom has only moderate aggradation rates. Dipping beds may also explain an inverted date from an arctic ground squirrel nest (DF10-25) that was originally thought to be stratigraphically below Dawson tephra, but contains graminoid vegetation dated *ca.* 1,150 years after Dawson tephra time. Cryostratigraphy and paleoenvironmental indicators in this unit are in good agreement with a unit that is similar in age from the Upper Goldbottom site in this study. This unit is comparable to the Quartz Creek Member from Kotler and Burn (2000).

Upper Goldbottom

The Upper Goldbottom site is located in a valley 28 km south of Dawson on a tributary to the Klondike River. The Upper Goldbottom site consists of an 28.5 m high exposure of fine-grained sediment above a sharp contact with basal auriferous gravels. This exposure is subdivided into five units, from bottom to top: (1) 12.6 m of brown and grey organic silts with *in situ* shrub to graminoid vegetation, (2) 5.4 m of brown and grey silts with *in situ* graminoid vegetation and reworked twigs, (3) 4.5 m of grey silts with *in situ* graminoid vegetation,

(4) up to 4 m of black and grey organic-rich silts with abundant shrub and wood macrofossils, and (5) at least 2 m of silt with abundant large wood macrofossils (Figure 3-21, 3-22).

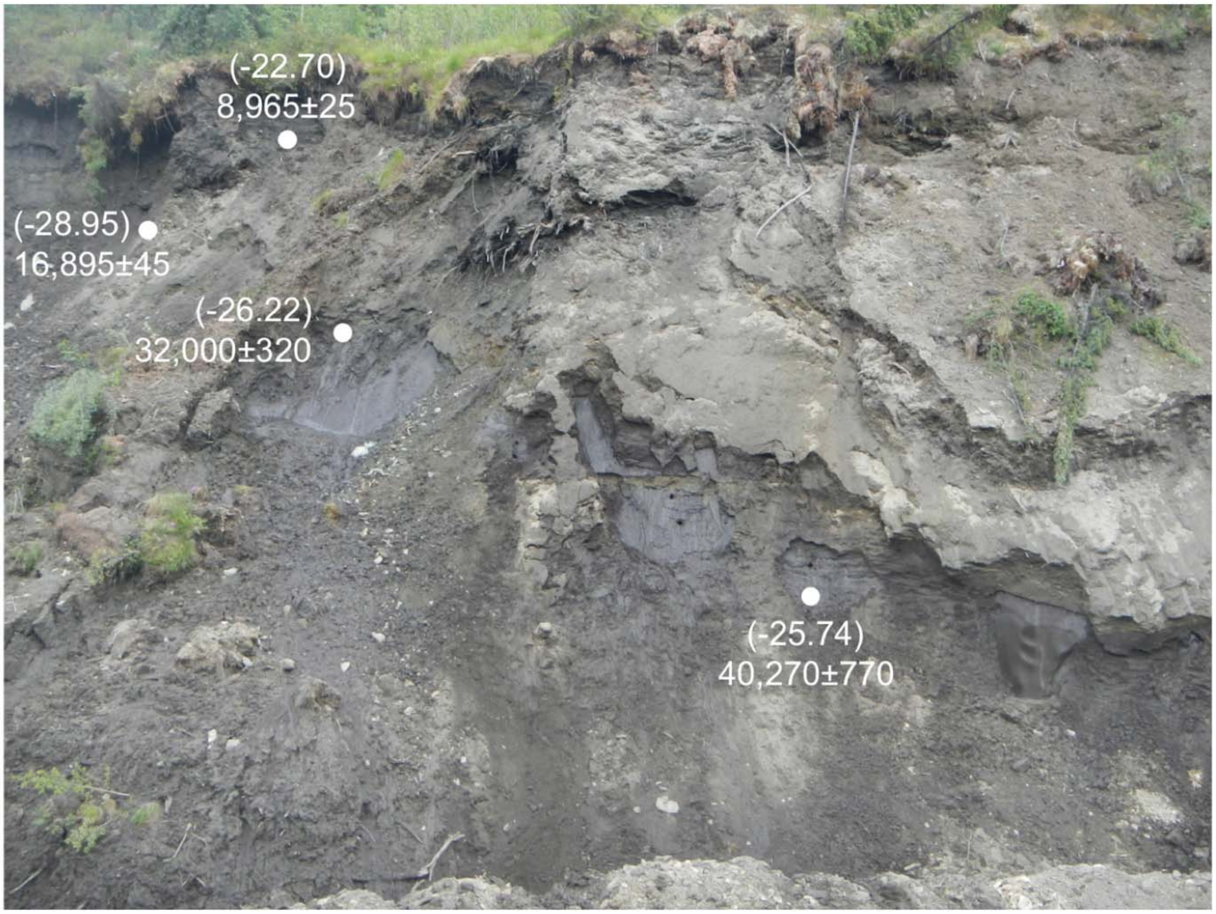

Figure 3-21 : The Upper Goldbottom site with a few of the dated samples. Contacts between units are obscured by slumped material.

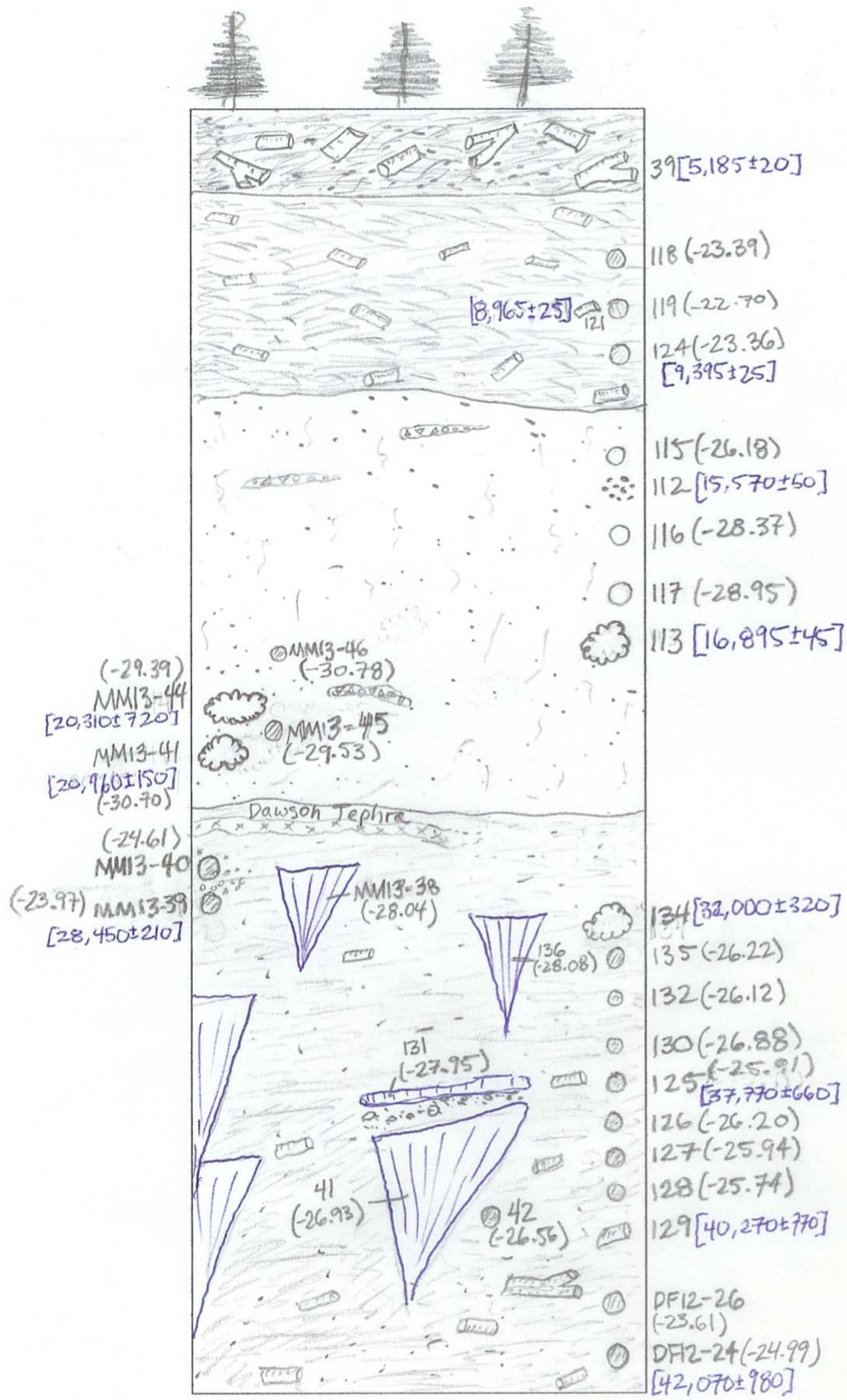

Figure 3-22 : Stratigraphic sketch of the Upper Goldbottom site. Sample numbers correspond to MM12 sample number unless otherwise specified.

Description

The lowermost unit, exposed from 0 to 12.6 m, consists of brown and grey silts including *in situ* fibrous organics, graminoid vegetation, and infrequent wood and shrub macrofossils (Figure 3-23). Lenses 10 – 20 cm thick of rust-brown sandy gravel and one 10 – 20 cm thick layer of clear segregated ice are present in this unit (Figure 3-24). The contact with underlying gravels is obscured by slumped material. Total carbon ranges from 4.6 to 6.3% and total nitrogen from 0.3 to 0.5%. Syngenetic ice wedges (1 – 3 m wide) are common throughout this unit. Non-parallel wavy lenticular (2 – 4 mm thick) and microlenticular cryostructures are present in otherwise structureless sediment. Water isotopes range from -28.08‰ to -23.61‰ $\delta^{18}O$ and -218.9‰ to -190.6‰ $\delta^{2}H$. Four radiocarbon dates indicate deposition between 45,650 and 35,895 cal yrs BP (42,070±980, UCIAMS-122274; 32,000±320, UCIAMS-114714). One arctic ground squirrel nest is present and dated to 35,895 cal yrs BP (32,000±320, UCIAMS-114714), which is the oldest arctic ground squirrel nest from the Klondike area with a finite radiocarbon date. Aggradation of this unit is estimated to be 0.08 cm/year from 43,985 to 35,895 cal yrs BP (Figure 3-25). Several *in situ* bones are present in the lower few meters and many detrital large mammal bones are found at the base of this unit, consisting of mostly bison and mammoth.

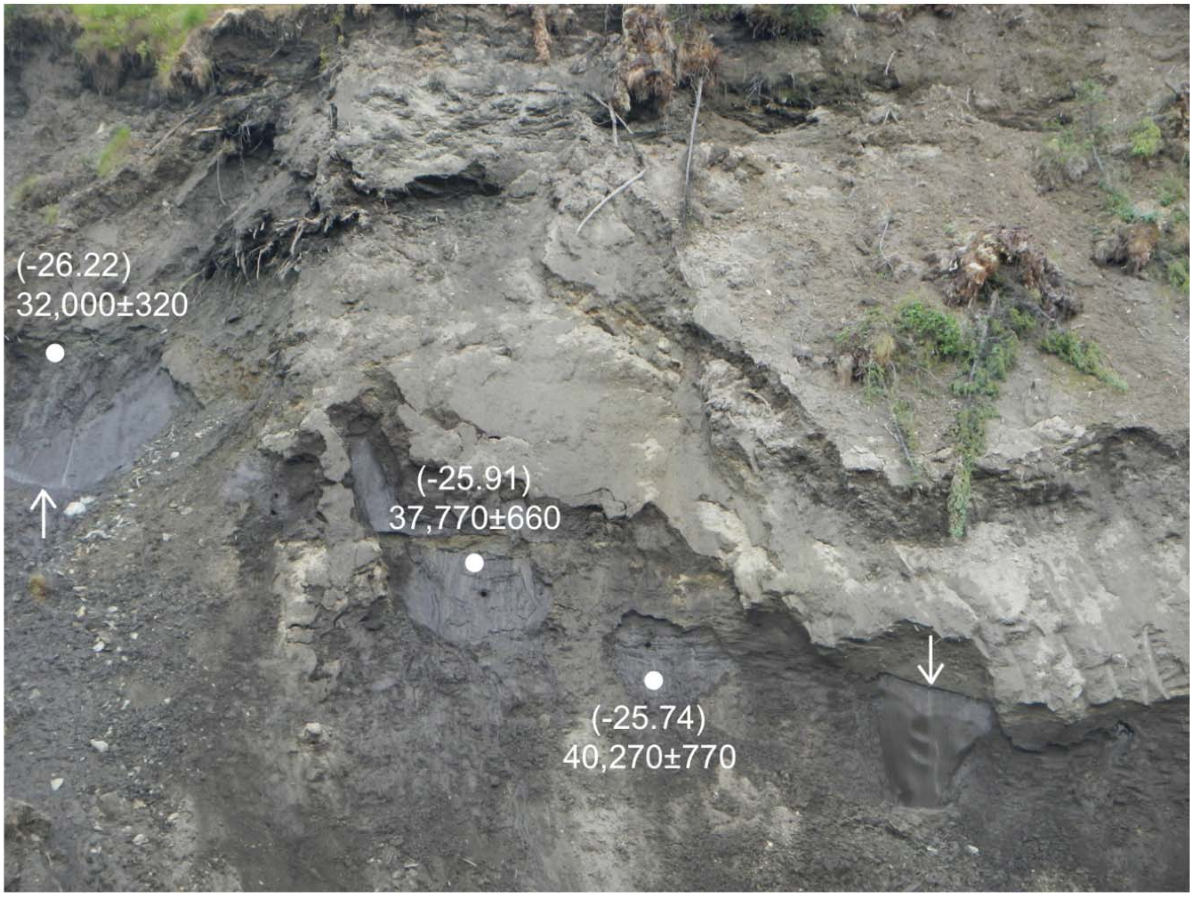

Figure 3-23 : The lowermost unit at the Upper Goldbottom site is exposed from 0 to 12.6 m and consists of brown silt including wood and shrub macrofossils in the lower 6 m and graminoid-dominated vegetation in the upper 6.6 m. Syngenetic ice wedges are indicated by the two arrows. Water isotopes have a general trend of becoming more depleted with height in the section. One arctic ground squirrel nest is present at 12.6 m (the uppermost sample indicated on the figure).

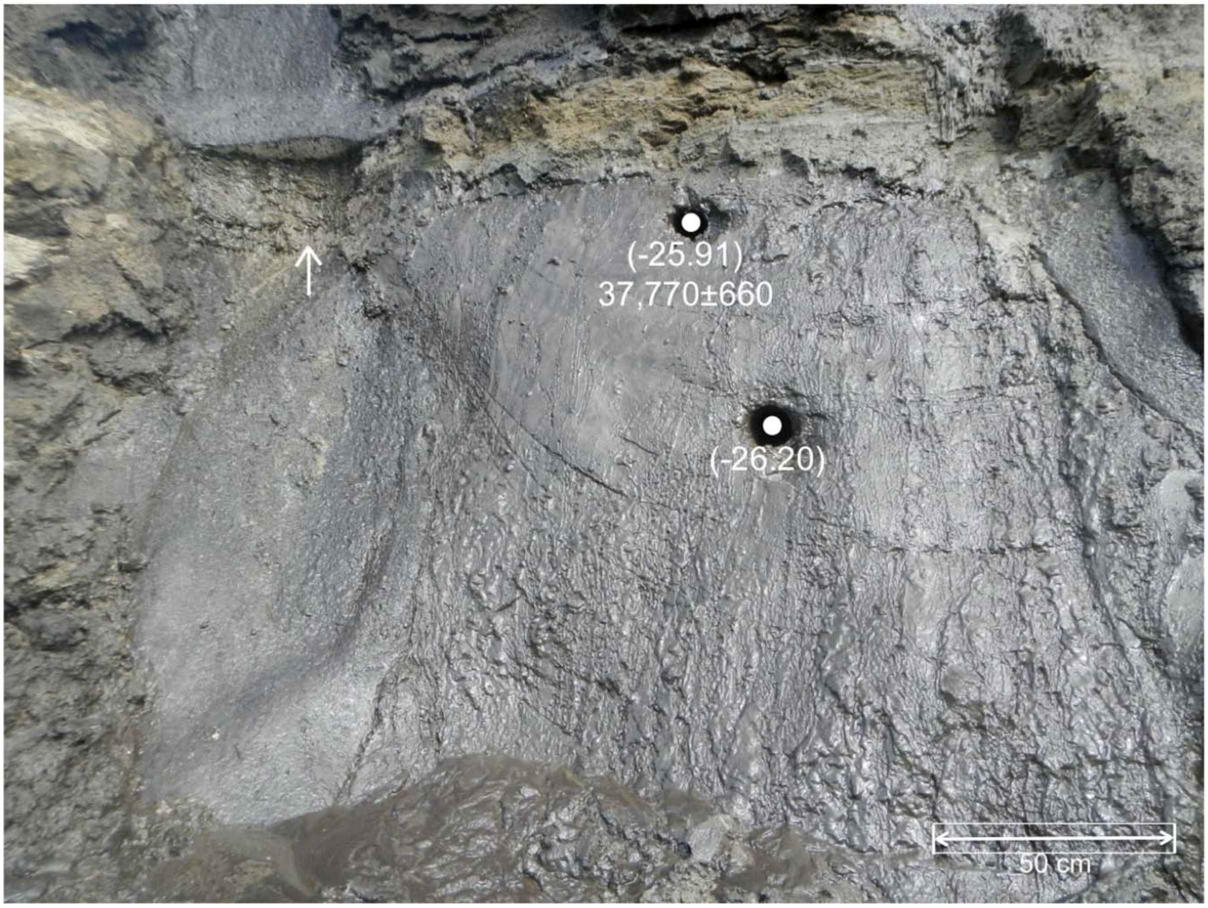

Figure 3-24 : The lowermost unit from ~7.0 to 9.0 m at Upper Goldbottom. This unit is characterized by brown silts including *in situ* graminoid and infrequent shrubby vegetation. A 10 – 20 cm layer of sandy gravels (at arrow) is overlain by 10 – 20 cm thick layer of clear ice.

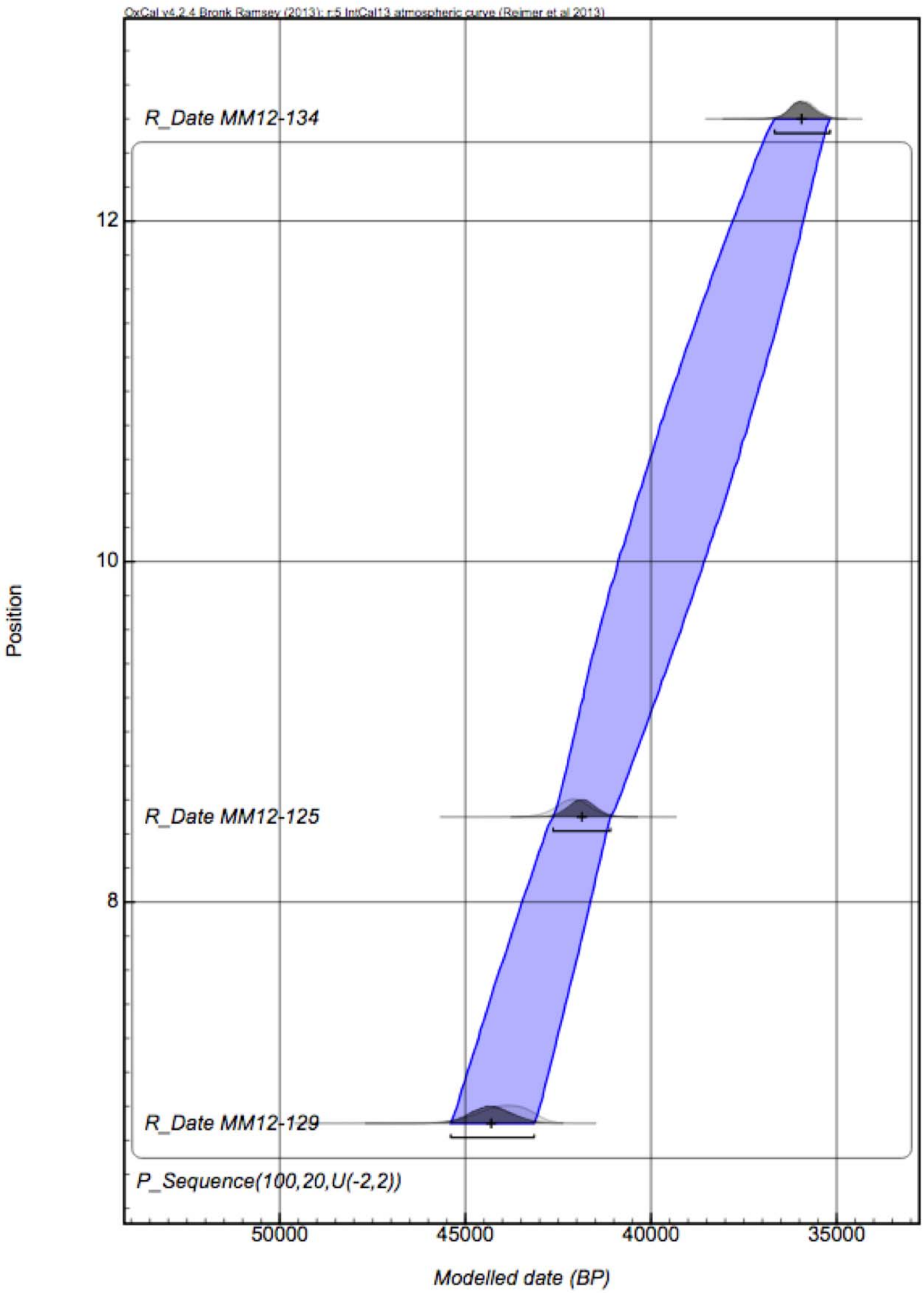

Figure 3-25 : Deposition model for the lowermost unit based on three radiocarbon dates from 6.7 to 12.6 m at the Upper Goldbottom site. The estimated aggradation rate for this interval is 0.08 cm/year. The relative position between samples is measured in meters.

The second unit, exposed from 12.6 to 18.0 m, consists of brown and grey silts including *in situ* fibrous organics, graminoid vegetation, and infrequent reworked wood and shrub macrofossils in sandy gravel lenses. No photographs of this unit were taken. Dawson tephra is present in a 10 cm thick layer at 17.7 m. The contact with the underlying unit is obscured by slumped material. Large syngenetic ice wedges (up to 3 m wide) are common throughout this unit. Water isotope values range from -28.04‰ to -23.97‰ $\delta^{18}O$ and -224.9‰ to -188.1‰ $\delta^{2}H$. One radiocarbon date below Dawson tephra indicates deposition rates of 0.07 cm/year between 32,385 and 29,400 cal yrs BP (28,450±210, UCIAMS-142201; Dawson tephra age from Zazula et al., 2006) (Figure 3-26). No other paleoenvironmental indicators were analyzed from this unit.

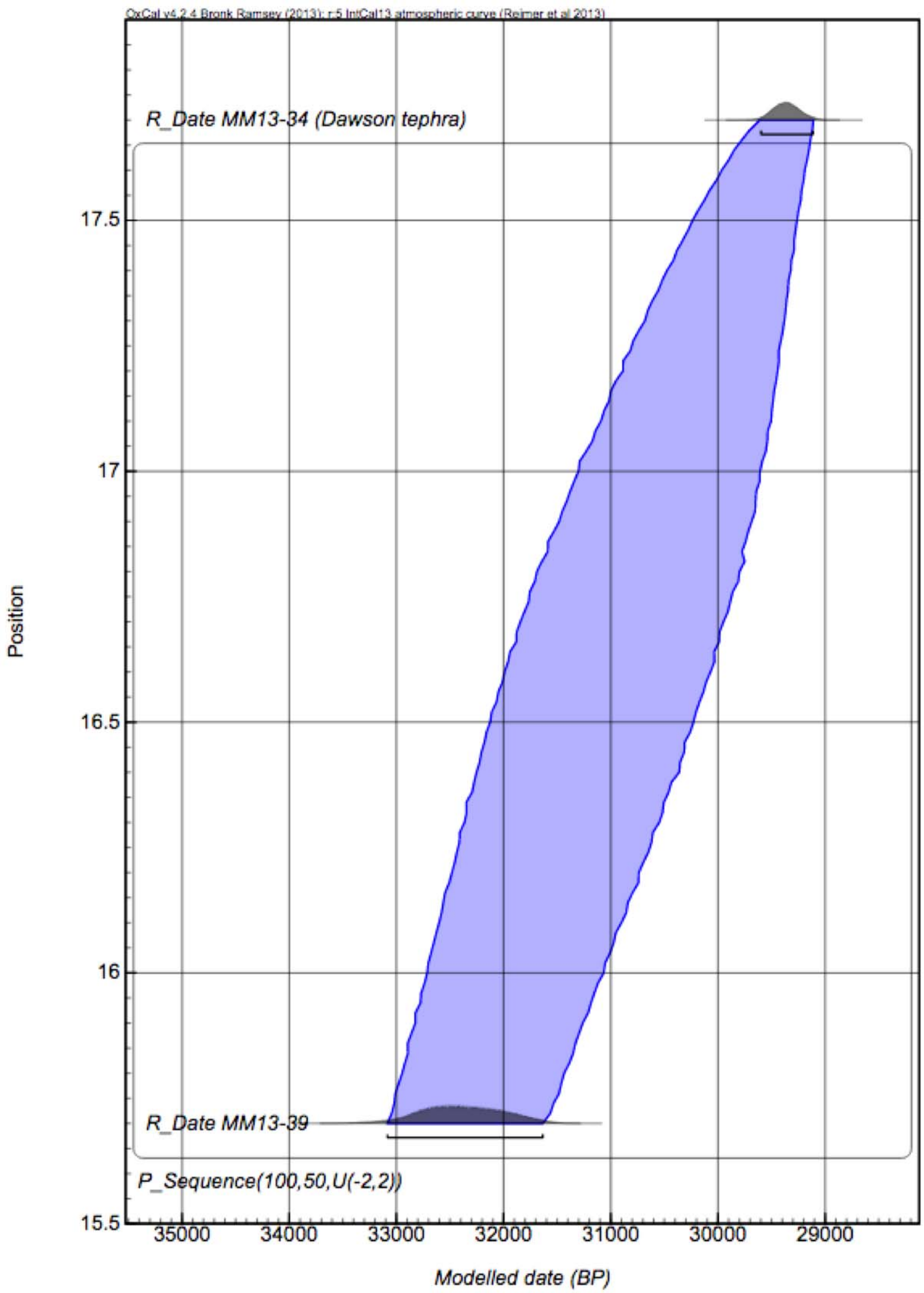

Figure 3-26 : Deposition model for the second unit based on one radiocarbon date at 15.7 m and the presence of Dawson tephra at 17.7 m from the Upper Goldbottom site. The estimated aggradation rate for this interval is 0.07 cm/year. The age of Dawson tephra is from Zazula et al. (2006). The relative position between samples is measured in meters.

The third unit, exposed from 18.0 to 22.5 m, consists of grey silts including *in situ* graminoid vegetation and a few thin (up to ~15 cm thick) lenses of gravel (Figure 3-27). We were unable to observe any contacts with other units due to slumping of material. Total carbon ranges from 1.2 to 2.1% and total nitrogen from 0.1 to 0.2%. This unit lacks syngenetic ice wedges, albeit one thin (20 cm wide) epigenetic ice wedge extends down from an overlying black organic-rich silt unit. The overlying black silt unit is unable to be sampled. Cryostratigraphy is characterized by zones of parallel wavy lenticular (2 – 4 mm thick) to microlenticular ice in otherwise structureless silts. Water isotopes in this unit range from -30.78‰ to -26.18‰ $\delta^{18}O$ and -232.6‰ to -208.2‰ $\delta^{2}H$. Based on four radiocarbon dates, this unit was deposited 25,285 to 18,820 cal yrs BP (20,960±150, UCIAMS-131095; 15,570±50, UCIAMS-122282). Aggradation rates are estimated to be 0.13 cm/year from 25,285 to 24,525 cal yrs BP, and 0.03 cm/year from 20,375 to 18,490 cal yrs BP (Figure 3-28, 3-29). Four arctic ground squirrel nests are present, three of which are radiocarbon dated from 25,285 to 20,375 cal yrs BP (20,960±150, UCIAMS-131095; 16,895±45, UCIAMS-114712).

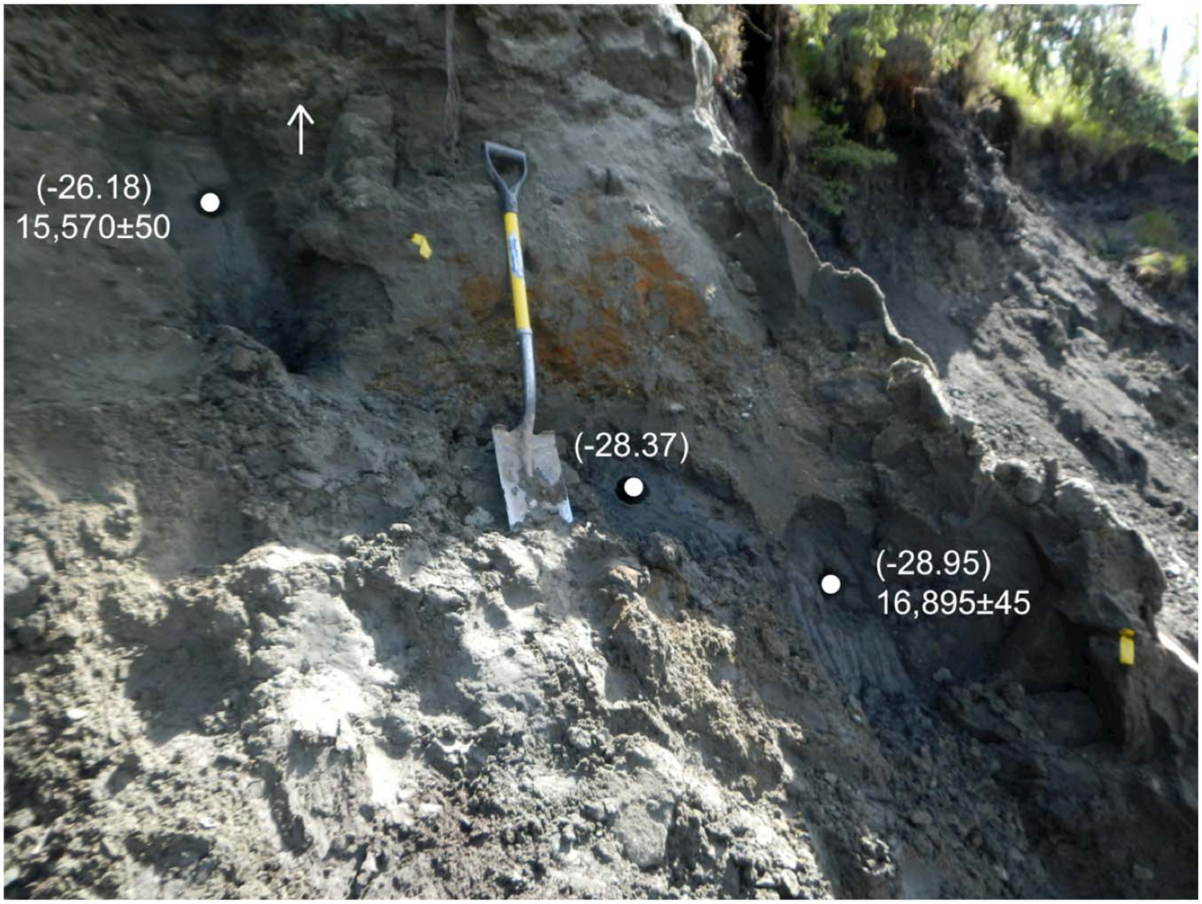

Figure 3-27 : The third unit at the Upper Goldbottom site is exposed from 18.0 to 22.5 m and consists of grey silts including *in situ* graminoid vegetation and arctic ground squirrel nests. Overlying sandy gravels are indicated by the arrow. Shovel is ~1.2 m high.

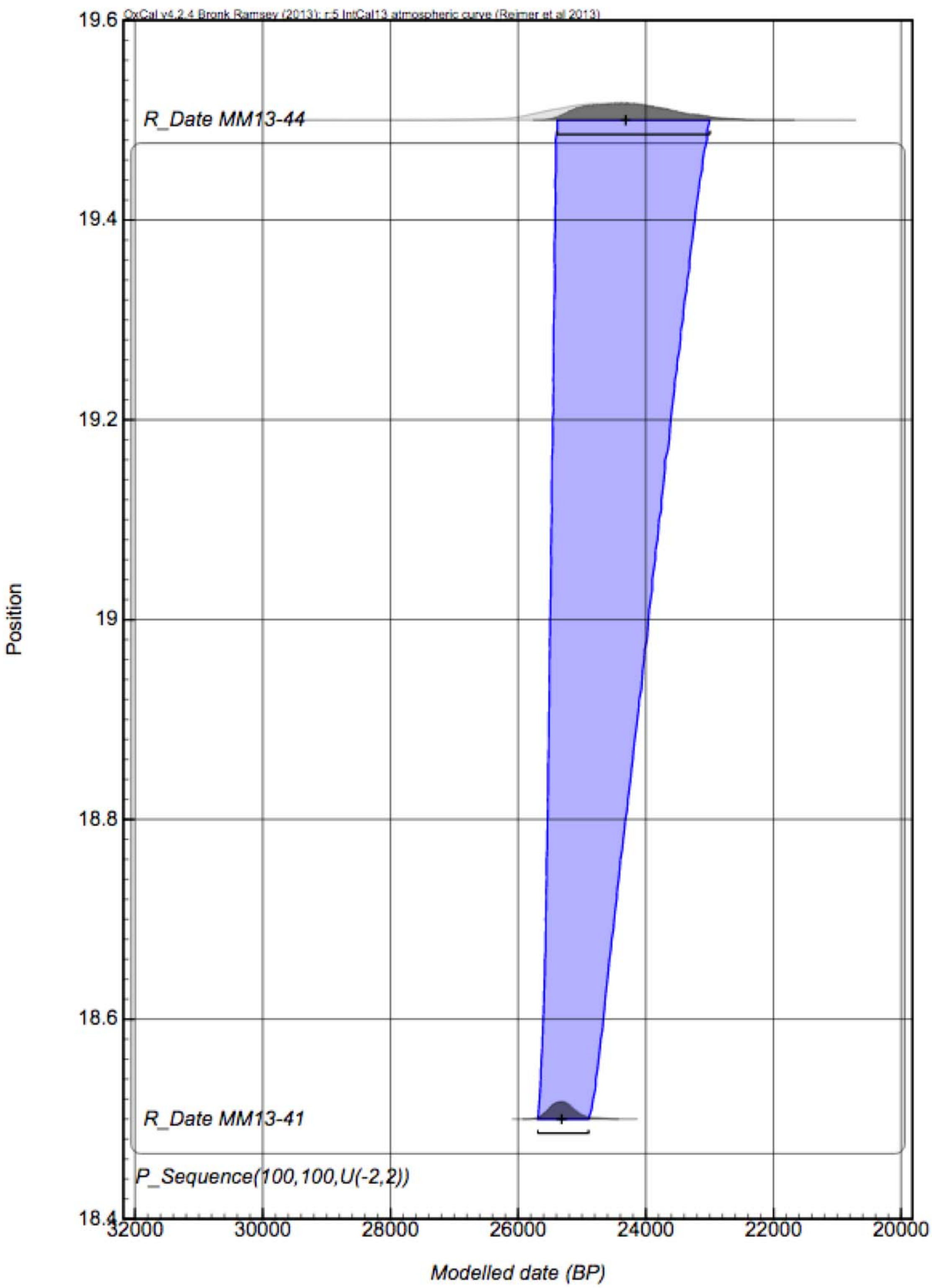

Figure 3-28 : Deposition model for the third unit based on two radiocarbon dates at 18.5 and 19.5 m from the Upper Goldbottom site. The estimated aggradation rate for this interval is 0.13 cm/year. The relative position between samples is measured in meters.

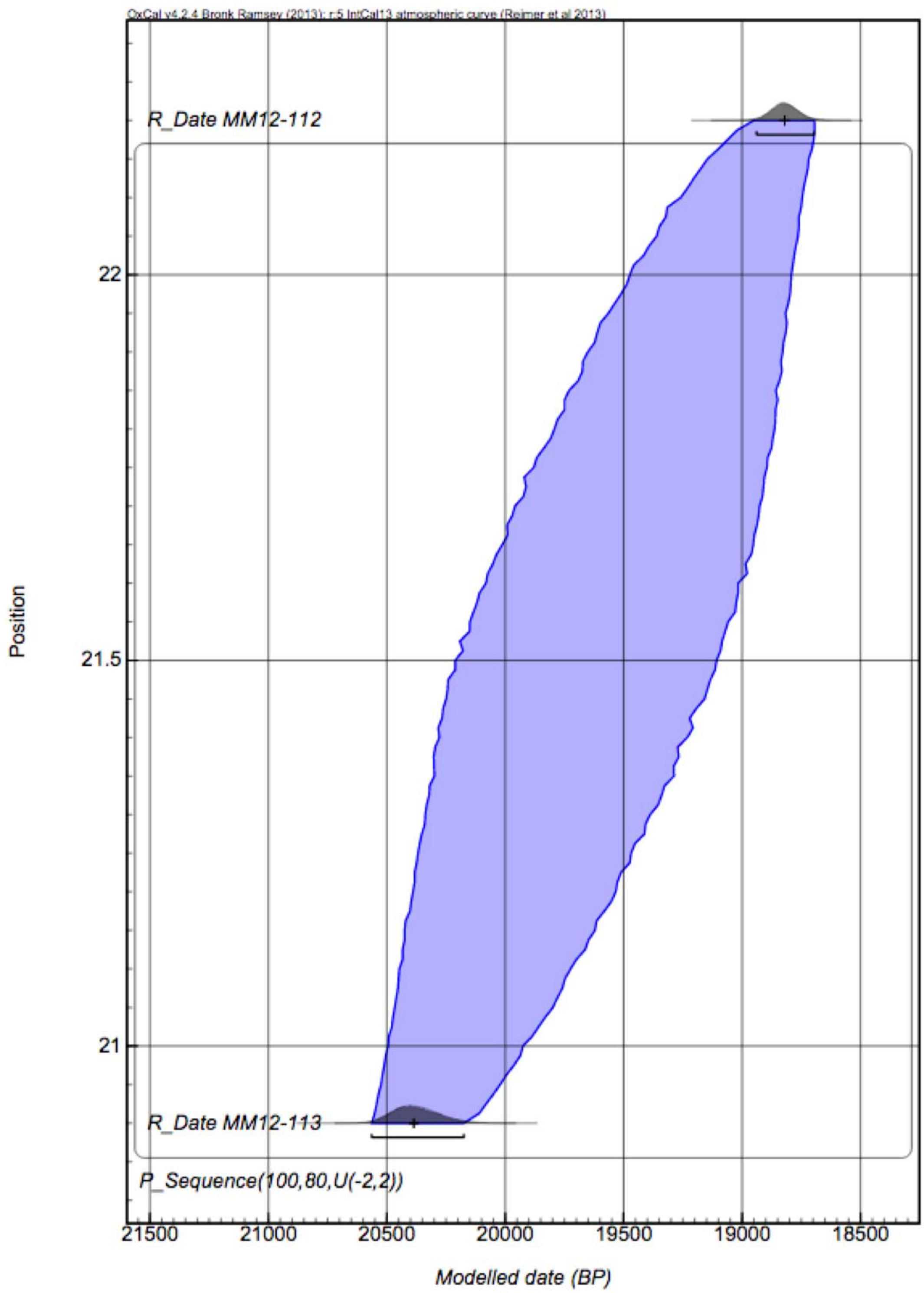

Figure 3-29 : Deposition model for the third unit based on two radiocarbon dates at 20.9 and 22.2 m from the Upper Goldbottom site. The estimated aggradation rate for this interval is 0.03 cm/year. The relative position between samples is measured in meters.

The fourth unit, exposed from 22.5 to 26.5 m, consists of black and grey organic-rich silts including *in situ* graminoid and shrub vegetation with thin (5 – 15 cm) interbedded lenses of sand and gravels (Figure 3-30). An adjacent exposure dated to the same interval has relatively less plant material in green-grey silts and interbedded humified brown organics, reworked shrub and graminoid vegetation, and lenses of sands and gravels up to 15 cm thick (Figure 3-31). A sharp basal contact separates the underlying sediment. The upper 2 m of this unit is sediment-rich aggradational ice that is unable to be sampled. Total carbon ranges from 3.6 to 5.4% and total nitrogen from 0.25 to 0.34%. No ice wedges are present. Cryostructures are characterized by non-parallel wavy lenticular (4 – 16 mm thick) within otherwise structureless (ice-poor) sediment. Water isotopes range from -23.39‰ to -22.70‰ $\delta^{18}O$ and -180.0‰ to -172.8‰ $\delta^{2}H$. Based on three radiocarbon dates, deposition of this unit began *ca.* 10,600 cal yrs BP (9,395±25, UCIAMS-114910). Aggradation rates are not estimated for this unit due to the radiocarbon samples being laterally-offset ~10 m.

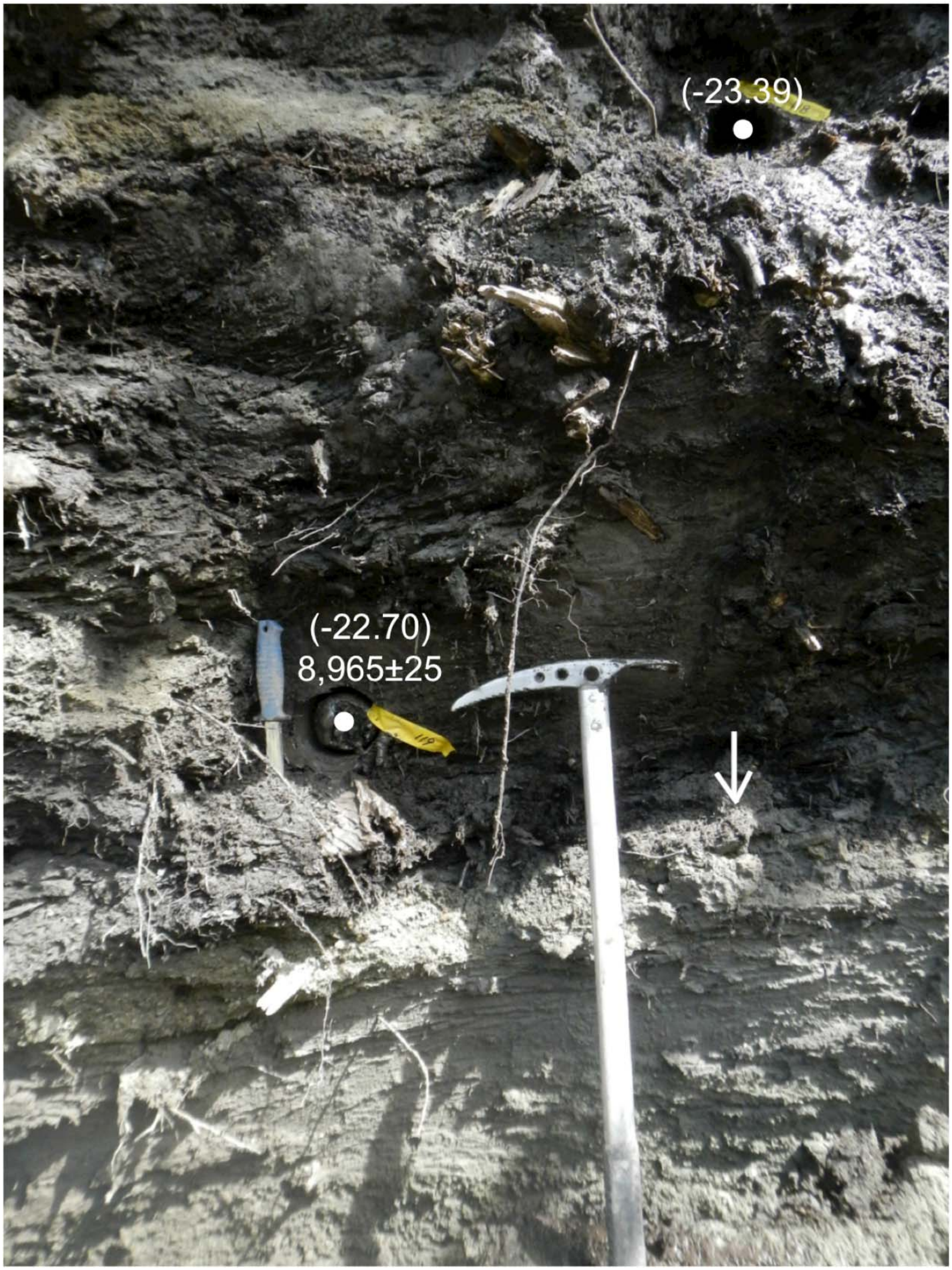

Figure 3-30 : The fourth unit at the Upper Goldbottom site (above arrow) is exposed from 22.5 to 26.5 m and consists of organic-rich black and grey silts with graminoid and shrubby vegetation. There is a sharp basal contact (at arrow) with underlying grey silts of the second unit. Width of ice axe head is 21 cm.

Figure 3-31 : The upper 2 m of the fourth unit exposed from 24.5 to 26.5 m at the Upper Goldbottom site. This unit consists of green-grey silts and gravelly sands including interbedded humified brown silts with shrub and graminoid vegetation. Knife handle is 11 cm long.

The uppermost unit, exposed from 26.5 to 28.5 m, consists of a layer of black silts including abundant randomly-oriented broken wood macrofossils. This unit is unable to be reached for sampling except to recover a piece of wood for radiocarbon dating. This unit has a sharp, undulating basal contact. One large woody macrofossil is radiocarbon dated to 5,945 cal yrs BP (5,185±20, UCIAMS-114898).

Interpretations

Radiocarbon dates in the lowermost unit suggests the sediment from 0 to 12.6 m was deposited during the late MIS 3. Basal contact is obscured by slumped material. Vegetation trends from graminoid vegetation with numerous wood and shrub macrofossils from 0 to 6.0 m to graminoid-dominated vegetation from 6.0 to 12.6 m, which suggests a trend to more arid conditions during the MIS 3 – MIS 2 transition. The earliest arctic ground squirrel nest in this study is at 12.6 m, suggesting the presence of steppe-tundra vegetation by *ca.* 36,000 cal yrs BP. Lenses of rust-brown sandy gravels suggest the presence of minor local tributary influences at the site during this interval. A 10 – 20 cm thick layer of pure ice may be a buried snowbank, which has isotopic values comparable to an adjacent ice wedge. Total carbon and nitrogen contents are high in the lower 6 m and suggest productive environments during this interval. Carbon and nitrogen contents are not determined from 6.0 to 12.6 m. Large syngenetic ice wedges and lenticular and microlenticular cryostructures suggest syngenetic aggradation of permafrost. Moderately depleted isotopes suggest slightly colder-than-present mean annual air temperatures associated with interstadial conditions. Water isotopes become more depleted with height, suggesting dropping air temperatures associated with the onset of cold stage conditions during the MIS 3 – MIS 2 transition. Aggradation rates during this interval are moderate. Cryostratigraphy and paleoenvironmental indicators in this unit are in good agreement with a unit of similar age from the Upper Hunker site in this study, albeit with less abundant vegetation and colluvium. Water isotopes from this unit are comparable to the Last Chance Creek Member values from Kotler and Burn (2000).

One radiocarbon date and the presence of Dawson tephra in the second unit suggests the sediment from 12.6 to 18.0 m was deposited during the late MIS 3 to early MIS 2. Basal contact is obscured by slumped material. Sediment contains *in situ* graminoid vegetation with few reworked shrub macrofossils, which suggests a trend more arid conditions during the MIS 3 – MIS 2 transition. Total carbon and nitrogen contents are not determined for this unit. Large syngenetic ice wedges suggest syngenetic aggradation of permafrost. Moderately depleted isotopes suggest slightly colder-than-present mean annual air temperatures associated with interstadial conditions. Aggradation rates during this interval are lower than the estimated rate from Lower Quartz (0.34 cm/year). Lower Quartz stratigraphic relations may be compromised however by dipping bedding planes along the exposed face (D. Froese 2014, *pers. comm.*). Water isotopes in this unit are slightly enriched compared to the Lower Quartz site. The presence of reworked woody material in sandy gravel lenses in this unit suggests that there may be local reworking of material. This unit is comparable to the Quartz Creek Member from Kotler and Burn (2000).

Radiocarbon dates from the third unit suggest the sediment from 18.0 to 22.5 m was deposited during the height of the last cold stage. The basal contact of this unit is obscured by slumped material. The presence of arctic ground squirrels and *in situ* graminoids indicate steppe-tundra vegetation. Low total carbon and nitrogen values suggest relatively sparse vegetation cover when compared to MIS 3 values in the lowermost unit. One enriched epigenetic ice wedge extends downward from overlying organic-rich sediment which is unable to be sampled. Cryostructures are lenticular and microlenticular, suggesting syngenetic aggradation of permafrost. The most depleted water isotopes from this site are from this unit, suggesting cold temperatures associated with cold stage conditions. Aggradation is moderate to low, possibly due to a lack of woody vegetation that would entrap windblown silts (loess). Cryostratigraphy and paleoenvironmental indicators in this unit are in good agreement with units of similar age from the Black Hills and Lower Hunker sites. This unit is comparable to the Quartz Creek Member from Kotler and Burn (2000).

Radiocarbon dates from the fourth unit suggest the sediment from 22.5 to 26.5 m was deposited during the early Holocene. The basal contact with the third unit is sharp and unconformable. Shrub vegetation is present, suggesting warmer and wetter conditions than were present during the last cold stage. Total carbon and nitrogen contents are higher than last cold stage soils and slightly less than the boreal forest soils of the lowermost unit. The presence of lenticular cryostructures suggests syngenetic aggradation of permafrost. Water isotopes are similar to modern precipitation, suggesting warm temperatures associated with interglacial conditions. Aggradation rates are not determined. Cryostratigraphy and paleoenvironmental indicators in this unit are in good agreement with a unit similar in age from the Lucky Lady II and Lower Hunker sites in this study. This unit is comparable to the "Organic unit" from Kotler and Burn (2000).

Radiocarbon dates from the fifth unit suggest the sediment from 26.5 to 28.5 m was deposited during the mid-Holocene. The contact with underlying sediment is sharp and unconformable. Large Holocene wood is indicative of boreal forests. Cryostructures, total carbon and nitrogen, and other paleoecological indicators in this unit are not defined. The broken, randomly-oriented wood may be the result of thaw slumping of organic-rich sediment into valley-bottoms, and is in good agreement with the mid-Holocene unit at Upper Quartz. This unit may be comparable to the “Organic unit” from Kotler and Burn (2000).

Lucky Lady II

The Lucky Lady II site is located in the middle of a broad valley 46 km south of Dawson on a tributary to the Indian River. An 11.5 m section of the exposure is sampled and can be divided into two units: (1) 3.5 m of grey silts with *in situ* graminoid vegetation, overlain by (2) 8 m of organic-rich grey and black silts with *in situ* shrub vegetation (Figure 3-32, 3-33). The contact between the two units is defined by the appearance of shrubby vegetation. This site has had a series of five vertical cores drilled that range from 2.4 to 4.3 m each, which allow for high-resolution isotope and radiocarbon analyses across the boundary between the silt and organic units (scans of all cores are in Appendix F). In all, 96 water isotope values and 27 radiocarbon dates from Lucky Lady II are included in this study.

Figure 3-32 : General view of the Lucky Lady II section. A sharp contact (at arrow) separates grey silts including *in situ* graminoid vegetation of the lower unit, sampled from 0 to 3.5 m, from the upper unit, which is sampled from 3.5 to 11.5 m and consists of organic-rich black and grey silts including *in situ* shrub and graminoid vegetation.

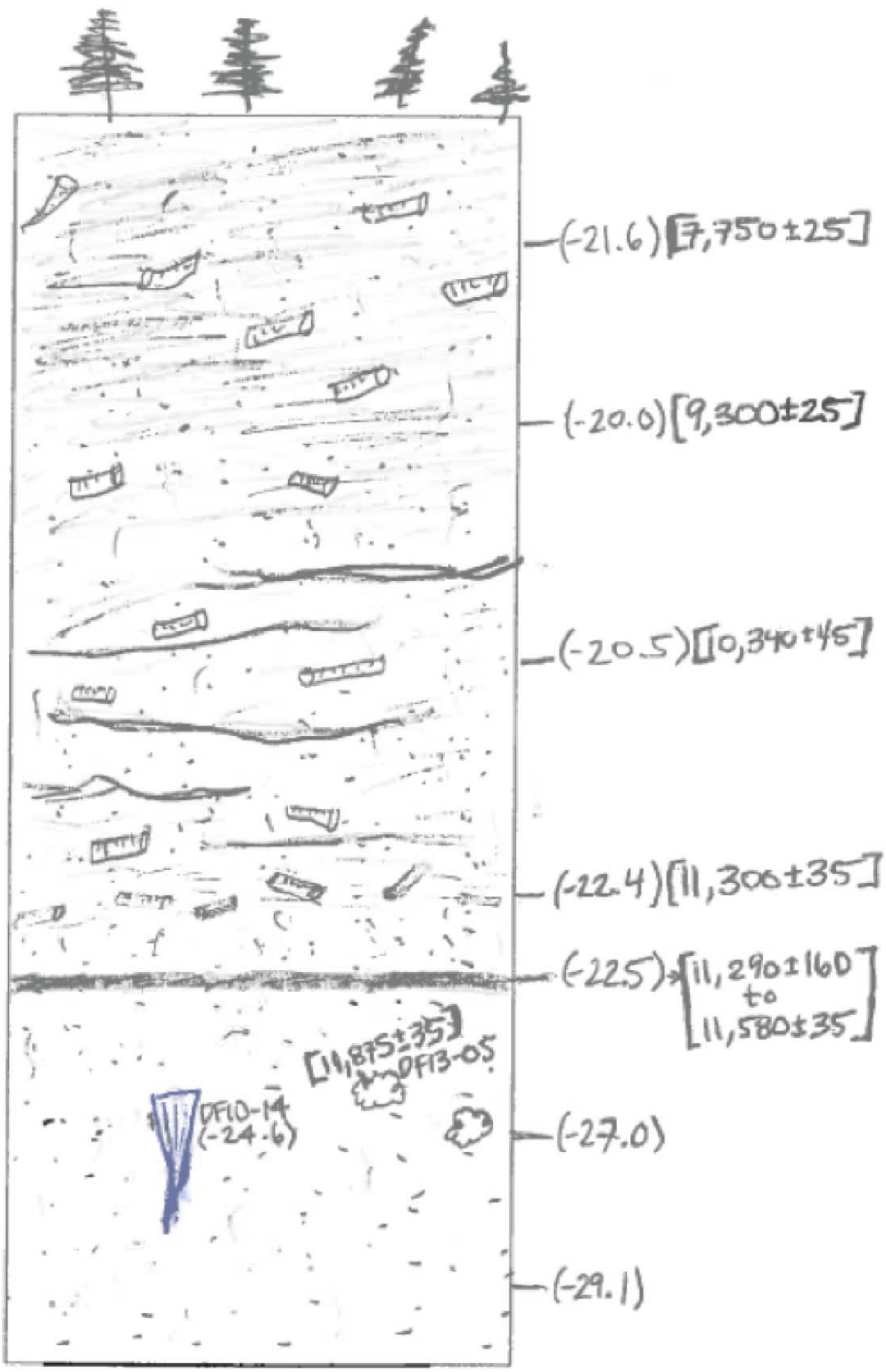

Figure 3-33 : Stratigraphic sketch of the Lucky Lady II exposure. Water and radiocarbon samples in the figure are only a few of the total number of samples analyzed from the five vertical cores (LL2A, LL2B, LL2C, LL2S, and LL2-12).

Description

The lowermost unit, exposed from 0 to 3.5 m, consists of grey silts including *in situ* graminoid vegetation (Figure 3-34). A ~4 – 6 cm laterally-continuous black organic-rich horizon is present 80 cm below the overlying unit in otherwise grey silts including *in situ* graminoid vegetation (Figure 3-35). This black horizon has four radiocarbon dates between 13,410 to 13,140 cal yrs BP (11,580±35, UCIAMS-143308; 11,290±160, UCIAMS-56390). A series of thinner black horizons are interspersed from 2.7 to 3.5 m. Total carbon ranges from 1.0 to 1.9% and total nitrogen ranges from 0.1 to 0.2%. One thin syngenetic ice wedge (~30 cm wide) is located ~3 m below the top of this unit. Cryostratigraphy is characterized by 1 – 3 mm thick parallel wavy lenticular cryostructures in otherwise structureless (ice-poor) sediment. Water isotopes range from -29.14‰ to -21.18‰ $\delta^{18}O$ and -220.3‰ to -167.7‰ $\delta^{2}H$. The isotopic ratios generally become more enriched with height. This unit was deposited from *ca.* 16,500 to 13,150 cal yrs BP (13,680±35, UCIAMS-51324; 11,290±160, UCIAMS-56390). Aggradation of this unit is estimated to be 0.12 to 0.62 cm/year (Figure 3-36, 3-37). Three arctic ground squirrel nests have been dated from this unit and range in age from 16,500 to 13,675 cal yrs BP (13,680±35, UCIAMS-51324; 11,875±35, UCIAMS-131092). Several *in situ* horse and bison bones are present.

Figure 3-34 : The lowermost unit at the Lucky Lady II site is exposed from 0 to 3.5 m and consists of grey silts with *in situ* graminoid vegetation and a ~4 – 6 cm laterally-continuous black organic-rich horizon (at arrow) 80 cm below the top of this unit. Ice axe is 80 cm high.

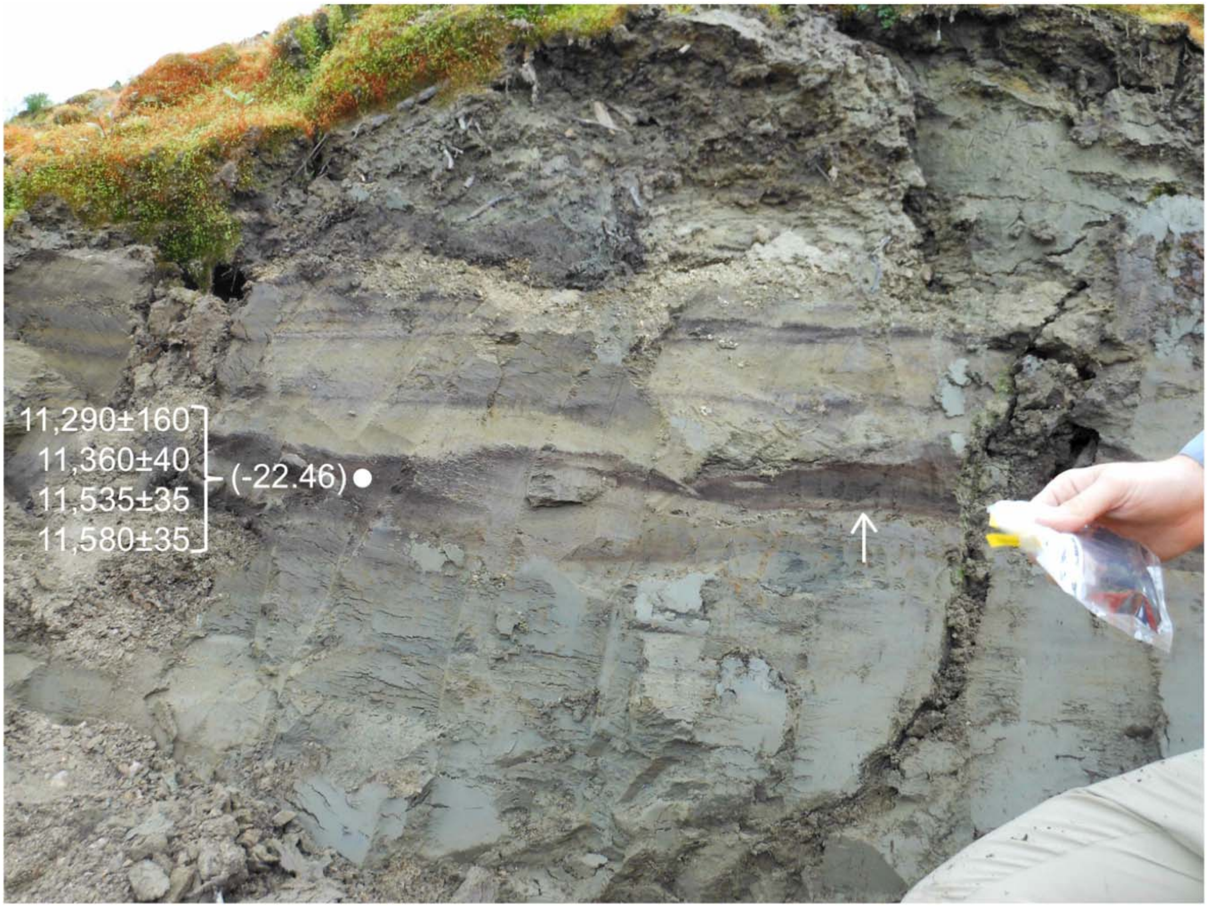

Figure 3-35 : The lowermost unit at Lucky Lady II includes a distinct ~4 – 6 cm thick, laterally-continuous black organic horizon at 2.7 m (at arrow). This black horizon has four radiocarbon dates ranging from 13,410 to 13,140 cal yrs BP (11,580±35, UCIAMS-143308; 11,290±160, UCIAMS-56390). A series of thinner black horizons are present throughout the section above this black layer.

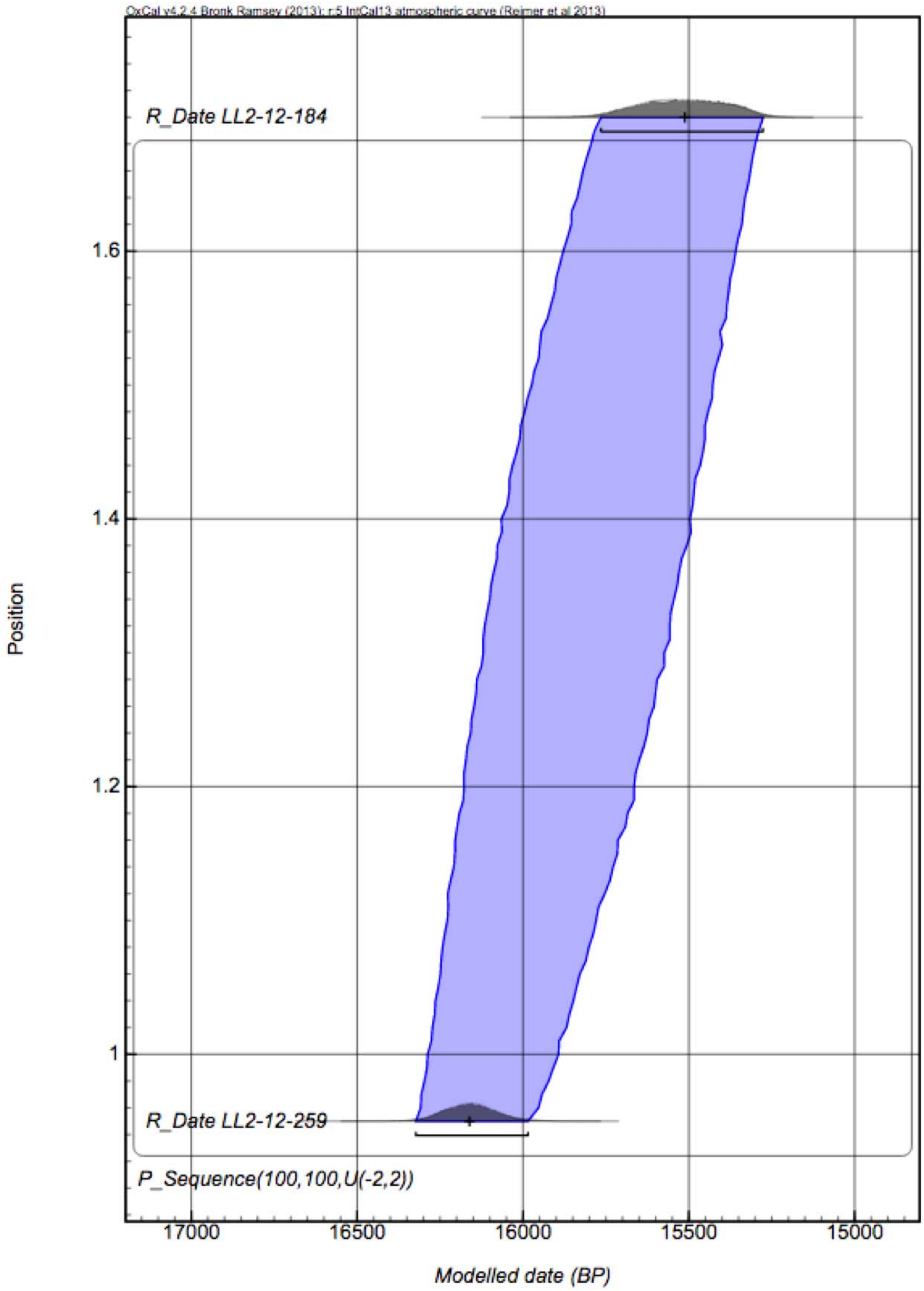

Figure 3-36 : Deposition model for the lower unit at Lucky Lady II based on two radiocarbon dates from 0.95 to 1.70 m. The estimated aggradation rate for this interval is 0.12 cm/year. The relative position between samples is measured in meters.

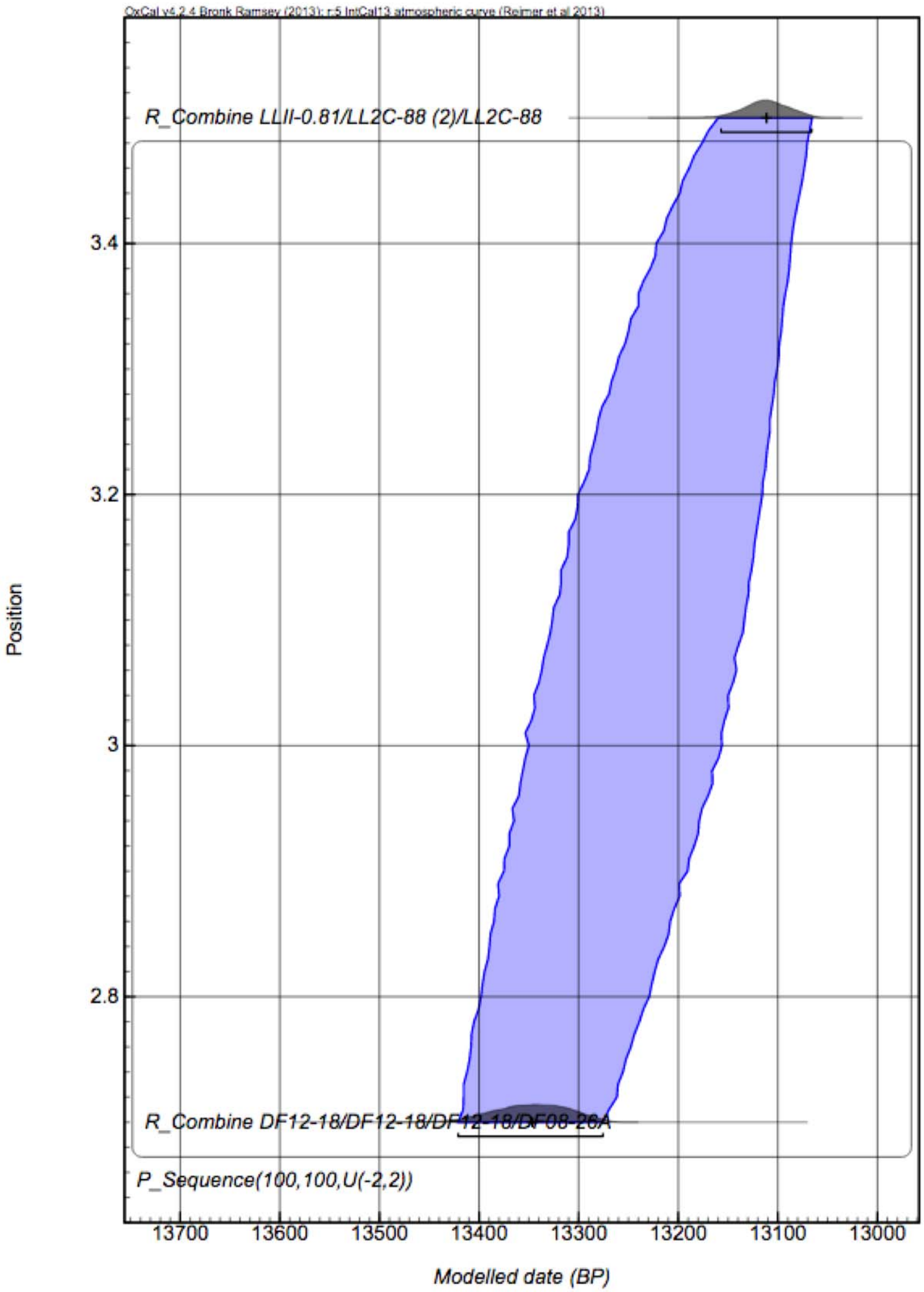

Figure 3-37 : Deposition model for the lower unit at Lucky Lady II based on seven radiocarbon dates from 2.70 to 3.50 m. The estimated aggradation rate for this interval is 0.62 cm/year. The relative position between samples is measured in meters.

The second unit, exposed from 3.5 to 11.5 m, consists of grey and black silts including *in situ* shrub and graminoid vegetation (Figure 3-38). The sediment in this unit generally becomes more organic-rich with height. Black organic horizons typically ~2 – 6 cm thick are interspersed throughout this unit. Total carbon ranges from 1.1 to 6.0% and total nitrogen ranges from 0.1 to 0.5%. No ice wedges are present. Cryostructures are mainly parallel lenticular (~2 mm thick) and microlenticular to structureless. Water isotopes average -21.02‰ $\delta^{18}O$ ($1\sigma = 0.62$‰) and -166.0‰ $\delta^{2}H$ ($1\sigma = 4.7$‰). This unit was deposited 13,150 to 8,525 cal yrs BP (11,300±35, UCIAMS-142197; 7,750±25, UCIAMS-143296). Aggradation of this unit is estimated to be 0.12 to 0.19 cm/year (Figure 3-39, 3-40, 3-41). No fossils are present *in situ* in this unit.

Figure 3-38 : The upper unit (above arrow) is sampled from 3.5 to 11.5 m at Lucky Lady II and consists of black and grey silts with abundant *in situ* shrub and graminoid vegetation. This unit generally becomes more organic-rich with height.

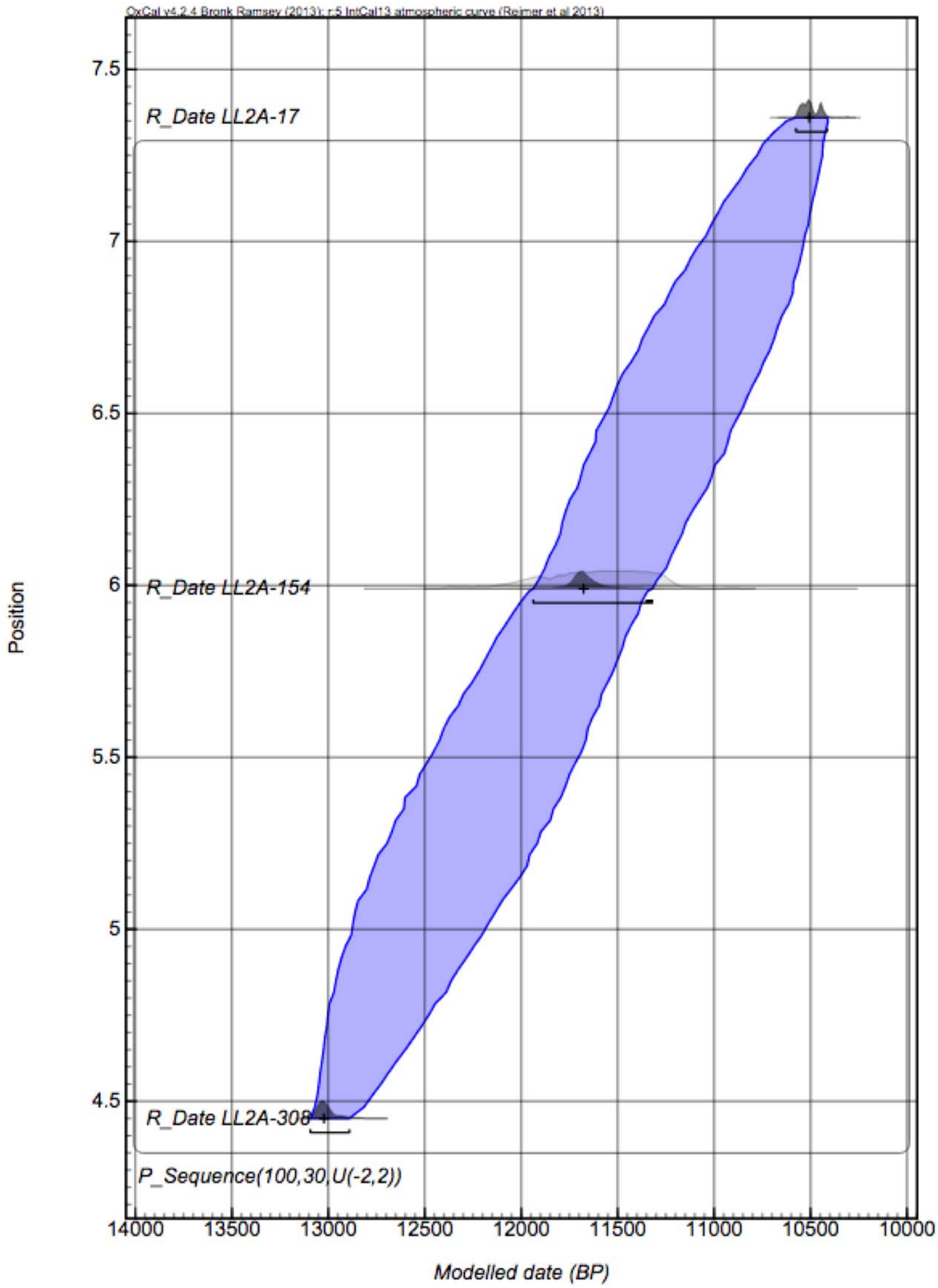

Figure 3-39 : Deposition model for the upper unit at Lucky Lady II based on three radiocarbon dates from 4.45 to 7.36 m. The estimated aggradation rate for this interval is 0.12 cm/year. The relative position between samples is measured in meters.

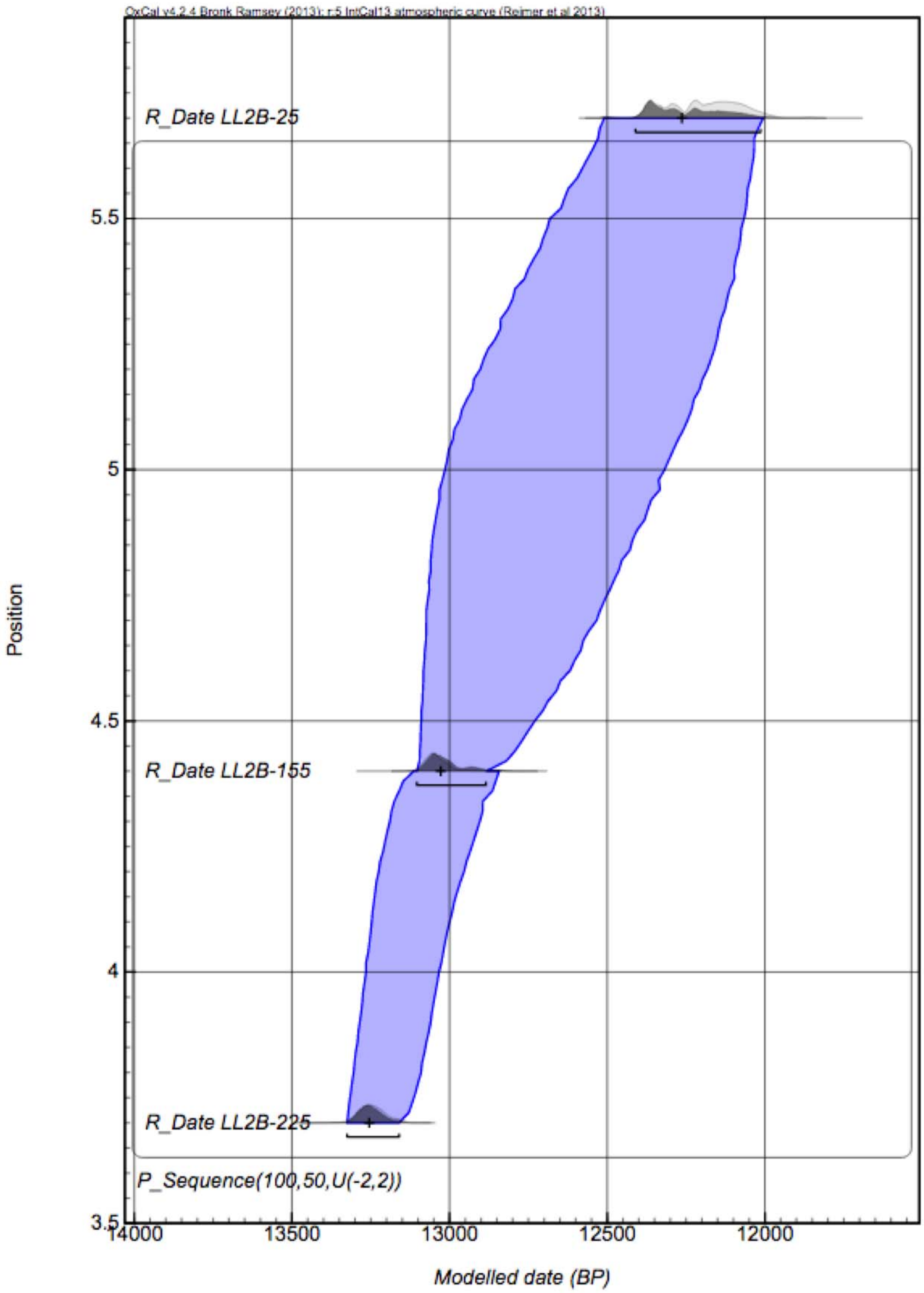

Figure 3-40 : Deposition model for the upper unit at Lucky Lady II based on three radiocarbon dates from 3.70 to 5.70 m. The estimated aggradation rate for this interval is 0.19 cm/year. The relative position between samples is measured in meters.

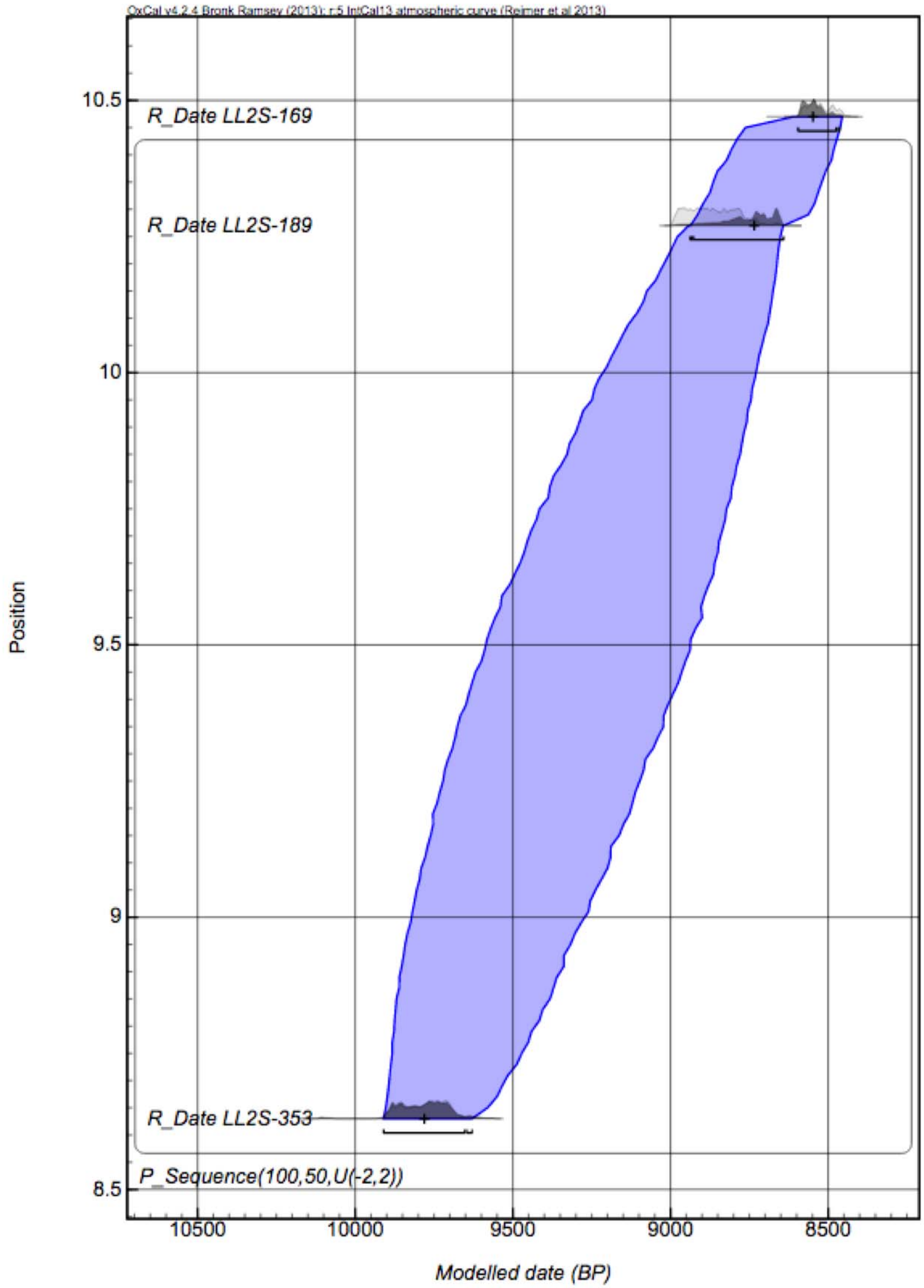

Figure 3-41 : Deposition model for the upper unit at Lucky Lady II based on three radiocarbon dates from 8.63 to 10.47 m. The estimated aggradation rate for this interval is 0.15 cm/year. The relative position between samples is measured in meters.

Interpretations

Radiocarbon dates from the lower unit suggest the sediment from 0 to 3.5 m was deposited during the latest Pleistocene. Basal contact is not visible. The presence of graminoid vegetation, mineral soils, and arctic ground squirrel nests suggest a steppe-tundra landscape with deep, well-drained active layers. The distinct black layer at 2.7 m is a paleosol. Increasing carbon and nitrogen contents from 2.7 to 3.5 m suggests increasing vegetation cover in response to warming air temperatures during the last glacial-interglacial transition. Lenticular cryostructures suggest syngenetic aggradation of permafrost. Enrichment of water isotopes with height in the section suggests rising air temperatures. Aggradation rates for the lower unit are moderate and comparable to the upper unit, with the exception of the upper 80 cm between the paleosol and earliest shrub appearance, which is estimated to be approximately half the rate. This unit is comparable to the Quartz Creek Member from Kotler and Burn (2000).

Radiocarbon dates from the upper unit suggest that the sediment from 3.5 to 11.5 m began deposition during the Bølling-Allerød interstadial and continued through the early Holocene. The appearance of shrub vegetation in the upper unit defines the conformable contact with the underlying Pleistocene silts. A lack of arctic ground squirrel nests, the presence of shrub vegetation, and enriched water isotopes suggest a shift from steppe-tundra to shrub vegetation by the start of the second unit. Total carbon and nitrogen contents are higher in the upper unit than in the lower unit, suggesting a more productive environment. Lenticular and microlenticular cryostructures indicate syngenetic aggradation of permafrost. Warmer-than-present temperatures of the early Holocene thermal maximum are suggested by a ~1.5‰ enrichment in $\delta^{18}O$ from 11,000 to 9,000 cal yrs BP. Aggradation rates for this unit are moderate. This unit may be comparable to the Dago Hill and "Organic unit" from Kotler and Burn (2000).

Brimstone

The Brimstone site is located in the middle of a broad valley 46 km south of Dawson on a tributary to the Indian River. Situated near the middle of a broad valley this 6 m exposure is subdivided into two units: (1) lower 3 m of ice-rich grey silts and black organic-rich silt horizons with large woody macrofossils, and (2) upper 3 m grey silts with woody and fibrous macrofossils (Figure 3-42, 3-43). No mammal fossils are present at the site.

Figure 3-42 : General view of Brimstone site. The lower unit is exposed 0 to 3.0 m and overlain by a sharp contact with the upper unit, which is exposed from 3.0 to 6.0 m. Both units consist of crudely stratified organic-rich grey, brown, and black silts including abundant wood and fibrous organics. Syngenetic ice wedges are present in both units (not pictured). Ice axe is 80 cm high.

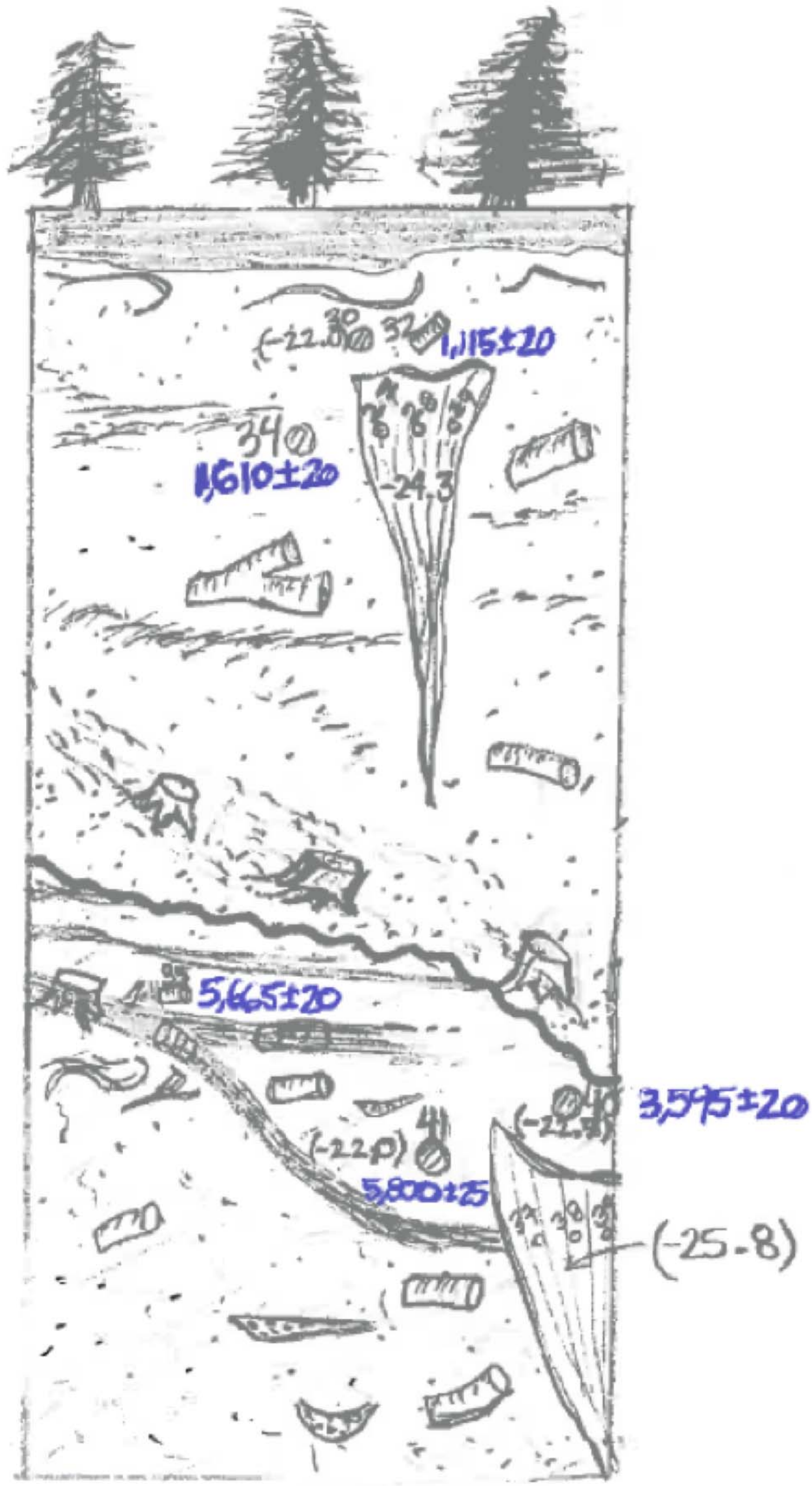

Figure 3-43 : Sketch of the Brimstone site stratigraphy. Sample numbers correspond to DF12 samples (*e.g.* 41 is DF12-41).

Description

The lower unit, exposed from 0 to 3.0 m, consists of crudely stratified ice-rich grey and black organic silts including large woody macrofossils (Figure 3-44). Sections of dry grey silt horizons ~15 cm thick are present. Surrounding sediments in this unit are sandy and wood-rich. Total carbon ranges from 2.2 to 3.4% and total nitrogen from 0.15 to 0.2%. A syngenetic ice wedge sampled at 2.0 m is ~50 cm wide. Lenticular and layered ice (1 – 1.5 cm thick) is present in this unit, with mostly structureless grey silts in the upper ~1 m. Water isotopes range from -24.96‰ to -21.98‰ $\delta^{18}O$ and -190.0‰ to -169.9‰ $\delta^{2}H$. Three samples are radiocarbon dated to 6,600, 6,445, and 3,900 cal yrs BP (5,800±25, UCIAMS-122287; 5,665±20, UCIAMS-114900; 3,595±20, UCIAMS-114916). The youngest of these is located between a sharp overlying contact and the top of a truncated syngenetic ice wedge and may be reworked material. Excluding this sample, aggradation rates for this unit are estimated to be 0.48 cm/year (Figure 3-45).

Figure 3-44 : The lower unit at the Brimstone site is exposed from 0 to 3.0 m and consists of black and grey silts with black organic silt lenses and layers including *in situ* fibrous and woody organic macrofossils. This unit contains one syngenetic ice wedge at 2.0 m (not pictured) that is ~50 cm wide. Ice axe is 80 cm high.

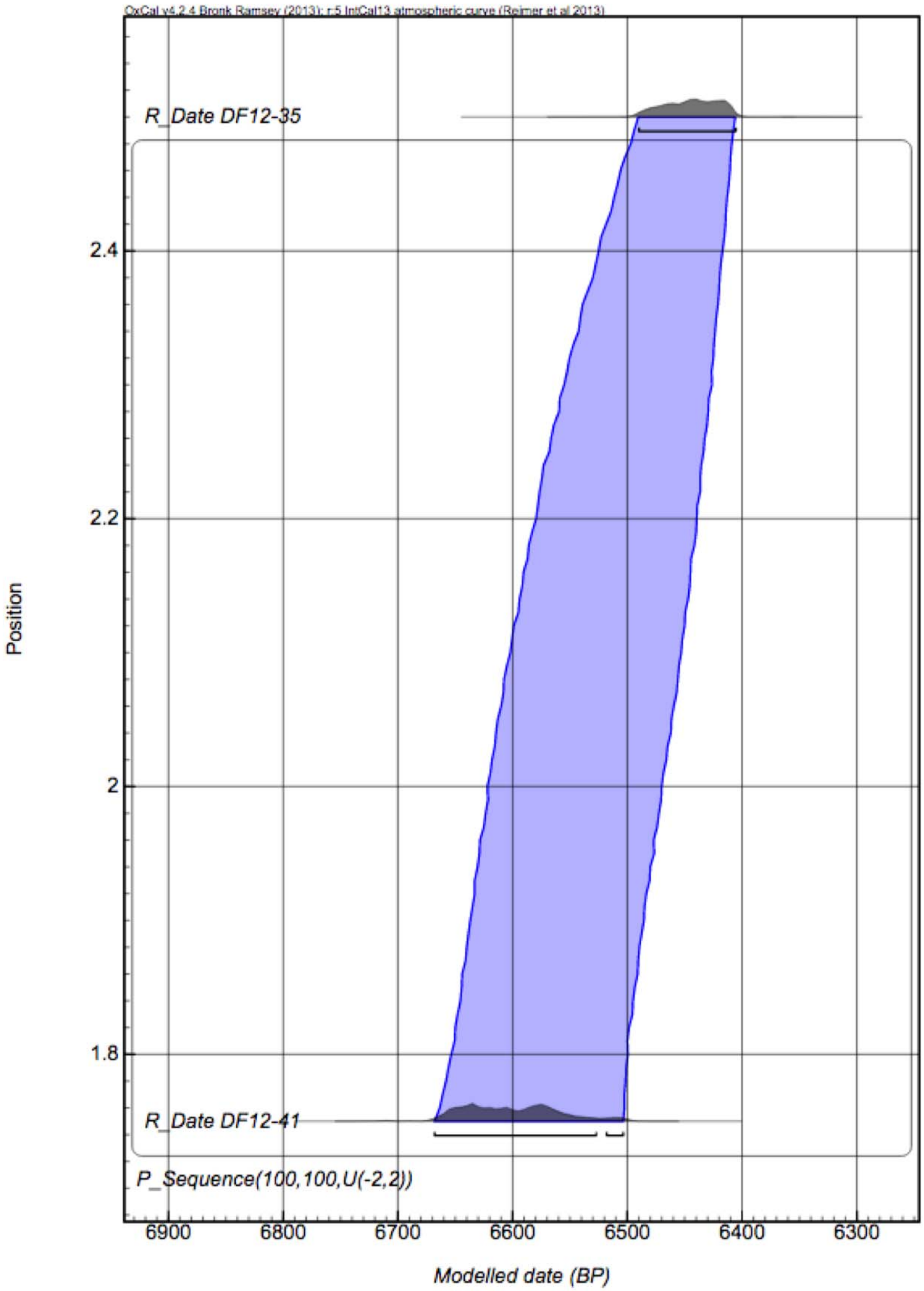

Figure 3-45 : Deposition model for the lower unit based on two radiocarbon dates at 1.75 and 2.5 m at the Brimstone site. The estimated aggradation rate for this interval is 0.48 cm/year. The relative position between samples is measured in meters.

The upper unit, exposed from 3.0 to 6.0 m, consists of crudely stratified organic-rich grey, brown, and black silts including abundant wood and fibrous organics (Figures 3-46, 3-47). The contact with the underlying unit is sharp. Total carbon ranges from 2.1 to 4.4% and total nitrogen from 0.15 to 0.2%. One syngenetic ice wedge (~45 cm wide) is present at 5.0 m. Above the truncated ice wedge, 60 cm of crudely stratified sandy silt and woody macrofossils up to 5 cm in diameter are overlain by 45 cm of retranslocated fibrous organics and grey silts (Figure 3-48). Lenticular and layered ice (up to 1 cm thick) is present in this unit. Water isotopes range from -25.84‰ to -21.96‰ $\delta^{18}O$ and -200.9‰ to -167.4‰ $\delta^{2}H$. This unit was deposited 1,485 to 1,015 cal yrs BP (1,610±20, UCIAMS-114915; 1,115±20, UCIAMS-114917). Aggradation of this unit is estimated to be 0.48 cm/year (Figure 3-49).

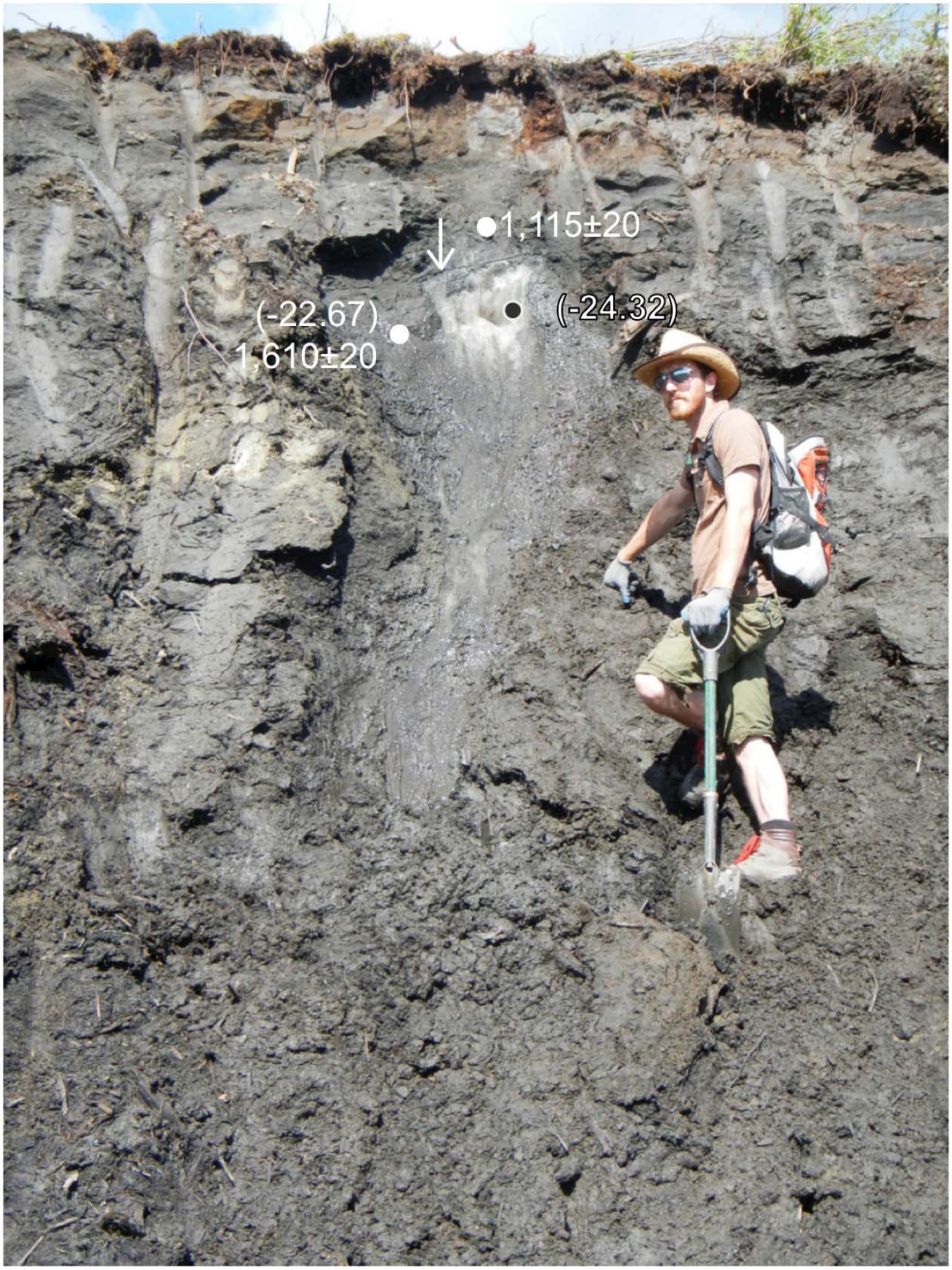

Figure 3-46 : The upper unit at the Brimstone site is exposed from 3.0 to 6.0 m and consists of crudely stratified grey, brown, and black silt with *in situ* and reworked fibrous organic and woody macrofossils. The arrow indicates the top of a truncated syngenetic ice wedge. Shovel is ~1.2 m high.

Figure 3-47 : Closer view of syngenetic ice wedge at 5.0 m in the upper unit at the Brimstone site. The arrow indicates the top of the truncated ice wedge.

Figure 3-48 : The uppermost 80 cm in the upper unit at the Brimstone site, which consists of massive to crudely stratified grey and brown sandy silts with retranslocated fibrous and woody macrofossils. Bottom of the photo is ~20 cm above a truncated syngenetic ice wedge. Ice axe head is 21 cm wide.

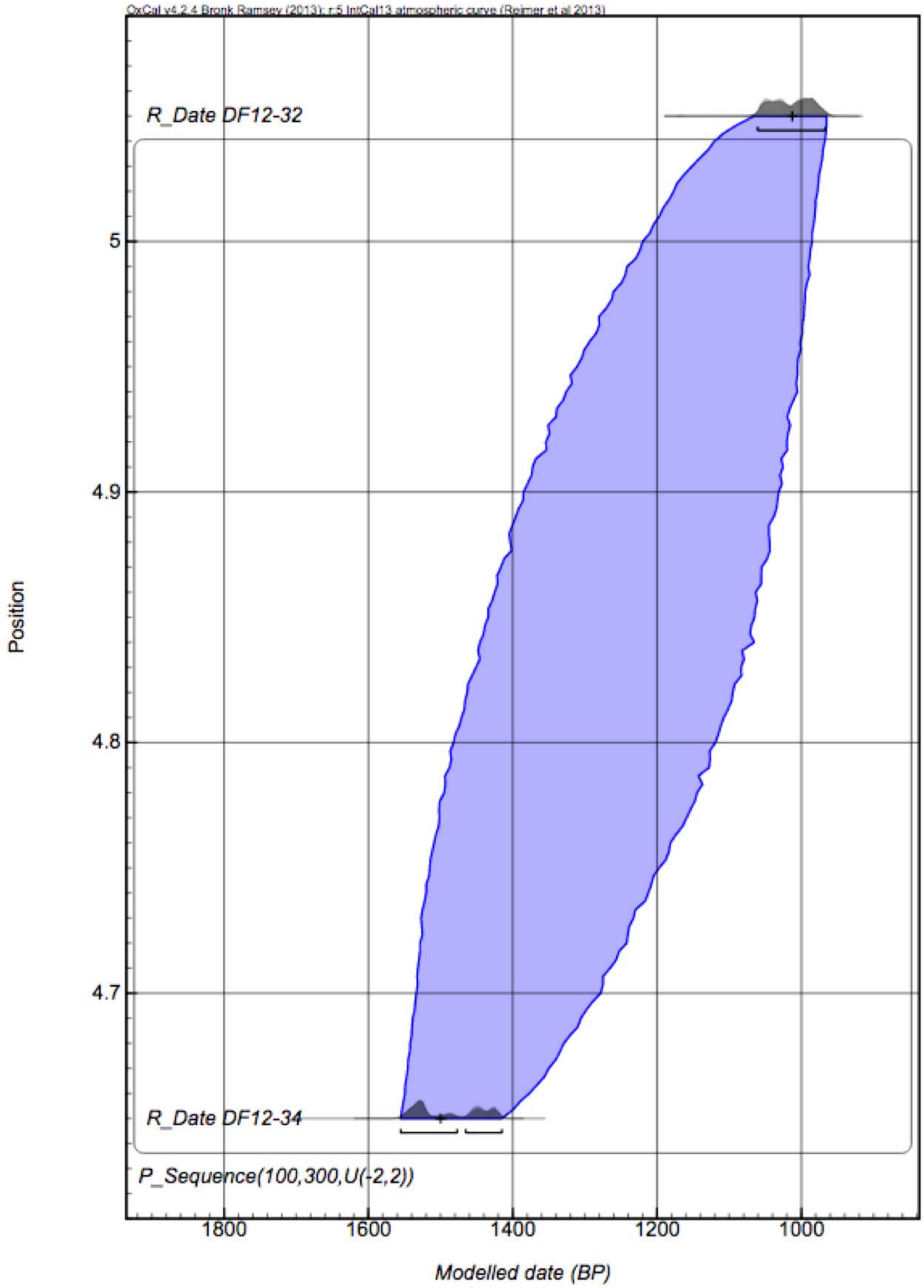

Figure 3-49 : Deposition model for the upper unit based on two radiocarbon dates at 4.6 and 5.1 m at the Brimstone site. The estimated aggradation rate for this interval is 0.09 cm/year. The relative position between samples is measured in meters.

Interpretations

Radiocarbon dates from the lower unit suggest that the sediment from 0 to 3.0 m was deposited during the mid-Holocene. The basal contact is obscured by slumped material. Large Holocene wood macrofossils indicate boreal forest. Total carbon and nitrogen content is slightly less than early Holocene units from Lower Hunker and Upper Goldbottom, which may be the result of rapid aggradation as suggested by the radiocarbon dates in this unit. One small syngenetic ice wedge is present at 2.0 m. Cryostructures are lenticular and layered, suggesting syngenetic aggradation of permafrost. The water isotopes are comparable to modern precipitation, suggesting air temperatures similar to today. Aggradation rates of 0.48 cm/year indicate high rates of deposition during this interval, which is in good agreement with aggradation rates from the mid-Holocene unit at Upper Quartz. This unit may be comparable to the “Organic unit” from Kotler and Burn (2000).

Radiocarbon dates from the upper unit suggest that the sediment from 3.0 to 6.0 m was deposited during the late Holocene. A sharp, undulating contact with the lower unit is likely an unconformity that occurred sometime between *ca.* 6,500 and 2,000 cal yrs BP, as suggested by organic material dated to 3,900 cal yrs BP located just below the unconformity and above a truncated syngenetic ice wedge. This is *ca.* 2,500 years younger than sediments surrounding the ice wedge and may have been reworked into the active layer at the time of the unconformity. Large wood and fibrous organics indicate a full boreal environment. Total carbon and nitrogen content is similar to the lower unit, which is slightly lower than expected probably due to high rates of aggradation. One thin syngenetic ice wedge is present at 5.0 m. Cryostructures are layered and lenticular, suggesting syngenetic aggradation of permafrost. Water isotopes are comparable to modern precipitation, suggesting air temperatures similar to today. Aggradation rates of 0.09 cm/year suggest lower aggradation rates compared to the mid-Holocene. This unit may be comparable to the “Organic unit” from Kotler and Burn (2000).

Upper Hunker

The Upper Hunker site is located in a valley 26 km south of Dawson on a tributary to the Klondike River. Auriferous gravels are ~7 m below the described section. This exposure is

13.2 m thick and can be subdivided into four units, from bottom to top: (1) 5.1 m of grey silts, (2) 3.7 m wood-rich silts, (3) 2 m of silt-rich ice with woody macrofossils, and (4) 2.4 m of diamict interbedded with *in situ* fibrous organics (Figure 3-50, 3-51). Contacts between units are sharp. Aggradation rates were not able to be determined from this exposure.

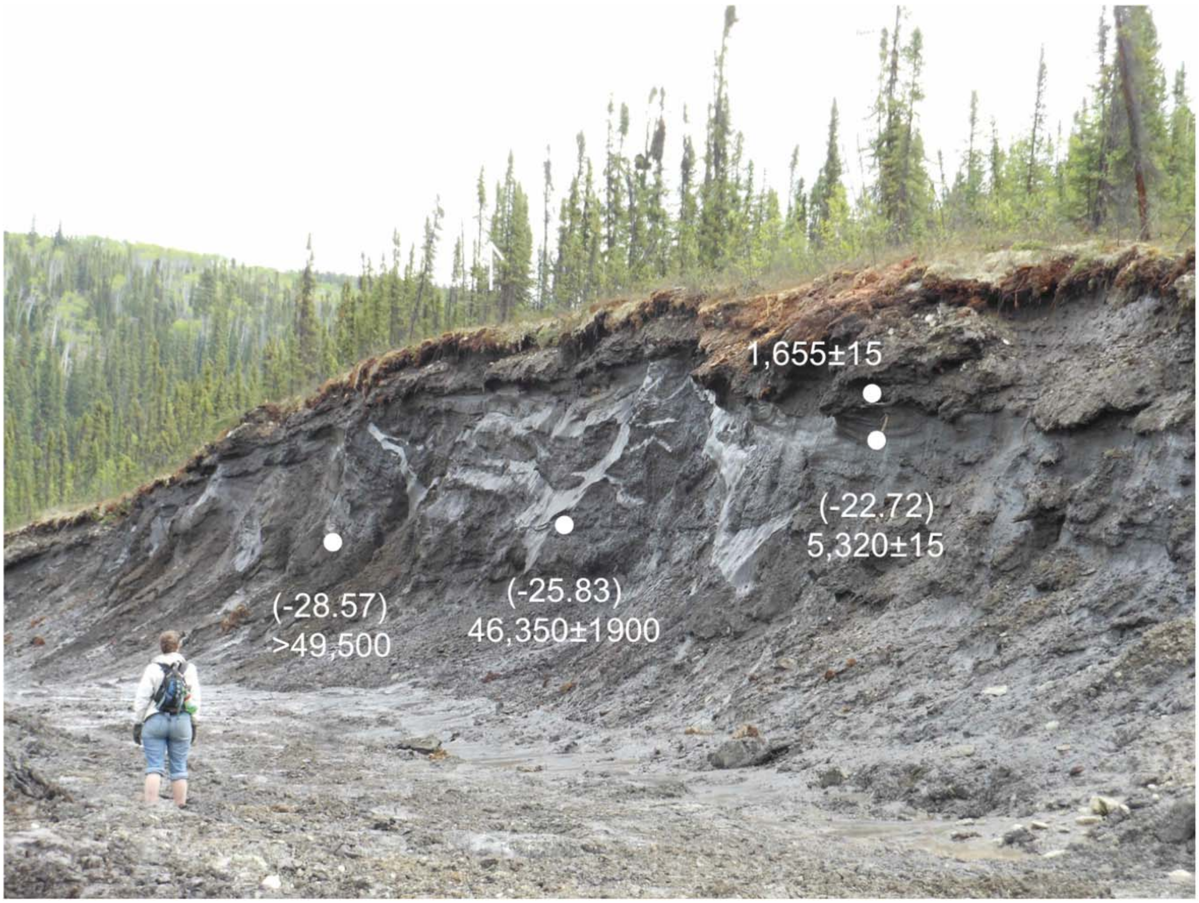

Figure 3-50 : General view of Upper Hunker site.

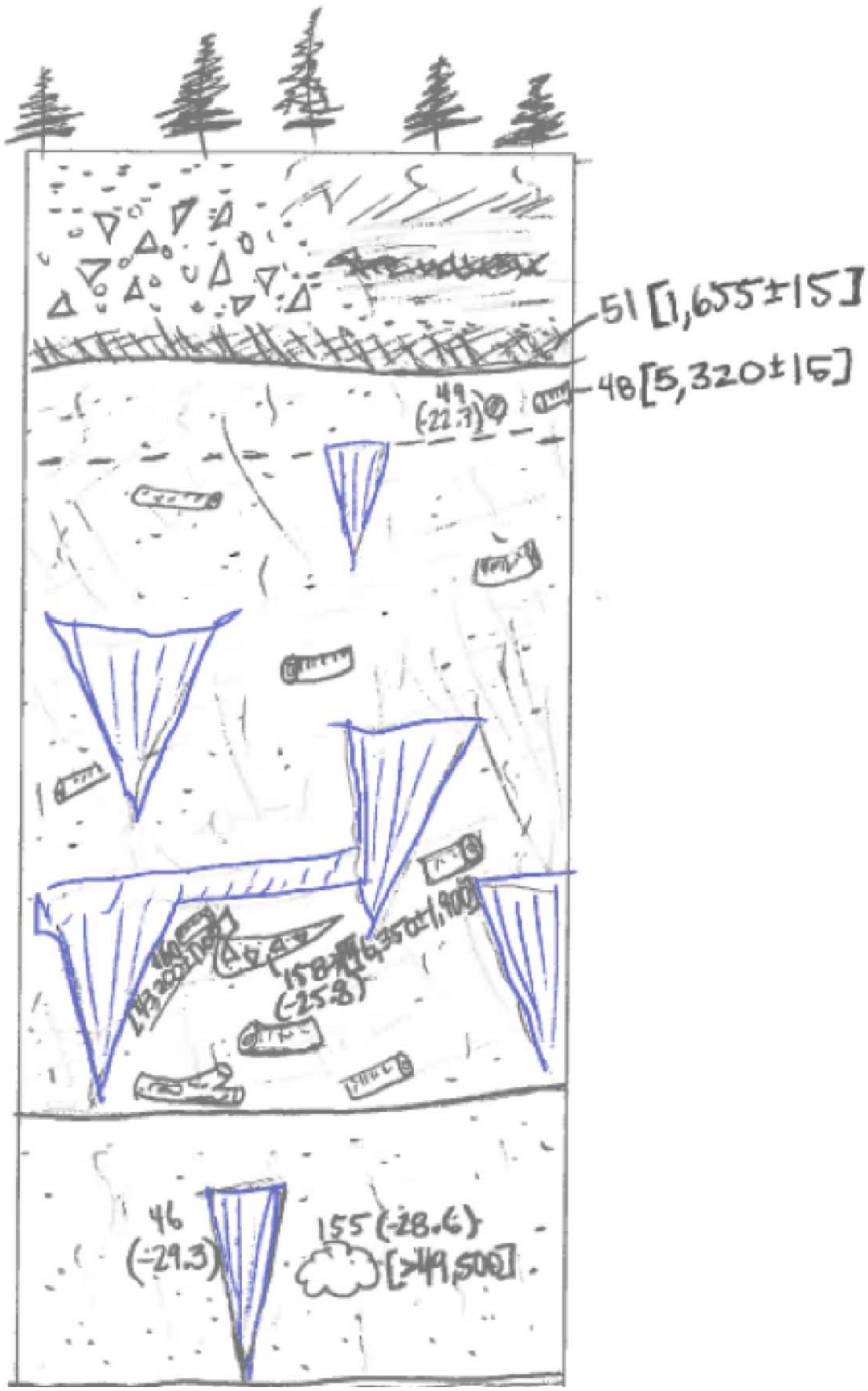

Figure 3-51 : Stratigraphic sketch of Upper Hunker. Sample numbers correspond to MM12 samples.

Description

The lowermost unit, exposed from 0 to 5.1 m, consists of grey silts including *in situ* graminoid vegetation (Figure 3-52). Basal contact obscured by slumped material. Total carbon is 2.8% and total nitrogen is 0.2%. One syngenetic ice wedge (40 cm wide) is present at 1.0 m in otherwise relatively ice-poor sediment. Cryostructures are primarily structureless with microlenticular ice. Water isotopes range from -30.02‰ to -29.12‰ $\delta^{18}O$ and -231.0‰ to -224.9‰ $\delta^{2}H$. One radiocarbon date from an arctic ground squirrel nest is non-finite (>49,500 ^{14}C yrs BP, UCIAMS-114717).

Figure 3-52 : The lowermost unit at the Upper Hunker site is exposed from 0 to 5.1 m and consists of grey silts with *in situ* graminoid vegetation. One non-finite arctic ground squirrel nest is indicated by the white dot. This unit has one 40 cm wide ice wedge (not pictured). Ice axe is 80 cm high.

The second unit, exposed from 5.1 to 8.8 m, consists of grey and brown organic silts including abundant woody macrofossils and roots (Figure 3-53). The contact with the lowermost unit is obscured by slumped material. This unit also contains thick (up to 50 cm) lenses of wood-rich diamict. Total carbon and nitrogen are not determined. The organic silts contain large syngenetic ice wedges (up to 1.5 m wide). Cryostructures are mainly parallel planar layered and lenticular ice (up to 1 cm thick). Water from the only pore ice sample in this unit has isotopic values of -25.8‰ $\delta^{18}O$ and -198.0‰ $\delta^{2}H$. This unit was deposited *ca.* 48,550 to 46,800 cal yrs BP based on two radiocarbon dates (46,350±1,900, UCIAMS-122276; 43,200±1,100, UCIAMS-114724). This unit is particularly fossiliferous, containing abundant bison fossils and, to a lesser extent, horse and mammoth.

Figure 3-53 : The second unit at Upper Hunker, exposed from 5.1 to 8.8 m, containing *in situ* wood, shrub, and graminoid vegetation. Multi-generational syngenetic ice wedges (up to 1.5 m thick) are present throughout this unit. A sharp contact with the third unit at 8.8 m is indicated by arrow.

The third unit, exposed from 8.8 to 10.8 m, consists of ice-rich grey silt including lenses of silt-rich ice containing *in situ* graminoid and reworked woody vegetation (Figure 3-54). The boundary separating the underlying unit is sharp. The contact with the overlying layer is a sharp boundary with a distinct change to *in situ* fibrous organics with interspersed diamict and abundant wood macrofossils. Total carbon and nitrogen are not determined. Cryostructures are mainly parallel wavy layered and lenticular ice (up to 8 mm thick). Water isotopes range from -23.42‰ to -22.40‰ $\delta^{18}O$ and -179.5‰ to -170.1‰ $\delta^{2}H$. One radiocarbon date indicates deposition of this unit began *ca.* 6,000 cal yrs BP (5,320±15, UCIAMS-114727).

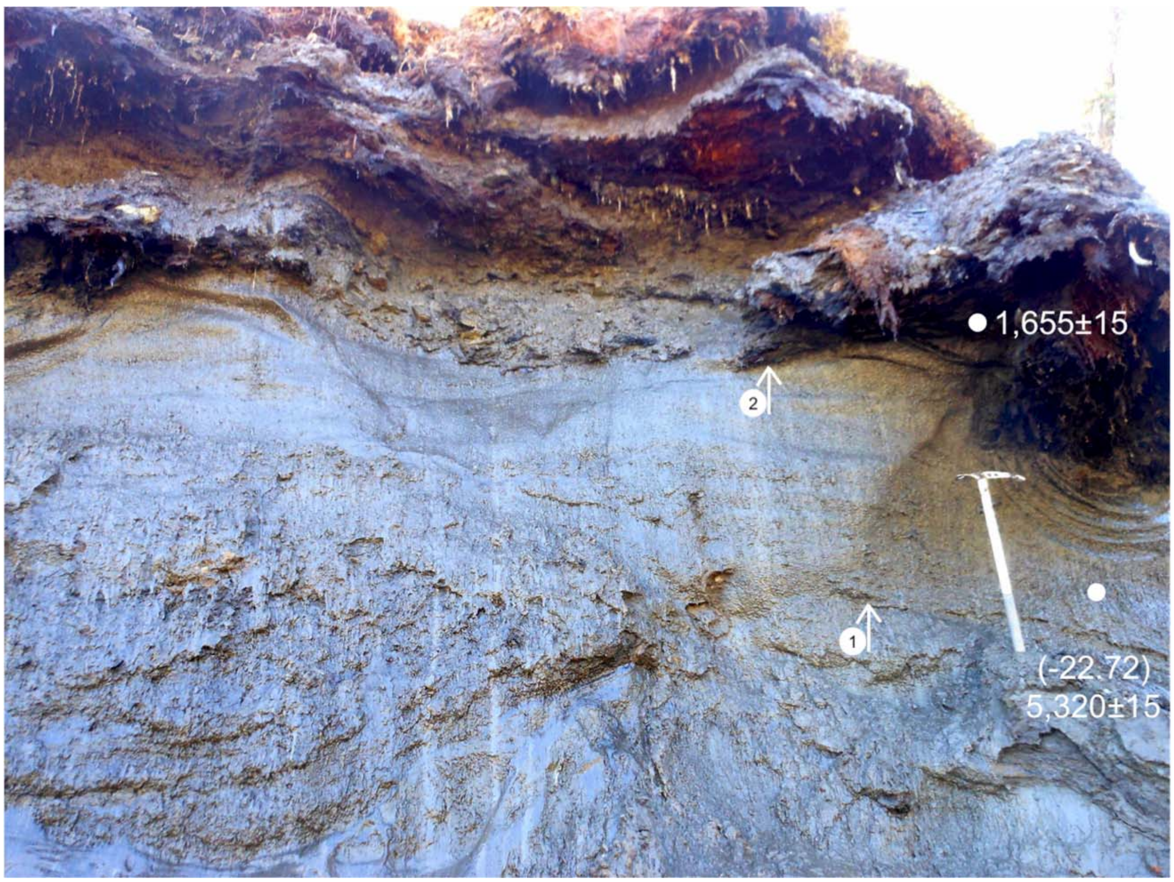

Figure 3-54 : Numbered arrows indicate sharp contacts at the base of the third and fourth units at the Upper Hunker site. Arrow “1” marks the base of the third unit, exposed 8.8 to 10.8 m, which consists of ice-rich grey silts with *in situ* graminoid and reworked woody vegetation. Arrow “2” marks the base of the uppermost unit, exposed 10.8 to 13.2 m, which consists of *in situ* fibrous organics in grey silts and thick layers (up to 1 m) of wood-rich diamict. Ice axe is 80 cm high.

The uppermost unit, exposed from 10.8 to 13.2 m, consists of grey and black silts including layers of *in situ* fibrous organics and diamict (see Figure 3-54). The basal contact of this unit is sharp. Cryostructures, total carbon and nitrogen, and other paleoecological indicators are not determined for this unit. Radiocarbon dates from the base of this unit indicate deposition began *ca.* 1,500 cal yrs BP (1,655±15, UCIAMS-114732).

Interpretations

Radiocarbon dates from the lowermost unit suggest that the sediment from 0 to 5.1 m was deposited >50,000 years ago. Basal contact is obscured by slumped material. Sediment contains *in situ* graminoid vegetation and arctic ground squirrel nests indicating steppe-tundra. Total carbon and nitrogen contents are slightly above typical cold stage values and are more similar to contents from late MIS 3 sediment at Upper Quartz. One syngenetic wedge is present. Depleted water isotopes suggest lowered temperatures associated with cold stage conditions. Aggradation rates are not estimated. Water isotopes from this unit are slightly more depleted than the Last Chance Creek Member values from Kotler and Burn (2000).

Radiocarbon dates from the second unit suggest that the sediment from 5.1 to 8.8 m was deposited during the MIS 3 interstadial. The contact with the lowermost unit is sharp and unconformable. Large wood in this unit suggests a boreal forest environment. Ice-rich permafrost with large ice wedges suggests syngenetic aggradation of permafrost**.** Moderately depleted isotopes suggest slightly colder-than-present mean annual air temperatures associated with interstadial conditions. Cryostructures, total carbon and nitrogen, and other paleoecological indicators in this unit are not determined. Water isotopes from this unit are comparable to the Last Chance Creek Member values from Kotler and Burn (2000).

Radiocarbon dates from the third unit suggest that the sediment from 8.8 to 10.8 m was deposited during the mid-Holocene. The basal contact of this unit is sharp and unconformable. This unit generally corresponds with the first widespread appearances of large Holocene wood macrofossils from other mid-Holocene deposits in this study. Ice-rich silts and syngenetic ice wedges suggest relatively moist conditions during syngenetic aggradation of permafrost. Water isotopes are comparable to modern precipitation, indicating warm temperatures in interglacial conditions. Cryostructures, total carbon and nitrogen, and other paleoecological indicators in this unit are not defined. This unit may be comparable to the "Organic unit" from Kotler and Burn (2000).

Radiocarbon dates from the uppermost unit suggest that the sediment from 10.8 to 13.2 m was deposited during the late Holocene. Contact with the underlying unit is sharp and unconformable. Abundant *in situ* fibrous and woody organics suggest warm and moist environments. Thick layers of colluvium with randomly-oriented wood pieces suggest deposition by mass movement, possibly resulting from slope failure associated with thawing permafrost. Cryostructures, total carbon and nitrogen, and other paleoecological indicators are not defined. This unit may be comparable to the "Organic unit" from Kotler and Burn (2000).

Lower Hunker

The Lower Hunker site is located in the middle of a broad valley 15 km south of Dawson on a tributary to the Klondike River. The Lower Hunker section is 20.5 m thick and can be divided into four units, from bottom to top: (1) 3 m organic-rich black and grey silt with abundant wood macrofossils, (2) 5 m of organic-rich black and grey silt with graminoid vegetation, (3) 8.5 m of grey silt with graminoid vegetation, and (4) 4 m of organic-rich black and grey silts with abundant wood and shrub macrofossils (Figure 3-55, 3-56). Contacts between units are sharp, albeit the contacts above and below the second unit are obscured by slumped material. No arctic ground squirrel nests are present at the site. Many detrital mammal bones were found, mostly horse, and to a lesser extent bison and mammoth.

Figure 3-55 : General view of the Lower Hunker exposure. The lowermost unit, exposed from 0 to 3.0 m, consists of black and grey silts including woody macrofossils and syngenetic ice wedges (marker “1”). The third unit, exposed from 8.0 to 16.5 m, consists of grey silt with *in situ* graminoid vegetation (marker “2”). The second and fourth units are not pictured.

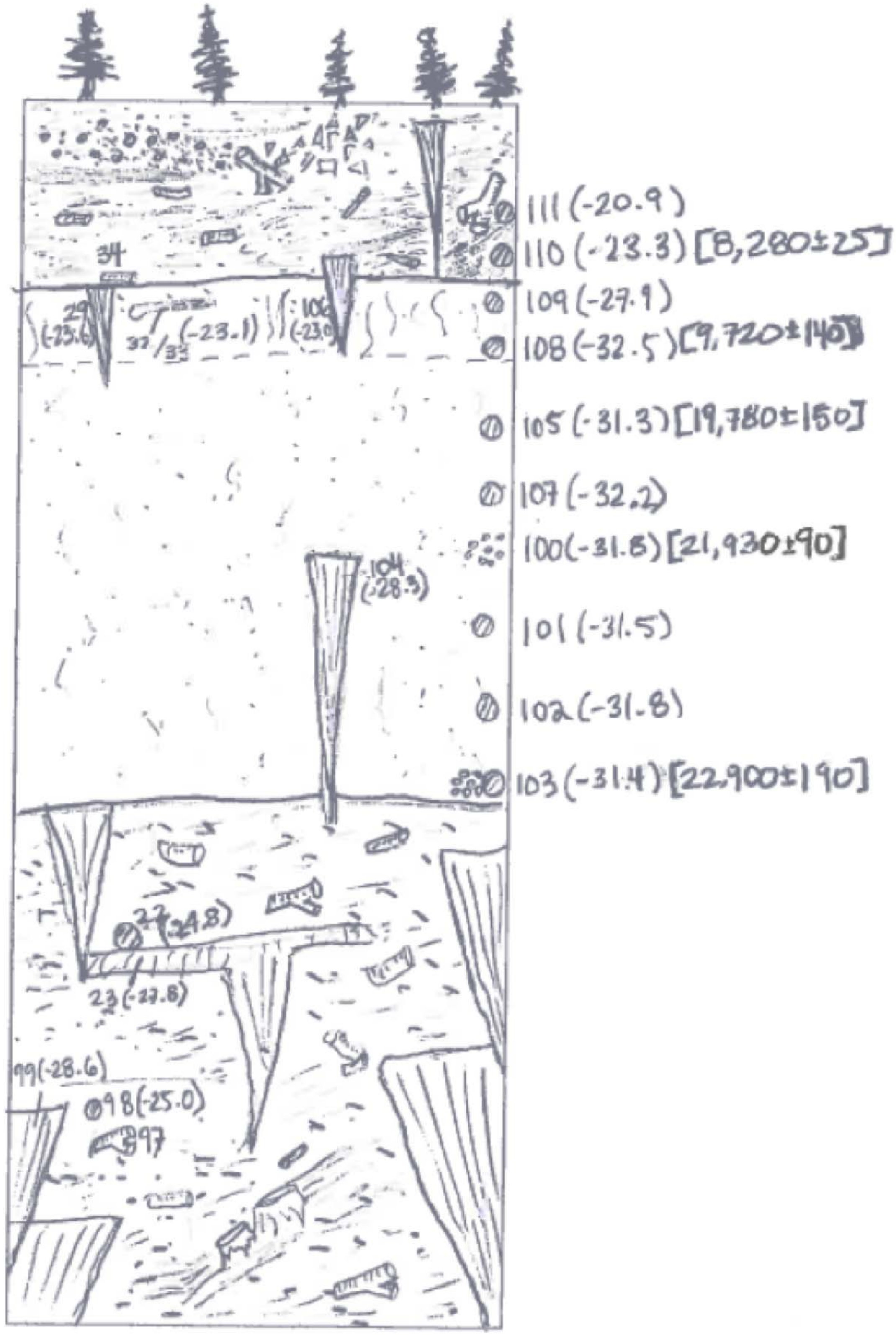

Figure 3-56 : Sketch of the Lower Hunker exposure. Sample numbers correspond to MM12 samples.

Description

The lowermost unit, exposed from 0 to 3.0 m, consists of organic-rich black and grey silts including abundant shrub and wood macrofossils (Figure 3-57). The contact with the overlying unit is sharp, while the contact with the underlying gravels is covered by slumped material. Total carbon is 5.7% and total nitrogen is 0.4%. One syngenetic ice wedge 1.5 m wide is truncated 1.5 m below the upper contact. This unit is characterized by non-parallel wavy microlenticular ice. Water isotopes range from -28.88‰ to -25.07‰ $\delta^{18}O$ and -225.7‰ to -194.6‰ $\delta^{2}H$. One radiocarbon sample is non-finite (49,600±2,400, UCIAMS-114715).

Figure 3-57 : The lowermost unit at the Lower Hunker site is exposed from 0 to 3.0 m and consists of organic-rich black and brown silts with *in situ* shrub and wood macrofossils. A thick syngenetic ice wedge (at arrow) is present. This unit is beyond the limits of radiocarbon dating.

The second unit, exposed from 3.0 to 8.0 m, consists of ~0.5 to 2 m thick layers of grey to brown silts including *in situ* graminoid vegetation and twigs (Figure 3-58). The basal contact is obscured by slumped material between the two units, which are laterally-offset. Total carbon is 5.1% and total nitrogen is 0.5%. Four generations of syngenetic ice wedges (up to 1 m wide) are present in this unit. The silts are generally structureless with lenticular ice (1 – 3 mm thick). One sampled ice wedge has water isotopic values of -27.75‰ $\delta^{18}O$ and -214.5‰ $\delta^{2}H$. Associated organic-rich silts have isotopic values of -24.77‰ $\delta^{18}O$ and -197.6‰ $\delta^{2}H$. An organic macrofossil from the unit dates to 34,950 cal yrs BP (31,020±250, UCIAMS-114726).

Figure 3-58 : The second unit at the Lower Hunker site is exposed from 3.0 to 8.0 m and consists of grey to brown silts including abundant *in situ* graminoid vegetation and twigs. Ice wedges up to 1 m wide are present throughout this unit. Graminoid vegetation is dated to 34,950 cal yrs BP (31,020±250, UCIAMS-114726).

The third unit, exposed from 8.0 to 16.5 m, consists of grey silts including *in situ* graminoid vegetation (Figure 3-59). The basal contact is obscured by slumped material. Total carbon ranges from 1.0 to 1.6% and total nitrogen from 0.06 to 0.1%. One thin syngenetic ice wedge (~30 cm wide) is sampled at 12.0 m. Another thin ice wedge is sampled at 14.0 m but is likely epigenetic and may have formed during the deposition of the overlying organic-rich unit. This unit is characterized by microlenticular and microlayered cryostructures in otherwise structureless permafrost. One instance of reticulate-chaotic ice is present at 8.0 m in the lowermost sample from this unit. Sediment is increasingly ice-rich in the upper 1 m, from 15.5 to 16.5 m. Water isotopes range from -32.48‰ to -27.86‰ $\delta^{18}O$ and -245.6‰ to -213.6‰ $\delta^{2}H$. Based on four radiocarbon dates, this unit was deposited from 27,295 to 22,720 cal yrs BP (22,900±190, UCIAMS-122281; 19,780±150, UCIAMS-122283). Aggradation rates are estimated to be 0.17 cm/year from 27,295 to 23,810 cal yrs BP (Figure 3-60). No arctic ground squirrel nests are present, however there are several zones containing small clusters of fecal pellets which are believed to be from arctic ground squirrels (Zazula et al., 2005).

Figure 3-59 : The third unit at the Lower Hunker site is exposed from 8.0 to 16.5 m and contains grey silts with *in situ* graminoid vegetation. Shovel is ~1.2 m high.

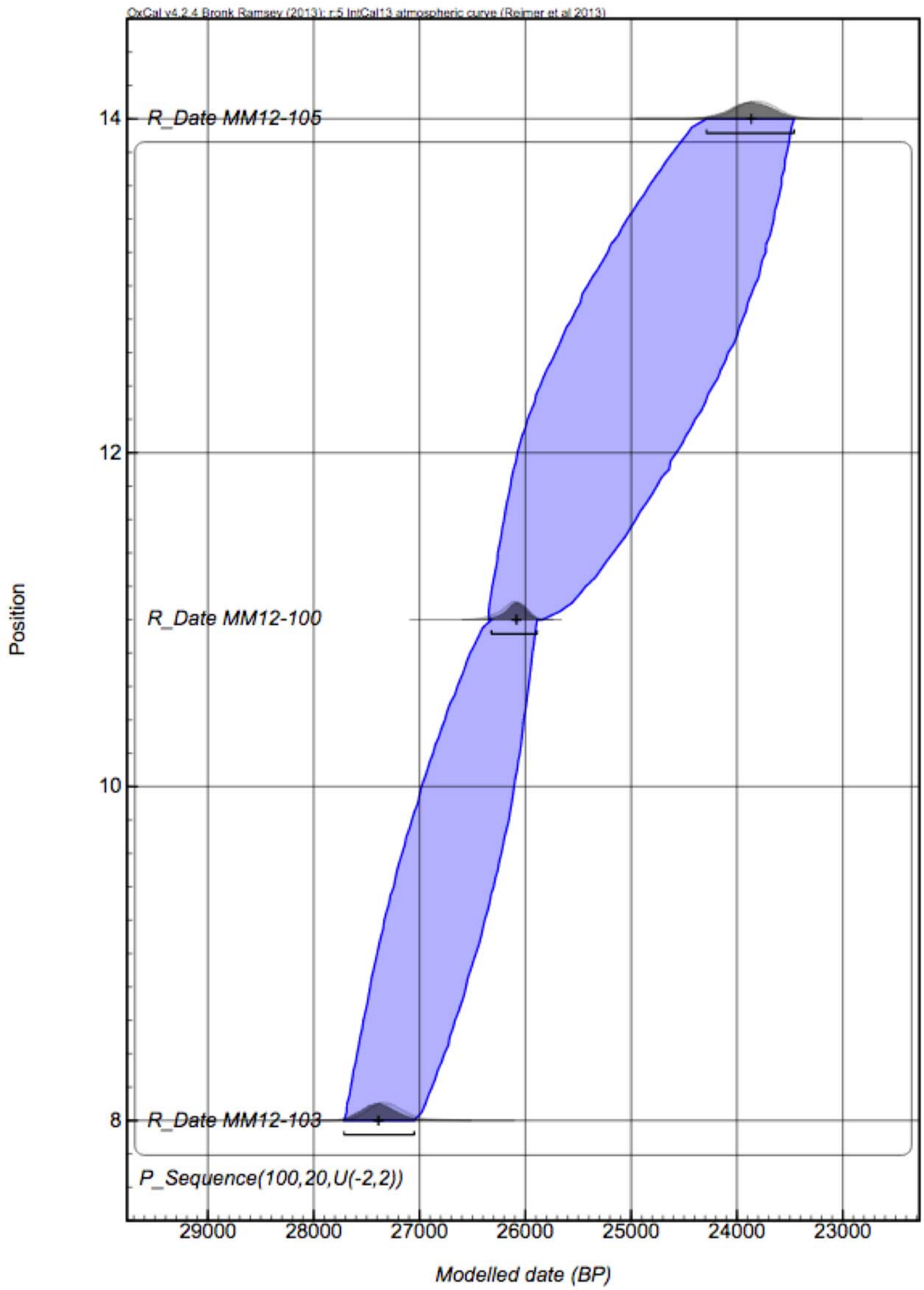

Figure 3-60 : Deposition model for the third unit based on three radiocarbon dates from 8.0 to 14.0 m at the Lower Hunker site. The estimated aggradation rate for this interval is 0.17 cm/year. The relative position between samples is measured in meters.

The uppermost unit, exposed 16.5 to 20.5 m, consists of black to grey organic-rich silt up to 4 m thick including reworked woody organic macrofossils (Figure 3-61). The contact with the underlying unit is sharp and undulating. Total carbon ranges from 2.8 to 5.4% and total nitrogen from 0.2 to 0.25%. Several thin ice wedges (up to 30 cm wide) and segregated ice lenses (up to 15 cm thick) are present in this unit. This unit is characterized by non-parallel wavy lenticular ice (1 – 3 mm thick) and microlayered cryostructure. Water isotopes range from -23.31‰ to -20.85‰ $\delta^{18}O$ and -166.5‰ to -160.3‰ $\delta^{2}H$. This unit is dated to 9,290 cal yrs BP (8,280±25, UCIAMS-114901).

Figure 3-61 : The third unit (below arrow) at the Lower Hunker site is exposed from 8.0 to 16.5 m and consists of grey silts with *in situ* graminoid vegetation. The uppermost unit, exposed from 16.5 to 20.5 m, has a sharp basal contact (at arrow) and consists of organic-rich black and grey silts with *in situ* shrub and graminoid vegetation. Ice axe is 80 cm high.

Interpretations

Radiocarbon dates from the lowermost unit suggest the sediment from 0 to 3.0 m was deposited >50,000 years ago. The basal contact is obscured by slumped material. Black and grey silts including woody plants, syngenetic ice wedges, and microlenticular cryostructures suggest syngenetic permafrost aggradation during relatively warmer and wetter conditions. Depleted water isotopes suggest moderately cold temperatures most likely associated with interstadial conditions. Aggradation rates cannot be estimated. Water isotopes from this unit are comparable to Last Chance Creek Member values from Kotler and Burn (2000).

Radiocarbon dates from the second unit suggest that the sediment from 3.0 to 8.0 m was deposited during the late MIS 3 interstadial. Contact with the lowermost unit is obscured by slumped material. Abundant graminoid vegetation suggests a productive environment. Total carbon and nitrogen contents are high, similar to other MIS 3 samples from Upper Goldbottom. Large syngenetic ice wedges and lenticular cryostructures suggest syngenetic aggradation of permafrost. Moderately depleted isotopes suggest slightly colder-than-present mean annual air temperatures associated with interstadial conditions. Aggradation rates cannot be estimated. Cryostratigraphy and paleoenvironmental indicators in this unit are in good agreement with a unit of similar age from the Upper Goldbottom site. Water isotopes from this unit are comparable to the Last Chance Creek Member values from Kotler and Burn (2000).

Radiocarbon dates from the third unit suggest the sediment from 8.0 to 16.5 m was deposited during the last cold stage. The basal contact of this unit is sharp and unconformable. Graminoid vegetation suggests a cryoxeric environment. Low total carbon and nitrogen suggest sparse vegetative cover compared to the other three units in the exposure. The presence of a thin syngenetic ice wedge in sediment with microlenticular and microlayered cryostructures suggests syngenetic aggradation of permafrost. Reticulate-chaotic structure in the lowermost sample may have resulted from local thaw. One ice wedge in the upper 2.5 m contains enriched isotopes, suggesting an epigenetic origin of the ice wedge as the water isotopes indicate warmer temperatures associated with interglacial conditions. This unit contains some of the most depleted water isotopes in this study, suggesting the coldest conditions occurred *ca*. 27,000 to 23,000 cal yrs BP. Aggradation rates are moderate and are comparable to cold stage rates from the Upper Goldbottom site. Cryostratigraphy and paleoenvironmental indicators in this unit are in good agreement with units similar in age from the Black Hills and Upper Goldbottom sites in this study. This unit may be comparable to the Quartz Creek Member from Kotler and Burn (2000).

Radiocarbon dates from the uppermost unit suggest that the sediment from 16.5 to 20.5 m was deposited during the early Holocene thermal maximum. The basal contact of this unit is sharp and unconformable. Abundant shrub macrofossils and relatively high total carbon and nitrogen contents suggest a productive environment during this interval. Thin syngenetic and epigenetic wedges are present. Cryostructures are lenticular and microlayered, suggesting syngenetic aggradation of permafrost. Enriched water isotopes suggest warm air temperatures associated with interglacial conditions. Aggradation rates are not determined. Cryostratigraphy and paleoenvironmental indicators in this unit are in good agreement with units similar in age from the Upper Goldbottom and Lucky Lady II sites in this study. This unit may be comparable to the "Organic unit" from Kotler and Burn (2000).

Discussion and conclusions

In this study we have proxy records from eight sites spanning 50,000 cal yrs BP. Ages of 175 pore ice samples and 16 ice wedge samples are constrained by 85 radiocarbon dates. Cryostratigraphic and paleoecological indicators are consistent between sites over 60 km apart allowing us to create a composite long-term record. The $\delta^2H/\delta^{18}O$ and paleoecological data are coherent between multiple sites, indicating the composite record can be used to unravel the climatic history of the region over the last 50,000 years.

The height of last cold stage in the Klondike may have broad correspondence with the LGM, which is defined by Clark et al. (2009) to have spanned from 26,500 to *ca.* 20,000 cal yrs BP. The most isotopically-depleted samples in this study range from *ca.* 27,000 to 23,000 cal yrs BP, suggesting Klondike ground ice records regional climate trends. Additional discussion of the water isotope trends follows in Chapter 4.

Kotler and Burn (2000) also provide a multi-site record of cryostratigraphy, plant macrofossils, and ground ice $\delta^2H/\delta^{18}O$ for the Klondike, but their $\delta^2H/\delta^{18}O$ record is constrained by only nine radiocarbon dates. Moreover, the oldest macrofossils (>40,000 ^{14}C

years) constraining the Kotler and Burn (2000) record were beyond the limit of conventional radiocarbon beta-decay dating. AMS dating allowed us to date older materials with comparatively less uncertainty, and the 85 dated samples in this study allow us to compile a relatively high-resolution sequence spanning the last *ca.* 50,000 cal yrs BP. Meyer et al. (2010) developed a high-resolution $\delta^2H/\delta^{18}O$ record from a relict ice wedge complex near Barrow, Alaska, but theirs is restricted to 14,400 to 11,300 cal yrs BP. Our record is unique in northwestern North America in terms of its temporal resolution and duration. The only comparable ground ice $\delta^2H/\delta^{18}O$ record outside of North America was developed for an Ice Complex in northern Siberia by Schirrmeister et al. (2002), which spans the last 60,000 ^{14}C years.

References

Buck, C.L., Barnes, B.M., 1999. Temperatures of hibernacula and changes in body composition of arctic ground squirrels over winter. Journal of Mammalogy, 80 (4), 1264-1276.

Bronk Ramsey, C., 2008. Deposition models for chronological records. Quaternary Science Reviews, 27 (1-2), 42-60.

Bronk Ramsey, C., 2009. Bayesian analysis of radiocarbon dates. Radiocarbon, 51 (1), 337-360. Oxcal Version 4.2, http://c14.arch.ox.ac.uk/oxcal.html.

Bronk Ramsey, C., Lee, S., 2013. Recent and Planned Developments of the Program OxCal. Radiocarbon, 55 (2-3), 720-730.

Clark, P.U., Dyke, A.S., Shakun, J.D., Carlson, A.E., Clark, J., Wohlfarth, B., Mitrovica, J.X., Hostetler, S.W., McCabe, A.M., 2009. The Last Glacial Maximum. Science, 325, 710-714.

Fraser, T.A., Burn, C.R., 1997. On the nature and origin of "muck" deposits in the Klondike area, Yukon Territory. Canadian Journal of Earth Sciences, 34 (10), 1333-1344.

Froese, D.G., Zazula, G.D., Westgate, J.A., Preece, S.J., Sanborn, P.T., Reyes, A.V., Pearce, N.J.G., 2009. The Klondike goldfields and Pleistocene environments of Beringia. GSA Today, 19 (8), 4-10.

Kotler, E., Burn, C.R., 2000. Cryostratigraphy of the Klondike “muck” deposits, west-central Yukon Territory. Canadian Journal of Earth Sciences, 37, 849-861.

Meyer, H., Schirrmeister, L., Yoshikawa, K., Opel, T., Wetterich, S., Hubberten, H.-W., Brown, J., 2010. Permafrost evidence for severe winter cooling during the Younger Dryas in northern Alaska. Geophysical Research Letters, 37, L03501.

Reimer, P.J., Baillie, M.G.L., Bard, E., Bayliss, A., Beck, J.W., Blackwell, P.G., Bronk Ramsey, C., Buck, C.E., Burr, G.S., Edwards, R.L., Friedrich, M., Grootes, P.M., Guilderson, T.P., Hajdas, I., Heaton, T., Hogg, A.G., Hughen, K.A., Kaiser, K.F., Kromer, B., McCormac, F.G., Manning, S.W., Reimer, R.W., Richards, D.A., Southon, J.R., Talamo, S., Turney, C.S.M., van der Plicht, J., Weyhenmeyer, C.E., 2013. IntCal13 and Marine13 radiocarbon age calibration curves 0–50,000 years cal BP. Radiocarbon, 55 (4), 1869-1887.

Sanborn, P.T., Smith, C.A., Froese, D.G., Zazula, G.D., Westgate, J.A., 2006. Full-glacial paleosols in perennially frozen loess sequences, Klondike goldfields, Yukon Territory, Canada. Quaternary Research, 66 (1), 147-157.

Schirrmeister, L., Siegert, C., Kuznetsova, T., Kuzmina, S., Andreev, A., Kienast, F., Meyer, H., Bobrov, A., 2002. Paleoenvironmental and paleoclimatic records from permafrost deposits in the Arctic region of Northern Siberia. Quaternary International, 89 (1), 97-118.

Zazula, G.D., Froese, D.G., Westgate, J.A., La Farge, C., Mathewes, R.W., 2005. Paleoecology of Beringian “packrat” middens from central Yukon Territory, Canada. Quaternary Research, 63, 189-198.

Zazula, G.D., Froese, D.G., Elias, S.A., Kuzmina, S., La Farge, C., Reyes, A.V., Sanborn, P.T., Schweger, C.E., Scott Smith, C.A., Mathewes, R.W., 2006. Vegetation buried under Dawson tephra (25,300 ^{14}C years BP) and locally diverse late Pleistocene paleoenvironments of Goldbottom Creek, Yukon, Canada. Palaeogeography, Palaeoclimatology, Palaeoecology, 242 (3-4), 253-286.

Zazula, G.D., Froese, D.G., Elias, S.A., Kuzmina, S., Mathewes, R.W., 2007. Arctic ground squirrels of the mammoth-steppe. Paleoecology of Late Pleistocene middens (~24,000 – 29,450 ^{14}C yr BP), Yukon Territory, Canada. Quaternary Science Reviews, 26, 979-1003.

Chapter 4: A 50,000 year record of meteoric water isotopes ($\delta^2H/\delta^{18}O$) and paleoenvironments from central Yukon permafrost

A version of this chapter will be submitted for publication with the following authorship: Matt Mahony, Trevor Porter, Joel Pumple, Fabrice Calmels and Duane Froese. In this work, I did primary descriptions of the Black Hills, Upper Quartz, Upper Goldbottom, Upper Hunker, and Lower Hunker sites. Fabrice Calmels drilled the Lucky Lady II site, which I subsequently re-analyzed for this chapter. Joel Pumple provided samples from the Lower Quartz site, while Duane Froese provided the samples and radiocarbon dates from the Lucky Lady II, Brimstone and Lower Quartz sites. Trevor Porter provided assistance with the modern Global Network of Isotopes in Precipitation (GNIP) dataset and interpretations of the stable isotope record.

Introduction

Permafrost is an exceptional archive of late Quaternary environmental conditions owing to slow rates of organic matter decomposition in frozen sediments (Guthrie, 1990; Shapiro and Cooper, 2003; Froese et al., 2009; Zazula et al., 2003, 2007). These archives are best known for the preservation of Quaternary mammalian (Guthrie, 1990) and plant remains (Yashina et al., 2012) but ice-rich permafrost can also serve as an archive for meteoric water isotopes ($\delta^2H/\delta^{18}O$), which are closely associated with air temperatures in high-latitude regions (Dansgaard, 1964). Over the last two decades, syngenetic ground ice from unglaciated sites in Yukon, Alaska, and Siberia, collectively Beringia, has been developed as an isotopic paleoclimate proxy (Kotler and Burn, 2000; Schirrmeister et al., 2002; Lacelle et al., 2004; Popp et al., 2006; Meyer et al., 2010; Opel et al., 2011; Wetterich et al., 2011; Fritz et al., 2012). These records are generally restricted to the radiocarbon timescale and are of coarser temporal resolution than ice cores, but they do provide an opportunity to improve the spatial coverage of late Pleistocene meteoric water isotope records and knowledge of regional climate dynamics. Furthermore, when permafrost isotopes are paired with paleoecological and cryostratigraphic data, a fuller interrogation of the paleoclimate record may be possible (Schirrmeister et al., 2002). Here we present a new, multi-proxy composite record of paleoenvironmental change spanning the last *ca.* 50,000 cal yrs BP based on the cryostratigraphy, paleoecological indicators and $\delta^2H/\delta^{18}O$ of frozen ‘muck’ deposits in the Klondike goldfields of central Yukon (Froese et al., 2009). We use this record to provide new insight into past climatic and ecological changes in the region during this interval, including additional discussions on reduced ice wedge formation during the last cold stage, megafauna records, and the last glacial-interglacial transition.

Study area and methods

The Klondike goldfields of central Yukon (Figure 4-1) are within the largely unglaciated region of eastern Beringia (Froese et al., 2009). The area hosts widespread syngenetic permafrost, reflecting the aggradation of sediments (primarily loess) during Pleistocene cold stages, thus preserving a record of these past environments (Fraser and Burn, 1997). Placer mining exposures through the area provide convenient access to these deposits. For this study, eight sites where stratigraphic sections were revealed by placer mining activities were surveyed for cryostratigraphy, paleoecological indicators, and water isotopes. The locations of these sites were recorded with a handheld GPS, while elevations for samples were measured via a laser range finder (Lasertech 200XL) with 0.1 m vertical precision; given challenges with operator position and target accuracy, we estimate vertical accuracy to be 0.5 m. We developed a composite record of $\delta^2H/\delta^{18}O$ from syngenetic ice wedges and pore ice from eight sites up to 60 km apart.

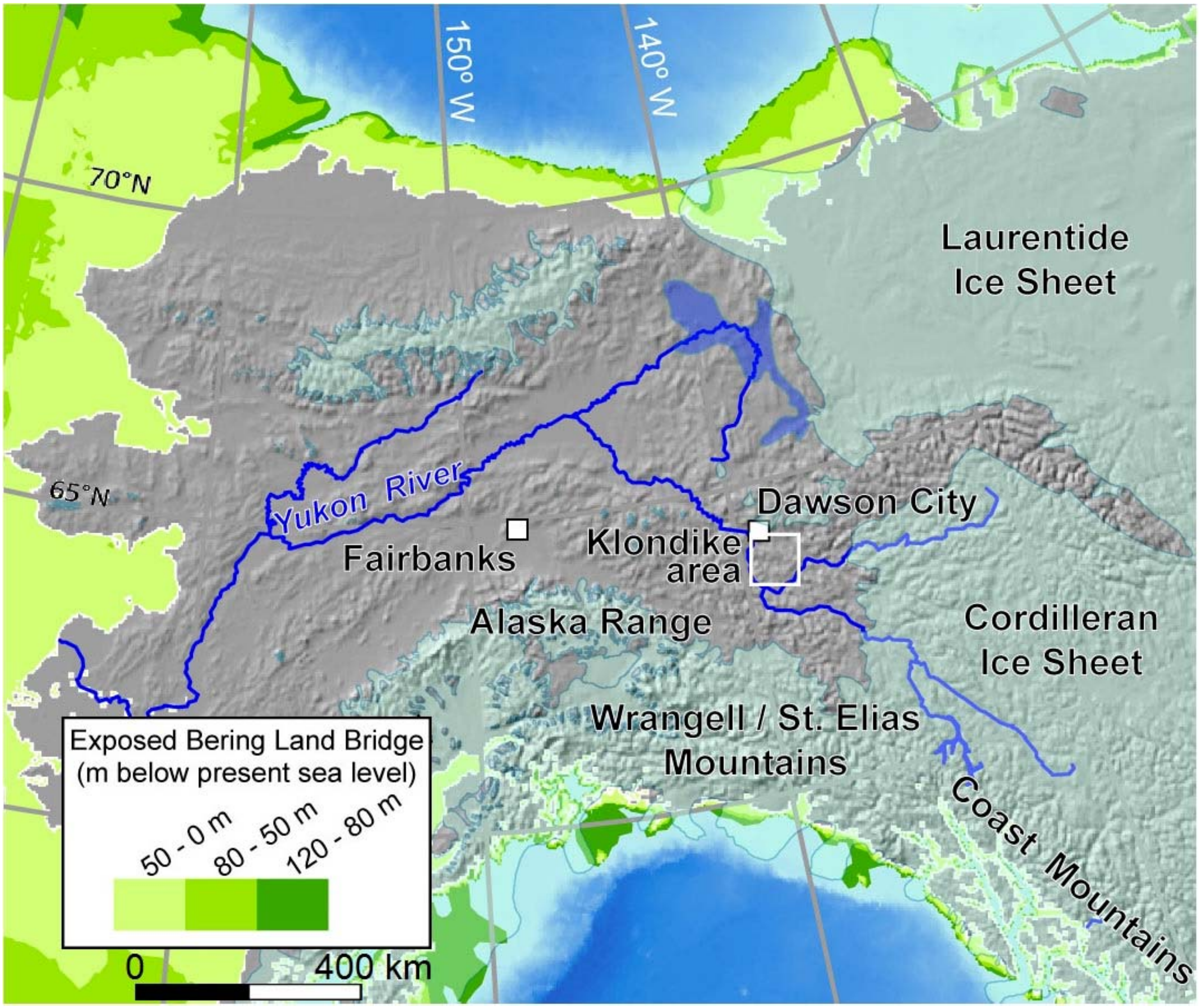

Figure 4-1 : Extent of glacial ice cover and exposed land during the late Pleistocene (adapted from Froese et al., 2009). The Klondike area, located just outside of Dawson City, is outlined by the white square.

Radiocarbon dates and the presence of Dawson tephra (*ca.* 29,400 cal yrs BP) provide chronology for sites (Zazula et al., 2006; Demuro et al., 2008). Pretreatment of organic samples for ^{14}C dating by accelerator mass spectrometry (AMS) was completed at the University of Alberta. Plant macrofossil samples were placed in sterilized glass culture tubes for an acid-base-acid (ABA) wash, consisting of heating samples to 70°C and submerging them for 30 minutes in 1M HCl, followed by 60 minute washes of 1M NaOH until solution was clear, and finally a 30 minute 1M HCl wash. Samples were rinsed with ultrapure water until neutral and freeze-dried. Prepared samples were shipped to the Keck Carbon Cycle

Accelerator Mass Spectrometer facility (University of California, Irvine). Radiocarbon dates of 85 plant macrofossils were calibrated via the IntCal13 calibration curve (Table 4-1a, 4-1b) (Bronk Ramsey, 2009; Reimer et al., 2013). In total, 175 pore ice and 16 ice wedge samples were analyzed for $\delta^2H/\delta^{18}O$ at the University of Alberta using an LGR (model DLT-100) and a Picarro (model L2130-i), which utilize laser absorption spectrometry. Waters from 10 samples were also analyzed via isotope-ratio mass spectrometry, and were indistinguishable from samples measured using the laser absorption spectrometry method (see Chapter 2). $\delta^2H/\delta^{18}O$ values were calibrated to the VSMOW scale based on two international standards (USGS45 and USGS46) run at the same time as the unknowns. Measurement precision in this study was 1.0‰ for δ^2H and 0.2‰ for $\delta^{18}O$ based on routine measurement of Evian water, which is a secondary water standard with isotopic values defined in Chesson et al. (2010) (Table 4-2).

Ages for the organic materials were interpolated between dated macrofossils. Estimations of aggradation rates are compiled in Appendix B. Ages of pore ice in syngenetic permafrost is thought to be younger than the organic material in the sediment due to the ability of surface waters to penetrate down into sediment at the base of the active layer which hosts relatively older organics. Pore ice is preserved at the bottom of the active layer over a number of years, as deposition at the surface causes the permafrost table to aggrade. The result is pore ice values that are younger than the radiocarbon ages of organics obtained at the same depth (Figure 4-2). Estimation of the age of pore waters is calculated based on aggradation rates and active layer depths, such that:

$$Age_{waters} = Age_{organics} - (\text{Paleoactive layer depth} * \text{Aggradation rate})$$

Paleoactive layers during the last cold stage were likely deeper than present due to bare patches of soil, reduced cloud cover, and well-drained active layers (Guthrie, 1990; Guthrie, 2001; Froese et al., 2009). In this study we assume last cold stage active layers to be 0.8 m, which may be a relatively conservative estimate. Active layer depths for the remainder of the record are assumed to be 0.6 m (Figure 4-3).

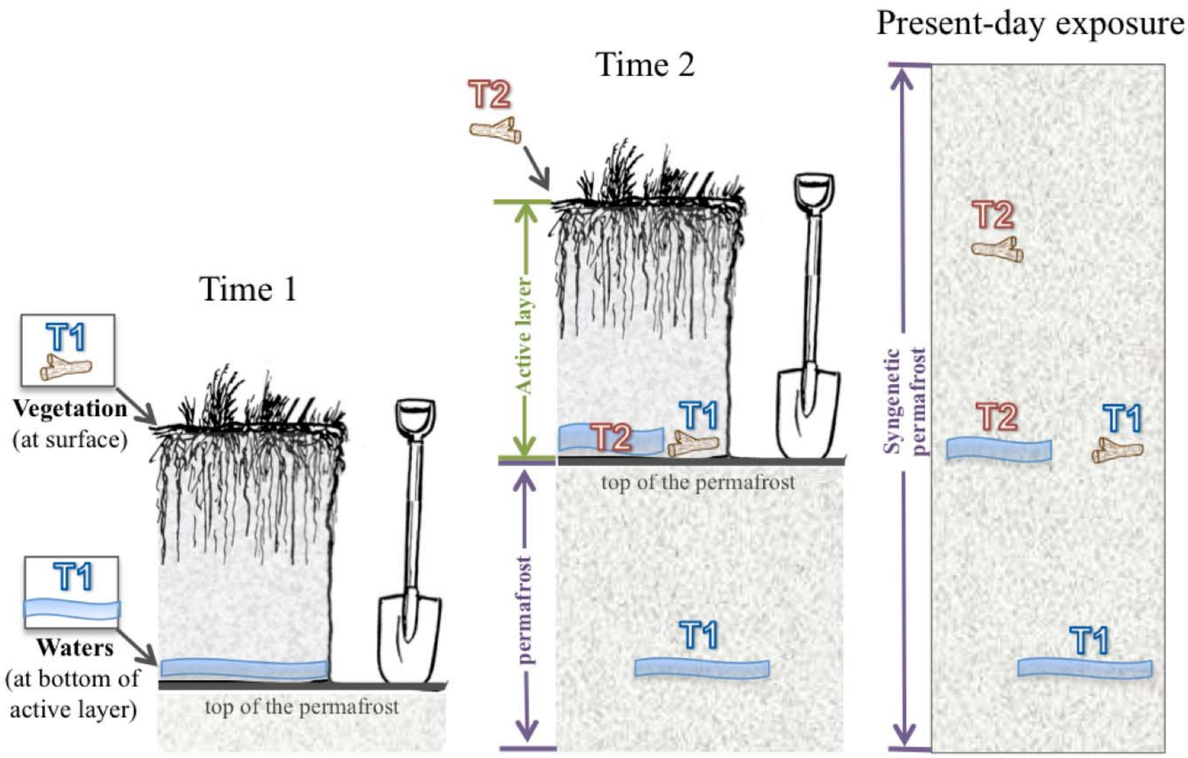

Figure 4-2 : Age relations between organics and pore ice in aggrading permafrost (adapted from Guthrie, 2001). Pore ice is assumed to be a record of waters that froze at the base of the active layer and became incorporated into the permafrost. Because of this assumption, we adjust the ages of pore waters based on paleoactive layer depths and aggradation rates. Calibrated radiocarbon ages used for estimating the age of the waters. Active layer depths in this study are assumed to be 0.8 m for the last cold stage sediment and 0.6 m for interstadial and interglacial sediment.

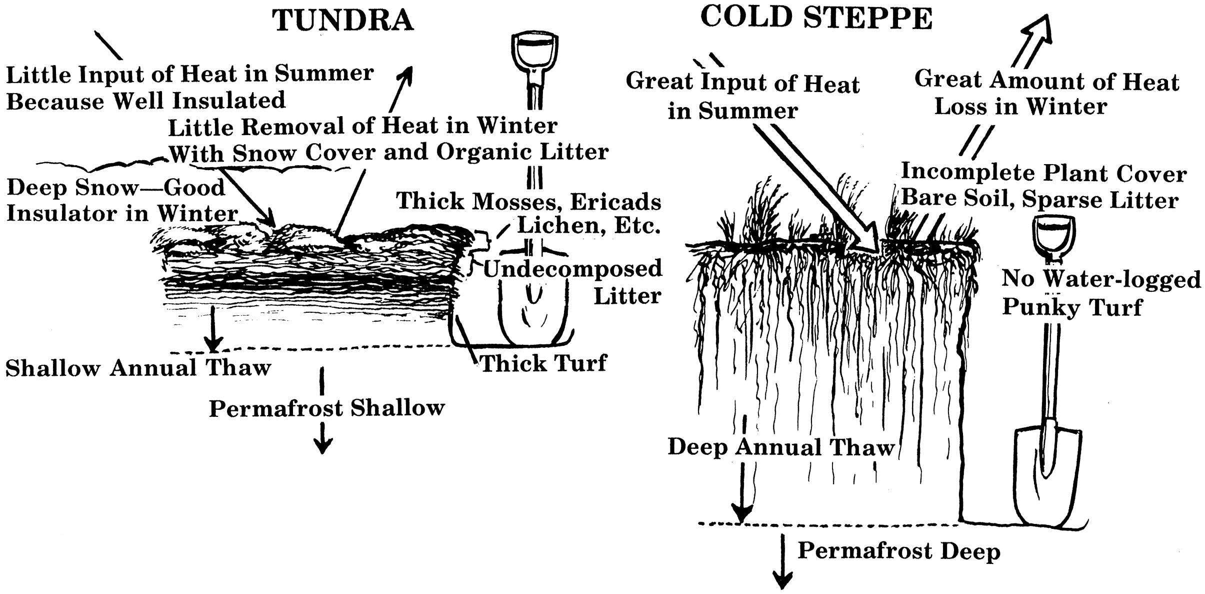

Figure 4-3 : Illustration of active layer depths in organic soils (left) and mineral soils (right) (from Guthrie, 2001). Paleoactive layer depths are assumed to be 0.8 m in steppe-tundra environments of the last cold stage and 0.6 m in interstadial and interglacial environments.

Table 4-1a : Details of the 85 radiocarbon dates in this study. Full calibrated age ranges are in Appendix A.

Site	Sample	Cal yrs BP	^{14}C yrs BP	±	Lab ID	Material
Black Hills	MM12-64	145	140	20	UCIAMS-114904	peat
Black Hills	MM12-63	3,040	2,905	20	UCIAMS-114902	twigs
Black Hills	MM12-68	>25,655	>21,300	-	UCIAMS-150831	grass
Black Hills	MM12-70	25,840	21,550	140	UCIAMS-114923	grass
Black Hills	MM12-70	26,775	22,490	310	UCIAMS-122279	grass
Black Hills	MM12-75	27,220	22,930	810	UCIAMS-131097	grass
Black Hills	MM12-67	27,575	23,360	100	UCIAMS-114718	AGSN
Brimstone	DF12-32	1,015	1,115	20	UCIAMS-114917	wood
Brimstone	DF12-34	1,485	1,610	20	UCIAMS-114915	grass
Brimstone	DF12-40	3,900	3,595	20	UCIAMS-114916	peat
Brimstone	DF12-35	6,445	5,665	20	UCIAMS-114900	wood
Brimstone	DF12-41	6,600	5,800	25	UCIAMS-122287	wood
Lower Hunker	MM12-110	9,290	8,280	25	UCIAMS-114901	wood
Lower Hunker	MM12-108	11,070	9,720	140	UCIAMS-122280	twigs/grass
Lower Hunker	MM12-LH2-259-09	22,720	18,780	380	UCIAMS-122277	grass
Lower Hunker	MM12-105	23,810	19,780	150	UCIAMS-122281	grass
Lower Hunker	MM12-100	26,145	21,930	90	UCIAMS-114711	fecal pellets
Lower Hunker	MM12-103	27,295	22,990	190	UCIAMS-122283	fecal pellets
Lower Hunker	MM12-22	34,950	31,020	250	UCIAMS-114726	shrub twigs
Lower Hunker	MM12-97	non-finite	49,600	2,400	UCIAMS-114715	wood
Lower Quartz	DF10-25	28,210	23,990	560	UCIAMS-101864	AGSN
Lower Quartz	DF10-24	30,160	25,920	180	UCIAMS-101914	AGSN
Lower Quartz	DF10-37	30,305	26,030	140	UCIAMS-96042	grass
Lower Quartz	DF10-37b	30,330	26,070	180	UCIAMS-101901	grass
Lower Quartz	DF10-36	30,685	26,300	1,300	UCIAMS-101859	grass
Upper Goldbottom	MM12-39	5,945	5,185	20	UCIAMS-114898	wood
Upper Goldbottom	MM12-121	10,135	8,965	25	UCIAMS-114906	wood
Upper Goldbottom	MM12-124	10,625	9,395	25	UCIAMS-114910	wood
Upper Goldbottom	MM12-112	18,820	15,570	50	UCIAMS-122282	fecal pellets
Upper Goldbottom	MM12-113	20,375	16,895	45	UCIAMS-114712	AGSN
Upper Goldbottom	MM13-44b	24,525	20,310	720	UCIAMS-131093	AGSN
Upper Goldbottom	MM13-41a	25,285	20,960	150	UCIAMS-131095	AGSN
Upper Goldbottom	MM13-39	32,385	28,450	210	UCIAMS-142201	wood
Upper Goldbottom	MM12-134	35,895	32,000	320	UCIAMS-114714	AGSN
Upper Goldbottom	MM12-125	42,100	37,770	660	UCIAMS-142208	wood
Upper Goldbottom	MM12-129	43,985	40,270	770	UCIAMS-114716	wood
Upper Goldbottom	DF12-24	45,650	42,070	980	UCIAMS-122274	wood
Upper Hunker	MM12-51	1,555	1,655	15	UCIAMS-114732	peat
Upper Hunker	MM12-48	6,090	5,320	15	UCIAMS-114727	wood
Upper Hunker	MM12-160	46,800	43,200	1,100	UCIAMS-114724	wood
Upper Hunker	MM12-158	48,550	46,350	1,900	UCIAMS-122276	wood bits/grass
Upper Hunker	MM12-155	non-finite	>49,500	-	UCIAMS-114717	AGSN

Table 4-1b : Details of the 85 radiocarbon dates in this study. Full calibrated age ranges are in Appendix A.

Site	Sample	Cal yrs BP	^{14}C yrs BP	±	Lab ID	Material
Lucky Lady II	LL2S-169	8,525	7,750	25	UCIAMS-143296	twigs
Lucky Lady II	LL2S-189	8,865	7,975	25	UCIAMS-142212	needle/leaves
Lucky Lady II	LL2S-353	9,780	8,770	30	UCIAMS-142211	leaves/twigs
Lucky Lady II	LLII-5.25(+)	10,340	9,195	20	UCIAMS-67149	shrub twigs
Lucky Lady II	LL2A-17	10,505	9,300	25	UCIAMS-143297	leaves/twigs
Lucky Lady II	LLII-4.0(+)	10,730	9,480	20	UCIAMS-67155	shrub twigs
Lucky Lady II	LL2A-154	11,620	10,020	170	UCIAMS-143298	twigs
Lucky Lady II	LL2B-25	12,195	10,340	45	UCIAMS-143302	twig
Lucky Lady II	LLII-2.25(+)	12,850	11,000	20	UCIAMS-67153	shrub twigs
Lucky Lady II	LL2C-37	12,935	11,070	30	UCIAMS-143306	twigs/grass
Lucky Lady II	LL2A-308	13,010	11,125	30	UCIAMS-143299	twigs
Lucky Lady II	LLII-1.0(+)	13,035	11,145	25	UCIAMS-67154	shrub twigs
Lucky Lady II	LL2B-155	13,045	11,165	35	UCIAMS-143303	twigs/grass
Lucky Lady II	LLII-0.81(+)	13,105	11,250	20	UCIAMS-67152	shrub twigs
Lucky Lady II	DF08-26A	13,140	11,290	160	UCIAMS-56390	twigs/grass
Lucky Lady II	LL2C-88(2)	13,145	11,290	40	UCIAMS-142198	shrub twigs
Lucky Lady II	LL2C-88	13,150	11,300	35	UCIAMS-142197	shrub twigs
Lucky Lady II	DF12-18	13,200	11,360	40	UCIAMS-114725	twigs/grass
Lucky Lady II	LL2B-225	13,240	11,405	30	UCIAMS-143304	twigs/grass
Lucky Lady II	DF12-18	13,375	11,535	35	UCIAMS-143307	twigs/grass
Lucky Lady II	DF12-18	13,410	11,580	35	UCIAMS-143308	twigs/grass
Lucky Lady II	DF13-05	13,675	11,875	35	UCIAMS-131092	AGSN
Lucky Lady II	LL2A-425	13,675	11,870	50	UCIAMS-143301	twig
Lucky Lady II	LL2-12-184	15,520	12,980	60	UCIAMS-122284	grass
Lucky Lady II	DF12-61b	15,990	13,300	30	UCIAMS-114721	AGSN
Lucky Lady II	LL2-12-259	16,160	13,430	35	UCIAMS-122273	grass
Lucky Lady II	DF08-97	16,500	13,680	35	UCIAMS-51324	AGSN
Upper Quartz	MM13-16	5,165	4,520	25	UCIAMS-142207	wood
Upper Quartz	MM12-96	5,840	5,115	25	UCIAMS-114911	wood
Upper Quartz	MM12-95	5,925	5,160	20	UCIAMS-114899	wood
Upper Quartz	MM12-QC-06	12,805	10,960	35	UCIAMS-114733	grass
Upper Quartz	MM13-28	13,110	11,245	40	UCIAMS-150828	twigs/grass
Upper Quartz	MM13-30	13,160	11,315	35	UCIAMS-142205	wood
Upper Quartz	MM13-15	13,255	11,420	35	UCIAMS-131098	wood
Upper Quartz	MM13-14	13,510	11,690	35	UCIAMS-131100	wood
Upper Quartz	MM13-28	13,655	11,835	35	UCIAMS-150832	twigs/grass
Upper Quartz	MM13-29	13,685	11,885	35	UCIAMS-142206	wood
Upper Quartz	MM13-25	14,080	12,190	35	UCIAMS-142199	leaves/twigs
Upper Quartz	MM13-12	14,335	12,340	35	UCIAMS-142196	grass
Upper Quartz	MM13-11	15,740	13,110	35	UCIAMS-142195	AGSN
Upper Quartz	MM13-22	16,270	13,510	45	UCIAMS-131096	AGSN
Upper Quartz	MM13-17	16,310	13,520	170	UCIAMS-131094	grass
Upper Quartz	MM12-QC-02	16,560	13,680	390	UCIAMS-114710	grass

Table 4-2 : Isotopic deviation (‰) of 42 Evian waters analyzed as unknown quality control standards in this study from the published values in Chesson et al. (2010) (sorted in ascending $\delta^{18}O$ deviation). Deviation of isotopic ratios presented as absolute values.

QC #	δ^2H (‰)	$\delta^{18}O$ (‰)	QC #	δ^2H (‰)	$\delta^{18}O$ (‰)
QC1	2.6	0.02	**QC23**	1.3	0.20
QC2	1.3	0.03	**QC24**	0.8	0.20
QC3	0.2	0.03	**QC25**	0.7	0.20
QC4	0.3	0.03	**QC26**	1.7	0.24
QC5	1.9	0.03	**QC27**	0.4	0.25
QC6	1.2	0.05	**QC28**	0.0	0.25
QC7	0.2	0.05	**QC29**	1.4	0.25
QC8	1.2	0.06	**QC30**	1.7	0.27
QC9	1.8	0.07	**QC31**	1.3	0.27
QC10	0.2	0.09	**QC32**	0.6	0.28
QC11	1.4	0.10	**QC33**	2.1	0.28
QC12	0.3	0.12	**QC34**	0.3	0.28
QC13	0.4	0.13	**QC35**	1.1	0.33
QC14	0.5	0.15	**QC36**	0.9	0.34
QC15	1.1	0.15	**QC37**	0.4	0.37
QC16	0.5	0.15	**QC38**	1.1	0.39
QC17	0.9	0.15	**QC39**	0.0	0.52
QC18	1.6	0.16	**QC40**	1.5	0.53
QC19	0.0	0.16	**QC41**	0.9	0.68
QC20	1.1	0.17	**QC42**	1.9	0.74
QC21	1.2	0.18	**AVG**	**1.0**	**0.22**
QC22	0.5	0.19	**STDEV**	**0.6**	**0.17**

Results

Four units are defined below based on the cryostratigraphy, $\delta^2H/\delta^{18}O$, and paleoecological indicators from the study sites (Figure 4-4a, 4-4b, 4-5). The three lowermost units are late Pleistocene, while the uppermost unit is largely Holocene in age. Volumetric ice content of 18 samples are in Appendix G. Co-isotope relations for the ground ice samples have a slope of 7.1 with an r^2 value of 0.98, in close agreement with the local meteoric water line of modern precipitation for Whitehorse and Mayo, Yukon (Figure 4-6) (GNIP dataset, 2013). Isotopic ratios ($\delta^2H/\delta^{18}O$) of permafrost waters are in close agreement between sites, giving us confidence that the changes are a reflection of regional phenomena (Figure 4-7, 4-8, 4-9).

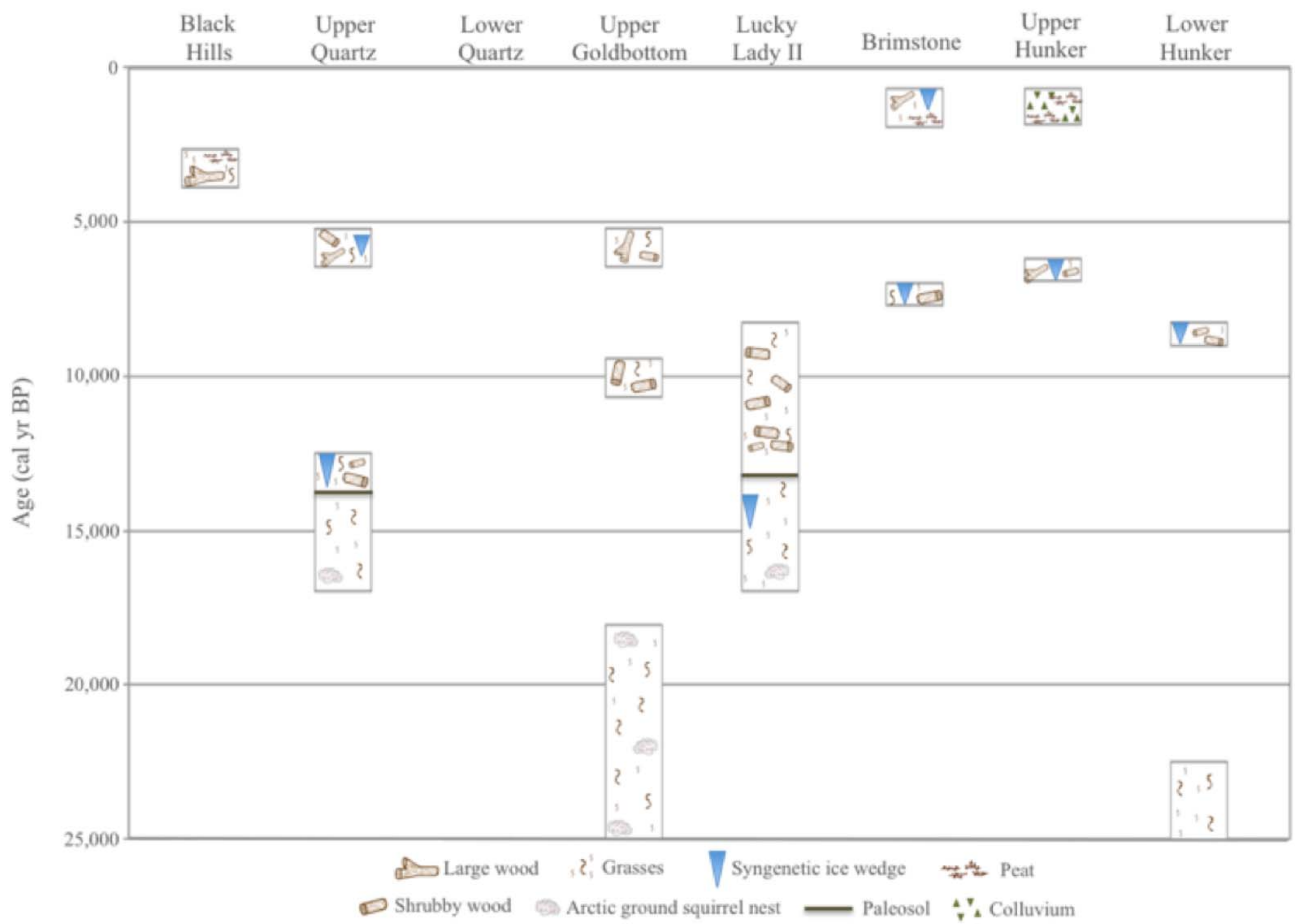

Figure 4-4a : Permafrost units in the eight exposures included in this study, spanning 0 – 25,000 cal yrs BP. The symbols are included to characterize the units, and are not intended to reflect the precise chronology of cryostratigraphic or vegetational changes within the units.

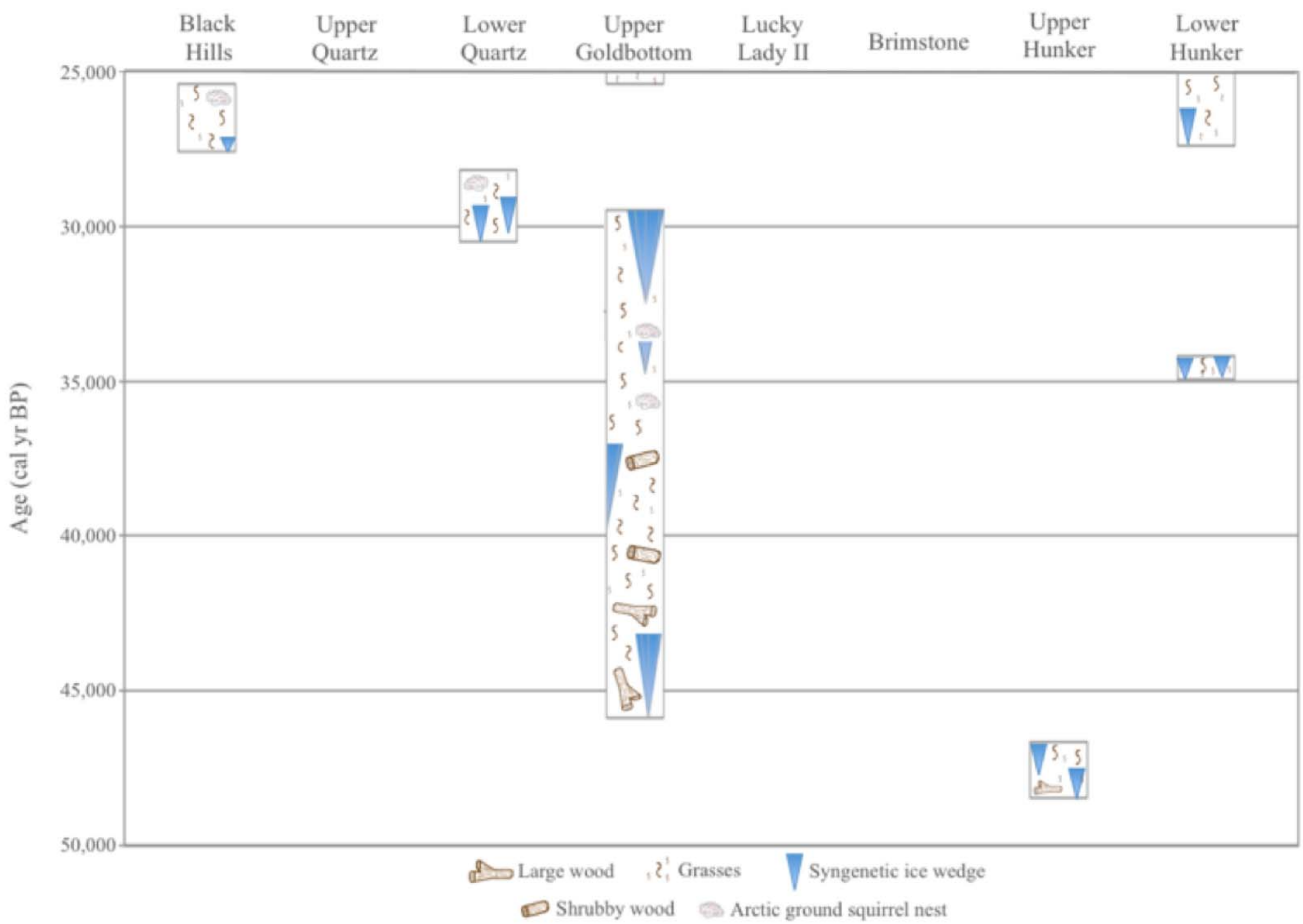

Figure 4-4b : Permafrost units in the eight exposures included in this study, spanning 50,000 to 25,000 cal yrs BP. Symbols characterize the units, and are not intended to reflect the precise chronology of cryostratigraphic or vegetational changes

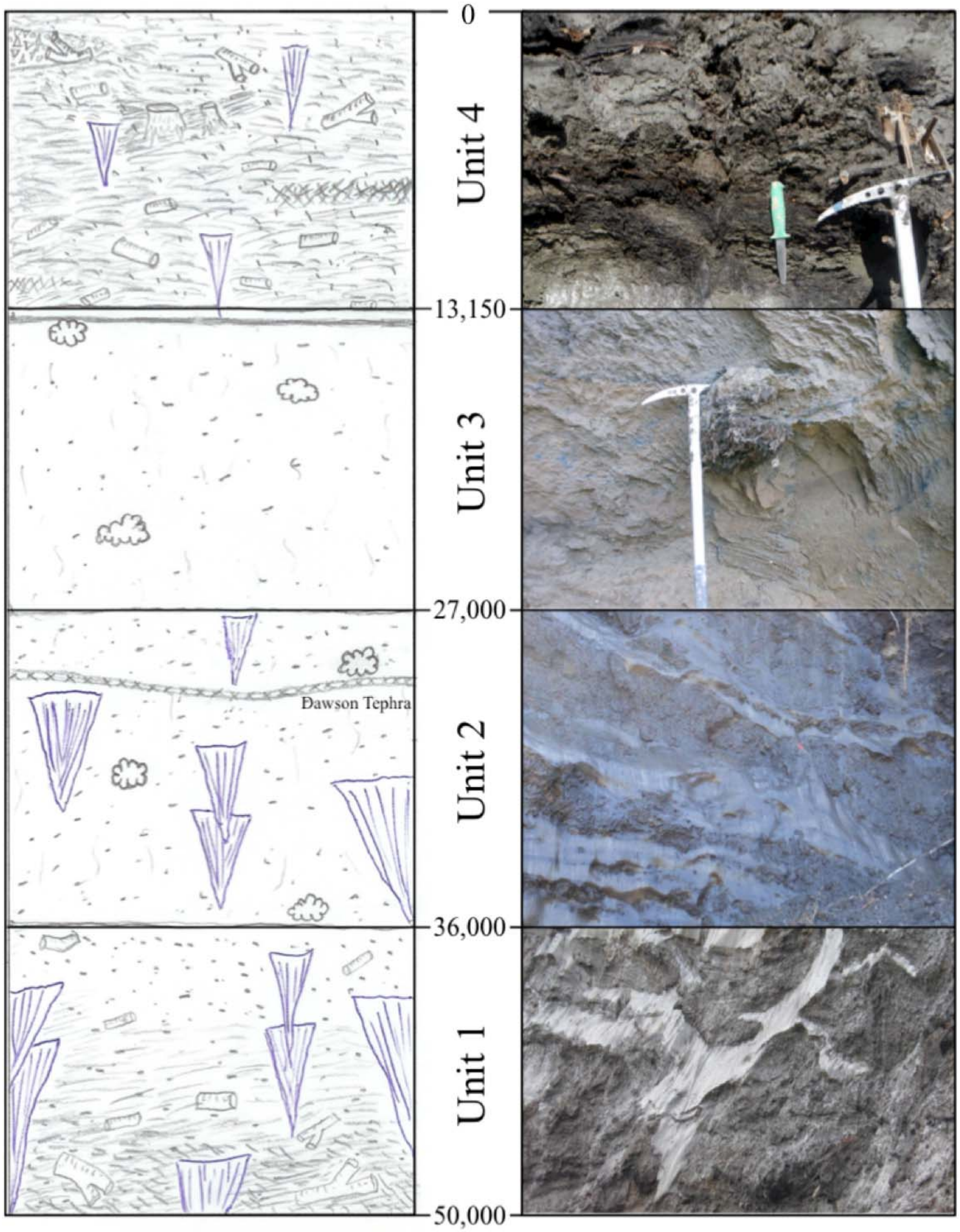

Figure 4-5 : Four permafrost units defined in this study from the Klondike area, Yukon. Ages are in cal yrs BP. Unit 1 photo shows organic-rich sediments with abundant woody macrofossils and syngenetic ice wedges at the Upper Hunker site, Unit 2 photo shows brown organic silts and large ice wedges at Lower Hunker, Unit 3 photo shows grey silts with graminoid vegetation and an arctic ground squirrel nest at Black Hills, and Unit 4 photo shows black organic silt with wood-rich detritus and small ice wedges at Brimstone.

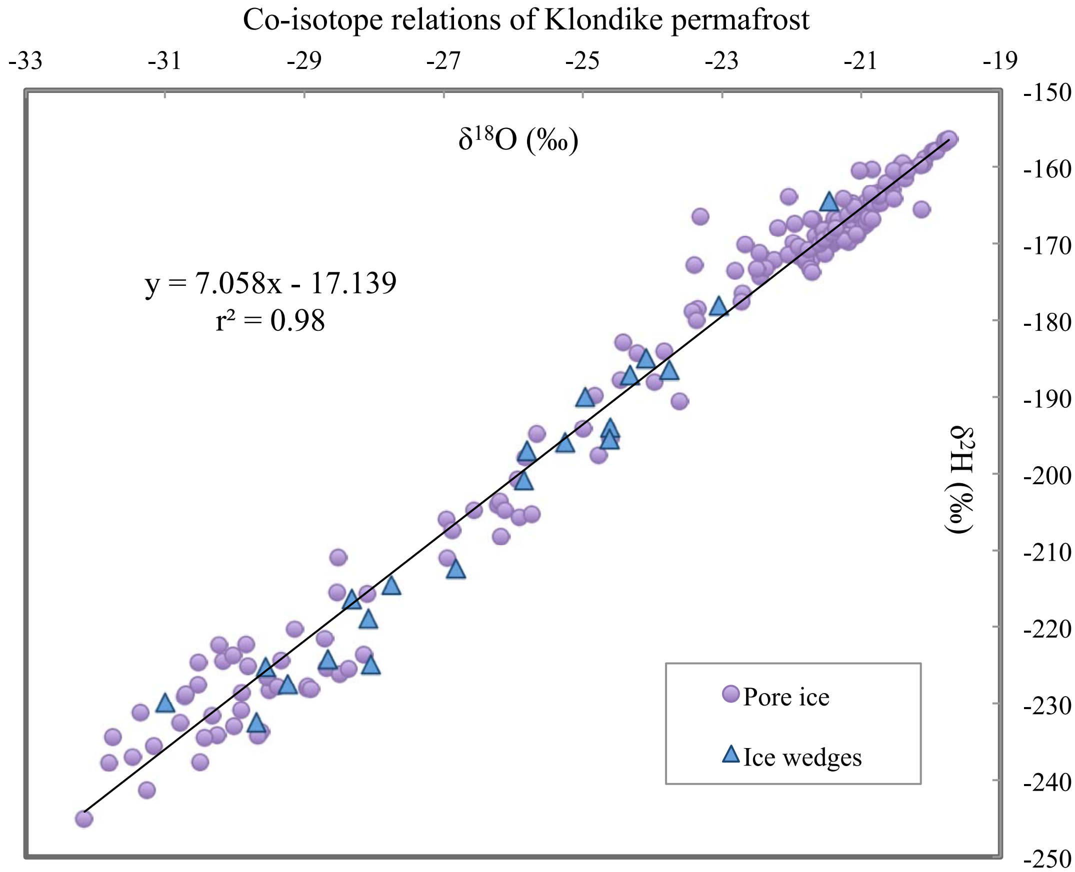

Figure 4-6 : Co-isotope relations between $\delta^{18}O$ and $\delta^{2}H$ for the samples in this study. These include 175 pore ice samples and values from 16 individual ice wedges (two of which were sampled multiple times). The slope of the best-fit line is 7.1 with an r^2 value of 0.98.

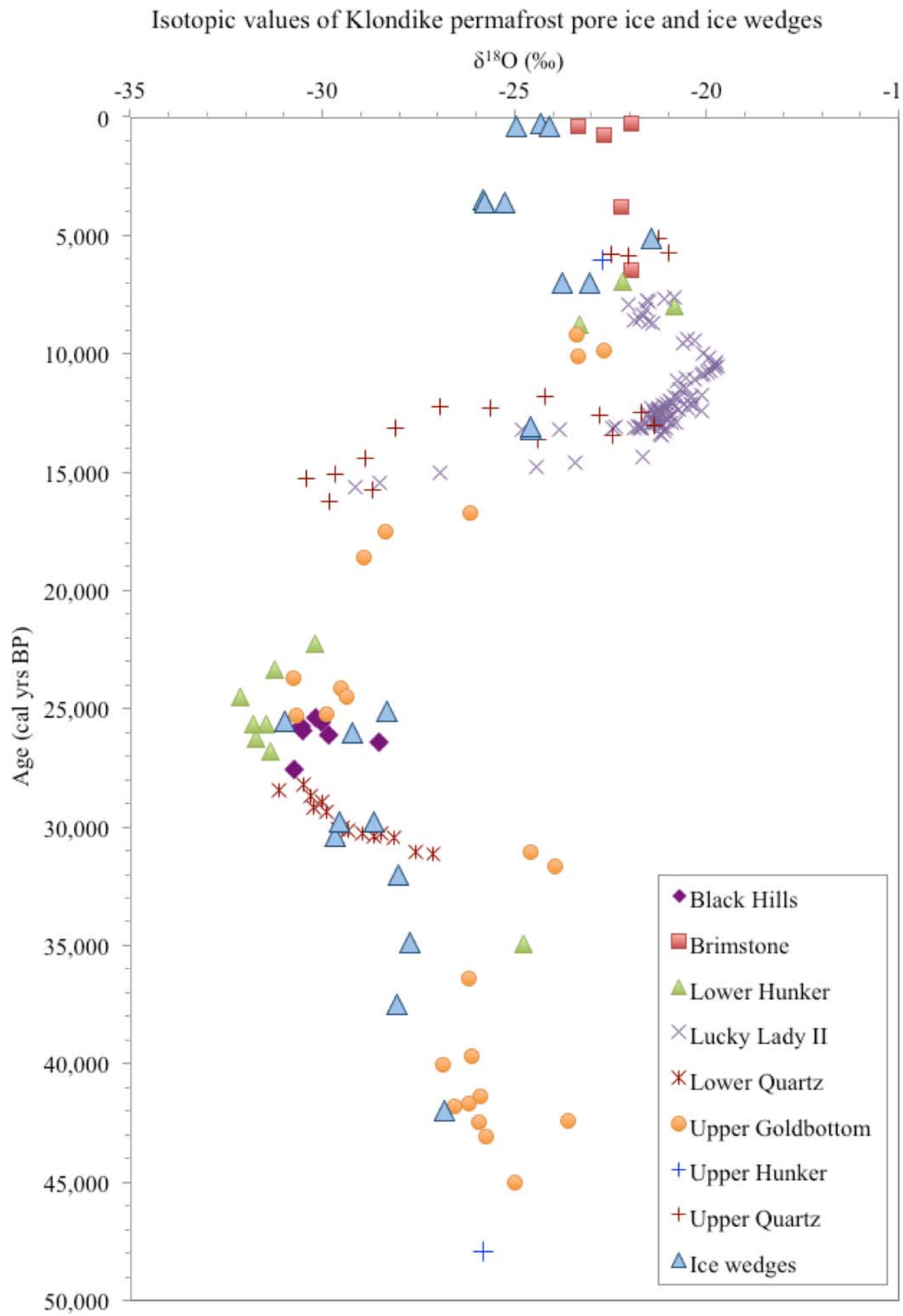

Figure 4-7 : $\delta^{18}O$ (‰) of 175 pore samples and 16 ice wedge samples in this study. The ages of samples are estimated from 85 radiocarbon dates and corrected for the organic-water age offset illustrated in Figure 4-2.

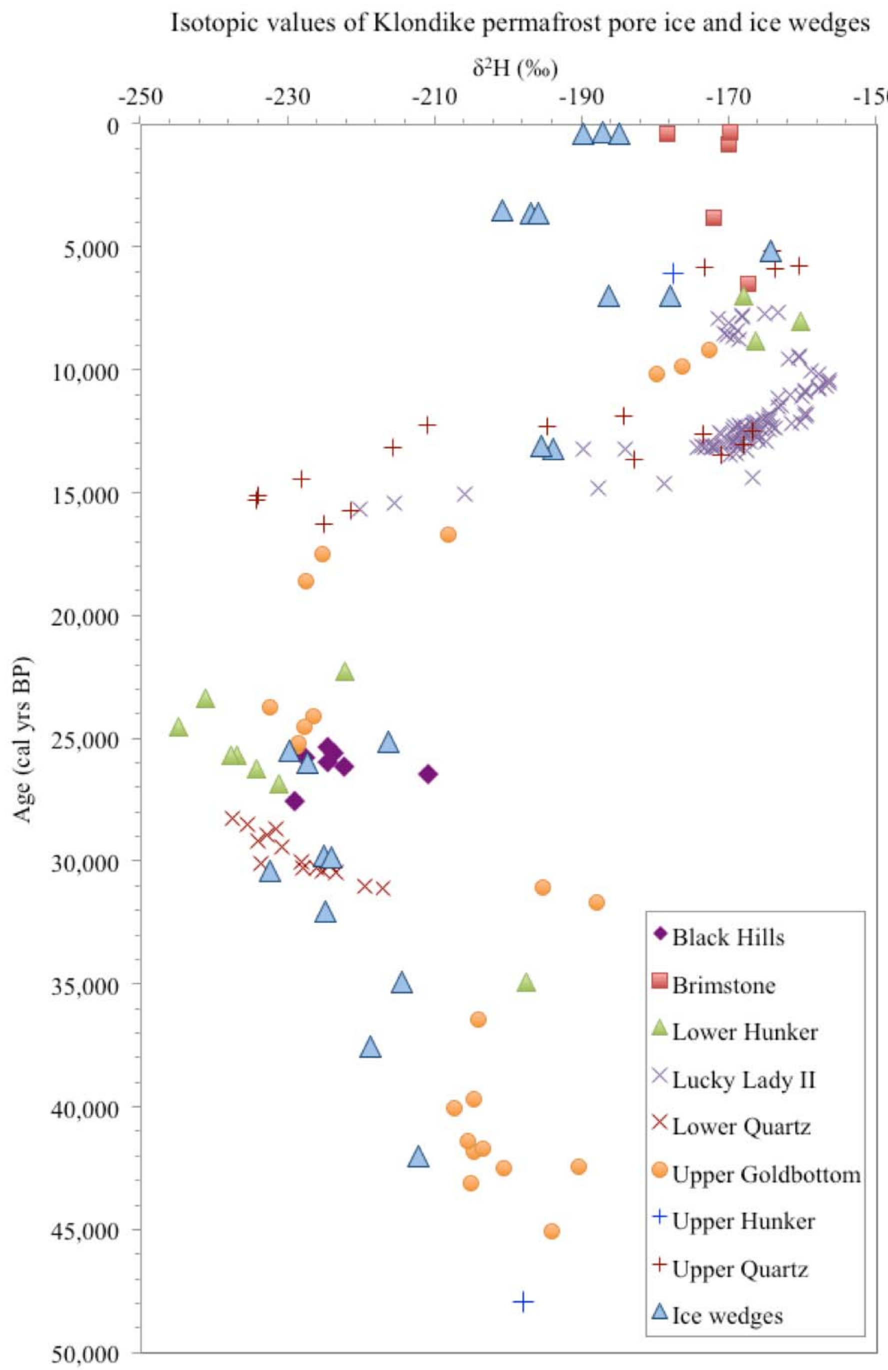

Figure 4-8 : δ^2H (‰) of 175 pore ice and 16 ice wedge samples in this study. The ages of samples are estimated from 85 radiocarbon dates and corrected for the organic-water age offset illustrated in Figure 4-2.

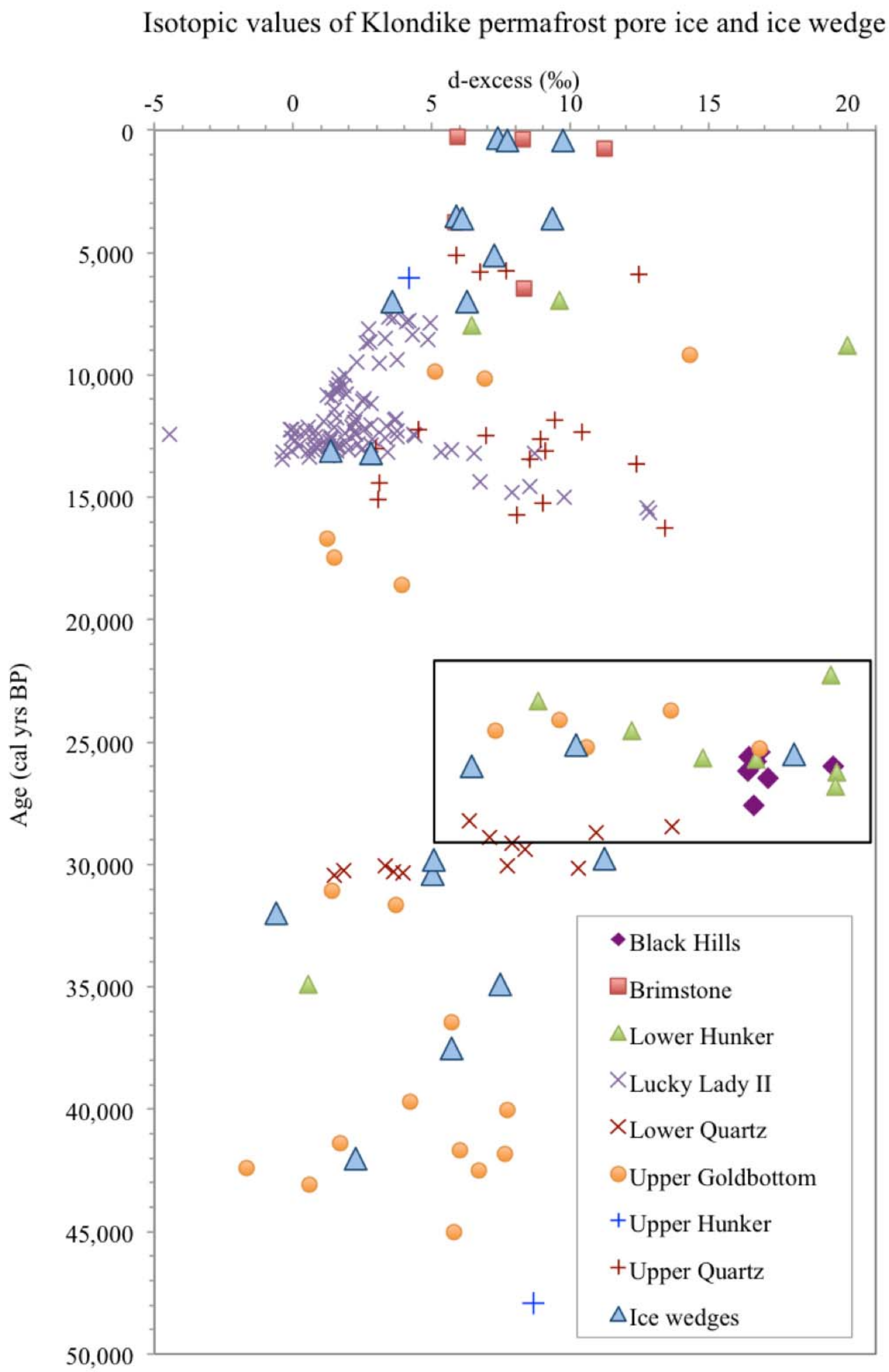

Figure 4-9 : D-excess (‰) of samples through the last 50,000 cal yrs BP. The black rectangle outlines a distinct +9‰ enrichment period from *ca.* 29,000 to 22,000 cal yrs BP from the Black Hills, Lower Hunker, Lower Quartz, and Upper Goldbottom sites. The ages of samples are estimated from 85 radiocarbon dates and corrected for the organic-water age offset illustrated in Figure 4-2.

Unit 1 — 50,000 to 36,000 cal yrs BP

Unit 1 is characterized by organic-rich sediments with abundant woody macrofossils and large syngenetic ice wedges up to ~3 m wide. This unit is present at Upper Goldbottom and Upper Hunker sites and is at least 12.6 m thick. Carbon and nitrogen contents of the sediment average 5.2% and 0.4% ($n = 5$; $1\sigma = 0.7\%$; 0.1%), respectively. The ice present within the sediments is generally non-parallel and parallel wavy lenticular (typically 2 – 4 mm thick, up to 16 mm thick) and microlenticular ice in otherwise structureless sediment with volumetric ice contents of 57 – 119% from three samples (ice content of all 18 samples in Appendix G). δ^2H and $\delta^{18}O$ exhibit little overall trend during this interval, with mean values of -202‰ (1σ = 5‰) and -25.8‰ (1σ = 0.9‰), respectively. Vegetation shifts from abundant spruce (*Picea sp.*) macrofossils at the base of the unit to shrub and graminoid vegetation in the upper ~6 m. This unit does not contain any evidence of arctic ground squirrel nests. Five radiocarbon dates of wood macrofossils obtained from within this unit range from *ca.* 48,500 to 36,000 cal yrs BP. Aggradation is estimated to have been moderate, with one rate from Upper Goldbottom indicating 0.08 cm/year.

Unit 2 — 36,000 to 27,000 cal yrs BP

Unit 2 contains brown organic silts and large syngenetic ice wedges (up to 2.5 m wide) with vegetation ranging from small twigs near the base of the unit to largely graminoid vegetation towards the top. This unit is present at Lower Quartz, Upper Goldbottom, and Lower Hunker sites and is at least 15 m thick. Carbon and nitrogen contents of the sediment averages 3.2% and 0.3% ($n = 17$; $1\sigma = 0.9\%$; 0.1%), respectively. The ice present within the sediments is generally non-parallel planar layered (~1 mm thick) to wavy lenticular (~1 – 2 mm thick) in otherwise structureless sediment with volumetric ice content of 57% from one sample. Arctic ground squirrel nests are present throughout the unit. Organic-rich sediments with large woody macrofossils are noticeably absent from this unit. Mean δ^2H and $\delta^{18}O$ values are -223‰ (1σ = 14‰) and -28.6‰ (1σ = 2.1‰), respectively. Both δ^2H and $\delta^{18}O$ exhibit negative trends over this interval, but the $\delta^{18}O$ trend is relatively steep compared to that of δ^2H resulting in a sharp rise in deuterium-excess (hereafter, 'd-excess'). D-excess results from non-equilibrium effects, primarily due to the relative humidity at the moisture source (Dansgaard, 1964). The 11 radiocarbon dates obtained within this unit range from *ca.* 36,000 to 27,200 cal yrs BP. Most of these dates are from arctic ground squirrel nests and grasses. Aggradation is estimated to have been moderate to high, with two rates ranging from 0.07 to 0.34 cm/year.

Unit 3 — 27,000 to 13,150 cal yrs BP

Unit 3 is characterized by grey silts that contain less organic matter than the lower units and include graminoid vegetation and arctic ground squirrel nests. This unit is present at Black Hills, Upper Quartz, Upper Goldbottom, Lucky Lady II, and Lower Hunker sites and is at least 8.5 m thick. Carbon and nitrogen contents of the sediment averages 1.5% and 0.1% ($n = 28$; $1\sigma = 0.5\%$; 0.1%), respectively. The ice present within the sediments is generally parallel wavy microlenticular, lenticular, and layered ice up to 2 mm thick. Sediments commonly lack visible excess ice (structureless) and have volumetric ice contents of 40 – 64% from eight samples. Large woody plant macrofossils are absent, as in Unit 2. The negative water isotope trend from Unit 2 continues through Unit 3, but the trend is not as steep. This unit contains the most isotopically depleted water of the record, centered on the interval from *ca.* 27,000 to 23,000 cal yrs BP, with lows of -245‰ for δ^2H and -32.2‰ for $\delta^{18}O$. D-excess is elevated for much of this interval, with a mean value of +15.1‰ (2σ = +7.8‰) from *ca.* 29,000 to 22,000 cal yrs BP. This d-excess anomaly occurs at the Black Hills, Lower Quartz, and Upper Goldbottom sites, which are separated by up to 60 km, suggesting it is a regional phenomenon. Following this period, d-excess returns to typical mean values of +6.6‰ (2σ = +8.6‰, from 22,000 to 13,500 cal yrs BP). From *ca.* 15,000 to 13,150 cal yrs BP, δ^2H and $\delta^{18}O$ increase steadily to highs of -167‰ and -21.1‰, respectively. Multiple sites record either pre- or post-isotopic shift values, but two sites *ca.* 13 km apart (Upper Quartz and Lucky Lady II) record this isotopic shift from *ca.* 15,000 to 13,150 yrs BP. The 31 radiocarbon dates obtained within this unit range from 26,775 to 13,150 cal yrs BP. These are mostly from arctic ground squirrel nests and graminoid vegetation, with several twigs and woody bits towards the top of the unit. A ~4 – 6 cm thick paleosol is present at the top of the unit with four radiocarbon dates ranging from 13,410 to 13,140 cal yrs BP (11,580±35, UCIAMS-143308; 11,290±160, UCIAMS-56390). The aggradation rate is estimated to have been low to moderate, with a total of seven rates ranging from 0.03 to 0.62 cm/year (average 0.18 cm/year).

Unit 4 — < 13,150 cal yrs BP

Unit 4 is characterized by interbedded black, wood-rich detritus and organic silts with small ice wedges. Abundant small woody shrub macrofossils are present at the base of Unit 4, distinguishing it from Unit 3. This unit is present at the Black Hills, Upper Quartz, Upper Goldbottom, Lucky Lady II, Brimstone, Upper Hunker, and Lower Hunker sites, and is at least 8 m thick. Carbon and nitrogen contents of the sediment averages 3.8% and 0.2% ($n = 17$; $1\sigma = 1.5\%; 0.1\%$), respectively. The ice present within the sediments is generally non-parallel to parallel wavy lenticular and layered (1 – 10 mm thick), and microlenticular ice in otherwise structureless sediments with volumetric ice contents of 50 – 76% from six samples. Several lenses of segregated ice (typically up to 2 cm thick) are interspersed throughout the unit. No arctic ground squirrel nests are present. Deposits dating from *ca.* 6,000 cal yrs BP and onward have large wood macrofossils. δ^2H and δ^{18}O reach peak values of -156‰ and -19.7‰, respectively, by *ca.* 11,000 – 9,000 cal yrs BP. Subsequently, both isotopes follow a slight negative trend to means of -169‰ and -21.8‰ over the last 9,000 cal yrs BP. D-excess remains low through this unit with a mean value of +3.4‰ (2σ = +6.8‰). The 36 radiocarbon dates obtained within this unit range from 13,150 to 145 cal yrs BP from shrub and large woody macrofossils. Aggradation is estimated to have been moderate to high, with six rates ranging from 0.09 to 2.0 cm/year (average 0.50 cm/year). General results of the four permafrost units are summarized in Table 4-3.

Unit	Thickness (m)	Age (cal yrs BP)	Number of sites containing units	δ^2H (‰) (approx. avg.)	$\delta^{18}O$ (‰) (approx. avg.)	Average C (%)	Average N (%)	Vegetation	Ice wedges (size and abundance)
4	>12.6	< 13,150	7	-167	-21.3	3.8	0.2	Shrubs to trees	Small, common
3	>15.0	27,000 - 13,150	5	-215*	-28.2*	1.5	0.1	Graminoids	Small, rare
2	>8.5	36,000 - 27,000	3	-223	-28.6	3.2	0.3	Graminoids	Large, abundant
1	>8.0	50,000 - 36,000	2	-202	-25.8	5.2	0.4	Trees to shrubs	Large, abundant

*Unit 3 contains waters from the height of the last cold stage and the last glacial-interglacial transition. From 27,000 to 20,000 cal yrs BP, δ^2H averages -230‰ and $\delta^{18}O$ averages -30.6‰. From 20,000 to 13,150 cal yrs BP, δ^2H averages -203‰ and $\delta^{18}O$ averages -26.3‰.

Table 4-3 : General results of the permafrost record from eight sites in the Klondike area.

The cryostratigraphic observations, chronology, vegetation, and isotopic data provide a record of changing environmental dynamics in the Klondike region over the last 50,000 cal yrs BP. The consistency of changes between sites through the region gives added confidence these observations represent regional dynamics. Paleoenvironmental interpretations of general lithostratigraphic, cryostratigraphic, and paleoecological indicators are discussed in the next section, followed by sections discussing more details of the water isotope record, the nature and timing of the last glacial-interglacial transition, reduced ice wedge formation during the last cold stage, and faunal trends. The conclusions of all discussion sections are presented in Chapter 5.

Radiocarbon dates from Unit 1 indicate this unit largely corresponds with Marine Isotope Stage (MIS) 3 interstadial conditions. Large woody macrofossils, syngenetic ice wedges, and high carbon and nitrogen contents indicate a productive full boreal forest in a relatively warm, wet environment. Sediment-rich ice with regular layered and lenticular cryostructures suggest aggradation of syngenetic permafrost through regular accumulation of loess at the surface. Average water isotopes are depleted ~29‰ δ^2H and ~3.2‰ $\delta^{18}O$ compared to late Holocene (water isotope trends are discussed in more detail in the following section). Aggradation rates during this interval are estimated to have been moderate.

Radiocarbon dates and Dawson tephra from Unit 2 correspond with the latest MIS 3 and early MIS 2. The appearance of arctic ground squirrels and graminoid vegetation indicates an environmental shift to steppe-tundra vegetation (Zazula et al., 2005, 2007). This change most likely affected active layer depths in the Klondike because well-drained mineral soils during the last cold stage probably developed thicker active layers compared to poorly-drained organic soils in boreal forest environments of MIS 3. Carbon and nitrogen contents fall between the high values of Unit 1 and the low values of Unit 3, suggesting a transition in the environment to less-productive steppe-tundra. Large syngenetic ice wedges and regular layered and lenticular ice suggests aggradation of syngenetic permafrost. Average water isotopes are depleted ~50‰ δ^2H and ~6.0‰ $\delta^{18}O$ compared to late Holocene. Aggradation rates during this interval are estimated to have been moderate to high.

Radiocarbon dates from Unit 3 indicate this unit was deposited during MIS 2, including the height of the last cold stage and latest Pleistocene climate amelioration. Low carbon and nitrogen contents suggest less productive environments than those in Unit 1 and Unit 2. The prominent black horizon at the top of Unit 3 is a paleosol that formed at the Lucky Lady II site between *ca*. 13,400 to 13,100 cal yrs BP resulting from the stabilization of the landscape and accumulation of organic material. This paleosol lies 80 cm below Unit 4, which is defined by the appearance of shrub vegetation at Lucky Lady II. Regular microlenticular ice and structureless (ice-poor) cryostructures suggests aggradation of syngenetic permafrost during arid conditions. The most depleted water isotopes in this unit are from *ca.* 25,000 cal yrs BP, with a general depleted trend *ca.* 27,000 – 23,000 cal yrs BP during the height of the last cold stage. Average water isotopes during this interval are depleted ~57‰ δ^2H and ~8.0‰ δ^{18}O compared to late Holocene. D-excess during much of this interval (trend from 29,000 to 22,000 cal yrs BP) was elevated on average +9‰, possibly due to changing seasonality of precipitation (discussed in the following section). Aggradation rates during this interval are estimated to have been moderate to low, possibly due to a lack of large woody vegetation that would otherwise entrap loess.

Radiocarbon dates from Unit 4 indicate Holocene environments were present *ca.* 13,150 cal yrs BP in central Yukon. No arctic ground squirrel nests are present in this unit. Water isotopes are the most enriched during the early Holocene thermal maximum (Kaufman et al., 2004). The first appearance of shrub vegetation at the Lucky Lady II site dates to 13,150 cal yrs BP, which suggests established shrub cover in the Klondike by this time. Shrub vegetation dating several hundred years earlier is present in the Upper Quartz site, however the setting of this exposure is in a more narrow, poorly-drained valley setting compared to the Lucky Lady II site. The shift to shrub vegetation would have also changed active layer depth in the Klondike from being thick, well-drained mineral soils during the last cold stage to thinner, poorly-drained organic soils. Large woody macrofossils and *in situ* conifer stumps that are present from *ca.* 6,000 cal yrs BP onwards indicate the establishment of full boreal forest by this time. Carbon and nitrogen contents double from Unit 3, which suggest more productive environments. Regular layered and lenticular ice suggests aggradation of syngenetic permafrost. During the early Holocene, water isotopes are enriched ~11‰ δ^2H and ~2.0‰ δ^{18}O compared to late Holocene. Aggradation rates during this interval are estimated to have been moderate to very fast. Many wood-rich deposits have a complex texture, possibly representing reworked forest vegetation from thaw slumping or deposition into thermokarst features during the Holocene (*e.g.* Reyes et al., 2010). Additional discussion of the nature and timing of the last glacial-interglacial transition is presented after the following water isotope trends section.

Water isotope trends

Secular trends in the Klondike $\delta^2H/\delta^{18}O$ record appear to agree with temperature trends in arctic ice cores (Figure 4-10) (Johnsen et al., 2001; Lowe et al., 2008). The negative $\delta^2H/\delta^{18}O$ trend in the Klondike record from 50,000 to 23,000 cal yrs BP suggests a persistent cooling trend, with the most depleted values occurring between *ca.* 27,000 to 23,000 cal yrs BP. The most depleted values are coincident with the maximum extent of the Laurentide Ice Sheet in northwestern North America (Dyke et al., 2002) and of most ice sheets globally (Clark et al., 2009). Kotler and Burn (2000) report similar full glacial values for this area. Our $\delta^2H/\delta^{18}O$ record exhibits a slight increase from *ca.* 23,000 to 17,000 cal yrs BP and then increases sharply at 15,000 to enriched values which we interpret as the Pleistocene-Holocene climate amelioration. Klondike $\delta^2H/\delta^{18}O$ values peaked in the early Holocene around 11,000 to 9,000 cal yrs BP, coinciding with maximum summer solar insolation and peak warmth inferred from a temperature proxies in Alaska and northwestern Canada (Kaufman et al., 2004). Subsequently, $\delta^2H/\delta^{18}O$ declined gradually over the remainder of the Holocene, which agrees with broader cooling trends (Kaufman et al., 2004).

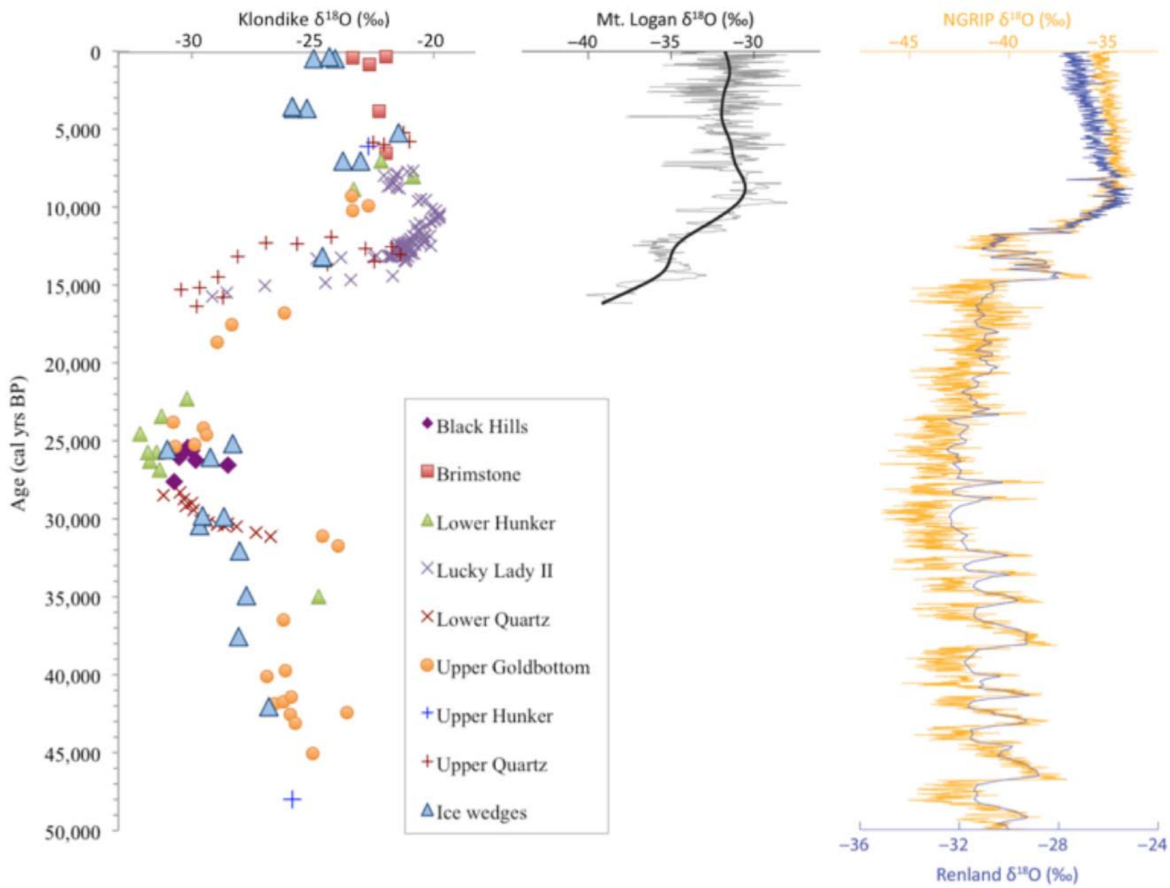

Figure 4-10 : Comparison of temporal trends in $\delta^{18}O$ in Klondike permafrost to Mt. Logan, NGRIP and Renland ice core records. The Klondike record has comparable trends to the other three isotopic records, suggesting a robust record of meteoric precipitation. Ice core records plotted by T. Porter.

Paleotemperature estimates from pore water isotopes

Using isotope-temperature models we can make estimates of paleotemperatures from Klondike pore ice over the past 50,000 cal yrs BP. By applying Dansgaard's paleothermometry equation from Greenland ice cores (temp = $1.45 * \delta^{18}O + 19.7$), we get a reasonable estimate of last cold stage (*ca.* 25,000 cal yrs BP) and late Holocene temperatures, which suggest a difference of 11.4°C across this interval (-24.5°C; -13.1°C, respectively) (Dansgaard, 1964). This record is from Greenland ice cores however and may not have the best estimation of the temperature-isotope relation for Yukon. The GNIP database (2013) provides temperature-isotope relations from 22 stations in North America and may be a better estimate for reconstructing temperatures in this study (Figure 4-11). A regression line for this data was created in collaboration with D. Froese and T. Porter. Because the amount of monthly temperature and precipitation data varies between stations, only the mean isotopic value for each month is used from the sites in order to represent each station equally in the regression line dataset. Four coastal stations have different temperature-$\delta^{18}O$ relations from continental North America and are not included in the linear regression (see Figure 4-11).

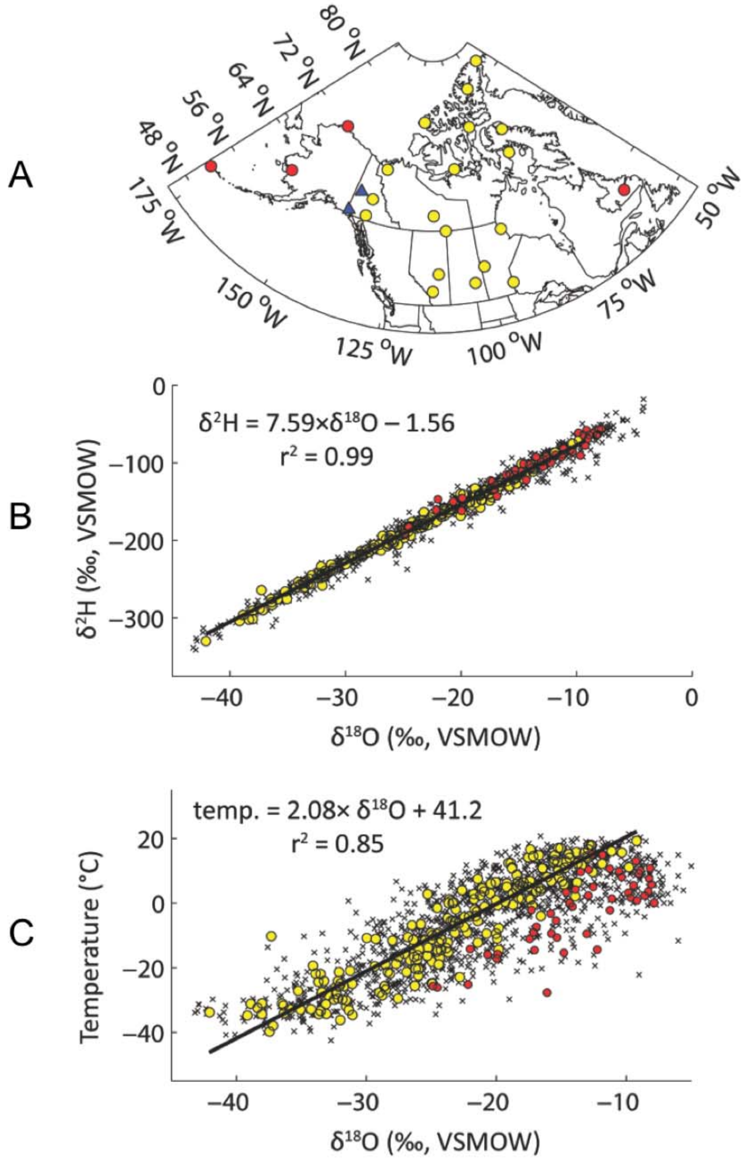

Figure 4-11 : (a) The locations of 22 GNIP stations. Red markers indicate coastal stations that are not included because they have isotopes in precipitation that differ from the cold, dry climate of Yukon. The two blue triangles represent records from Mt. Logan and the Klondike; (b) GNIP co-isotope relations. Grey x's are all the isotope values from the stations, yellow and red markers are averaged monthly values from each station. This regression line is used for more accurate paleotemperature estimations to replace the Dansgaard line (temp = 1.45 * $\delta^{18}O$ + 19.7) (Dansgaard, 1964); (c) temperature-$\delta^{18}O$ relations. Red markers indicate stations that are not included in the North American regression line. Figure and analysis by T. Porter.

Using the GNIP temperature-$\delta^{18}O$ regression line ($T = 2.08 * \delta^{18}O + 41.2$) the pore ice record suggests a 16.4°C difference between the height of the last cold stage and late Holocene mean annual air temperatures (-22.3°C; -5.8°C, respectively). The magnitude of this temperature difference is most likely exaggerated however, as the reduced excess ice, graminoid vegetation, and elevated d-excess during the last cold stage suggests changing seasonality of precipitation. Ice wedges in this study suggest a 9.4°C difference between last cold stage and late Holocene mean winter temperatures (-20.2°C; -10.8°C, respectively).

Development of a quantitative model requires improved knowledge of snow-rain mixing ratios for these sites and how mixing ratios might change by vegetation type. According to the paleoecological record, vegetation types have varied greatly over the last 50,000 cal yrs BP, likely affecting snow entrapment (Rouse et al., 1984), and precipitation seasonality has also likely changed during the last cold stage as evidenced by the d-excess anomaly (see discussion in the following section), both of which would have affected the seasonal mixture of soil water $\delta^2H/\delta^{18}O$. This is important since the slope of the temperature-$\delta^{18}O$ relation varies by season (Fricke and O'Neill, 1999; also evident from the GNIP data for Mayo, Yukon). Additional work may be possible for estimating the relative amount of summer vs. winter precipitation in pore ice by comparing the isotopes in wedge ice, a direct measurement of winter precipitation from snowmelt, to the isotopic signal in pore ice, which is typically more enriched from summer precipitation.

D-excess

A positive d-excess anomaly in Unit 3, centered on the last cold stage (*ca.* 29,000 to 22,000 cal yrs BP) is unique in the 50,000 year record and is present at the Black Hills, Lower Hunker, Lower Quartz, and Upper Goldbottom sites. Empirical studies have demonstrated that d-excess varies seasonally, peaking during winter in the Northern Hemisphere (Feng et al., 2009) and is related to evaporative conditions at the moisture source impacting kinetic fractionation, whereby under-saturated air at the ocean surface results in greater d-excess (Jouzel et al., 2007; Uemura et al., 2008). Based on this understanding, the positive d-excess anomaly can be interpreted in one of two ways. If precipitation seasonality in the Klondike area remained more or less constant, the d-excess anomaly could reflect reduced relative humidity over the North Pacific (*i.e.* the source of Klondike precipitation). Alternatively, the d-excess anomaly could represent a precipitation seasonality change with a bias towards winter precipitation. It seems unlikely that precipitation seasonality in the Klondike would have remained constant during the last cold stage given its close proximity and potentially changing dynamics of the Laurentide Ice Sheet, which had a marked effect on North American atmospheric circulation and precipitation in other regions of North America (COHMAP, 1988).

GNIP data for Mayo, Yukon (AD 1986-1989), indicate d-excess values that are *ca.* +12‰ during winter (DJF) compared to summer (JJA) (Figure 4-12). Excluding the d-excess anomaly in the Klondike record, the mean d-excess of soil water in this area over the last 50,000 cal yrs BP is estimated to be *ca.* +5.4‰ (2σ = 10.2‰), in relatively close agreement with modern GNIP values. The +9‰ d-excess anomaly may signal a precipitation seasonality shift with a bias toward winter precipitation, either due to increased winter or decreased summer precipitation, or both. The accumulation of windblown snow in Klondike valley-bottoms may be responsible for the d-excess anomaly, which is discussed in a section below. In addition, the transition from boreal trees/shrubs in Unit 1 to grassy, steppe-tundra in Unit 3 is indicative of a shift towards drier summer conditions. The modern boundary between grasslands and the boreal forest in western Canada is strongly influenced by moisture during the warm season (Hogg, 1997). Therefore, the paleoecological transition from Unit 1 to Unit 3 may represent an increase in summer moisture deficits, which would also reinforce a positive d-excess anomaly.

Figure 4-12 : Monthly d-excess in precipitation from Whitehorse and Mayo, Yukon (GNIP database, 2013). Median values for each month are plotted in red.

Timing and nature of the last glacial-interglacial transition (LGIT) in permafrost from the Klondike area, Yukon

The last glacial-interglacial transition (LGIT) was a significant shift in the global climate that changed virtually all environments on Earth. A series of smaller-scale climatic events across the LGIT are recorded by water isotopes in Greenland ice cores and include the Bølling-Allerød interstadial (14,700 – 12,900 cal yrs BP), Younger Dryas stadial (12,900 – 11,700 cal yrs BP), and early Holocene thermal maximum (11,300 – 9,100 cal yrs BP) (Figure 4-13) (Kaufman et al., 2004; Lowe et al., 2008). This interval is exceptionally well-preserved in syngenetic permafrost at the Lucky Lady II site. This section presents and discusses the nature and timing of the LGIT from the cryostratigraphy, vegetation, meteoric water isotopes, and total carbon contents of the Lucky Lady II site (Figure 4-14).

Permafrost studies in the Klondike area have largely characterized the nature of the boundary between Pleistocene silts and Holocene organics to be an unconformity generally dating to the early Holocene thermal maximum (Figure 4-15) (Dyck and Fyles, 1963; Hunter and Langston, 1964; Burn et al., 1986; Burn, 1997; Fraser and Burn, 1997; Kotler and Burn, 2000). It has also been referred to as the early Holocene thaw unconformity (*e.g.* Burn et al., 1986) and has been reported as a widespread feature in northwestern Canada (*e.g.* Kaufman et al., 2004). The organic units at three sites in this study (Lower Hunker, Upper Goldbottom, and Upper Quartz) have unconformable contacts with underlying Pleistocene silts similar in age to previously reported exposures in eastern Beringia (Table 4-4). The Lucky Lady II section however has a continuous record from >16,500 to 8,500 cal yrs BP, which spans the LGIT without a distinct thaw unconformity (Figure 4-16).

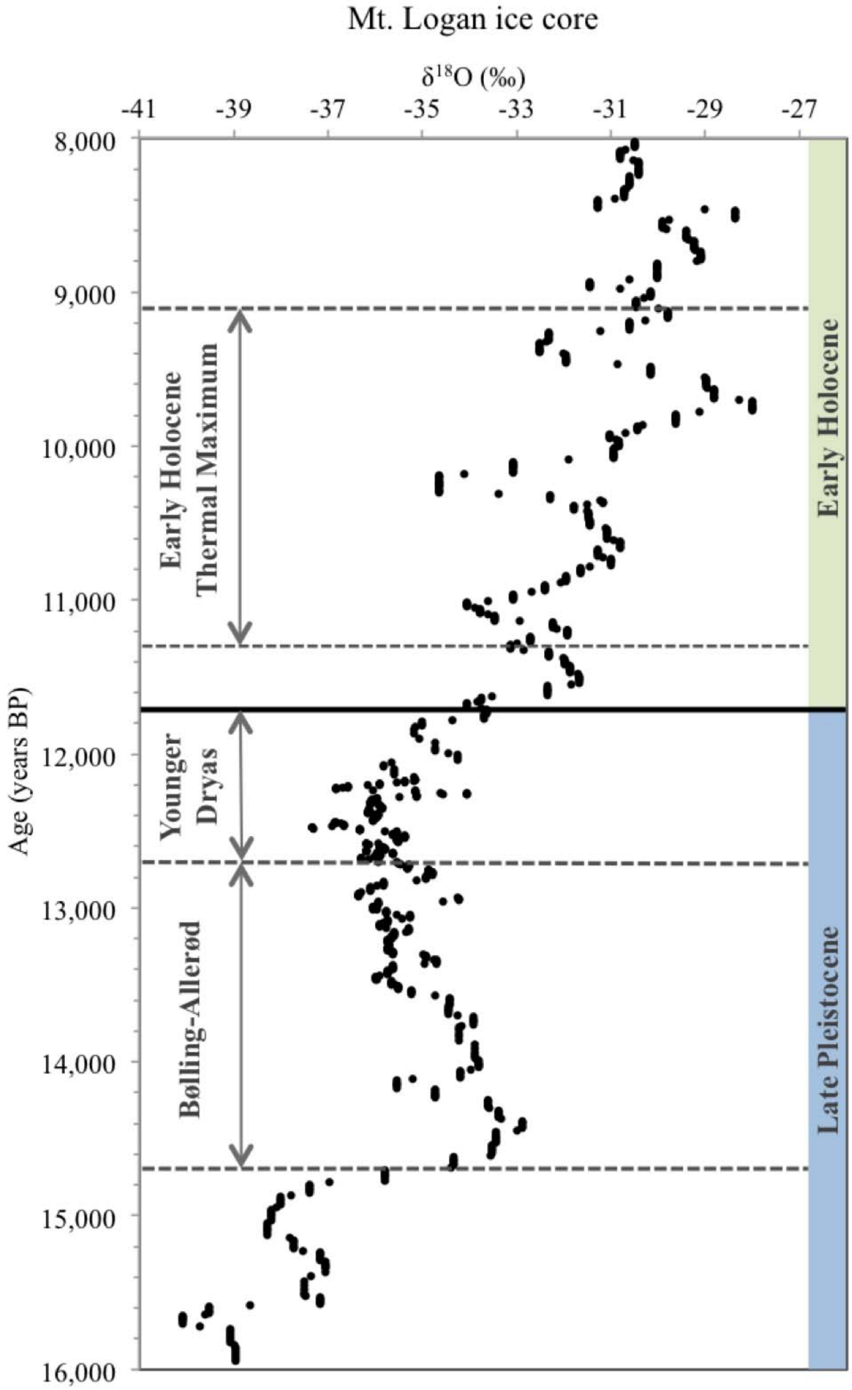

Figure 4-13 : $\delta^{18}O$ record across the LGIT from the Mt. Logan ice core (Fisher et al., 2008). The approximate timing of late Pleistocene (Lowe et al., 2008) and early Holocene (Kaufman et al., 2004) climatic events are included.

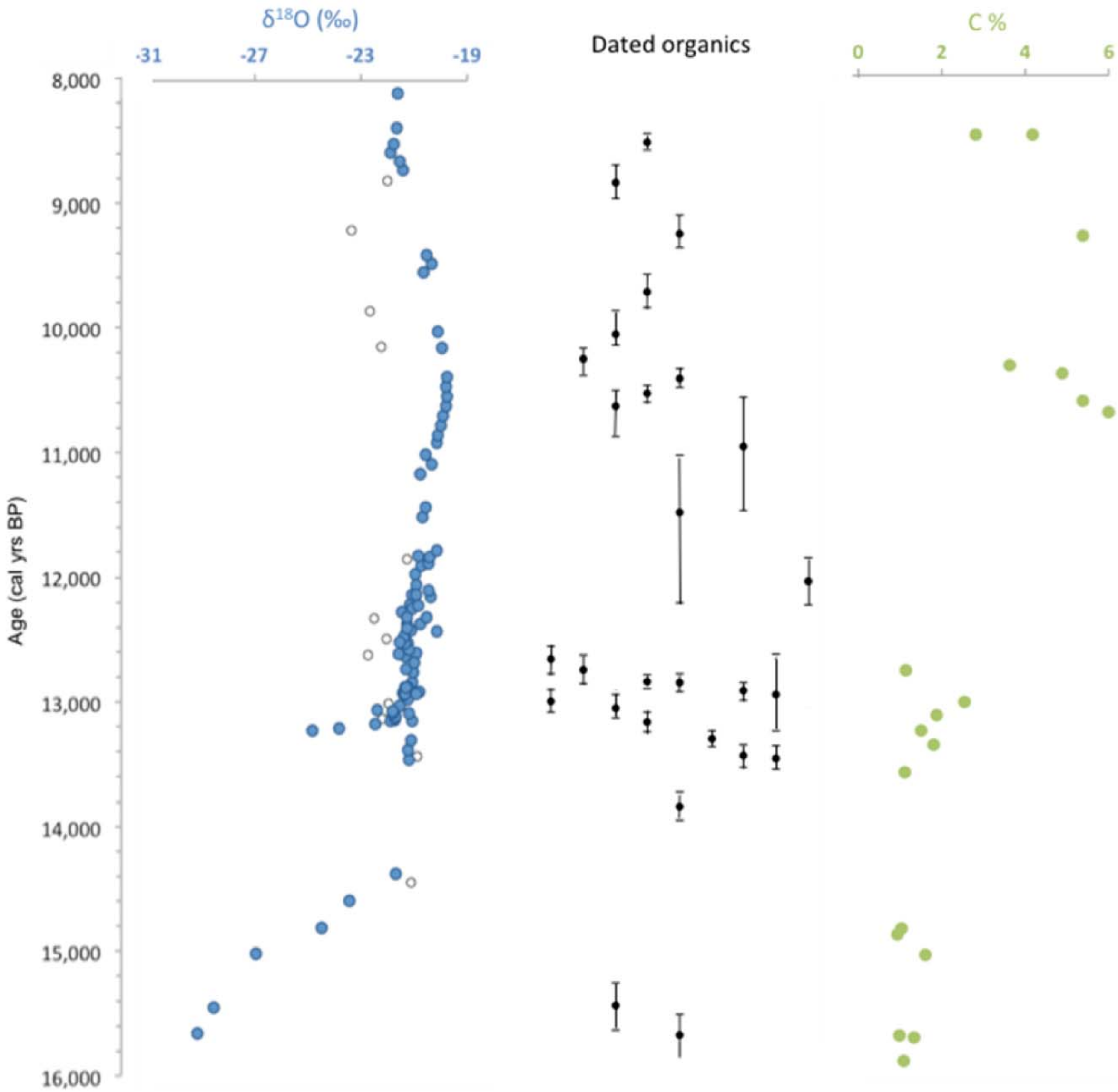

Figure 4-14 : Water isotopes, calibrated radiocarbon ages, and carbon content of permafrost from Lucky Lady II across the LGIT. Blue markers indicate water isotope samples from Lucky Lady II, white circles are values from other sites in this study.

Table 4-4 : Previously reported ages of the contact between Pleistocene silts and Holocene organics in eastern Beringia.

Locality	Region	Cal yrs BP	^{14}C yrs BP	±	Lab number	Material	Reference
Klondike	subarctic	6,320	5,525	200	BGS-1757	wood	Fraser and Burn, 1997
Klondike	subarctic	7,290	6,360	80	BGS-1756	tree root	Fraser and Burn, 1997
Klondike	subarctic	7,365	6,450	80	BGS-1769	peat	Fraser and Burn, 1997
Pelly Isl.	arctic	8,865	7,950	280	GSC-2305	rhizomes	Mackay, 1978
Pelly Isl.	arctic	8,935	8,060	70	TO-5889	rhizomes	Burn, 1997
Garry Isl.	arctic	9,090	8,130	70	TO-3608	rhizomes	Burn, 1997
Tuktoyaktuk	arctic	9,145	8,220	230	BGS-1668	wood	Burn, 1997
Garry Isl.	arctic	9,175	8,245	230	GX-4540	peat	Mackay, 1978
Klondike	subarctic	9,190	8,215	105	BGS-1771	peat/wood	Fraser and Burn, 1997
Hooper Isl.	arctic	9,860	8,765	230	GX-4352	rhizomes	Mackay, 1978
Summer Isl.	arctic	9,935	8,860	180	Beta-46223	wood	Murton and French, 1993
Mayo	subarctic	9,950	8,870	200	WAT-1144	wood	Burn et al., 1986
Pelly Isl.	arctic	10,380	9,180	110	GSC-2197	wood	Mackay, 1978
Mayo	subarctic	10,695	9,400	200	BGS-1026	wood	Burn, 1997
Mackenzie	arctic	10,810	9,480	100	Beta-46224	wood	Murton and French, 1993
Klondike	subarctic	10,830	9,510	220	GSC-196	peat	Hunter and Langston, 1964
Klondike	subarctic	10,850	9,520	130	GSC-73	wood	Dyck and Fyles, 1963
Klondike	subarctic	11,510	9,945	150	BGS-1772	twigs	Fraser and Burn, 1997
Tuktoyaktuk	arctic	11,550	9,980	140	Gak-5433	wood	Fukuda, 1975
Tuktoyaktuk	arctic	12,105	10,440	530	BGS-1797	wood	Burn, 1997

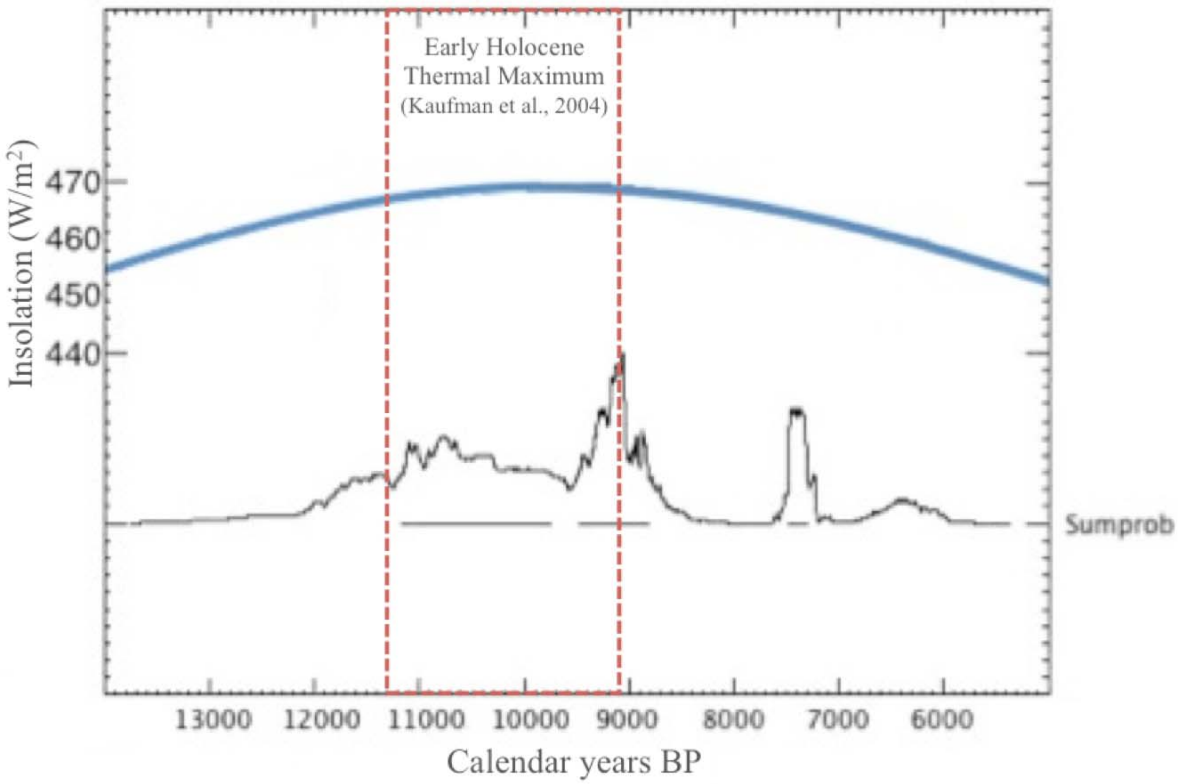

Figure 4-15 : Summed plot distribution of previously reported radiocarbon ages of the organic-rich unit (Unit 4) overlying Pleistocene silts (Unit 3) in eastern Beringia plotted with summer insolation (June) at 60°N across the LGIT (blue line) (Berger, 1992). The approximate timing of the early Holocene thermal maximum across eastern Beringia is indicated by red dashed lines (Kaufman et al., 2004).

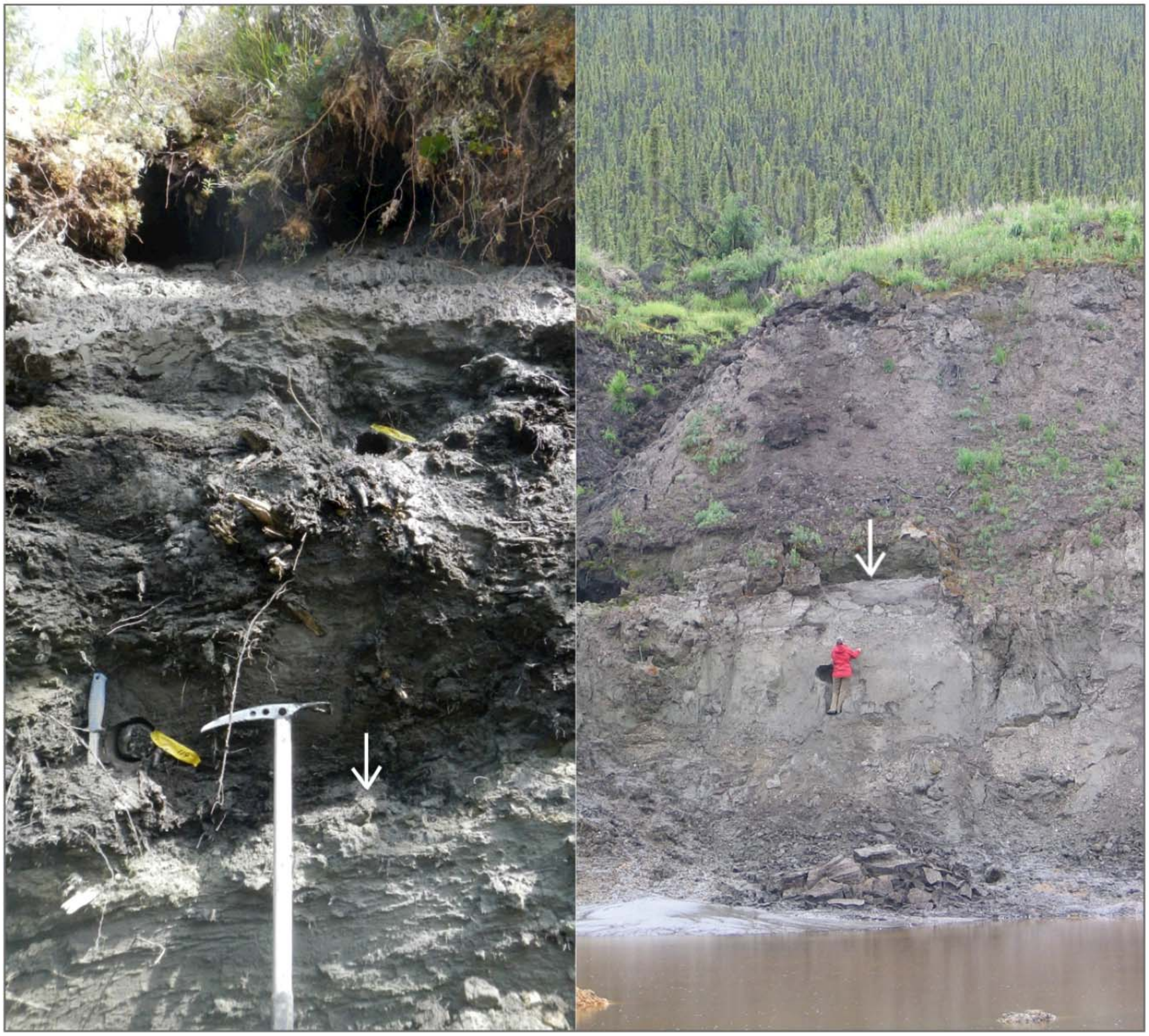

Figure 4-16 : The LGIT is characterized by grey Pleistocene silts with *in situ* graminoid vegetation which is distinctly bound (at arrows) by a sharp contact with organic-rich silts with *in situ* shrub macrofossils. This contact can be unconformable (left, Upper Goldbottom site) or conformable (right, Lucky Lady II site). The head of the ice axe is 21 cm wide.

The cryostratigraphy of four separate cores from the Lucky Lady II site have been photographed to create one composite stratigraphic log from *ca.* 13,700 to 8,500 cal yrs BP (all of the scanned Lucky Lady II core sections are in Appendix F). The stratigraphically lowest core (LL2-12) consists of 1.25 m of grey organic-poor silts which had not yet been obtained at the time the other cores were scanned, but three radiocarbon dates indicate it extends the Lucky Lady II record back to *ca.* 16,200 cal yrs BP. Water isotopes in the silt and organic units exhibit a general trend of enrichment with height during the LGIT, suggesting the Lucky Lady II exposure preserves a robust record of increasing air temperatures during this interval. The timing and nature of the boundary between the Pleistocene silt and organic units at the Lucky Lady II exposure is replicated in a similar exposure at Upper Quartz, which spans *ca.* 16,500 to 12,800 cal yrs BP. Various proxies from these two exposures record similar paleoecological shifts.

The composite log for the Lucky Lady II sequence is an excellent example of the LGIT in central Yukon and could be considered a reference section due to the high-resolution sampling from the vertical cores from the site. The general trends of the LGIT are discussed in following sections.

Bølling-Allerød (14,700 to 12,900 cal yrs BP)

The boundary between Pleistocene silt and Holocene organic units in the Klondike date during this interval, *ca.* 13,150 cal yrs BP. Additional paleoenvironmental changes include enrichment in water isotopes, a vegetation shift from grasses to shrubs, increasing total carbon contents, and an increase in the amount of visible ice, to name a few. The timing of these changes are discussed in more detail in the final section of this chapter.

Two small syngenetic ice wedges from Upper Quartz and Lucky Lady II are present in sediments dating to the Bølling-Allerød. Twigs and grass from the Upper Quartz ice wedge have been radiocarbon dated two separate times to 13,655 and 13,110 cal yrs BP, just prior to the start of the Younger Dryas. Organic material for radiocarbon dating was unable to be recovered from the Lucky Lady II ice wedge.

Younger Dryas (12,900 to 11,700 cal yrs BP)

Several samples from Upper Quartz, which are estimated to contain waters from *ca.* 13,000 to 12,000 cal yrs BP, have instances of depleted isotopes (-25‰ $\delta^{18}O$), however there are also instances of enriched waters (-23 to -21‰ $\delta^{18}O$) dating to this interval (see Figure 4-14). This may be the result of water mixing in the active layer, which could mask isotopic signals from brief climatic ameliorations such as the Younger Dryas. Environmental factors such as the rate of deposition, active layer depth, and the seasonality of precipitation affect the degree of mixing in the permafrost record, which determines whether or not short-lived climatic events are well-preserved.

Sediment horizons dated around Younger Dryas time in the Lucky Lady II cores are distinctly ice-poor, possibly due to more arid conditions. Additional work needs to be done with these samples using an induction module in order to analyze the isotopic ratios of waters from the exceedingly dry samples. No other obvious indicators suggest significant changes in the sediment dating around Younger Dryas time.

Early Holocene thermal maximum (11,300 to 9,100 cal yrs BP)

The early Holocene thermal maximum had an impact on paleoenvironments in central Yukon over *ca.* 2,200 years from 11,300 to 9,100 cal yrs BP (Kaufman et al., 2004). During this interval there is a 1.5% rise in total carbon and a ~1.5‰ enrichment of $\delta^{18}O$ in the water isotopes in Klondike permafrost from 11,000 to 9,000 cal yrs BP. Evidence from the continuous permafrost sequence from Lucky Lady II does not indicate any other significant markers in the permafrost record from this interval.

Reduced thermal contraction cracking in last cold stage permafrost

Klondike permafrost dating to the last cold stage (Unit 3) generally lacks ice wedges, especially from *ca.* 27,000 to 15,000 cal yrs BP. The few syngenetic ice wedges that are present are tall and narrow (< 30 cm wide). This is a significant change from the other late Pleistocene units in this study (Figure 4-17). Kotler and Burn (2000) propose that the lack of ice wedges were probably the result of thin snow depths, which did not produce enough spring melt to fill thermal contraction cracks. However, cracks tend to be ~2 m deep, well into the permafrost table (Mackay and Burn, 2002) and it seems more plausible that these cracks would have probably infilled with material eventually, in which case we should see evidence of the cracks in syngenetic permafrost. This finding leads us to believe that there were conditions during this time that inhibited thermal contraction cracking in the Klondike. This section discusses the potential factors that reduce the frequency of thermal contraction cracking and ice wedge formation during the last cold stage.

Mackay (1993) determined that thermal contraction cracks occur during rapid changes in air temperature, specifically daily changes in temperature averaging 1.8°C over four days, or ~7°C total. Cracking occurs most frequently in poorly-drained tundra lowlands between mid-January and March, but also can occur infrequently in November and December if snow cover is thin (Mackay, 1993). The most significant condition reported by Mackay (1993) to inhibit thermal contraction cracking is snow cover at least 60 cm thick. Additional studies have determined that modern, active ice wedges are experiencing a lowering frequency of cracking in part due to more snow entrapment from increased vegetation cover, deep active layers, and winter ground temperatures (Kokelj et al., 2007). Proxy results from this study suggest the combination of two factors may have sufficiently ceased thermal contraction cracking for *ca.* 12,000 years: thick snow drifts in valley-bottoms (at least 60 cm thick) and deep, dry active layers that are believed to have been present during the mammoth-steppe (Guthrie, 1990; Mackay, 1993; Froese et al., 2009). These two factors are explained in detail below.

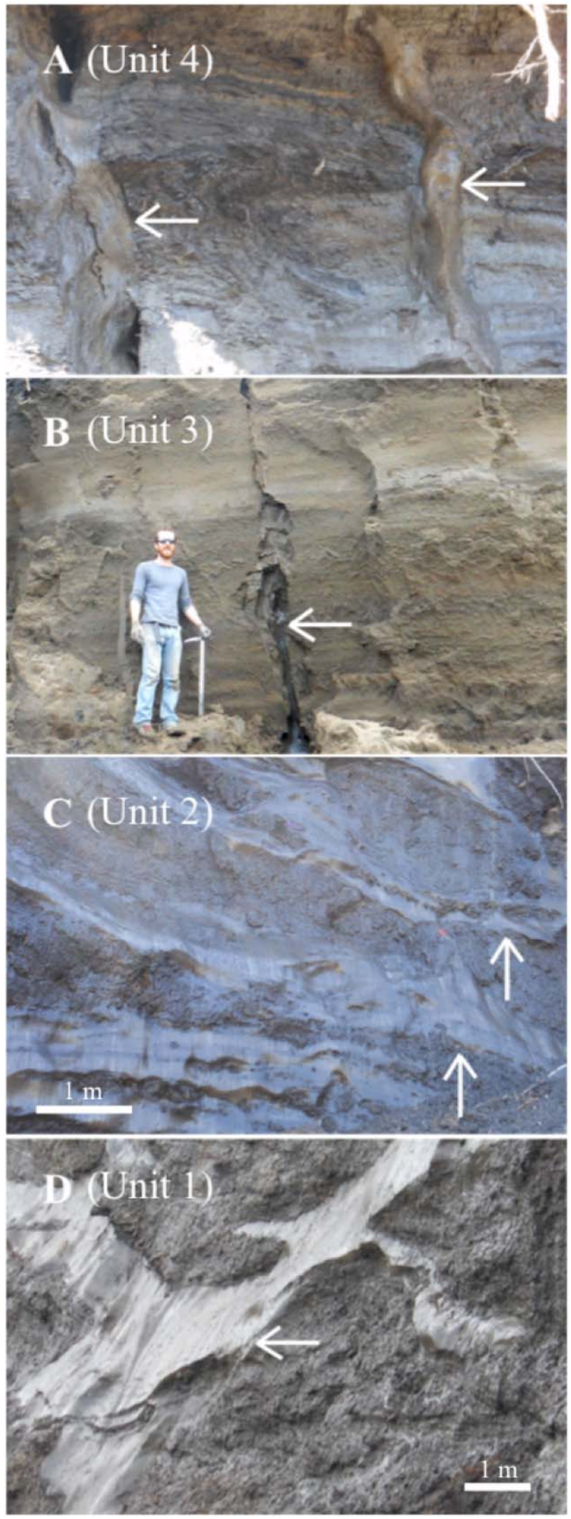

Figure 4-17 : Syngenetic ice wedges in Klondike permafrost (indicated by arrows) in (a) Unit 4, (b) Unit 3, (c) Unit 2, and (d) Unit 1.

Blowing snow across the open, treeless uplands may have resulted in drifted snow in Klondike valley-bottoms. By mid-January, when cracking is most frequent, snow depths may have exceeded 60 cm and thus prevented late winter cracking. Two additional lines of evidence from this study may support this interpretation: a distinct rise in d-excess during much of this interval, and a significant drop in the number of dated fossils of bison, which are known to avoid regions with thick snow cover (Figure 4-18) (Guthrie, 1990).

D-excess is elevated in winter precipitation. This record has a distinct +9‰ d-excess anomaly during much of Unit 3. This anomaly could be due to an increase in snow cover, which would result in an increase in the d-excess of pore ice.

Based on the fossil record, bison were not nearly as common in interior Yukon from *ca.* 31,000 to 16,000 cal yrs BP (all compiled fossil dates are presented and discussed in the following section). Bison avoid snow depths over 60 cm thick because the energy expended in clearing away that much snow is not replenished by the nutrients from the food they are able to access (Guthrie, 1990). This also happens to be the snow depth reported by Mackay (1993) to inhibit thermal contraction cracking. Fossil dates of saiga antelope in the Yukon, another species that are known to avoid deep snow, are only dated twice to 16,210 and 15,930 cal yrs BP (13,390±180, RIDDL-279; 13,250±70, CAMS-18416).

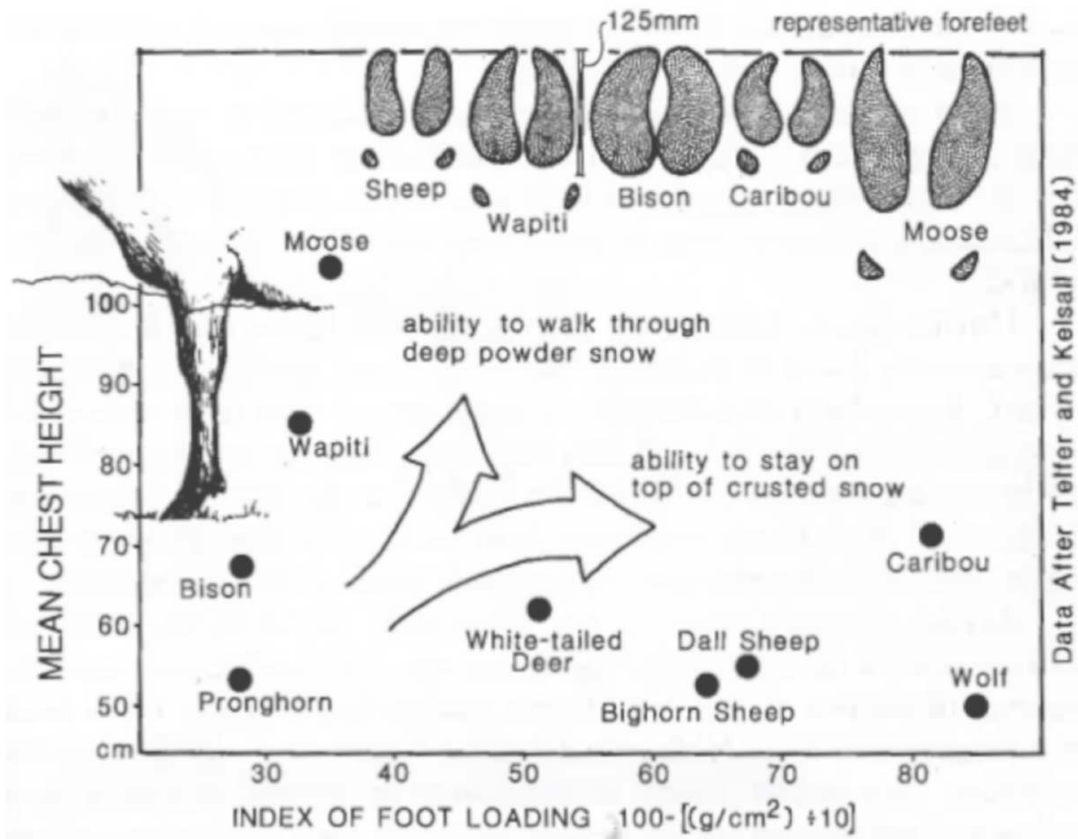

Figure 4-18 : Diagram comparing of hoof morphology and loading indices to mean chest heights of several Pleistocene megafauna in order to obtain information regarding the mobility of large mammals in snow depths between 50 and 100 cm (from Guthrie, 1990). Information for saiga antelope is not readily available, however Guthrie (1990) notes they avoid regions with deep snow cover.

The second factor that may have effectively inhibited thermal contraction cracking is deep active layers. The late Pleistocene had well-drained mineral soils (Froese et al., 2009), as opposed to the poorly-drained tundra lowlands that Mackay (1993) determined cracking occurs most frequently in. Mackay (1993) found that thermal contraction cracking is the result of air temperature changes over several days, so deep active layers may have acted as an effective thermal buffer between the top of the permafrost and fluctuating air temperatures. In addition, the active layer probably had little moisture, evidenced by lower ice volumes compared the other permafrost in this study. The extreme aridity was due to a number of factors, mainly the combination of reduced precipitation, changing seasonality, increased winds, and clear summer skies (Guthrie, 1990; Guthrie, 2001). The summer and fall is believed to have had even less precipitation, as the seasonality of precipitation shifted towards the spring months, and therefore the soils were most likely extremely dry going into the winter (Guthrie, 1990). Air is a more effective insulator than water and so this dry layer may have enhanced the thermal buffer between the top of the permafrost and sudden changes in air temperature, potentially inhibiting thermal contraction cracking.

Pleistocene megafauna in interior Yukon

Well-preserved remains of mammals are common in Beringian permafrost. Some environmental factors potentially influencing the presence (or absence) of certain species of the late Pleistocene megafauna in the Yukon interior can be proposed based on the proxy records in this study. In this section, a dataset of compiled published an unpublished fossil mammal radiocarbon dates is presented and then discussed in relation to the paleoenvironmental records from the four permafrost units defined in this study.

Only AMS radiocarbon dates of high quality are included in the dataset, specifically those from: Center for Accelerator Mass Spectrometry, USA (CAMS) (n = 89); NSF – Arizona Accelerator Mass Spectrometry, USA (AA) (n = 48); University of California – Irvine, USA (UCIAMS) (n = 27); Oxford Radiocarbon Accelerator Unit, UK (OxA) (n = 15); and Simon Fraser University, CAN (RIDDL) (n = 10). Reported mammal ages that were not specific as to which region of eastern Beringia the fossils originated (*e.g.* Alaska vs. Yukon, coastal vs. interior) are not included in the dataset. Published dates are from Shapiro et al. (2004), Guthrie (2006), Debruyne et al. (2008) and unpublished dates from B. Shapiro and D. Froese labs (Figure 4-19).

Three of the main grazing members of the mammoth-steppe which are included in this dataset are bison (*Bison sp.*, n = 48), horse (*Equus sp.*, n = 59), and mammoth (*Mammuthus sp.*, n = 54) (Guthrie, 2001; Froese et al., 2009). Two additional species are included: arctic ground squirrel (*Spermophilus parryii,* n = 18), an ecological indicator and archive of steppe-tundra (Zazula et al., 2003, 2005, 2007), and moose (*Alces alces*, n = 10) because there are an ample number of high-quality dates. Other large mammals did not have enough high-quality AMS dates to be included.

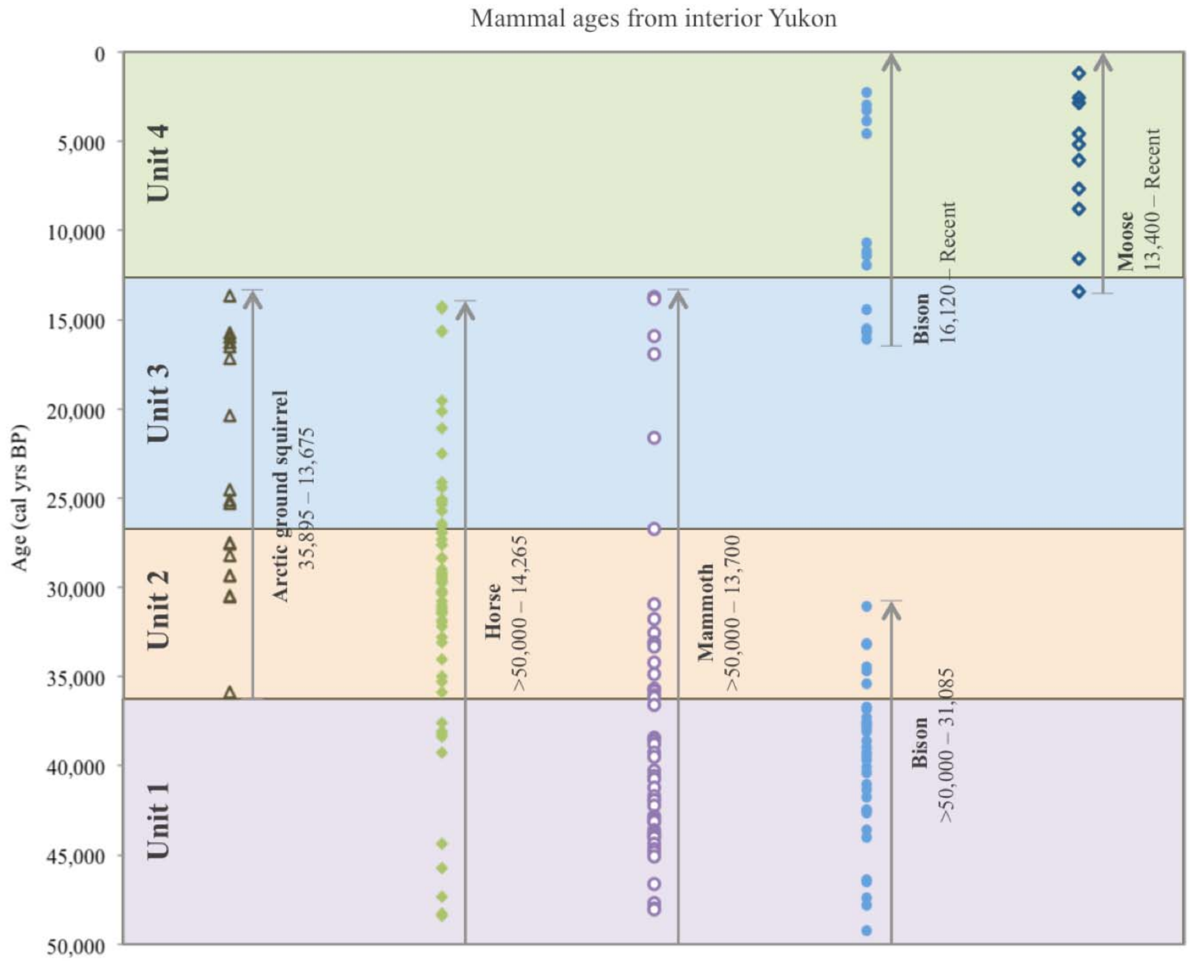

Figure 4-19 : Ages of radiocarbon dated bison, horse, mammoth, arctic ground squirrel, and moose spanning the last 50,000 cal yrs BP. The dataset is a compilation of 189 high-quality AMS radiocarbon dates from interior Yukon. Presence of arctic ground squirrels is thought to be an indicator of steppe-tundra (Zazula et al., 2003, 2005, 2007).

Unit 1 (50,000 to 36,000 cal yrs BP)

Vegetation and other paleoecological indicators in this record suggest the MIS 3 environment underwent significant changes throughout this interval from boreal forest to an arid treeless landscape. The mammals included in this study that were present are bison, mammoth, and, to a lesser extent, horse. Arctic ground squirrels are absent from this interval.

Unit 2 (36,000 to 27,000 cal yrs BP)

The beginning of this interval coincides with the earliest dated arctic ground squirrel nest in this study, indicating an established steppe-tundra vegetation. This may have been ideal for horses, which is suggested by the large number of dated fossils. The beginning of this interval is around the same time as reported reductions in genetic diversity of bison in Beringia *ca.* 37,000 cal yrs BP, indicating a significant drop in population sizes close to the onset of the last cold stage (Shaprio et al., 2004). In the fossil record, a significant drop in the number of bison dated after *ca.* 31,000 cal yrs BP suggest a steep decline in interior Yukon populations, which may have been the result of environmental changes and possibly thicker snow depths during the last cold stage.

Unit 3 (27,000 to 13,150 cal yrs BP)

The mammals which are present for the majority of this unit are arctic ground squirrels, horse, and mammoth. These three mammals all have latest dated fossils dating to a brief interval *ca.* 14,300 to 13,700 cal yrs BP. Bison are absent from interior Yukon until *ca.* 16,000 cal yrs BP, with the earliest fossil date from the Klondike at 15,500 cal yrs BP. Moose, which were not present in the late Pleistocene, appear during the LGIT *ca.* 13,400 cal yrs BP.

This abrupt shift in late Pleistocene fauna and other paleoecological indicators beginning *ca.* 16,000 cal yrs BP suggest a significant paleoenvironmental shift in the Klondike over *ca.* 3,000 years centering around the Bølling-Allerød interstadial (Table 4-5). The significance of these environmental changes is reinforced by a distinct enrichment in both Klondike and Mt. Logan ice records *ca.* 14,750 cal yrs BP (Fisher et al., 2008).

Table 4-5 : The timing of numerous paleoenvironmental and faunal changes in the Klondike area from *ca.* 16,000 to 13,150 cal yrs BP. The timing of isotopic enrichment of Klondike permafrost waters is based on the mean timing of enrichment from three syngenetic exposures across this interval. The timing of Mt. Logan isotopic enrichment is based on the record from Fisher et al. (2008).

Age (cal yrs BP)	**Event**	**Age (^{14}C yrs BP)**	**±**	**Lab number**
16,120	Bison re-appearance in Yukon	13,390	180	RIDDL-279
15,495	Bison re-appearance in Klondike	12,960	60	OxA-11197
14,830	Isotopic enrichment, this study (>-30‰ $\delta^{18}O$)	-	-	-
14,750	Mt. Logan isotopic enrichment (>-37‰ $\delta^{18}O$)	-	-	-
14,700	Approximate start of the Bølling-Allerød	-	-	-
14,265	Latest dated horse	12,310	35	CAMS-157477
13,700	Latest dated mammoth	11,860	120	AA-17559
13,685	Earliest dated shrub macrofossil (Upper Quartz site)	11,885	35	UCIAMS-142206
13,675	Latest dated arctic ground squirrel nest	11,875	35	UCIAMS-131092
13,400	Earliest dated moose	11,570	60	CAMS-23472
13,150	Established shrub vegetation (Lucky Lady II site)	11,300	35	UCIAMS-142197

Unit 4 (13,150 cal yrs BP to Recent)

This unit corresponds to the Holocene, which had shrub and tree vegetation. This unit lacks horses, mammoth, and arctic ground squirrels. Bison and moose are present throughout the Holocene. The presence of moose also may indicate widespread thermokarst development, as aquatic plants make up a significant part of moose summer diet (Rogers, 2001).

References

Berger, A., 1992. Orbital Variations and Insolation Database. IGBP PAGES/World Data Center for Paleoclimatology Data Contribution Series # 92-007. NOAA/NGDC Paleoclimatology Program, Boulder CO, USA.

Bronk Ramsey, C., 2009. Bayesian analysis of radiocarbon dates. Radiocarbon, 51 (1), 337-360. Oxcal Version 4.2, http://c14.arch.ox.ac.uk/oxcal.html.

Burn, C.R., 1997. Cryostratigraphy, paleogeography, and climate change during the early Holocene warm interval, western Arctic coast, Canada. Canadian Journal of Earth Sciences, 34 (7), 912-925.

Burn, C.R., Michel, F.A., Smith, M.W., 1986. Stratigraphic, isotopic, and mineralogical evidence for and early Holocene thaw unconformity at Mayo, Yukon-territory. Canadian Journal of Earth Sciences, 23 (6), 794-803.

Chesson, L.A., Bowen, G.J., Ehleringer, J.R., 2010. Analysis of the hydrogen and oxygen stable isotope ratios of beverage waters without prior water extraction using isotope ratio infrared spectroscopy. Rapid Communications in Mass Spectrometry, 24, 3205-3213.

Clark, P.U., Dyke, A.S., Shakun, J.D., Carlson, A.E., Clark, J., Wohlfarth, B., Mitrovica, J.X., Hostetler, S.W., McCabe, A.M., 2009. The Last Glacial Maximum. Science, 325, 710-714.

COHMAP Project Members, 1988. Climatic Changes of the Last 18,000 Years: Observations and Model Simulations. Science, 241, 1043-1052.

Dansgaard, W., 1964. Stable isotopes in precipitation. Tellus, 16, 436-468.

Debruyne, R., Chu, G., King, C.E., Bos, K., Kuch, M., Schwarz, C., Szpak, P., Gröcke, D.R., Matheus, P., Zazula, G., Guthrie, D., Froese, D., Buigues, B., de Marliave, C., Flemming, C., Poinar, D., Fisher, D., Southon, J., Tikhonov, A.N., MacPhee, R.D.E., Poinar, H.N., 2008. Out of America: ancient DNA evidence for a new world origin of late quaternary woolly mammoths. Current Biology, 18 (17), 1320-1326.

Demuro, M., Roberts, R.G., Froese, D.G., Arnold, L.J., Brock, F., Ramsey, C.B., 2008. Optically stimulated luminescence dating of single and multiple grains of quartz from perennially frozen loess in western Yukon Territory, Canada: comparison with radiocarbon chronologies for the late Pleistocene Dawson tephra. Quaternary Geochronology, 3 (4), 346-364.

Dyck, W., Fyles, J.G., 1963. Geological Survey of Canada radiocarbon dates II. Radiocarbon, 5, 39-55.Dyke, A.S., Andrews, J.T., Clark, P.U., England, J.H., Miller, G.H., Shaw, J., Veillette, J.J., 2002. The Laurentide and Innuitian ice sheets during the last glacial maximum. Quaternary Science Reviews, 21 (1), 9-31.

Feng, X., Faiia, A.M., Posmentier, E.S., 2009. Seasonality of isotopes in precipitation: A global perspective. Journal of Geophysical Research, 114, D08116.

Fisher, D., Osterberg, E., Dyke, A., Dahl-Jensen, D., Demuth, M., Zdanowicz, C., Bourgeois, J., Koerner, R.M., Mayewski, P., Wake, C., Kreutz, K., Steig, E., Zheng, J., Yalcin, K., Goto-Azuma, K., Luckman, B., Rupper, S., 2008. The Mt Logan Holocene-Late Wisconsinan isotope record: Tropical Pacific-Yukon connections. Holocene, 18 (5), 667-677.

Fraser, T.A., Burn, C.R., 1997. On the nature and origin of "muck" deposits in the Klondike area, Yukon Territory. Canadian Journal of Earth Sciences, 34 (10), 1333-1344.

Fricke, H.C., O'Neil, J.R., 1999. The correlation between $^{18}O/^{16}O$ ratios of meteoric water and surface temperature: its use in investigating terrestrial climate change over geologic time. Earth and Planetary Science Letters, 170, 181-196.

Fritz, M., Wetterich, S., Schirrmeister, L., Meyer, H., Lantuit, H., Preusser, F., Pollard, W.H., 2012. Eastern Beringia and beyond: Late Wisconsinan and Holocene landscape dynamics along the Yukon Coastal Plain, Canada. Palaeogeography, Palaeoclimatology, Palaeoecology, 319, 28-45.

Froese, D.G., Westgate, J.A., Preece, S.J., Storer, J., 2002. Age and significance of the late Pleistocene Dawson tephra in eastern Beringia. Quaternary Science Reviews, 21 (20), 2137-2142.

Froese, D.G., Zazula, G.D., Westgate, J.A., Preece, S.J., Sanborn, P.T., Reyes, A.V., Pearce, N.J.G., 2009. The Klondike goldfields and Pleistocene environments of Beringia. GSA Today, 19 (8), 4-10.

Fukuda, M., 1975. Quaternary histories of landform development in permafrost. Joint studies on physical and biological environments in the permafrost. Alaska and north Canada, June to July 1974. Institute of Low Temperature Science, Hokkaido University, Japan, pp. 62-84.

Guthrie, R.D., 1990. Frozen fauna of the mammoth-steppe: The story of Blue Babe. University of Chicago Press, Chicago IL, USA, 323 p.

Guthrie, R.D., 2001. Origin and causes of the mammoth steppe: a story of cloud cover, woolly mammal tooth pits, buckles, and inside-out Beringia. Quaternary Science Reviews, 20 (1), 549-574.

Guthrie, R.D., 2006. New carbon dates link climatic change with human colonization and Pleistocene extinctions. Nature, 441 (7090), 207-209.

Hogg, E.H., 1997. Temporal scaling of moisture and the forest-grassland boundary in western Canada. Agricultural and Forest Meteorology, 84, 115-122.

Hunter, H.A., Langston, W., Jr., 1964. Odontoma in a northern mammoth. Palaeontology, 7, 674-681.

Johnsen, S.J., Dahl-Jensen, D., Gundestrup, N., Steffensen, J.P., Clausen, H.B., Miller, H., Masson-Delmotte, V., Sveinbjörnsdottir, A.E., White, J., 2001. Oxygen isotope and palaeotemperature records from six Greenland ice-core stations: Camp Century, Dye-3, GRIP, GISP2, Renland and NorthGRIP. Journal of Quaternary Science, 16, 299-307.

Jouzel, J., Stiévenard, M., Johnsen, S.J., Landais, A., Masson-Delmotte, V., Sveinbjörnsdottir, A., Vimeux, F., Von Grafenstein, U., White, J.W.C., 2007. The GRIP deuterium-excess record. Quaternary Science Reviews, 26, 1-17.

Kaufman, D.S., Ager, T.A., Anderson, N.J., Anderson, P.M., Andrews, J.T., Bartlein, P.T., Brubaker, L.B., Coats, L.L., Cwynar, L.C., Duvall, M.L., Dyke, A.S., Edwards, M.E., Eisner, W.R., Gajewski, K., Geirsdottir, A., Hu, F.S., Jennings, A.E., Kaplan, M.R., Kerwin, M.W., Lozhkin, A.V., MacDonald, G.M., Miller, G.H., Mock, C.J., Oswald, W.W., Otto-Bliesner, B.L., Porinchu, D.F., Ruhland, K., Smol, J.P., Steig, E.J., Wolfe, B.B., 2004. Holocene thermal maximum in the western Arctic (0-180 degrees W). Quaternary Science Reviews, 23 (5), 529-560.

Kokelj, S.V., Pisaric, M.F.J., Burn, C.R., 2007. Cessation of ice-wedge development during the 20th century in spruce forests of eastern Mackenzie Delta, Northwest territories, Canada.

Canadian Journal of Earth Sciences, 44 (11), 1503-1515.

Kotler, E., Burn, C.R., 2000. Cryostratigraphy of the Klondike "muck" deposits, west-central Yukon Territory. Canadian Journal of Earth Sciences, 37 (6), 849-861.

Lacelle, D., Bjornson, J., Lauriol, B., Clark, I.D., Troutet, Y., 2004. Segregated-intrusive ice of subglacial meltwater origin in retrogressive thaw flow headwalls, Richardson Mountains, NWT, Canada. Quaternary Science Reviews, 23, 681-696.

Lowe, J.J., Rasmussen, S.O., Björck, S., Hoek, W.Z., Steffensen, J.P., Walker, M.J., Yu, Z.C., 2008. Synchronisation of palaeoenvironmental events in the North Atlantic region during the Last Termination: a revised protocol recommended by the INTIMATE group. Quaternary Science Reviews, 27 (1), 6-17.

Mackay, J.R., 1978. Freshwater shelled invertebrate indicators of paleoclimate in northwestern Canada during late glacial times: Discussion. Canadian Journal of Earth Sciences, 15 (3), 461-462.

Mackay, J.R., 1993. Air temperature, snow cover, creep of frozen ground, and the time of ice wedge cracking, western Arctic coast. Canadian Journal of Earth Sciences, 30 (8), 1720-1729.

Mackay, J.R., Burn, C.R., 2002. The first 20 years (1978-1979 to 1998-1999) of ice-wedge growth at the Illisarvik experimental drained lake site, western Arctic coast, Canada. Canadian Journal of Earth Sciences, 39, 95-111.

Meyer, H., Schirrmeister, L., Yoshikawa, K., Opel, T., Wetterich, S., Hubberten, H.-W., Brown, J., 2010. Permafrost evidence for severe winter cooling during the Younger Dryas in northern Alaska. Geophysical Research Letters, 37, L03501.

Murton, J.B., French, H.M., 1993. Thermokarst Involutions, Summer Island, Pleistocene Mackenzie Delta, Western Canadian Arctic. Permafrost and Periglacial Processes, 4 (3), 217-229.

Opel, T., Dereviagin, A.Y., Meyer, H., Schirrmeister, L., Wetterich, S., 2011. Palaeoclimatic information from stable water isotopes of Holocene ice wedges on the Dmitrii Laptev Strait, northeast Siberia, Russia. Permafrost and Periglacial Processes, 22, 84–100.

Popp, S., Diekmann, B., Meyer, H., Siegert, C., Syromyatnikov, I., Hubberten, H.-W., 2006. Palaeoclimate signals as inferred from stable-isotope composition of ground ice in the Verkhoyansk foreland, Central Yakutia. Permafrost and Periglacial Processes, 17, 119-132.

Reimer, P.J., Baillie, M.G.L., Bard, E., Bayliss, A., Beck, J.W., Blackwell, P.G., Bronk Ramsey, C., Buck, C.E., Burr, G.S., Edwards, R.L., Friedrich, M., Grootes, P.M., Guilderson, T.P., Hajdas, I., Heaton, T., Hogg, A.G., Hughen, K.A., Kaiser, K.F., Kromer, B., McCormac, F.G., Manning, S.W., Reimer, R.W., Richards, D.A., Southon, J.R., Talamo, S., Turney, C.S.M., van der Plicht, J., Weyhenmeyer, C.E., 2013. IntCal13 and Marine13 radiocarbon age calibration curves 0–50,000 years cal BP. Radiocarbon, 55 (4), 1869-1887.

Reyes, A.V., Froese, D.G., Jensen, B.J.L., 2010. Permafrost response to last interglacial warming: field evidence from non-glaciated Yukon and Alaska. Quaternary Science Reviews, 29, 3256-3274.

Rogers, A., 2001. Moose. Colin Baxter Photography Ltd., Scotland, UK, 72 p.

Rouse, W.R., 1984. Microclimate at Arctic tree line 1. Radiation balance of tundra and forest. Water Resources Research, 20, 57-66.

Schirrmeister, L., Siegert, C., Kuznetsova, T., Kuzmina, S., Andreev, A., Kienast, F., Meyer, H., Bobrov, A., 2002. Paleoenvironmental and paleoclimatic records from permafrost deposits in the Arctic region of Northern Siberia. Quaternary International, 89, 97-118.

Shapiro, B., Cooper, A., 2003. Beringia as an Ice Age genetic museum. Quaternary Research, 60 (1), 94-100.

Shapiro, B., Drummond, A.J., Rambaut, A., Wilson, M.C., Matheus, P.E., Sher, A.V., Pybus, O.G., Gilbert, M.T.P., Barnes, I., Binladen, J., Willerslev, E., Hansen, A.J., Baryshnikov, G.F., Burns, J.A., Davydov, S., Driver, J.C., Froese, D.G., Harington, C.R., Keddie, G., Kosintsev, P., Kunz, M.L., Martin, L.D., Stephenson, R.O., Storer, J., Tedford, R., Zimov, S., Cooper, A., 2004. Rise and fall of the Beringian steppe bison. Science, 306 (5701), 1561-1565.

Uemura, R., Matsui, Y., Yoshimura, K., Motoyama, H., Yoshida, N., 2008. Evidence of deuterium excess in water vapor as an indicator of ocean surface conditions. Journal of

Geophysical Research, 113, D19114.

Wetterich, S., Rudaya, N., Tumskoy, V., Andreev, A.A., Opel, T., Schirrmeister, L., Meyer, H., 2011. Last Glacial Maximum records in permafrost of the East Siberian Arctic. Quaternary Science Reviews, 30, 3139-3151.

Yashina, S., Gubin, S., Maksimovich, S., Yashina, A., Gakhova, E., Gilichinsky, D., 2012. Regeneration of whole fertile plants from 30,000-y-old fruit tissue buried in Siberian permafrost, Proceedings of the National Academy of Sciences, 109, 4008-4013.

Zazula, G.D., Froese, D.G., Schweger, C.E., Mathewes, R.W., Beaudoin, A.B., Telka, A.M., Harington, C.R., Westgate, J.A., 2003. Palaeobotany: Ice-age steppe vegetation in east Beringia. Nature, 423 (6940), 603.

Zazula, G.D., Froese, D.G., Westgate, J.A., La Farge, C., Mathewes, R.W., 2005. Paleoecology of Beringian "packrat" middens from central Yukon Territory, Canada. Quaternary Research, 63 (2), 189-198.

Zazula, G.D., Froese, D.G., Elias, S.A., Kuzmina, S., La Farge, C., Reyes, A.V., Sanborn, P.T., Schweger, C.E., Scott Smith, C.A., Mathewes, R.W., 2006. Vegetation buried under Dawson tephra (25,300 ^{14}C years BP) and locally diverse late Pleistocene paleoenvironments of Goldbottom Creek, Yukon, Canada. Palaeogeography, Palaeoclimatology, Palaeoecology, 242 (3-4), 253-286.

Zazula, G.D., Froese, D.G., Elias, S.A., Kuzmina, S., Mathewes, R.W., 2007. Arctic ground squirrels of the mammoth-steppe: paleoecology of Late Pleistocene middens (~24,000–29,450 yr BP), Yukon Territory, Canada. Quaternary Science Reviews, 26 (7), 979-1003.

Chapter 5: Conclusions and Future Work

In the Klondike area, widespread syngenetic permafrost contains a rich multi-proxy perspective on past climate and environmental change. Paleoecological and cryostratigraphic indicators in this study provide critical insights for the interpretation of pore ice as a robust long-term record of meteoric precipitation. This record is complementary to ice cores, lake sediments, and other commonly used paleo-archives.

This study expands on the initial work by Kotler and Burn (2000) by redefining four units based on the litho-, cryo-, and chronostratigraphy of Klondike permafrost, including 85 AMS radiocarbon, water isotopes from 175 pore ice samples and 16 ice wedge samples, and coeval paleoecological indicators. The consistency of changes between sites through the region gives added confidence that these observations represent regional rather than site-specific dynamics. The meteoric water isotope record is the first long-term paleoclimate proxy of its kind in North America constructed from syngenetic permafrost.

In this study we also determined that laser absorption spectroscopy is an effective method for permafrost water analyses based on results that were in excellent agreement with identical samples analyzed via IRMS. This gives us confidence the results are accurate in this study and permafrost waters do not contain significant amounts of problematic DOCs, which have been shown in previous studies to be an issue when analyzing plant waters.

This study recognizes four units based on results from eight permafrost exposures up to 60 km apart. Unit 1 was deposited *ca.* 50,000 to 36,000 cal yrs BP during the MIS 3 interstadial. This unit is present at two sites and is estimated to be at least 12.6 m thick. It is characterized by organic-rich grey and black silts including abundant spruce (*Picea sp.*) and shrub macrofossils at the base of this unit, which are gradually replaced by graminoid-dominated vegetation towards the top of this unit. Large woody vegetation and high average carbon and nitrogen contents (5.2% and 0.4%, respectively) suggest a productive boreal forest in a relatively warm and wet environment associated with interstadial conditions. No arctic ground squirrel nests are present in this unit. This unit has abundant large syngenetic ice wedges. Cryostructures are characterized by regular layered and lenticular ice, suggesting aggradation of syngenetic permafrost through regular accumulation of loess at the surface. $\delta^2H/\delta^{18}O$

exhibit little overall trend during this interval, with mean values of -202‰ and -25.8‰, respectively. Fossil ages suggest horses, bison, and mammoth thrived in Yukon during this interval.

Unit 2 was deposited *ca.* 36,000 to 27,000 cal yrs BP during the MIS 3 – MIS 2 transition. It is present at three sites and is at least 15 m thick. This unit is characterized by brown silts including graminoid vegetation and arctic ground squirrel nests. Average contents of carbon and nitrogen are 3.2% and 0.3%, respectively. This unit has large syngenetic ice wedges. Cryostructures are characterized by regular layered and lenticular ice, suggesting aggradation of syngenetic permafrost through regular accumulation of loess at the surface. Mean $\delta^2H/\delta^{18}O$ values are -223‰ for δ^2H and -28.6‰ for $\delta^{18}O$ and exhibit a negative trend through this interval, suggesting colder air temperatures than Unit 1. Fossil dates indicate horses, bison, mammoth, and arctic ground squirrels thrived in Yukon during this interval.

Unit 3 was deposited *ca.* 27,000 to 13,150 cal yrs BP during the MIS 2 stadial. It is present at five sites and is at least 8.5 m thick. This unit is characterized by grey silts including graminoid vegetation and arctic ground squirrel nests. Average contents of carbon and nitrogen are 1.5% and 0.1%, respectively. Ice wedges are noticeably reduced in this unit, which may be due to environmental conditions that inhibited thermal contraction cracking from occurring. This may have been due to dry, deeper-than-present active layers and drifted snow at least 60 cm thick in valley-bottoms during the last cold stage. Cryostructures are characterized by regular microlenticular ice, suggesting aggradation of syngenetic permafrost through regular accumulation of loess at the surface. Water isotopes in this record reach lows of -245‰ for δ^2H and -32.2‰ for $\delta^{18}O$ during the height of the last cold stage *ca*. 27,000 to 23,000 cal yrs BP. Elevated d-excess values are present for much of this interval, with a mean value of +15.1‰ from *ca.* 29,000 to 22,000 cal yrs BP. From *ca*. 15,000 to 13,150 cal yrs BP, δ^2H and $\delta^{18}O$ increase to highs of -167‰ and -21.1‰, respectively. Paleoenvironmental trends across the last glacial-interglacial transition suggest: (1) shrub vegetation became established in the Klondike *ca.* 13,150 cal yrs BP; (2) significant environmental changes during the last glacial-interglacial transition centered around the Bølling-Allerød in the Klondike, as suggested by the timing of isotopic enrichment in pore ice, the appearance of shrub macrofossils, the appearance of bison and moose fossils, and last dated mammoth, horse, and arctic ground squirrel fossils; (3) the boundary between Pleistocene silts and the interglacial organic unit is conformable at Lucky Lady II, suggesting continuous deposition of silt and aggradation of syngenetic permafrost in the Klondike.

Unit 4 began deposition *ca.* 13,150 cal yrs BP in the early Holocene. It is present at seven sites and is at least 8 m thick. This unit is characterized by grey and black silts including *in situ* shrub and graminoid vegetation. After *ca.* 6,000 cal yrs BP, spruce (*Picea sp.*) macrofossils are present. Average contents of carbon and nitrogen are 3.8% and 0.2%, respectively. Small infrequent syngenetic and epigenetic wedges are present throughout this unit. Cryostructures are characterized by regular layered and lenticular ice, suggesting aggradation of syngenetic permafrost. δ^2H and $\delta^{18}O$ reach maximum values of -156‰ and -19.7‰, respectively, between 11,000 – 9,000 cal yrs BP during the early Holocene thermal maximum. Subsequently, both isotopes follow a negative trend to mean values of -168‰ and -21.8‰ over the last 9,000 cal yrs BP. No arctic ground squirrel nests are present. Fossil dates indicate bison and moose have thrived in the Klondike throughout the Holocene.

A paleoenvironmental record similar to this study could span well beyond the limits of radiocarbon dating if tephrochronology and additional dating techniques, such as optically stimulated luminescence dating, are applied. An interesting comparison between permafrost units in Alaska and Yukon could be made if similar permafrost records are developed. Additional work includes identifying organic material at the base of Unit 4 and during the early Holocene thermal maximum, additional ice volume measurements, especially in Unit 2, water isotope analyses of dry Lucky Lady II core samples using an induction module on a liquid isotope analyzer, and also improved knowledge of snow-rain mixing ratios in pore ice and how mixing ratios change by vegetation type in an effort to improve the quantitative paleotemperature estimates in this study.

Appendix A: Radiocarbon dates of organic samples

Site	Sample	Cal yr BP (mean)	Cal yr BP max (1σ)	Cal yr BP min (1σ)	^{14}C date	±	Lab ID	Low mass samples (mgC)	Material
Upper Goldbottom	MM12-39	5,945	5,990	5,910	5,185	20	UCIAMS-114898	-	wood
Upper Goldbottom	MM12-121	10,135	10,225	9,935	8,965	25	UCIAMS-114906	-	wood
Upper Goldbottom	MM12-124	10,625	10,700	10,560	9,395	25	UCIAMS-114910	-	wood
Upper Goldbottom	MM12-112	18,820	18,940	18,700	15,570	50	UCIAMS-122282	-	fecal pellets
Upper Goldbottom	MM12-113	20,375	20,555	20,175	16,895	45	UCIAMS-114712	-	arctic ground squirrel nest
Upper Goldbottom	MM13-44b	24,525	26,085	22,865	20,310	720	UCIAMS-131093	0.042	arctic ground squirrel nest
Upper Goldbottom	MM13-41a	25,285	25,695	24,845	20,960	150	UCIAMS-131095	0.170	arctic ground squirrel nest
Upper Goldbottom	MM13-39	32,385	33,080	31,650	28,450	210	UCIAMS-142201	-	wood
Upper Goldbottom	MM12-134	35,895	36,580	35,150	32,000	320	UCIAMS-114714	-	arctic ground squirrel nest
Upper Goldbottom	MM12-125	42,100	43,075	41,130	37,770	660	UCIAMS-142208	-	wood
Upper Goldbottom	MM12-129	43,985	45,320	42,750	40,270	770	UCIAMS-114716	-	wood
Upper Goldbottom	DF12-24	45,650	47,805	43,750	42,070	980	UCIAMS-122274	-	wood
Upper Hunker	MM12-51	1,555	1,605	1,525	1,655	15	UCIAMS-114732	-	peat
Upper Hunker	MM12-48	6,090	6,185	6,000	5,320	15	UCIAMS-114727	-	wood
Upper Hunker	MM12-160	46,800	49,235	44,760	43,200	1,100	UCIAMS-114724	-	wood
Upper Hunker	MM12-158	48,550	-	46,615	46,350	1,900	UCIAMS-122276	-	wood bits/grass
Upper Hunker	MM12-155	non-finite	>50,000	-	>49,500	-	UCIAMS-114717	-	arctic ground squirrel nest
Upper Quartz	MM13-16	5,165	5,305	5,050	4,520	25	UCIAMS-142207	-	wood
Upper Quartz	MM12-96	5,840	5,925	5,750	5,115	25	UCIAMS-114911	-	wood
Upper Quartz	MM12-95	5,925	5,985	5,895	5,160	20	UCIAMS-114899	-	wood
Upper Quartz	MM12-QC-06	12,805	12,930	12,710	10,960	35	UCIAMS-114733	0.190	grass
Upper Quartz	MM13-28	13,110	13,190	13,045	11,245	40	UCIAMS-150828		twigs/grass
Upper Quartz	MM13-30	13,160	13,260	13,080	11,315	35	UCIAMS-142205	-	wood
Upper Quartz	MM13-15	13,255	13,340	13,145	11,420	35	UCIAMS-131098	-	wood
Upper Quartz	MM13-14	13,510	13,580	13,445	11,690	35	UCIAMS-131100	-	wood
Upper Quartz	MM13-28	13,655	13,750	13,560	11,835	35	UCIAMS-150832		twigs/grass
Upper Quartz	MM13-29	13,685	13,775	13,575	11,885	35	UCIAMS-142206	-	wood
Upper Quartz	MM13-25	14,080	14,200	13,960	12,190	35	UCIAMS-142199	-	leaves/twigs
Upper Quartz	MM13-12	14,335	14,635	14,110	12,340	35	UCIAMS-142196	-	grass
Upper Quartz	MM13-11	15,740	15,950	15,550	13,110	35	UCIAMS-142195	-	arctic ground squirrel nest
Upper Quartz	MM13-22	16,270	16,485	16,075	13,510	45	UCIAMS-131096	-	arctic ground squirrel nest
Upper Quartz	MM13-17	16,310	16,850	15,810	13,520	170	UCIAMS-131094	0.069	grass
Upper Quartz	MM12-QC-02	16,560	17,650	15,435	13,680	390	UCIAMS-114710	0.021	grass

Site	Sample	Cal yr BP (mean)	Cal yr BP max (1σ)	Cal yr BP min (1σ)	^{14}C date	±	Lab ID	Low mass samples (mgC)	Material
Black Hills	MM12-64	145	280	5	140	20	UCIAMS-114904	-	peat
Black Hills	MM12-63	3,040	3,145	2,960	2,905	20	UCIAMS-114902	-	twigs
Black Hills	MM12-68	>25,655	-	-	>21,300	-	UCIAMS-150831	0.023	grass
Black Hills	MM12-70	25,840	26,080	25,590	21,550	140	UCIAMS-114923	0.160	grass
Black Hills	MM12-70	26,775	27,400	26,110	22,490	310	UCIAMS-122279	0.100	grass
Black Hills	MM12-75	27,220	28,845	25,725	22,930	810	UCIAMS-131097	0.052	grass
Black Hills	MM12-67	27,575	27,760	27,385	23,360	100	UCIAMS-114718	-	arctic ground squirrel nest
Brimstone	DF12-32	1,015	1,060	965	1,115	20	UCIAMS-114917	-	wood
Brimstone	DF12-34	1,485	1,555	1,415	1,610	20	UCIAMS-114915	-	grass
Brimstone	DF12-40	3,900	3,970	3,840	3,595	20	UCIAMS-114916	0.250	peat
Brimstone	DF12-35	6,445	6,490	6,405	5,665	20	UCIAMS-114900	-	wood
Brimstone	DF12-41	6,600	6,670	6,505	5,800	25	UCIAMS-122287	-	wood
Lower Hunker	MM12-110	9,290	9,405	9,135	8,280	25	UCIAMS-114901	-	wood
Lower Hunker	MM12-108	11,070	11,605	10,660	9,720	140	UCIAMS-122280	0.058	twigs/grass
Lower Hunker	MM12-LH2-259-09	22,720	23,615	21,845	18,780	380	UCIAMS-122277	0.075	grass
Lower Hunker	MM12-105	23,810	24,195	23,430	19,780	150	UCIAMS-122281	0.140	grass
Lower Hunker	MM12-100	26,145	26,400	25,925	21,930	90	UCIAMS-114711	-	fecal pellets
Lower Hunker	MM12-103	27,295	27,670	26,905	22,990	190	UCIAMS-122283	0.170	fecal pellets
Lower Hunker	MM12-22	34,950	35,515	34,460	31,020	250	UCIAMS-114726	-	shrub twigs
Lower Hunker	MM12-97	non-finite	-	-	49,600	2,400	UCIAMS-114715	-	wood
Lower Quartz	DF10-25	28,210	29,360	27,255	23,990	560	UCIAMS-101864	0.075	arctic ground squirrel nest
Lower Quartz	DF10-24	30,160	30,690	29,620	25,920	180	UCIAMS-101914	-	arctic ground squirrel nest
Lower Quartz	DF10-37	30,305	30,735	29,810	26,030	140	UCIAMS-96042	-	grass
Lower Quartz	DF10-37b	30,330	30,800	29,775	26,070	180	UCIAMS-101901	-	grass
Lower Quartz	DF10-36	30,685	33,630	28,075	26,300	1,300	UCIAMS-101859	0.042	grass

Site	Sample	Cal yr BP (mean)	Cal yr BP max (1σ)	Cal yr BP min (1σ)	^{14}C date	±	Lab ID	Low mass samples (mgC)	Material
Lucky Lady II	LL2S-169	8,525	8,590	8,450	7,750	25	UCIAMS-143296	-	twigs
Lucky Lady II	LL2S-189	8,865	8,995	8,720	7,975	25	UCIAMS-142212	-	needle/leaves
Lucky Lady II	LL2S-353	9,780	9,910	9,630	8,770	30	UCIAMS-142211	-	leaves/twigs
Lucky Lady II	LLII-5.25(+)	10,340	10,480	10,250	9,195	20	UCIAMS-67149	-	shrub twigs
Lucky Lady II	LL2A-17	10,505	10,575	10,420	9,300	25	UCIAMS-143297	-	leaves/twigs
Lucky Lady II	LLII-4.0(+)	10,730	10,990	10,605	9,480	20	UCIAMS-67155	-	shrub twigs
Lucky Lady II	LL2A-154	11,620	12,375	11,145	10,020	170	UCIAMS-143298	0.044	twigs
Lucky Lady II	LL2B-25	12,195	12,395	12,000	10,340	45	UCIAMS-143302	0.180	twig
Lucky Lady II	LLII-2.25(+)	12,850	12,970	12,740	11,000	20	UCIAMS-67153	-	shrub twigs
Lucky Lady II	LL2C-37	12,935	13,050	12,815	11,070	30	UCIAMS-143306	-	twigs/grass
Lucky Lady II	LL2A-308	13,010	13,090	12,895	11,125	30	UCIAMS-143299	-	twigs
Lucky Lady II	LLII-1.0(+)	13,035	13,095	12,975	11,145	25	UCIAMS-67154	-	shrub twigs
Lucky Lady II	LL2B-155	13,045	13,115	12,970	11,165	35	UCIAMS-143303	-	twigs/grass
Lucky Lady II	LLII-0.81(+)	13,105	13,150	13,060	11,250	20	UCIAMS-67152	-	shrub twigs
Lucky Lady II	DF08-26A	13,140	13,450	12,805	11,290	160	UCIAMS-56390	0.052	twigs/grass
Lucky Lady II	LL2C-88(2)	13,145	13,235	13,065	11,290	40	UCIAMS-142198	-	shrub twigs
Lucky Lady II	LL2C-88	13,150	13,240	13,070	11,300	35	UCIAMS-142197	-	shrub twigs
Lucky Lady II	DF12-18	13,200	13,295	13,105	11,360	40	UCIAMS-114725	0.160	twigs/grass
Lucky Lady II	LL2B-225	13,240	13,315	13,150	11,405	30	UCIAMS-143304	-	twigs/grass
Lucky Lady II	DF12-18	13,375	13,455	13,290	11,535	35	UCIAMS-143307	-	twigs/grass
Lucky Lady II	DF12-18	13,410	13,485	13,310	11,580	35	UCIAMS-143308	-	twigs/grass
Lucky Lady II	DF13-05	13,675	13,770	13,575	11,875	35	UCIAMS-131092	-	arctic ground squirrel nest
Lucky Lady II	LL2A-425	13,675	13,775	13,560	11,870	50	UCIAMS-143301	0.210	twig
Lucky Lady II	LL2-12-184	15,520	15,760	15,280	12,980	60	UCIAMS-122284	0.190	grass
Lucky Lady II	DF12-61b	15,990	16,160	15,815	13,300	30	UCIAMS-114721	-	arctic ground squirrel nest
Lucky Lady II	LL2-12-259	16,160	16,320	15,990	13,430	35	UCIAMS-122273	-	grass
Lucky Lady II	DF08-97	16,500	16,730	16,295	13,680	35	UCIAMS-51324	-	arctic ground squirrel nest

Appendix B: Permafrost aggradation rates

Unit	Site	Aggradation rate (cm/year)	Age (from) cal yrs BP	Age (to) cal yrs BP	Sample (from)	Sample (to)
Unit 4	Brimstone	0.085	1,485	1,015	DF12-34	DF12-32
Unit 4	Upper Quartz	2.00	5,925	5,840	MM12-95	MM12-96
Unit 4	Brimstone	0.484	6,600	6,445	DF12-41	DF12-35
Unit 4	Lucky Lady II	0.147	9,780	8,525	LL2S-353	LL2S-169
Unit 4	Lucky Lady II	0.116	13,010	10,505	LL2A-308	LL2A-17
Unit 4	Lucky Lady II	0.191	13,240	12,195	LL2B-225	LL2B-25
Unit 4	Lucky Lady II	0.615	13,280	13,150	LL2C-197	LL2C-117
Unit 3	Lucky Lady II	0.117	16,160	15,520	LL2-12-259	LL2-12-184
Unit 3	Upper Quartz	0.142	16,270	15,740	MM13-22	MM13-11
Unit 3	Upper Quartz	0.061	16,560	12,805	MM12-QC-02	MM12-QC-06
Unit 3	Upper Goldbottom	0.032	20,375	18,820	MM12-113	MM12-112
Unit 3	Upper Goldbottom	0.132	25,285	24,525	MM13-41	MM13-44
Unit 3	Lower Hunker	0.172	27,295	23,810	MM12-103	MM12-105
Unit 2	Lower Quartz	0.335	30,330	28,210	DF10-37	DF10-25
Unit 2	Upper Goldbottom	0.066	32,385	29,375	MM13-39	MM13-34
Unit 1	Upper Goldbottom	0.083	43,985	35,895	MM12-129	MM12-134

Appendix C: Carbon and nitrogen content of Klondike permafrost

Unit	Site	Sample	Age (cal yr BP)	%C	%N	C:N
Unit 4	Brimstone	DF12-30	1,000	2.10	0.15	14.0
Unit 4	Brimstone	DF12-31	1,075	4.37	0.23	19.4
Unit 4	Brimstone	DF12-34	1,485	3.67	0.22	16.7
Unit 4	Brimstone	DF12-40	3,900	2.19	0.15	15.1
Unit 4	Brimstone	DF12-41	6,600	3.38	0.18	18.6
Unit 4	Lower Hunker	MM12-111	8,475	4.16	0.24	17.4
Unit 4	Lower Hunker	MM12-35	8,500	2.81	0.19	15.0
Unit 4	Lower Hunker	MM12-110	9,290	5.37	0.25	21.4
Unit 4	Upper Goldbottom	MM12-119	10,340	3.62	0.25	14.4
Unit 4	Lucky Lady 2	LLII-5.25(+)	10,340	4.89	0.36	13.5
Unit 4	Upper Goldbottom	MM12-124	10,625	5.37	0.34	15.6
Unit 4	Lucky Lady 2	LLII-4.0(+)	10,730	5.99	0.50	12.0
Unit 4	Lucky Lady 2	LLII-2.25(+)	12,850	1.12	0.08	15.0
Unit 4	Lucky Lady 2	LLII-1.0(+)	13,035	2.54	0.17	14.6
Unit 4	Lucky Lady 2	DF08-26A	13,140	1.80	0.17	10.4
Unit 3	Lucky Lady 2	LLII-0.75(+)	13,160	1.87	0.11	17.1
Unit 3	Lucky Lady 2	LL2-12-84	13,280	1.50	0.14	10.9
Unit 3	Upper Quartz	MM12-QC-05	13,620	1.11	0.06	17.5
Unit 3	Lucky Lady 2	LL2-12-109	13,840	1.04	0.04	24.0
Unit 3	Lucky Lady 2	LL2-12-134	14,400	1.59	0.07	22.8
Unit 3	Upper Quartz	MM12-QC-04	14,925	0.93	0.05	20.3
Unit 3	Lucky Lady 2	LL2-12-209	15,735	1.33	0.06	22.0
Unit 3	Upper Quartz	MM12-QC-03	15,745	0.99	0.05	18.4
Unit 3	Lucky Lady 2	LL2-12-234	15,945	1.07	0.06	18.9
Unit 3	Lucky Lady 2	LL2-12-259	16,160	1.01	0.05	21.7
Unit 3	Upper Quartz	MM12-QC-02	16,560	1.06	0.06	18.3
Unit 3	Upper Goldbottom	MM12-115	18,510	1.16	0.07	16.2
Unit 3	Upper Goldbottom	MM12-116	21,000	2.10	0.18	11.5
Unit 3	Upper Goldbottom	MM12-117	21,775	1.93	0.17	11.1
Unit 3	Lower Hunker	MM12-109	22,255	1.08	0.06	16.9
Unit 3	Lower Hunker	MM12-27	22,430	1.38	0.10	13.2
Unit 3	Lower Hunker	MM12-108	22,645	1.43	0.12	12.1
Unit 3	Lower Hunker	MM12-LH2-259-09	22,720	1.65	0.12	13.5
Unit 3	Lower Hunker	MM12-28	22,750	1.54	0.12	13.0
Unit 3	Lower Hunker	MM12-105	23,810	1.34	0.10	13.2
Unit 3	Lower Hunker	MM12-107	24,985	0.95	0.08	12.3
Unit 3	Black Hills	MM12-74	25,890	1.92	0.16	12.2
Unit 3	Black Hills	MM12-73	26,080	2.11	0.16	13.3
Unit 3	Black Hills	MM12-72	26,275	2.34	0.19	12.3
Unit 3	Lower Hunker	MM12-101	26,330	1.19	0.10	11.5
Unit 3	Black Hills	MM12-71	26,470	2.83	0.30	9.4
Unit 3	Lower Hunker	MM12-102	26,715	1.33	0.12	11.5
Unit 3	Black Hills	MM12-70	26,775	3.01	0.30	9.9
Unit 3	Black Hills	MM12-75	27,220	1.59	0.13	12.5
Unit 3	Lower Hunker	MM12-103	27,295	1.65	0.13	12.3

Unit	Site	Sample	Age (cal yr BP)	%C	%N	C:N
Unit 2	Lower Quartz	DF10-26	28,400	2.57	0.21	12.0
Unit 2	Lower Quartz	DF10-27	28,630	2.55	0.23	11.1
Unit 2	Lower Quartz	DF10-28	28,865	2.74	0.23	11.8
Unit 2	Lower Quartz	DF10-29	29,095	2.64	0.24	10.9
Unit 2	Lower Quartz	DF10-30	29,325	3.19	0.27	11.9
Unit 2	Lower Quartz	DF10-31	29,560	2.98	0.29	10.3
Unit 2	Lower Quartz	DF10-32	30,060	2.83	0.23	12.3
Unit 2	Lower Quartz	DF10-33	30,210	2.48	0.24	10.3
Unit 2	Lower Quartz	DF10-37	30,330	3.17	0.31	10.4
Unit 2	Lower Quartz	DF10-38	30,420	4.55	0.40	11.5
Unit 2	Lower Quartz	DF10-39	30,540	3.94	0.38	10.3
Unit 2	Lower Quartz	DF10-40	30,600	3.69	0.36	10.1
Unit 2	Lower Quartz	DF10-36	30,685	2.40	0.24	10.0
Unit 2	Lower Quartz	DF10-43	31,135	4.00	0.34	11.7
Unit 2	Lower Quartz	DF10-44	31,210	3.55	0.34	10.4
Unit 2	Lower Hunker	MM12-22	34,950	5.10	0.50	10.3
Unit 1	Upper Goldbottom	MM12-132	40,410	4.62	0.44	10.5
Unit 1	Upper Goldbottom	MM12-125	42,100	4.85	0.48	10.2
Unit 1	Upper Goldbottom	DF12-26	42,470	4.62	0.28	16.4
Unit 1	Upper Goldbottom	MM12-127	43,200	6.31	0.48	13.0
Unit 1	Upper Goldbottom	MM12-128	43,805	5.51	0.46	11.9
n.a.	Upper Hunker	MM12-45	non-finite	2.75	0.23	11.8
n.a.	Lower Hunker	MM12-98	non-finite	5.67	0.42	13.5

Appendix D: Sample data

Site	Unit	Sample	Material	Height in section (m)	Age of organics (cal yrs BP)	Age of waters (cal yrs BP)	δ^2H (‰)	$\delta^{18}O$ (‰)	D-excess (‰)	Aggradation rate (cm/year)
Black Hills	Unit 4	MM12-64	plant macros	5.10	**145**	-	-	-	-	-
Black Hills	Unit 4	MM12-63	plant macros	4.00	**3,040**	-	-	-	-	-
Black Hills	Unit 3	MM12-75	hand sample	3.30	**27,220**	26,755	-224.5	-30.16	16.8	0.172
Black Hills	Unit 3	MM12-67	arctic ground squirrel nest	2.90	**27,575**	27,575	-229.1	-30.72	16.6	0.172
Black Hills	Unit 3	MM12-74	hand sample	2.80	25,890	25,425	-223.7	-30.02	16.4	0.172
Black Hills	Unit 3	MM12-68	ice wedge	2.50	**>25,655**	25,700	-229.9	-31.00	18.1	0.172
Black Hills	Unit 3	MM12-73	hand sample	2.30	26,080	25,615	-227.6	-30.53	16.7	0.172
Black Hills	Unit 3	MM12-72	hand sample	1.80	26,275	25,810	-224.7	-30.52	19.5	0.172
Black Hills	Unit 3	MM12-69	ice wedge	1.30	26,000	26,000	-227.5	-29.24	6.4	0.172
Black Hills	Unit 3	MM12-71	hand sample	1.30	26,470	26,005	-222.3	-29.83	16.4	0.172
Black Hills	Unit 3	MM12-70	hand sample	0.50	**26,775**	26,310	-210.9	-28.51	17.1	0.172

Site	Unit	Sample	Material	Height in section (m)	Age of organics (cal yrs BP)	Age of waters (cal yrs BP)	δ^2H (‰)	$\delta^{18}O$ (‰)	D-excess (‰)	Aggradation rate (cm/year)
Lower Hunker	Unit 4	MM12-111	hand sample	18.00	8,475	7,985	-160.3	-20.85	6.4	0.123
Lower Hunker	Unit 3	MM12-35	hand sample	18.00	8,500	8,010	-166.1	-21.23	3.8	0.123
Lower Hunker	Unit 4	MM12-110	hand sample	17.00	**9,290**	8,800	-166.5	-23.31	20.0	0.123
Lower Hunker	Unit 4	MM12-29	ice wedge	16.00	8,500	8,500	-186.5	-23.76	3.6	0.123
Lower Hunker	Unit 3	MM12-109	hand sample	16.00	22,255	mixing btwn units	-213.6	-27.86	9.3	0.172
Lower Hunker	Unit 3	MM12-27	hand sample	16.00	22,430	mixing btwn units	-178.7	-23.65	10.5	0.172
Lower Hunker	Unit 3	MM12-108	hand sample	15.50	22,645	mixing btwn units	-245.6	-32.48	14.3	0.172
Lower Hunker	Unit 3	MM12-LH2-259	core sample	15.50	**22,720**	mixing btwn units	-222.4	-30.22	19.4	0.172
Lower Hunker	Unit 3	MM12-28	hand sample	15.50	22,750	mixing btwn units	-244.7	-33.11	20.2	0.172
Lower Hunker	Unit 4	MM12-106	ice wedge	14.00	-	unclear	-178.1	-23.04	6.3	-
Lower Hunker	Unit 3	MM12-105	hand sample	14.00	**23,810**	23,345	-241.3	-31.26	8.8	0.172
Lower Hunker	Unit 3	MM12-107	hand sample	13.00	24,985	24,520	-245.0	-32.16	12.2	0.172
Lower Hunker	Unit 3	MM12-104	ice wedge	12.00	23,500	23,500	-216.4	-28.32	10.2	0.172
Lower Hunker	Unit 3	MM12-100	fecal pellets	11.00	**26,145**	25,680	-237.8	-31.80	16.7	0.172
Lower Hunker	Unit 3	MM12-101	hand sample	10.00	26,330	25,865	-237.0	-31.47	14.8	0.172
Lower Hunker	Unit 3	MM12-102	hand sample	9.00	26,715	26,250	-234.4	-31.75	19.6	0.172
Lower Hunker	Unit 3	MM12-103	fecal pellets	8.00	**27,295**	26,830	-231.2	-31.35	19.6	0.172
Lower Hunker	Unit 2	MM12-22	hand sample	5.50	**34,950**	34,710	-197.6	-24.77	0.5	0.335
Lower Hunker	Unit 2	MM12-23	ice wedge	5.25	34,500	34,500	-214.5	-27.75	7.5	0.335
Lower Hunker	n.a.	MM12-97	plant macros	1.50	**non-finite**	non-finite	-	-	-	-
Lower Hunker	n.a.	MM12-98	hand sample	1.50	non-finite	non-finite	-194.6	-25.07	5.9	-
Lower Hunker	n.a.	MM12-99	ice wedge	1.00	non-finite	non-finite	-225.7	-28.88	5.3	-

Site	Unit	Sample	Material	Height in section (m)	Age of organics (cal yrs BP)	Age of waters (cal yrs BP)	δ^2H (‰)	$\delta^{18}O$ (‰)	D-excess (‰)	Aggradation rate (cm/year)
Upper Hunker	Unit 4	MM12-51	plant macros	10.85	**1,555**	-	-	-	-	-
Upper Hunker	Unit 4	MM12-48	plant macros	9.80	**6,090**	-	-	-	-	0.484
Upper Hunker	Unit 4	MM12-49	hand sample	9.80	6,090	5,965	-177.6	-22.72	4.2	0.484
Upper Hunker	Unit 1	MM12-160	plant macros	6.75	**46,800**	-	-	-	-	0.083
Upper Hunker	Unit 1	MM12-158	core sample	6.50	**48,550**	47,585	-198.0	-25.83	8.7	0.083
Upper Hunker	n.a.	MM12-155	arctic ground squirrel nest	2.00	**non-finite**	non-finite	-222.1	-28.57	6.5	-
Upper Hunker	n.a.	MM12-46	ice wedge	1.00	non-finite	non-finite	-228.6	-29.28	5.6	-
Upper Hunker	n.a.	MM12-45	hand sample	1.00	non-finite	non-finite	-227.7	-29.91	11.6	-
Upper Hunker	n.a.	MM12-44	arctic ground squirrel nest	1.00	non-finite	non-finite	-227.5	-29.79	10.8	-

Site	Unit	Sample	Material	Height in section (m)	Age of organics (cal yrs BP)	Age of waters (cal yrs BP)	δ^2H (‰)	$\delta^{18}O$ (‰)	D-excess (‰)	Aggradation rate (cm/year)
Lower Quartz	Unit 2	DF10-25	arctic ground squirrel nest	15.00	**28,210**	-	-	-	-	0.335
Lower Quartz	Unit 2	DF10-26	hand sample	15.00	28,400	28,220	-237.6	-30.50	6.3	0.335
Lower Quartz	Unit 2	DF10-27	hand sample	14.50	28,630	28,450	-235.6	-31.16	13.7	0.335
Lower Quartz	Unit 2	DF10-28	hand sample	14.00	28,865	28,685	-231.6	-30.32	10.9	0.335
Lower Quartz	Unit 2	DF10-29	hand sample	13.50	29,095	28,915	-233.0	-30.01	7.1	0.335
Lower Quartz	Unit 2	DF10-30	hand sample	13.00	29,325	29,150	-234.2	-30.25	7.9	0.335
Lower Quartz	Unit 2	DF10-31	hand sample	12.50	29,560	29,380	-230.9	-29.91	8.4	0.335
Lower Quartz	Unit 2	DF10-32	hand sample	11.00	30,060	29,820	-233.7	-29.63	3.3	0.335
Lower Quartz	Unit 2	DF10-24	arctic ground squirrel nest	10.80	**30,160**	-	-	-	-	0.335
Lower Quartz	Unit 2	DF10-34	ice wedge	10.75	29,750	29,750	-225.2	-29.55	11.2	0.335
Lower Quartz	Unit 2	DF10-33	hand sample	10.50	30,210	30,035	-228.3	-29.50	7.7	0.335
Lower Quartz	Unit 2	DF10-35	ice wedge	10.50	29,850	29,850	-224.2	-28.66	5.1	0.335
Lower Quartz	Unit 2	DF10-36	hand sample	8.80	**30,685**	30,275	-228.1	-28.96	3.6	0.335
Lower Quartz	Unit 2	DF10-37	hand sample	8.50	**30,330**	30,150	-224.4	-29.33	10.3	0.335
Lower Quartz	Unit 2	DF10-38	hand sample	8.20	30,420	30,240	-226.1	-28.49	1.8	0.335
Lower Quartz	Unit 2	DF10-39	hand sample	7.80	30,540	30,360	-225.4	-28.67	4.0	0.335
Lower Quartz	Unit 2	DF10-40	hand sample	7.60	30,600	30,420	-223.6	-28.14	1.5	0.335
Lower Quartz	Unit 2	DF10-41	ice wedge	7.30	30,100	30,100	-232.5	-29.69	5.0	0.335
Lower Quartz	Unit 2	DF10-43	hand sample	5.80	31,135	30,955	-220.2	-27.67	1.2	0.335
Lower Quartz	Unit 2	DF10-44	hand sample	5.55	31,210	31,030	-217.9	-27.49	2.0	0.335

Site	Unit	Sample	Material	Height in section (m)	Age of organics (cal yrs BP)	Age of waters (cal yrs BP)	δ^2H (‰)	$\delta^{18}O$ (‰)	D-excess (‰)	Aggradation rate (cm/year)
Upper Goldbottom	Unit 4	MM12-39	plant macros	26.60	**5,945**	-	-	-	-	-
Upper Goldbottom	Unit 4	MM12-124	core sample	24.60	**10,625**	10,135	-180.0	-23.36	6.9	0.123
Upper Goldbottom	Unit 4	MM12-118	core sample	23.40	9,685	9,200	-172.8	-23.39	14.3	0.123
Upper Goldbottom	Unit 4	MM12-121	plant macros	22.85	**10,135**	-	-	-	-	0.123
Upper Goldbottom	Unit 4	MM12-119	core sample	22.60	10,340	9,850	-176.5	-22.70	5.1	0.123
Upper Goldbottom	Unit 3	MM12-115	core sample	22.30	18,510	16,020	-208.2	-26.18	1.2	0.032
Upper Goldbottom	Unit 3	MM12-112	fecal pellets	22.20	**18,820**	-	-	-	-	0.032
Upper Goldbottom	Unit 3	MM12-116	core sample	21.40	21,000	18,510	-225.5	-28.37	1.5	0.032
Upper Goldbottom	Unit 3	MM12-117	core sample	21.15	21,775	19,290	-227.7	-28.95	3.9	0.032
Upper Goldbottom	Unit 3	MM12-113	arctic ground squirrel nest	20.90	**20,375**	-	-	-	-	0.032
Upper Goldbottom	Unit 3	MM13-46	core sample	19.75	24,940	24,330	-232.6	-30.78	13.6	0.132
Upper Goldbottom	Unit 3	MM13-44	arctic ground squirrel nest	19.50	**24,525**	24,525	-227.8	-29.39	7.3	0.132
Upper Goldbottom	Unit 3	MM13-45	core sample	19.25	25,325	24,720	-226.6	-29.53	9.6	0.132
Upper Goldbottom	Unit 3	MM13-42	arctic ground squirrel nest	18.60	25,210	25,210	-228.6	-29.90	10.6	0.132
Upper Goldbottom	Unit 3	MM13-41	arctic ground squirrel nest	18.50	**25,285**	25,285	-228.8	-30.70	16.8	0.132
Upper Goldbottom	Unit 2	MM13-34	tephra sample	17.70	**29,375**	-	-	-	-	0.066
Upper Goldbottom	Unit 2	MM13-40	core sample	16.20	31,635	30,730	-195.5	-24.61	1.4	0.066
Upper Goldbottom	Unit 2	MM13-39	core sample	15.70	**32,385**	31,480	-188.1	-23.97	3.7	0.066
Upper Goldbottom	Unit 2	MM13-38	ice wedge	14.95	32,000	32,000	-224.9	-28.04	-0.6	0.066
Upper Goldbottom	Unit 2	MM12-134	arctic ground squirrel nest	12.60	**35,895**	-	-	-	-	0.083
Upper Goldbottom	Unit 1	MM12-135	core sample	12.50	37,150	36,425	-204.1	-26.22	5.7	0.083
Upper Goldbottom	Unit 1	MM12-136	ice wedge	11.60	37,000	37,000	-218.9	-28.08	5.7	0.083
Upper Goldbottom	Unit 1	MM12-132	core sample	9.90	40,410	39,685	-204.8	-26.12	4.2	0.083
Upper Goldbottom	Unit 1	MM12-130	core sample	9.60	40,770	40,045	-207.4	-26.88	7.7	0.083
Upper Goldbottom	Unit 1	MM12-131	segregated ice	9.00	41,495	41,495	-217.8	-27.95	5.8	0.083
Upper Goldbottom	Unit 1	MM12-125	core sample	8.50	**42,100**	41,375	-205.7	-25.91	1.7	0.083
Upper Goldbottom	Unit 1	MM12-126	core sample	8.00	42,415	41,690	-203.6	-26.20	6.0	0.083
Upper Goldbottom	Unit 1	MM12-41	ice wedge	8.00	40,500	40,500	-212.3	-26.82	2.2	0.083
Upper Goldbottom	Unit 1	DF12-26	hand sample	7.95	42,470	41,745	-190.6	-23.61	-1.7	0.083
Upper Goldbottom	Unit 1	MM12-42	hand sample	7.90	42,535	41,810	-204.8	-26.56	7.6	0.083
Upper Goldbottom	Unit 1	MM12-127	core sample	7.35	43,200	42,475	-200.8	-25.94	6.7	0.083
Upper Goldbottom	Unit 1	MM12-128	core sample	6.85	43,805	43,080	-205.3	-25.74	0.6	0.083
Upper Goldbottom	Unit 1	MM12-129	plant macros	6.70	**43,985**	-	-	-	-	0.083
Upper Goldbottom	Unit 1	DF12-24	hand sample	5.70	**45,650**	44,925	-194.2	-24.99	5.8	0.083

Site	Unit	Sample	Material	Height in section (m)	Age of organics (cal yrs BP)	Age of waters (cal yrs BP)	δ^2H (‰)	$\delta^{18}O$ (‰)	D-excess (‰)	Aggradation rate (cm/year)
Upper Quartz	Unit 4	MM12-QC-10	core sample	7.00	5,765	5,735	-160.5	-21.02	7.7	2.000
Upper Quartz	Unit 4	MM12-92	segregated ice	5.80	5,825	5,795	-188.8	-24.48	7.1	2.000
Upper Quartz	Unit 4	MM12-QC-09	core sample	5.50	5,840	5,810	-173.3	-22.50	6.7	2.000
Upper Quartz	Unit 4	MM12-96	plant macros	5.50	**5,840**	5,810	-	-	-	2.000
Upper Quartz	Unit 4	MM12-QC-08	core sample	4.00	5,915	5,885	-163.9	-22.04	12.5	2.000
Upper Quartz	Unit 4	MM12-95	plant macros	3.80	**5,925**	5,895	-	-	-	2.000
Upper Quartz	Unit 4	MM12-91	segregated ice	3.80	5,925	5,895	-170.3	-21.92	5.1	2.000
Upper Quartz	Unit 4	MM12-QC-07	core sample	2.70	12,675	11,960	-166.8	-21.72	7.0	0.112
Upper Quartz	Unit 4	MM12-QC-06	core sample	2.30	**12,805**	12,090	-173.6	-22.81	8.9	0.112
Upper Quartz	Unit 3	MM12-QC-05	core sample	1.80	13,620	12,315	-194.9	-25.66	10.4	0.061
Upper Quartz	Unit 3	MM12-QC-04	core sample	1.00	14,925	13,620	-183.0	-24.42	12.4	0.061
Upper Quartz	Unit 3	MM12-QC-03	core sample	0.50	15,745	14,440	-228.2	-28.91	3.1	0.061
Upper Quartz	Unit 3	MM12-QC-02	core sample	0.00	**16,560**	15,255	-234.5	-30.43	9.0	0.061
Upper Quartz	Unit 4	MM13-19	plant macros	4.30	5,150	5,120	-	-	-	2.000
Upper Quartz	Unit 4	MM13-18	ice wedge	3.95	5,135	5,135	-164.5	-21.46	7.2	2.000
Upper Quartz	Unit 4	MM13-20	segregated ice	3.95	5,165	5,135	-157.1	-20.59	7.7	2.000
Upper Quartz	Unit 4	MM13-16	core sample	3.95	**5,165**	5,135	-164.2	-21.26	5.9	2.000
Upper Quartz	Unit 4	MM13-15	core sample	2.95	**13,255**	12,690	-168.0	-21.37	3.0	0.142
Upper Quartz	Unit 4	MM13-21	segregated ice	2.80	13,385	12,820	-162.8	-20.74	3.1	0.142
Upper Quartz	Unit 3	MM13-14	plant macros	2.65	**13,510**	-	-	-	-	0.142
Upper Quartz	Unit 3	MM13-13	core sample	2.65	13,510	12,945	-184.3	-24.22	9.4	0.142
Upper Quartz	Unit 3	MM13-12	core sample	1.80	**14,335**	13,770	-215.7	-28.10	9.1	0.142
Upper Quartz	Unit 3	MM13-17	core sample	0.80	**16,310**	15,745	-234.3	-29.67	3.1	0.142
Upper Quartz	Unit 4	MM13-30	plant macros	3.15	**13,160**	-	-	-	-	0.142
Upper Quartz	Unit 4	MM13-28	ice wedge	3.00	**13,110**	13,110	-195.5	-24.61	1.4	0.142
Upper Quartz	Unit 3/4	MM13-29	plant macros	2.95	**13,685**	-	-	-	-	0.142
Upper Quartz	Unit 3/4	MM13-27	core sample	2.85	13,940	13,375	-171.2	-22.47	8.5	0.142
Upper Quartz	Unit 3	MM13-26	segregated ice	2.10	14,010	13,445	-199.3	-26.01	8.8	0.142
Upper Quartz	Unit 3	MM13-25	core sample	2.00	**14,080**	13,515	-211.1	-26.95	4.5	0.142
Upper Quartz	Unit 3	MM13-11	arctic ground squirrel nest	1.00	**15,740**	-	-	-	-	0.142
Upper Quartz	Unit 3	MM13-24	core sample	1.00	16,305	15,740	-221.6	-28.71	8.1	0.142
Upper Quartz	Unit 4	MM13-22	arctic ground squirrel nest	0.25	**16,270**	16,270	-225.1	-29.81	13.4	0.142

Site	Unit	Sample	Material	Height in section (m)	Age of organics (cal yrs BP)	Age of waters (cal yrs BP)	δ^2H (‰)	$\delta^{18}O$ (‰)	D-excess (‰)	Aggradation rate (cm/year)
Brimstone	Unit 4	DF12-30	hand sample	5.10	1,000	295	-169.9	-21.98	5.9	0.085
Brimstone	Unit 4	DF12-32	plant macros	5.05	**1,015**	310	-	-	-	0.085
Brimstone	Unit 4	DF12-31	hand sample	5.00	1,075	370	-178.5	-23.35	8.3	0.085
Brimstone	Unit 4	DF12-27	ice wedge	5.00	300	300	-190.0	-24.96	9.7	0.085
Brimstone	Unit 4	DF12-28	ice wedge	5.00	200	200	-187.2	-24.32	7.4	0.085
Brimstone	Unit 4	DF12-29	ice wedge	5.00	300	300	-185.0	-24.09	7.7	0.085
Brimstone	Unit 4	DF12-34	hand sample	4.65	**1,485**	780	-170.1	-22.67	11.2	0.085
Brimstone	Unit 4	DF12-35	plant macros	2.50	**6,445**	3,850	-	-	-	0.484
Brimstone	Unit 4	DF12-40	hand sample	2.25	**3,900**	3,775	-172.2	-22.25	5.8	0.484
Brimstone	Unit 4	DF12-37	ice wedge	2.00	3,600	3,600	-195.9	-25.25	6.1	0.484
Brimstone	Unit 4	DF12-38	ice wedge	2.00	3,500	3,500	-200.9	-25.84	5.9	0.484
Brimstone	Unit 4	DF12-39	ice wedge	2.00	3,600	3,600	-197.0	-25.80	9.3	0.484
Brimstone	Unit 4	DF12-41	hand sample	1.75	**6,600**	6,475	-167.4	-21.96	8.3	0.484

Site	Unit	Sample	Material	Height in section (m)	Age of organics (cal yrs BP)	Age of waters (cal yrs BP)	δ^2H (‰)	$\delta^{18}O$ (‰)	D-excess (‰)	Aggradation rate (cm/year)
Lucky Lady II	Unit 4	LLII-5.25(+)	hand sample	7.95	**10,340**	-	-	-	-	-
Lucky Lady II	Unit 4	LLII-4.0(+)	hand sample	6.70	**10,730**	-	-	-	-	-
Lucky Lady II	Unit 4	LLII-2.25(+)	hand sample	4.95	**12,850**	-	-	-	-	-
Lucky Lady II	Unit 4	LLII-1.0(+)	hand sample	3.70	**13,035**	-	-	-	-	-
Lucky Lady II	Unit 4	LL2C-88 (2)	core sample	3.58	**13,145**	-	-	-	-	-
Lucky Lady II	Unit 4	LL2C-88	core sample	3.58	**13,150**	-	-	-	-	-
Lucky Lady II	Unit 4	LLII-0.81	hand sample	3.51	**13,105**	-	-	-	-	-
Lucky Lady II	Unit 3	LLII-0.75(+)	hand sample	3.45	13,160	-	-	-	-	-
Lucky Lady II	Unit 3	DF08-26A	paleosol	2.70	**13,140**	-	-	-	-	-
Lucky Lady II	Unit 3	DF12-18	paleosol	2.70	**13,200**	-	-	-	-	-
Lucky Lady II	Unit 3	DF12-18	paleosol	2.70	**13,375**	-	-	-	-	-
Lucky Lady II	Unit 3	DF12-18	paleosol	2.70	**13,410**	-	-	-	-	-
Lucky Lady II	Unit 3	DF13-05	arctic ground squirrel nest	1.70	**13,675**	-	-	-	-	-
Lucky Lady II	Unit 3	DF10-14A	ice wedge	0.50	13,200	13,200	-194.0	-24.60	2.8	-
Lucky Lady II	Unit 3	DF12-61b	arctic ground squirrel nest	0.40	**15,990**	-	-	-	-	-
Lucky Lady II	Unit 3	DF08-97	arctic ground squirrel nest	0.00	**16,500**	-	-	-	-	-

Site	Unit	Sample	Material	Height in section (m)	Age of organics (cal yrs BP)	Age of waters (cal yrs BP)	δ^2H (‰)	$\delta^{18}O$ (‰)	D-excess (‰)	Aggradation rate (cm/year)
Lucky Lady II	Unit 4	LL2A-14	core sample	7.39	10,480	9,990	-158.9	-20.09	1.8	0.129
Lucky Lady II	Unit 4	LL2A-17	core sample	7.36	**10,505**	10,015	-	-	-	0.129
Lucky Lady II	Unit 4	LL2A-24	core sample	7.29	10,560	10,070	-157.9	-19.94	1.6	0.129
Lucky Lady II	Unit 4	LL2A-54	core sample	6.99	10,805	10,315	-156.5	-19.76	1.6	0.129
Lucky Lady II	Unit 4	LL2A-64	core sample	6.89	10,885	10,395	-156.6	-19.80	1.8	0.129
Lucky Lady II	Unit 4	LL2A-74	core sample	6.79	10,970	10,480	-156.4	-19.74	1.6	0.129
Lucky Lady II	Unit 4	LL2A-84	core sample	6.69	11,050	10,560	-156.9	-19.81	1.6	0.129
Lucky Lady II	Unit 4	LL2A-94	core sample	6.59	11,130	10,640	-157.9	-19.93	1.6	0.129
Lucky Lady II	Unit 4	LL2A-104	core sample	6.49	11,215	10,725	-157.9	-19.98	1.9	0.129
Lucky Lady II	Unit 4	LL2A-114	core sample	6.39	11,295	10,805	-159.6	-20.11	1.2	0.129
Lucky Lady II	Unit 4	LL2A-122	core sample	6.31	11,360	10,870	-159.7	-20.14	1.4	0.129
Lucky Lady II	Unit 4	LL2A-134	core sample	6.19	11,455	10,965	-161.8	-20.55	2.6	0.129
Lucky Lady II	Unit 4	LL2A-144	core sample	6.09	11,540	11,050	-160.1	-20.33	2.5	0.129
Lucky Lady II	Unit 4	LL2A-154	core sample	5.99	**11,620**	11,130	-163.3	-20.76	2.8	0.129
Lucky Lady II	Unit 4	LL2A-164	core sample	5.89	11,710	11,170	-163.0	-20.56	1.5	0.129
Lucky Lady II	Unit 4	LL2A-174	core sample	5.79	11,800	11,260	-163.4	-20.70	2.2	0.129
Lucky Lady II	Unit 4	LL2A-214	core sample	5.39	12,160	11,620	-164.6	-20.85	2.2	0.129
Lucky Lady II	Unit 4	LL2A-224	core sample	5.29	12,250	11,710	-164.7	-20.72	1.1	0.129
Lucky Lady II	Unit 4	LL2A-233	core sample	5.20	12,335	11,795	-165.5	-20.96	2.2	0.129
Lucky Lady II	Unit 4	LL2A-244	core sample	5.09	12,430	11,890	-164.6	-20.93	2.8	0.129
Lucky Lady II	Unit 4	LL2A-254	core sample	4.99	12,525	11,985	-166.3	-21.06	2.1	0.129
Lucky Lady II	Unit 4	LL2A-264	core sample	4.89	12,615	12,075	-166.7	-21.16	2.6	0.129
Lucky Lady II	Unit 4	LL2A-272	core sample	4.81	12,685	12,145	-167.8	-21.44	3.8	0.129
Lucky Lady II	Unit 4	LL2A-284	core sample	4.69	12,795	12,255	-168.3	-21.27	1.9	0.129
Lucky Lady II	Unit 4	LL2A-294	core sample	4.59	12,885	12,345	-168.3	-21.32	2.2	0.129
Lucky Lady II	Unit 4	LL2A-304	core sample	4.49	12,975	12,435	-168.6	-21.24	1.4	0.129
Lucky Lady II	Unit 4	LL2A-308	core sample	4.45	**13,010**	12,610	-	-	-	0.129
Lucky Lady II	Unit 4	LL2A-314	core sample	4.39	13,095	12,780	-167.5	-20.93	0.0	0.129
Lucky Lady II	Unit 3	LL2A-334	core sample	4.19	13,200	12,780	-166.3	-21.02	1.9	0.129
Lucky Lady II	Unit 3	LL2A-344	core sample	4.09	13,250	12,830	-166.1	-21.05	2.3	0.129
Lucky Lady II	Unit 3	LL2A-354	core sample	3.99	13,305	12,885	-165.0	-20.82	1.6	0.129
Lucky Lady II	Unit 3	LL2A-384	core sample	3.69	13,460	13,040	-168.9	-21.07	-0.3	0.129
Lucky Lady II	Unit 3	LL2A-404	core sample	3.49	13,565	13,145	-167.7	-21.12	1.2	0.129
Lucky Lady II	Unit 3	LL2A-414	core sample	3.39	13,615	13,195	-169.2	-21.22	0.6	0.129
Lucky Lady II	Unit 3	LL2A-424	core sample	3.29	13,670	13,250	-169.8	-21.18	-0.4	0.129
Lucky Lady II	Unit 3	LL2A-425	core sample	3.28	**13,675**	13,255	-		-	0.129

Site	Unit	Sample	Material	Height in section (m)	Age of organics (cal yrs BP)	Age of waters (cal yrs BP)	δ^2H (‰)	$\delta^{18}O$ (‰)	D-excess (‰)	Aggradation rate (cm/year)
Lucky Lady II	Unit 4	LL2B-3	core sample	5.92	12,050	11,660	-159.7	-20.16	1.6	0.191
Lucky Lady II	Unit 4	LL2B-13	core sample	5.82	12,115	11,725	-159.5	-20.40	3.7	0.191
Lucky Lady II	Unit 4	LL2B-23	core sample	5.72	12,180	11,790	-159.8	-20.43	3.7	0.191
Lucky Lady II	Unit 4	LL2B-25	core sample	5.70	**12,195**	11,805	-	-	-	0.191
Lucky Lady II	Unit 4	LL2B-33	core sample	5.62	12,245	11,855	-160.3	-20.45	3.3	0.191
Lucky Lady II	Unit 4	LL2B-43	core sample	5.52	12,315	11,925	-161.5	-20.38	1.5	0.191
Lucky Lady II	Unit 4	LL2B-73	core sample	5.22	12,510	12,120	-164.2	-20.53	0.1	0.191
Lucky Lady II	Unit 4	LL2B-83	core sample	5.12	12,575	12,185	-163.8	-20.76	2.2	0.191
Lucky Lady II	Unit 4	LL2B-93	core sample	5.02	12,640	12,250	-164.7	-21.13	4.3	0.191
Lucky Lady II	Unit 4	LL2B-103	core sample	4.92	12,705	12,315	-166.7	-21.39	4.4	0.191
Lucky Lady II	Unit 4	LL2B-113	core sample	4.82	12,770	12,380	-166.9	-21.33	3.8	0.191
Lucky Lady II	Unit 4	LL2B-123	core sample	4.72	12,835	12,445	-166.2	-21.19	3.3	0.191
Lucky Lady II	Unit 4	LL2B-133	core sample	4.62	12,900	12,510	-167.9	-21.34	2.8	0.191
Lucky Lady II	Unit 4	LL2B-143	core sample	4.52	12,965	12,575	-167.7	-20.97	0.1	0.191
Lucky Lady II	Unit 4	LL2B-153	core sample	4.42	13,030	12,640	-169.2	-21.31	1.3	0.191
Lucky Lady II	Unit 4	LL2B-155	core sample	4.40	**13,045**	12,770	-	-	-	0.191
Lucky Lady II	Unit 4	LL2B-163	core sample	4.32	13,065	12,900	-169.5	-21.30	1.0	0.191
Lucky Lady II	Unit 4	LL2B-173	core sample	4.22	13,095	12,930	-169.6	-21.35	1.3	0.191
Lucky Lady II	Unit 4	LL2B-183	core sample	4.12	13,125	12,960	-168.0	-21.35	2.8	0.191
Lucky Lady II	Unit 3	LL2B-193	core sample	4.02	13,150	12,925	-167.2	-20.93	0.2	0.191
Lucky Lady II	Unit 3	LL2B-203	core sample	3.92	13,180	12,955	-168.9	-21.21	0.7	0.191
Lucky Lady II	Unit 3	LL2B-213	core sample	3.82	13,205	12,980	-169.5	-21.39	1.6	0.191
Lucky Lady II	Unit 3	LL2B-223	core sample	3.72	13,235	13,010	-170.1	-21.42	1.2	0.191
Lucky Lady II	Unit 3	LL2B-225	core sample	3.70	**13,240**	13,015	-	-	-	0.191
Lucky Lady II	Unit 3	LL2B-233	core sample	3.62	13,260	13,035	-169.0	-21.23	0.8	0.191
Lucky Lady II	Unit 3	LL2B-243	core sample	3.52	13,290	13,065	-170.9	-21.54	1.4	0.191
Lucky Lady II	Unit 3	LL2B-253	core sample	3.42	13,320	13,095	-168.9	-21.20	0.7	0.191
Lucky Lady II	Unit 3	LL2B-263	core sample	3.32	13,345	13,120	-172.3	-21.73	1.5	0.191

Site	Unit	Sample	Material	Height in section (m)	Age of organics (cal yrs BP)	Age of waters (cal yrs BP)	δ^2H (‰)	$\delta^{18}O$ (‰)	D-excess (‰)	Aggradation rate (cm/year)
Lucky Lady II	Unit 4	LL2C-7	core sample	4.60	12,855	12,695	-166.7	-20.90	0.5	0.372
Lucky Lady II	Unit 4	LL2C-17	core sample	4.50	12,880	12,720	-166.9	-20.85	-0.1	0.372
Lucky Lady II	Unit 4	LL2C-27	core sample	4.40	12,910	12,750	-169.3	-21.26	0.8	0.372
Lucky Lady II	Unit 4	LL2C-37	core sample	4.30	**12,935**	12,775	-169.5	-21.25	0.5	0.372
Lucky Lady II	Unit 4	LL2C-47	core sample	4.20	12,960	12,800	-168.7	-21.08	-0.1	0.372
Lucky Lady II	Unit 4	LL2C-67	core sample	4.00	13,015	12,855	-165.5	-20.14	-4.4	0.372
Lucky Lady II	Unit 4	LL2C-77	core sample	3.90	13,040	12,880	-171.4	-21.53	0.8	0.372
Lucky Lady II	Unit 4	LL2C-87	core sample	3.80	13,070	12,910	-171.1	-21.56	1.4	0.372
Lucky Lady II	Unit 4	LL2C-117	core sample	3.50	**13,150**	12,990	-173.3	-22.37	5.7	0.615
Lucky Lady II	Unit 3	LL2C-123	core sample	3.44	13,160	13,030	-172.4	-21.80	2.0	0.615
Lucky Lady II	Unit 3	LL2C-132	core sample	3.35	13,175	13,045	-172.0	-21.80	2.5	0.615
Lucky Lady II	Unit 3	LL2C-147	core sample	3.20	13,200	13,070	-173.7	-21.71	-0.1	0.615
Lucky Lady II	Unit 3	LL2C-157	core sample	3.10	13,215	13,085	-173.4	-21.74	0.5	0.615
Lucky Lady II	Unit 3	LL2C-167	core sample	3.00	13,230	13,100	-171.7	-21.89	3.4	0.615
Lucky Lady II	Unit 3	LL2C-187	core sample	2.80	13,265	13,135	-174.3	-22.46	5.3	0.615
Lucky Lady II	Unit 3	LL2C-197	core sample	2.70	**13,280**	13,150	-	-	-	0.615
Lucky Lady II	Unit 3	LL2C-207	core sample	2.60	13,295	13,165	-184.1	-23.83	6.5	0.615
Lucky Lady II	Unit 3	LL2C-217	core sample	2.50	13,315	13,185	-189.9	-24.82	8.7	0.615

Site	Unit	Sample	Material	Height in section (m)	Age of organics (cal yrs BP)	Age of waters (cal yrs BP)	δ^2H (‰)	$\delta^{18}O$ (‰)	D-excess (‰)	Aggradation rate (cm/year)
Lucky Lady II	Unit 4	LL2S-97	core sample	11.19	8,075	7,700	-163.5	-20.87	3.5	0.147
Lucky Lady II	Unit 4	LL2S-107	core sample	11.09	8,140	7,765	-165.2	-21.10	3.6	0.147
Lucky Lady II	Unit 4	LL2S-117	core sample	10.99	8,200	7,825	-168.2	-21.55	4.2	0.147
Lucky Lady II	Unit 4	LL2S-127	core sample	10.89	8,265	7,890	-168.2	-21.54	4.1	0.147
Lucky Lady II	Unit 4	LL2S-137	core sample	10.79	8,325	7,950	-171.5	-22.05	4.9	0.147
Lucky Lady II	Unit 4	LL2S-167	core sample	10.49	8,515	8,140	-170.1	-21.60	2.7	0.147
Lucky Lady II	Unit 4	LL2S-169	core sample	10.47	**8,525**	8,150	-	-	-	0.147
Lucky Lady II	Unit 4	LL2S-189	core sample	10.27	**8,865**	8,490	-	-	-	0.147
Lucky Lady II	Unit 4	LL2S-207	core sample	10.09	8,870	8,495	-169.0	-21.66	4.3	0.147
Lucky Lady II	Unit 4	LL2S-227	core sample	9.89	8,995	8,620	-170.8	-21.76	3.3	0.147
Lucky Lady II	Unit 4	LL2S-237	core sample	9.79	9,055	8,680	-170.4	-21.90	4.8	0.147
Lucky Lady II	Unit 4	LL2S-247	core sample	9.69	9,120	8,745	-169.5	-21.53	2.8	0.147
Lucky Lady II	Unit 4	LL2S-257	core sample	9.59	9,180	8,805	-168.8	-21.42	2.6	0.147
Lucky Lady II	Unit 4	LL2S-353	core sample	8.63	**9,780**	9,405	-	-	-	0.147
Lucky Lady II	Unit 4	LL2S-357	core sample	8.59	9,805	9,430	-160.5	-20.53	3.8	0.147
Lucky Lady II	Unit 4	LL2S-367	core sample	8.49	9,865	9,490	-160.5	-20.34	2.3	0.147
Lucky Lady II	Unit 4	LL2S-377	core sample	8.39	9,930	9,555	-162.0	-20.64	3.1	0.147

Site	Unit	Sample	Material	Height in section (m)	Age of organics (cal yrs BP)	Age of waters (cal yrs BP)	δ^2H (‰)	$\delta^{18}O$ (‰)	D-excess (‰)	Aggradation rate (cm/year)
Lucky Lady II	Unit 3	LL2-12-84	core sample	2.70	13,280	13,150	-	-	-	0.117
Lucky Lady II	Unit 3	LL2-12-109	core sample	2.45	13,840	13,710	-166.8	-21.69	6.7	0.117
Lucky Lady II	Unit 3	LL2-12-134	core sample	2.20	14,400	14,270	-178.8	-23.42	8.5	0.117
Lucky Lady II	Unit 3	LL2-12-159	core sample	1.95	14,960	14,830	-187.8	-24.46	7.9	0.117
Lucky Lady II	Unit 3	LL2-12-184	core sample	1.70	**15,520**	15,390	-205.9	-26.96	9.8	0.117
Lucky Lady II	Unit 3	LL2-12-209	core sample	1.45	15,735	15,605	-	-	-	0.117
Lucky Lady II	Unit 3	LL2-12-234	core sample	1.20	15,945	15,815	-215.5	-28.54	12.7	0.117
Lucky Lady II	Unit 3	LL2-12-259	core sample	0.95	**16,160**	16,030	-220.3	-29.14	12.8	0.117

Appendix E: Arctic ground squirrel nests in the Klondike

no.	Sample ID	Lab ID	Locality	Cal. yr BP	^{14}C yr BP	±	Source
1	UCIAMS-131092	DF13-05	Lucky Lady 2	13,675	11,875	35	This paper
2	-	DF13-06	Lucky Lady 2	14,000	estimated	-	Froese lab
3	GSC-2641	-	Hunker	14,135	12,200	100	Harington, 1977
4	UCIAMS-142195	MM13-11	Upper Quartz	15,740	13,110	35	This paper
5	UCIAMS-114721	DF12-61b	Lucky Lady 2	15,990	13,300	30	This paper
6	QC-664	-	Lower Sulfur	16,070	13,350	265	Guthrie, 1990
7	UCIAMS-131096	MM13-22	Upper Quartz	16,270	13,510	45	This paper
8	UCIAMS-51324	DF08-97	Lucky Lady 2	16,500	13,680	35	This paper
9	Beta-111606	DG-O-01	Lower Hunker	16,850	13,910	70	Kotler and Burn, 2000
10	UCIAMS-67157	DF-09-29	Hunker	17,155	14,100	40	Froese lab
11	GX-250	-	Chatanika	17,975	14,760	850	Guthrie, 1990
12	GX-251	-	Chatanika	18,110	14,860	860	Guthrie, 1990
13	-	MM13-09	Upper Quartz	20,000	estimated	-	Froese lab
14	-	MM13-10	Upper Quartz	20,000	estimated	-	Froese lab
15	UCIAMS-114712	MM12-113	Upper Goldbottom	20,375	16,895	45	This paper
16	QC-661	-	Cripple	21,760	17,980	575	Guthrie, 1990
17	QC-668	-	Engineer	22,045	18,230	410	Guthrie, 1990
18	QC-673	-	Little Eldorado	23,685	19,660	30	Guthrie, 1990
19	UCIAMS-131093	MM13-44b	Upper Goldbottom	24,525	20,310	720	This paper
20	-	MM13-42	Upper Goldbottom	25,000	estimated	-	This paper
21	UCIAMS-73889	GZ-2009-33	Little Blanche	25,140	20,840	100	Froese lab
22	OS-75964	-	?	25,225	20,900	110	Froese lab
23	UCIAMS-131095	MM13-41b	Goldbottom	25,285	20,960	150	This paper
24	QC-660	-	Cripple	26,250	21,750	1,400	Guthrie, 1990
25	Beta-136365		Hunker	26,320	22,090	140	Storer, 2002
26	QC-669	-	Cripple	26,630	22,280	870	Guthrie, 1990
27	UCIAMS-73888	-	Lindo	27,485	23,220	140	Froese lab
28	UCIAMS-114718	MM12-67	Black Hills	27,575	23,360	100	This paper
29	QC-667	-	Cripple	27,605	23,380	450	Guthrie, 1990
30	QC-670	-	Goldstream	27,995	23,130	1,765	Guthrie, 1990

no.	Sample ID	Lab ID	Locality	Cal. yr BP	^{14}C yr BP	±	Source
31	Beta-161238	-	Quartz	28,040	23,990	130	Froese et al., 2002
32	UCIAMS-101864	DF10-25	Quartz	28,210	23,990	560	Froese lab
33	Beta-161239	-	Quartz	28,315	24,280	130	Froese et al., 2002
34	QC-666	-	Goldstream	28,495	24,000	1,200	Guthrie, 1990
35	Beta-202416	GZ.04.07 (YG 343.15)	Quartz	28,935	24,880	170	Zazula et al., 2007
36	QC-675	-	Ester	29,095	24,525	1,390	Guthrie, 1990
37	OxA-16062	-	Quartz	29,320	25,270	120	Demuro et al., 2008
38	OxA-16063	-	Quartz	29,365	25,310	110	Demuro et al., 2008
39	Beta-202421	GZ.02.07.01.42 (YG 343.12)	Quartz	29,970	25,750	200	Zazula et al., 2007
40	-	GZ.02.07.01.36 (YG 343.8)	Quartz	30,000	estimated	-	Zazula et al., 2005
41	-	GZ.05.29 (YG 343.28)	Quartz	30,000	estimated	-	Zazula et al., 2007
42	-	GZ.05.32 (YG 343.31)	Quartz	30,000	estimated	-	Zazula et al., 2007
43	Beta-210522	GZ.04.44 (YG 343.42)	Quartz	30,025	25,800	240	Zazula et al., 2006a
44	Beta-210521	GZ.05.34 (YG 343.33)	Quartz	30,100	25,870	190	Zazula et al., 2006a
45	Beta-202419	GZ.04.69 (YG 343.3)	Quartz	30,210	25,970	200	Zazula et al., 2007
46	OxA-16044	-	Quartz	30,470	26,180	160	Demuro et al., 2008
47	OxA-18330	CQC 4	Quartz	30,530	26,220	140	Brock et al., 2010
48	Beta-202417	GZ.04.13 (YG 343.21)	Quartz	33,165	29,030	310	Zazula et al., 2007
49	Beta-202418	GZ.04.46 (YG.350.2)	Goldbottom	33,600	29,450	320	Zazula et al., 2006b
50	QC-672	-	Cripple	34,380	26,950	3,400	Guthrie, 1990
51	UCIAMS-114714	MM12-134	Upper Goldbottom	35,895	32,000	320	This paper
52	UCIAMS-96047	DF10-173	Quartz	>41,500	>41,500	-	Froese lab
53	-	DF10-171	Quartz	>41,500	estimated	-	Froese lab
54	UCIAMS-96046	DF10-165	Quartz	>46,100	>46,100	-	Froese lab
55	UCIAMS-114717	MM12-155	Upper Hunker	>49,500	>49,500	-	This paper
56	-	MM12-44	Upper Hunker	>49,500	estimated	-	This paper
57	UCIAMS-96045	DF10-QC-155	Quartz	>54,000	>54,000	-	Froese lab
58	-	MM12-145	Quartz	80,000	estimated		Froese lab
59	-	MM12-148	Quartz	80,000	estimated		Froese lab
60	-	DF12-53	Quartz	80,000	estimated	-	Froese lab
61	-	DF13-39b	Quartz	80,000	estimated	-	Froese lab

References

Brock, F., Froese, D.G., Roberts, R.G., 2010. Low temperature (LT) combustion of sediments does not necessarily provide accurate radiocarbon ages for site chronology. Quaternary Geochronology, 5, 625-630.

Demuro, M., Roberts, R.G., Froese, D.G., Arnold, L.J., Brock, F., Ramsey, C.B., 2008. Optically stimulated luminescence dating of single and multiple grains of quartz from perennially frozen loess in western Yukon Territory, Canada: comparison with radiocarbon chronologies for the late Pleistocene Dawson tephra. Quaternary Geochronology, 3 (4), 346-364.

Froese, D.G., Westgate, J.A., Preece, S.J., Storer, J., 2002. Age and significance of the late Pleistocene Dawson tephra in eastern Beringia. Quaternary Science Reviews, 21 (20), 2137-2142.

Guthrie, R.D., 1990. Frozen fauna of the mammoth-steppe: The story of Blue Babe. University of Chicago Press, Chicago IL, USA, 323 p.

Harington, C.R., 1977. Pleistocene mammals of the Yukon Territory. Ph.D. Thesis, University of Alberta, 1060 p.

Kotler, E., Burn, C.R., 2000. Cryostratigraphy of the Klondike "muck" deposits, west-central Yukon Territory. Canadian Journal of Earth Sciences, 37 (6), 849-861.

Storer, J.E., 2002. Vertebrate paleontology of the Dawson City area, in: Froese, D.G., Duk-Rodkin, A., Bond, J.D. (Eds.), Field Guide to Quaternary Research in Central and Western Yukon Territory. Occasional Papers in Earth Sciences No. 2, Heritage Branch, Government of Yukon, pp. 24–25.

Zazula, G.D., Froese, D.G., Westgate, J.A., La Farge, C., Mathewes, R.W., 2005. Paleoecology of Beringian ‘‘packrat’’ middens from central Yukon Territory, Canada. Quaternary Research, 63, 189–198.

Zazula, G.D., Telka, A.M., Harington, C.R., Schweger, C.E., Mathewes, R.W., 2006a. New spruce (Picea spp.) macrofossils from Yukon Territory: implications for late Pleistocene refugia in Eastern Beringia. Arctic, 59 (4), 391–400.

Zazula, G.D., Froese, D.G., Elias, S.A., Kuzmina, S., La Farge, C., Reyes, A.V., Sanborn, P.T., Schweger, C.E., Smith, C.A.S., Mathewes, R.W., 2006b. Vegetation buried under Dawson tephra (25,300 14C years BP) and locally diverse late Pleistocene paleoenvironments of Goldbottom Creek, Yukon, Canada. Palaeogeography, Palaeoclimatology, Palaeoecology, 242, 253–286.

Zazula, G.D., Froese, D.G., Elias, S.A., Kuzmina, S., Mathewes, R.W., 2007. Arctic ground squirrels of the mammoth-steppe: paleoecology of Late Pleistocene middens (~24,000–29,450 yr BP), Yukon Territory, Canada. Quaternary Science Reviews, 26 (7), 979-1003.

Appendix F: Scans of cores from the Lucky Lady II site

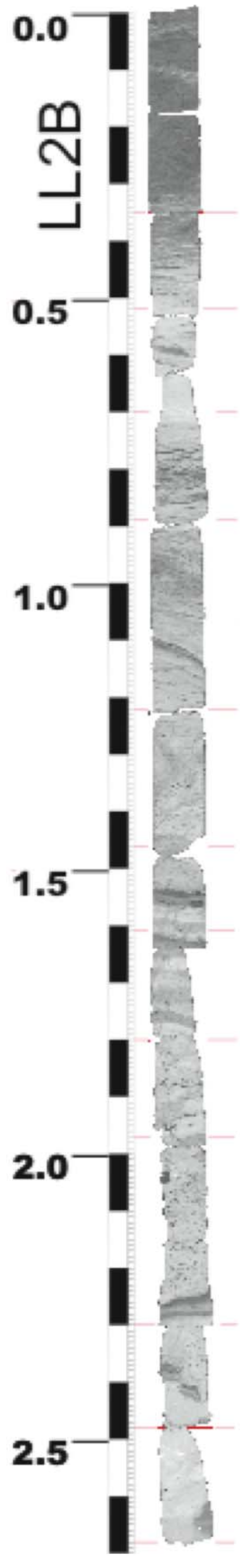

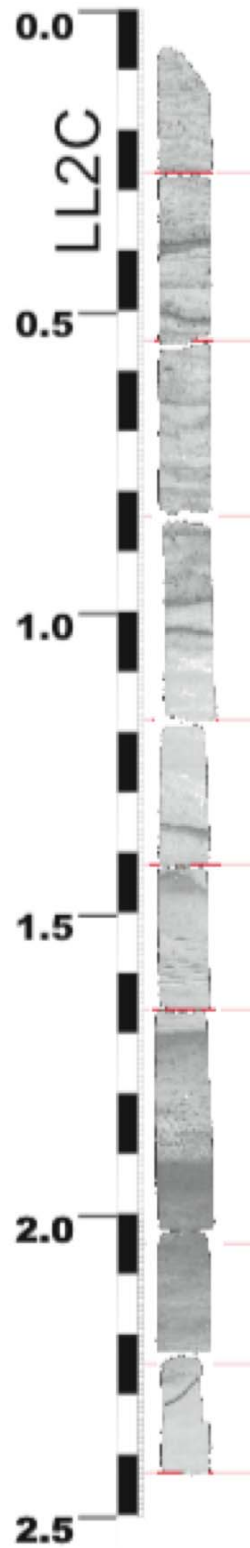

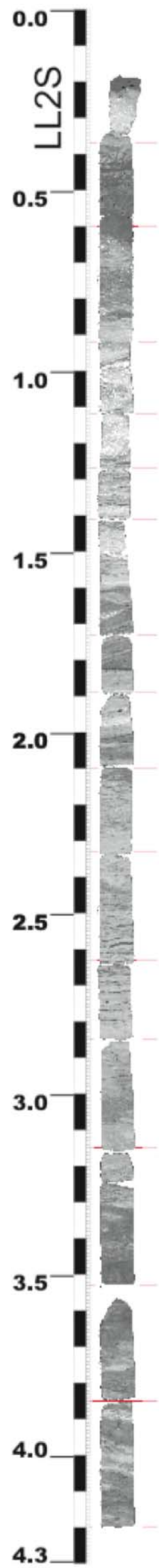
LL2S
0.0
0.5
1.0
1.5
2.0
2.5
3.0
3.5
4.0
4.3

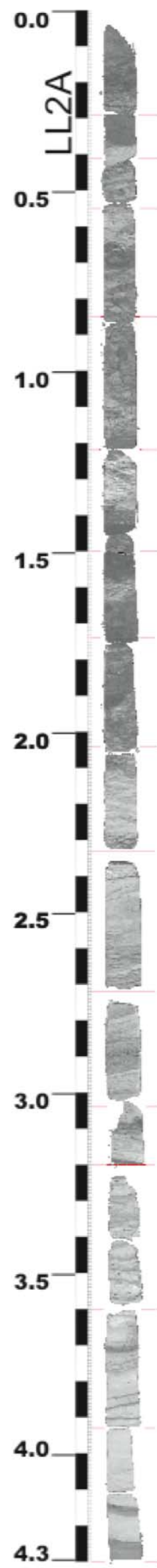
LL2A
0.0
0.5
1.0
1.5
2.0
2.5
3.0
3.5
4.0
4.3

Appendix G: Volumetric ice contents of 18 pore ice samples

Unit	Ice Volume (%)	Age (cal yrs BP)	Sample
Unit 4	75.9	5,895	MM12-QC-07
Unit 4	66.3	9,850	MM12-119
Unit 4	57.1	10,140	MM12-124
Unit 4	63.8	12,000	MM13-27
Unit 4	63.8	12,045	MM13-15
Unit 4	49.7	12,300	MM13-13
Unit 3	42.6	14,200	LL2-12-90
Unit 3	53.6	15,100	MM13-17
Unit 3	40.0	15,255	MM12-QC-02
Unit 3	51.5	15,740	MM13-24
Unit 3	55.0	17,490	MM12-116
Unit 3	46.5	18,600	MM12-117
Unit 3	57.9	26,160	MM12-71
Unit 3	63.9	26,990	MM12-103
Unit 2	57.2	28,355	DF10-27
Unit 1	70.0	39,855	MM12-130
Unit 1	119.1	41,470	MM12-125
Unit 1	56.8	42,400	DF12-26